Cover Page

Universiteit Leiden

Leiden University Repository

The handle http://hdl.handle.net/1887/138822 holds various files of this Leiden University dissertation.

Author: Tilburg, J.
Title: The role of solute carrier family 44 member 2 in the pathophysiology of venous thrombosis
Issue date: 2021-01-07

THE ROLE OF SOLUTE CARRIER FAMILY 44 MEMBER 2 IN THE PATHOPHYSIOLOGY OF VENOUS THROMBOSIS

Julia Tilburg

Colofon

The role of solute carrier family 44 member 2 in the pathophysiology of venous thrombosis
by JULIA TILBURG

ISBN/EAN: 978-94-6416-320-9

Copyright © 2020 Julia Tilburg
All rights reserved. No part of this thesis may be reproduced, stored or transmitted in any way or by any means without the prior permission of the author, or when applicable, of the publishers of the scientific papers.

Cover design: Daniëlle Balk | www.persoonlijkproefschrift.nl
Layout and design: Joppe Klein | www.persoonlijkproefschrift.nl
Printing: Ridderprint | www.ridderprint.nl

Cover figure based on Hinds. et al, Hum Mol Genet, 2016.

The role of solute carrier family 44 member 2 in the pathophysiology of venous thrombosis

Proefschrift

ter verkrijging van

de graad van Doctor aan de Universiteit Leiden

op gezag van de Rector Magnificus Prof. mr. C.J.J.M. Stolker

volgens besluit van het College voor Promoties

te verdedigen op donderdag 7 januari 2021

klokke 15.00 uur

door

Julia Tilburg

Geboren te Rotterdam in 1989

Promotor
Prof. dr. H.H. Versteeg

Copromotor
Dr. B.J.M. van Vlijmen

Leden promotiecommissie

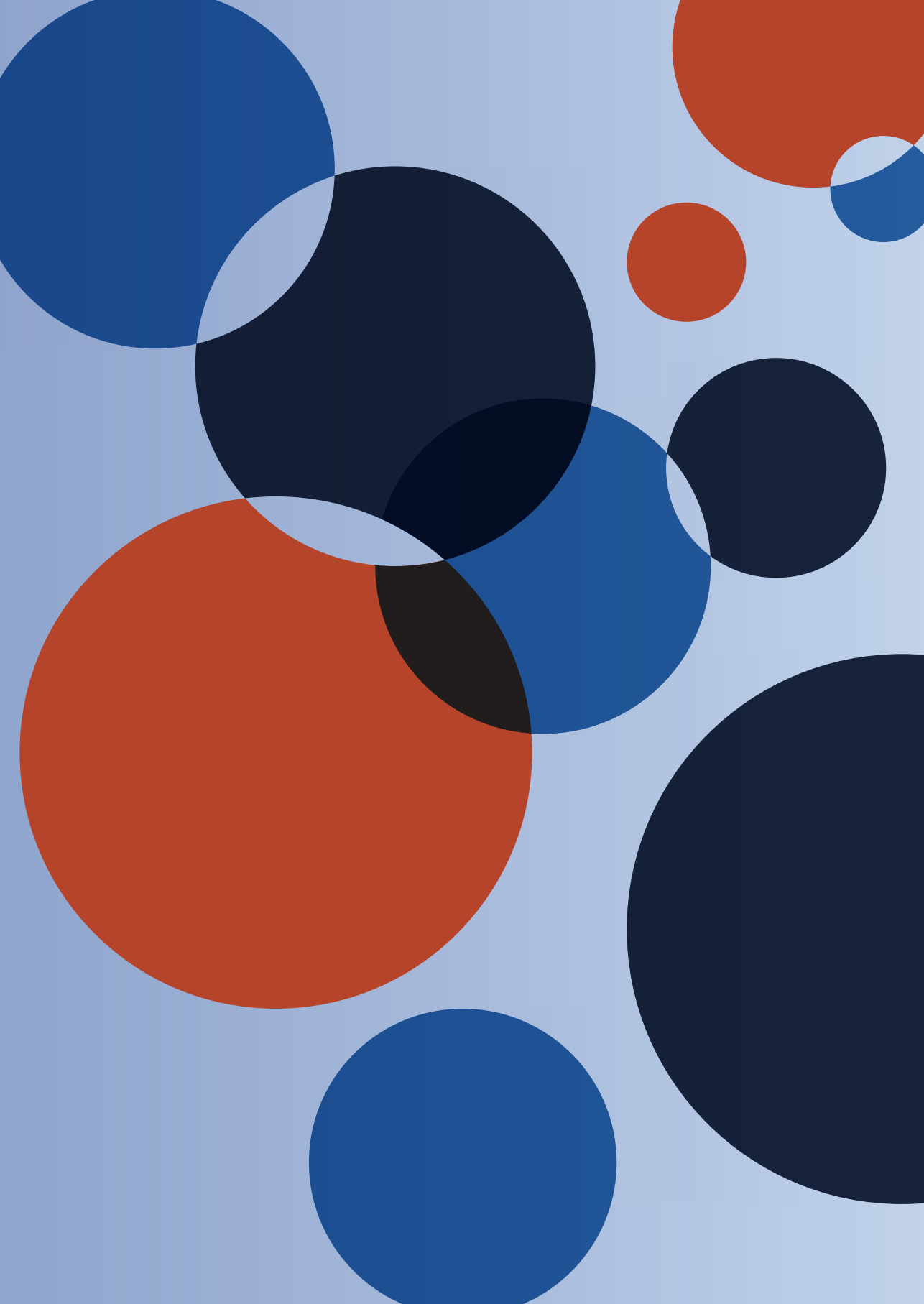
Prof. dr. S.C. Cannegieter	
Prof. dr. B.T. Heijmans	
Prof. dr. J.J. Voorberg	Universiteit van Amsterdam
Dr. J.A. Korporaal	Universiteit Utrecht

The research described in this thesis is financed by the Trombosestichting Nederland (#2015-4). The Landsteiner Foundation for Blood Transfusion Research (#1503) provided additional financial support.

Financial support from the Trombosestichting Nederland for the publication of this thesis is gratefully acknowledged.

Table of contents

Chapter 1	General introduction and outline of the thesis	7
Chapter 2	Characterization of hemostasis in mice lacking the novel thrombosis susceptibility gene *Slc44a2*	27
Chapter 3	SLC44A2 deficient mice have a reduced response in stenosis but not in hypercoagulability driven venous thrombosis	47
Chapter 4	Plasma protein signatures of a murine venous thrombosis model and *Slc44a2* knockout mice using quantitative-targeted proteomics	81
Chapter 5	SLC44A2/HNA3a is involved in neutrophil adhesion and activation to VWF in human and mice	117
Chapter 6	General discussion and perspectives	139
Chapter 7	Nederlandse samenvatting	157
Appendix	Curriculum Vitae	163
	Publications	165
	Dankwoord	166



GENERAL INTRODUCTION AND OUTLINE OF THE THESIS

Julia Tilburg

1

Venous Thrombosis

Hemostasis of the blood is essential to life as this keeps blood within the circulation upon the damage of a blood vessel. This process ensures that the transport of oxygen, nutrients and other necessities throughout the body is retained (1). A delicate interplay between vasoconstriction, blood platelets and several pro- and anticoagulant factors is responsible for the maintenance of hemostasis (1). A shift in this balance may lead to a reduced propensity to coagulate, possibly resulting in a bleeding disorder (2). On the other hand, a shift towards a more procoagulant condition can result in unwanted blood clotting known as thrombosis (3). Thrombosis can occur either in the arteries (arterial thrombosis; AT), or within a vein (venous thrombosis; VT). Together AT and VT are the main causes of death worldwide and a major burden on global health (4, 5). VT has an incidence of 1-2 in 1.000 people per year and usually occurs within the deep veins of the leg (deep vein thrombosis), where a blood clot causes obstruction of the vein (4). When a part of the clot embolises towards the lungs, it may cause a life-threatening condition called pulmonary embolism (PE) (6). VT has a mortality rate of 6% one month after diagnosis. When a patient survives, the recurrence is 25% after 5 years, thereby leaving patients with a lifelong risk (7, 8). Anticoagulant treatment is commonly used, both in treating thrombosis and as a prophylactic treatment in high risk patients (9). All currently available anticoagulant treatments (heparins, vitamin K antagonists and direct oral anticoagulants (DOACs)) introduce an imbalance of hemostasis (10-12). This imbalance can lead to adverse side effects, being serious and sometimes fatal bleedings (13).

The general principles of hemostasis

The pathophysiology of VT is well studied and relatively well understood (3). One of the first landmarks in thrombosis research was established in 1856 by the German physician Rudolph Virchow, when he described the elements contributing to thrombosis, also known as Virchow's triad (14, 15). He observed that thrombosis may develop if one of the following occurs: 1) Stasis of the blood flow, 2) Endothelial injury or 3) Hypercoagulability (14). To understand how these elements are linked to thrombosis, it is of importance to comprehend the general principles of hemostasis and the several different proteins and cell types that contribute to the development of a blood clot (16). Under normal conditions, the endothelium has an anticoagulant character as the surface is covered with the anticoagulant protein thrombomodulin (17). Damage of the vessel, however, will lead to the activation of the endothelial cells and the release of procoagulant von Willebrand factor (VWF) from the Weibel–Palade bodies. In addition, the subendothelial matrix is exposed, consisting of several procoagulant proteins (18). Platelets from the blood circulation are captured by VWF and subendothelial matrix proteins, thereby leading to activation and aggregation of these platelets and the formation of a hemostatic plug (19). This process of platelet recruitment is referred to as primary hemostasis and is followed by the activation of coagulation known as secondary hemostasis. Activation of the coagulation cascade is established by exposure of the blood to the procoagulant protein tissue factor (TF) upon vessel damage (20). This cascade, consisting of the subsequent activation of several serine proteases eventually results in the conversion of prothrombin into thrombin (16). Thrombin is central

to coagulation as thrombin leads to the polymerisation of fibrinogen to fibrin. Here, primary and secondary hemostasis come together as fibrin fibers interact with platelets and form a blood clot (21). An anticoagulant and fibrinolytic system is in place to avoid excessive blood clotting and to remove clots after wound healing is achieved (22, 23). This current concept of blood clot formation has been around for decades but new insights into the pathophysiology of VT are still being discovered (24).

The concept of immunothrombosis

The role of immune cells in VT initiation and propagation has recently been investigated extensively, although mainly in the setting of experimental mouse models (25). Neutrophils play an important role in the initiation of hypoxia- mediated VT (resulting from blood stasis), as they are recruited to the endothelial surface at an early phase of thrombus development (26). This accumulation of neutrophils is partially dependent on the mast cells residing in the vessel wall. Upon activation by hypoxia, these cells secrete histamine leading to endothelial activation and an enhanced exposure of adhesion molecules (27). Recruitment of neutrophils to the endothelial layer will result in release of neutrophil extracellular traps (NETs) forming a scaffold for platelets, VWF and fibrinogen, thereby propagating VT (28-30). Furthermore, NETs can activate the coagulation system as they trigger the activation of coagulation factor XII and consequently the intrinsic coagulation pathway (26). Monocytes are recruited to the vessel wall upon endothelial activation in a similar way as neutrophils, although to a lesser extent (26). These monocytes are the carrier of procoagulant TF, which initiates activation of blood coagulation via the extrinsic pathway (26). Besides their roles in hemostasis platelets also have a role in immunothrombosis, as specific adhesion molecules on their surface bind and activate neutrophils leading to an increased thrombus formation (31, 32). Together these concepts indicate a role for the immune system in VT at least in a murine VT setting. The relevance of this concept for human pathophysiology is of interest, as these mechanisms imply that systems other than classical hemostasis are influencing VT and therefore new insights into VT disease and potential therapeutic targets are to be discovered.

GWAS as a tool to identify novel genetic contributors to venous thrombosis

Risk factors for venous thrombosis

VT is a multifactorial disease and risk factors impacting one or more elements of Virchow's triad are commonly identified using human population studies (33-35). Amongst others, cancer, age, trauma, obesity, oral contraceptives, pregnancy, surgery, and air travel are identified as common environmental risk factors (36). In addition to acquired risk factors for VT, inheritable genetic predispositions also contribute to disease development (37). Although congenital deficiencies of natural coagulation inhibitors, protein C, protein S and antithrombin are rare, these deficiencies are major genetic risk factors for VT leading up to a 10-fold increased risk of developing a VT (38). Another well-known, but less strong, genetic contributor is Non-blood type O (ABO), which is associated with higher levels of VWF and subsequently a 2-fold higher VT risk (39). The first genetic mutation associated

with VT was discovered by linkage analysis of inheritable activated protein C-resistance (40). This increased resistance and thereby 3-fold increased risk for VT was denoted to a polymorphism in the coagulation factor V gene (Factor V Leiden mutation, rs6025) (40). Mutations located in the genes coding for prothrombin (*F2*, G20210A/rs1799963, 1.5-fold increased risk), fibrinogen (*FGG*, rs2066865, 1.5-fold increased risk*)* and coagulation Factor XI (*F11*, rs4253417, 2.8-fold increased risk*)* were later also linked to VT using conventional linkage analysis (41-43).

GWAS for venous thrombosis

Collectively, the known genetic factors described above do not fully explain how the genetic landscape contributes to VT risk. Therefore, to increase our understanding, advanced genetic studies are performed. Moreover, genome wide association studies (GWAS) provide a potentially powerful tool to determine single nucleotide polymorphisms (SNP) across the genome associated with diseases (44). By comparing allele frequencies of SNPs from a cohort displaying a phenotype or disease to a control group, GWAS can link genetic loci to certain traits (45). The hypothesis-free character of these studies opens up an opportunity to unravel unsuspected associations. This is relevant as these associations can provide biological insights and, in addition, may lead to the identification of novel therapeutic targets. The first GWAS was performed in 2002 for myocardial infarction and ever since GWAS have a proven track record in cardiovascular disease (CVD) (46-49). In order to identify novel genetic risk factors for VT and novel therapeutic targets potentially circumventing bleeding side effects, GWAS was first applied to this field in 2009 (50). This study, including 453 VT cases and 1327 controls confirmed previously reported genetic risk factors for VT, including Factor V Leiden and ABO loci, but did not reveal additional factors that contribute to the extent of these previously described factors (50). As estimations showed that the by then known genetic risk loci together explained 35% of the genetic predisposition for VT, novel factors were to be revealed (51). With the population studies and GWAS further emerging and the number of included subjects and measured SNPs radically increasing, studies became larger and more powerful. In 2015 a meta-analysis was published which combined the results of multiple VT GWAS studies that included a total of 7507 VT case subjects and 52632 controls (52). This was the first study to show the capacity of GWAS as a discovery method for VT as two novel risk factors were identified; *TSPAN15* and *SLC44A2* (with top associated SNPs: rs78707713 and rs2288904, respectively) (52). Importantly, these two loci were successfully replicated in three independent case-control studies. In addition, a second independent GWAS conducted in the 23andMe cohort, showed associations between these genes and self-reported blood clotting events (52, 53). Interestingly, *TSPAN15* and *SLC44A2* were not previously linked to coagulation, in contrast to all the previously identified genetic risk factors. This is further supported by the lack of an association of these genetic loci with 25 related quantitative biomarkers included in the GWAS such as the activated partial thromboplastin time, endogenous thrombin generation and activity levels of numerous coagulation (related) factors (52). Therefore, the association of these loci with VT implies

that there are undiscovered mechanisms to be revealed regarding the pathophysiology of VT involving TSPAN15 and SLC44A2.

GWAS have been widely used in CVD and other diseases or genomic traits. As an illustration, at start of the writing of this thesis, over 4000 GWAS were published and this number keeps on rapidly growing (54). Together these GWAS have provided a plethora of data and are an invaluable tool in uncovering genetic dispositions and biomarkers (55). However, the translation of these associations into novel therapeutic strategies remains limited (56). For a successful GWAS bench to bedside approach it is important to comprehend that gene discovery should not be a goal on itself. GWAS should be combined with further functional studies and treatment development to fully capture the biological relevance and potentially improve the disease outcome (57, 58). To this end, the work described in this thesis provides a functional follow up on one of the genes identified by GWAS as a VT susceptibility locus namely SLC44A2 and its role in the pathophysiology of VT.

SLC44A2 and its relation to disease

SLC44A2 is a relatively unknown gene and questions regarding the function of SLC44A2 still arise. In the following section, SLC44A2 and its relation to disease is further described.

The solute carrier family 44 member 2

SLC44A2 or solute carrier family 44 member 2 is encoded by a 42,115 nucleotide, 22 exon spanning gene located on chromosome 19p13.1 (59, 60). *SLC44A2* has two transcript variants; P2 and P1 which lead to proteins differing in the region at the N terminus and these transcripts have alternative promotors (60, 61). The SLC44A2 gene encodes a 68-72kDa transmembrane glycoprotein which is characterized by ten hydrophobic membrane-spanning domains, five extracellular loops and six intracellular regions (62). It is expressed in several tissues including cochlea, tongue, heart, colon, lung, kidney, liver and spleen (60). SLC44A2 is shown to be widely expressed in different blood cells such as neutrophils, platelets and erythrocytes (61, 63, 64). As the classification as a solute carrier transporter implies SLC44A2 is a presumed transporter enabling the passage of choline thought the cell membrane (65). Hence the alternative name of SLC44A2 is choline transporter-like protein 2 (CTL-2). Interestingly, however, this transport capacity is only associated with the longer transport variant P2 which is expressed on lung endothelial tissue (60). This was experimentally confirmed *in vitro* using brain microvascular endothelial cells (66). Neutrophils and platelets only express the P1 variant and therefore SLC44A2 on these components is not able to transport choline and the function here remains unknown (61, 64).

Human neutrophil antigen-3

In addition to the properties described above, SLC44A2 harbours one of the human neutrophil antigens (HNA), which were recently extensively reviewed (62). There are five HNAs (HNA1-5) and antibodies targeting these sites are known to be involved in immune diseases (62). SLC44A2 harbours the HNA3 epitope to which alloantibodies can arise. These

antibodies may lead to transfusion related acute lung injury (TRALI) or autoimmune hearing loss, both further described below (59, 67). The HNA3 epitope has two allelic variants, HNA3A and HNA3B, determined by a single point mutation SLC44A2*455G>A (SLC44A2*457G>A for transcript variant P2) (68). Interestingly, the same polymorphism, rs2288094, is linked to VT (52). More commonly, antibodies targeting HNA3A cause adverse effects as antibodies targeting HNA3B are less pathogenic (68). The prevalence of the HNA3A genetic variant, which is associated with an increased VT risk, is high with 0.79, 0.93 and 0.74 in Caucasians, African Americans and Chinese respectively (68-70). In the German population 64.1% is homozygous for HNA3A, 5.5% for HNA3B and 30.4% is heterozygous (68).

Transfusion Related Acute Lung Injury

HNA3 antibodies can arise in pregnant women, specifically when carrying a child with the opposite allelic variant (71). Upon blood or plasma transfusion with antibody contaminated blood from these women to recipients expressing the epitope targeted by these antibodies, an immune response can occur within hours after transfusion (67). Upon binding of the antibodies to the HNA3 epitope present on the SLC44A2 protein on neutrophils, these cells will become activated resulting in agglutination and the release of NETs (72, 73). Subsequently, the release of reactive oxygen species (ROS) from the neutrophils causes severe damage to the lung endothelium and when left untreated, this condition referred to as TRALI, can be fatal (74). A pre-existing pulmonary pathology is required for neutrophils to be present in the lung tissue and for TRALI to occur (67). TRALI is the most common transfusion related cause of death, therefore to lower the prevalence, women who delivered children should be excluded as a blood donor (75). The role of SLC44A2 is of interest as the transcript variant involved in TRALI is the same as the one associated with VT. Moreover, the cell type which is driving TRALI, neutrophils, has a known role in VT.

Autoimmune hearing loss and Slc44a2 deficient mice

In addition to its role in TRALI, SLC44A2 is also the target of antibodies inducing autoimmune hearing loss (59, 76, 77). Human autoantibodies can bind to the HNA3 epitope on SLC44A2 in the organ of Corti resulting in dysfunction of this organ (78). The organ of Corti, located in the cochlea of the inner ear, is pivotal to transduction of auditory signals and malfunctioning leads to severe hearing impairment (79). To study the role of SLC44A2 in hearing loss *Slc44a2* deficient mice were generated (80). By the insertion of *flox* sites surrounding the exon 3 to 10 region of the *Slc44a2* gene, and crossing of these mice to mice carrying a *Cre* recombinase behind the EIIa promotor (expressing *Cre* to the early mouse embryo) a full body knockout was developed. The mice appeared healthy and fertile and did not exhibit aberrant behaviour, size differences or other atypical features. However these mice exhibited extensive hair cell and spiral ganglion cell loss in the cochlea and subsequently progressive hearing loss (80). This finding further underlines a role for SLC44A2 in long term hair cell survival and in the maintenance of normal hearing.

SLC44A2 and von Willebrand factor

Further studies into the localization of SLC44A2 in the inner ear reported that this protein colocalizes with cochlin, one of the predominant proteins of the inner ear (81). Since cochlin harbours two VWF binding domains it was hypothesised that this colocalization is mediated by VWF (82). Bayat and colleagues created a human embryonic kidney (HEK293) cell line overexpressing SLC44A2. Interestingly, SLC44A2 positive cells displayed enhanced binding to VWF (83). Subsequently, by blocking specific VWF domains, SLC44A2 was shown to bind the A1 domain, the domain required for platelet-VWF interaction. Furthermore, it was established that neutrophil agglutination, induced by antibodies targeting SLC44A2, is reduced in plasma containing lower levels of VWF. Because of the predominant role of VWF in hemostasis the binding capacity of SLC44A2 to this protein is of interest when investigating the role of SLC44A2 in VT.

Modelling thrombosis using murine models

Selecting a study approach to investigate the role of SLC44A2 in the pathophysiology of VT is challenging as in VT several factors i.e. the endothelial, blood flow, coagulation factors and cellular components of the blood synergize to form a blood clot. Therefore, to study SLC44A2 in this interplay of different elements and the circulation, advanced experimental setups are necessary. The mouse is a frequently used model organism in VT research because of several advantages. First, the coagulation system is highly conserved in the mouse and all elements of Virchow's triad are present, making it suitable in mimicking VT (84). In addition, mice express SLC44A2 and the gene encoding SLC44A2 can be easily genetically manipulated to produce a mouse deficient in this protein (80, 85). Lastly, mice are also fast breeders, have low costs of maintenance and are relatively easy to handle (86). Although hemostasis is highly conserved, mice appear to be resistant to the development of a venous thrombus in the absence of any genetic, surgical or chemical manipulations. Therefore, to study thrombosis in a mouse model, a pro-thrombotic trigger has to be applied. As there are several factors that play a role in thrombosis, i.e. the elements of Virchow's triad (endothelial damage, blood flow and coagulation) there are also various ways to introduce thrombosis in mice (87). Endothelial activation is one method to modulate vascular injury or thrombosis in mice. Models such as the ferric chloride model, the laser injury model, or more systemic endothelial activation are widely accepted (88-90). Also models manipulating the blood flow are common practise, for instance by completely (stasis) or partially (stenosis) ligating the large veins in a mouse (26, 91, 92). Mouse models which interfere with expression of genes related to coagulation are used to study Virchow's third element of hemostasis; coagulation. For instance mice harbouring the Factor V Leiden mutation or tissue factor pathway inhibitor (TFPI) heterozygosity display mild to moderate pro-coagulant phenotypes (93, 94). Mice with more severe genetic deficiencies such as deletion of antithrombin, Protein C or TFPI will die perinatally (95-97). To overcome this early mortality, a mouse model using a transient imbalance of anticoagulant factors was established (98, 99). Overall, there are several different VT models available which all have advantages and disadvantages (100). A convenient algorithm including the 7 most used murine VT models was recently published

and although not complete, this guideline forms a solid foundation for VT model selection (101, 102). The murine VT models that are used throughout this thesis are summarized below and their advantages and disadvantages are discussed.

A challenge of hemostasis by endothelial damage of the cremaster arterioles
The recruitment of blood cells and other blood components towards the site of injury at the vessel wall is an important element in the maintenance of hemostasis (1). Intravital video microscopy upon laser injury of the cremaster muscle arterioles provides an opportunity to monitor this process live (103). In short; a laser is used to introduce injury on the luminal vessel wall of the cremaster muscle arterioles and within seconds, accumulation of fluorescently labelled elements at the site of injury may be recorded (89). This model was previously shown to be dependent on intravascular tissue factor, platelets and neutrophils (104, 105). Important to note, this model is not dependent on VWF. Thus to study VWF dependent mechanisms, other models might be more suitable (106). As the dissection of the cremaster muscle is a delicate procedure, a skilled animal surgeon is required to prepare the animal. One of the main advantages however, is that multiple injuries can be applied to one mouse leading to large experimental numbers per mouse (107). It should be pointed out that in this model the injury is applied to arterioles meaning that hemostasis is measured under arterial flow, therefore this model is not fully representative of VT. Besides its limitations, this model has been widely used to elucidate the contribution of several molecular components involved in thrombosis (107).

Neutrophil adherence to histamine stimulated endothelium
The model described above induces injury to monitor blood cell recruitment to a specific site. To introduce a more systemic endothelial activation resembling a state of inflammation, histamine can be used. In this model the venules of the mesentery bed are exposed and using intravital microscopy the recruitment of blood cells can be visualized and quantified (108, 109). Prior to laparotomy of the mesentery the mice is injected with histamine, resulting in endothelial degranulation and the release of VWF from the Weibel-Palade bodies (110). To monitor neutrophil adherence to the vessel wall these cells are fluorescently labelled. The advantages are again that multiple sites can be monitored in one mouse and the venous flow makes it suitable for studies on VT. As this model monitors the interaction of immune cell with the endothelial it is mainly used to study immunothrombosis.

Thrombosis induced by stenosis of the inferior vena cava
The inferior vena cava (IVC) is the largest vein in mice and is therefore a commonly used venous location to induce thrombosis. In the stenosis model, a partial ligation of the IVC is achieved by placing a ligature around the vein. A spacer is used to retain a small opening, resulting in a ~10% residual blood flow (92). In contrast to the previously commonly used St. Thomas model where a clip is used, the stenosis model is supposed to be endothelial damage free and endothelial activation is solely the result of hypoxia resulting from the reduced blood flow (101). Current understanding indicates the following sequence of events to result

in thrombus formation in this model. Upon endothelial activation, VWF-mediated platelet adhesion to the vessel wall occurs. Activation of these platelets leads to platelet-platelet aggregates which form a scaffold for coagulation activation via FXII activation into FXIIa (111). In addition, monocytes and neutrophils accumulate during the initiation phase. Remarkably within two hours after ligation neutrophils localize at the vessel wall (26, 112). Upon neutrophil activation NETs are formed, that will trap platelets and red blood cells forming the scaffold for a thrombus (29). Within 6 hours after ligation in the stenosis model a visible thrombus is formed and after 48 hours a multi layered thrombus consisting of white and red regions is developed (26). Because of the pivotal role of neutrophils and NETosis in the stenosis model, it is currently primarily used to study immunothrombosis.

Thrombosis induced by a hypercoagulable state

All models described above require advanced surgical procedures. On the contrary, the model driven by downregulation of anticoagulants is induced by a simple tail vein injection (98, 113). Following injection of small interfering RNAs (siRNA) against two anticoagulants, antithrombin and protein C, hepatic expression of these proteins is downregulated resulting in a hypercoagulable state. Within two days after treatment, the mice start to develop thrombi within the veins of the mandibular area of the head. Histologically, these obstructions present as a fibrin rich thrombus. As a secondary phenotype, mice display haemorrhaging in the area surrounding the eye which is likely due to rupture of the veins because of thrombus formation. This model was previously shown to be highly dependent on platelets and tissue factor (113). As neutrophils do not influence thrombosis in this model this model is not suitable for studies in immunothrombosis (113).

Mass spectrometry based targeted plasma proteomics

Mouse models for VT may be used to gain insight into the role of SLC44A2 in the pathophysiology of VT. To investigate a possible physiological effect of SLC44A2 on VT, the composition of the blood may be analyzed by various methods. For the work described in this thesis, we utilized a novel methodology to measure the plasma proteome in mice. Below, this method is introduced and the advantages above current assays are discussed.

The plasma proteome

Analysis of blood components yield important information regarding the state of health and disease in an individual. Blood counts and characteristics of the cellular components of blood i.e. erythrocytes, lymphocytes and thrombocytes may yield important information, for instance about ongoing inflammation, kidney malfunction or bleeding tendencies (114-116). Blood plasma contains, amongst others, proteins that are involved in blood coagulation, the acute phase response, cholesterol metabolism and the complement system (117, 118). In addition to these functional plasma proteins, the plasma proteome also contains proteins as a consequence of tissue leakage and signaling proteins (119). As the concentrations and activity of plasma proteins reflect the disease state, measuring these proteins in clinical diagnostics is common practice (120, 121). To measure protein abundance, antibody and

activity-based protein assays are nowadays frequently used. These assays have the ability to precisely determine protein concentrations, but often do not have the possibility to measure multiple proteins at once e.g. measure in multiplex (120). Another disadvantage of antibody based protein detection is the reliability on the availability and quality of an antibody for the protein of interest (122, 123).

Mass spectrometry based targeted plasma proteomics

As an alternative to the conventional protein assays, mass spectrometry can be applied to measure protein concentrations in multiplex (124). In short, a digested protein sample is loaded on a reversed phase column attached to a liquid chromatographer (125). After sample separation the peptides are converted to gas phase ions by electrospray ionization and the samples are then fragmented on a mass spectrometer (126). The originating mass spectra of these ions are used to identify and quantify the peptides and corresponding proteins (127). This method serves as a good tool for discovery-based proteomics, but is not suitable when a high precision is required, due to the spectral overlap in protein mass spectra (126). Mass spectrometry-based targeted proteomics, also called multiple reaction monitoring (MRM), incorporates stable isotope-labeled peptide standards to select and quantify specific peptides thereby overcoming the spectral overlap (127-130). By this means, MRM offers a technique to quantify preselected proteins with high precision and opens an opportunity to measure low abundance proteins in small volumes of for instance plasma (131, 132).

Murine plasma proteomics

Previously our group showed that protein quantification of several coagulation factors in human plasma by MRM strongly correlated with quantification by conventional antibody and activity assays (133). The protein signatures allowed for successful separation of patients with the diagnosis of VT and cancer-related VT emphasizing the potential of this technique for both diagnostics and for biomarker detection (133). MRM also holds potential in murine research as plasma volumes in mice are small and available antibodies required for conventional protein assays are limited. Therefore, recently, a large peptide panel was developed to quantify 500 plasma proteins in mouse using MRM (134). This panel was successful in separating different mouse strains based on the plasma proteome and in addition sex-dependent differences were reported (135). In the work described in this thesis, a modified version of this peptide panel is used to study the effects of VT and SLC44A2 on the plasma proteome in mice.

Aims and outline of this thesis

Within the context of this thesis, we aim to unravel the mechanism underlying the association between SLC44A2 and VT. As SLC44A2 does not belong to the coagulation or fibrinolytic system, dissecting these mechanisms is a powerful strategy to generate new biological insights into the pathophysiology of VT. In addition, as all current therapeutic strategies come with a risk for bleeding, novel pathways might present possibilities for new therapies.

From literature the following hypothesis arose regarding SLC44A2 and VT 1) SLC44A2 does not influences hemostasis, as GWAS do not link SLC44A2 2288904 SNP variances to haemostatic biomarkers included in the study. 2) SLC44A2 on endothelial and/or blood cells mediate the effect of SLC44A2 on VT, as these cell types express SLC44A2 and have a central role in VT. 3) SLC44A2 exhibits its effect on VT by neutrophil activation and NET release, similar as in TRALI, which also has a role for SLC44A2. 4) SLC44A2 exhibits its role in VT by binding of SLC44A2 on cells to VWF, as previous reports revealed these as binding partners. To test these hypotheses, a mouse deficient in SLC44A2 is used and throughout the chapters of the thesis, we will explore different aspects of hemostasis and thrombosis. To study the role of SLC44A2 rs2288904, human neutrophils expressing variations in this SNP are used.

Despite the deletion of the *Slc44a2* gene, mice appear relatively normal and no aberrancies were previously detected with the exception of hearing loss upon age. In **chapter 2** these mice are subjected to a general characterization of hemostasis to investigate whether SLC44A2 affects this process. Several parameters of hemostasis were studied i.e.: thrombin generation potential, expression of coagulation related genes, VWF characteristics and platelet aggregation. In addition a challenge of hemostasis was applied by introducing endothelial damage to the cremaster muscle arterioles.

In **chapter 3** we took our research a step further and moved from hemostasis to thrombosis. *Slc44a2* deficient mice were subjected to two independent models of VT. First, a model which challenges coagulation by siRNA-mediated inhibition of protein C and antithrombin resulting in a procoagulant state was used. Second, a model of VT that is driven by an inflammatory response upon flow restriction of the IVC was employed. To further elucidate the underlying mechanism, several elements of VT, i.e. blood, neutrophils and platelets were further investigated *ex vivo*.

Plasma protein levels hold important information on health and disease, and MRM can be used to measure the plasma proteome. In **chapter 4** we have employed a recently developed multiplex panel of peptide standards allowing measurement of 375 proteins (unbiased to pathway) in murine plasma. To first show the validity of this methodology, the plasma proteome was determined in wild type mice with VT induced by siRNA mediated inhibition of Protein C and antithrombin. Next, to determine the effect of SLC44A2 on the plasma proteome, we applied this panel to plasma of *Slc44a2* deficient mice.

In **chapter 5** we investigate the association between SLC44A2 and VWF in the setting of VT and move our research from mice to humans. To test the experimental set up and to replicate previous findings, HEK293 cell overexpressing the minor or major SLC44A2 rs2288904 allelic variant were perfused over VWF-coated flow chambers. Next, human neutrophil adhesion, activation and NET release was investigated in this perfusion set up. To study neutrophil adhesion in a more complex setting in *Slc44a2* deficient mice, neutrophil

mobilization towards the venules of the mesentery veins was determined upon endothelial activation.

In **chapter 6** the results described in this thesis are further discussed and **chapter 7** provides a Dutch summary of the findings.

References

1. Boon GD. An overview of hemostasis. *Toxicol Pathol*. 1993;21(2):170-9.
2. Peyvandi F, Garagiola I, Young G. The past and future of haemophilia: diagnosis, treatments, and its complications. *Lancet*. 2016;388(10040):187-97.
3. Furie B, Furie BC. Mechanisms of thrombus formation. *N Engl J Med*. 2008;359(9):938-49.
4. Raskob GE, Angchaisuksiri P, Blanco AN, et al. Thrombosis: a major contributor to global disease burden. *Arterioscler Thromb Vasc Biol*. 2014;34(11):2363-71.
5. Lozano R, Naghavi M, Foreman K, et al. Global and regional mortality from 235 causes of death for 20 age groups in 1990 and 2010: a systematic analysis for the Global Burden of Disease Study 2010. *Lancet*. 2012;380(9859):2095-128.
6. Essien EO, Rali P, Mathai SC. Pulmonary Embolism. *Med Clin North Am*. 2019;103(3):549-64.
7. Kyrle PA, Rosendaal FR, Eichinger S. Risk assessment for recurrent venous thrombosis. *Lancet*. 2010;376(9757):2032-9.
8. Naess IA, Christiansen SC, Romundstad P, et al. Incidence and mortality of venous thrombosis: a population-based study. *J Thromb Haemost*. 2007;5(4):692-9.
9. Harter K, Levine M, Henderson SO. Anticoagulation drug therapy: a review. *West J Emerg Med*. 2015;16(1):11-7.
10. Franchini M, Liumbruno GM, Bonfanti C, et al. The evolution of anticoagulant therapy. *Blood Transfus*. 2016;14(2):175-84.
11. Thaler J, Pabinger I, Ay C. Anticoagulant Treatment of Deep Vein Thrombosis and Pulmonary Embolism: The Present State of the Art. *Front Cardiovasc Med*. 2015;2:30.
12. Toorop MMA, van Rein N, Nierman MC, et al. Switching from vitamin K antagonists to direct oral anticoagulants: Treatment satisfaction and patient concerns. *J Thromb Haemost*. 2020.
13. Linkins LA, Choi PT, Douketis JD. Clinical impact of bleeding in patients taking oral anticoagulant therapy for venous thromboembolism: a meta-analysis. *Ann Intern Med*. 2003;139(11):893-900.
14. Kumar DR, Hanlin E, Glurich I, et al. Virchow's contribution to the understanding of thrombosis and cellular biology. *Clin Med Res*. 2010;8(3-4):168-72.
15. Turk JL. Rudolf Virchow--father of cellular pathology. *J R Soc Med*. 1993;86(12):688-9.
16. Versteeg HH, Heemskerk JW, Levi M, et al. New fundamentals in hemostasis. *Physiol Rev*. 2013;93(1):327-58.
17. Martin FA, Murphy RP, Cummins PM. Thrombomodulin and the vascular endothelium: insights into functional, regulatory, and therapeutic aspects. *Am J Physiol Heart Circ Physiol*. 2013;304(12):H1585-97.
18. Leebeek FW, Eikenboom JC. Von Willebrand's Disease. *N Engl J Med*. 2016;375(21):2067-80.
19. Li Z, Delaney MK, O'Brien KA, et al. Signaling during platelet adhesion and activation. *Arterioscler Thromb Vasc Biol*. 2010;30(12):2341-9.
20. Mackman N, Tilley RE, Key NS. Role of the extrinsic pathway of blood coagulation in hemostasis and thrombosis. *Arterioscler Thromb Vasc Biol*. 2007;27(8):1687-93.
21. Crawley JT, Zanardelli S, Chion CK, et al. The central role of thrombin in hemostasis. *J Thromb Haemost*. 2007;5 Suppl 1:95-101.

22. Rijken DC, Lijnen HR. New insights into the molecular mechanisms of the fibrinolytic system. *J Thromb Haemost*. 2009;7(1):4-13.
23. Dahlback B. Blood coagulation and its regulation by anticoagulant pathways: genetic pathogenesis of bleeding and thrombotic diseases. *J Intern Med*. 2005;257(3):209-23.
24. Esmon CT. Basic mechanisms and pathogenesis of venous thrombosis. *Blood Rev*. 2009;23(5):225-9.
25. Budnik I, Brill A. Immune Factors in Deep Vein Thrombosis Initiation. *Trends Immunol*. 2018;39(8):610-23.
26. von Bruhl ML, Stark K, Steinhart A, et al. Monocytes, neutrophils, and platelets cooperate to initiate and propagate venous thrombosis in mice in vivo. *J Exp Med*. 2012;209(4):819-35.
27. Ponomaryov T, Payne H, Fabritz L, et al. Mast Cells Granular Contents Are Crucial for Deep Vein Thrombosis in Mice. *Circ Res*. 2017;121(8):941-50.
28. Brill A, Fuchs TA, Savchenko AS, et al. Neutrophil extracellular traps promote deep vein thrombosis in mice. 2012;10(1):136-44.
29. Fuchs TA, Brill A, Duerschmied D, et al. Extracellular DNA traps promote thrombosis. *Proc Natl Acad Sci U S A*. 2010;107(36):15880-5.
30. Fuchs TA, Brill A, Wagner DD. Neutrophil extracellular trap (NET) impact on deep vein thrombosis. *Arterioscler Thromb Vasc Biol*. 2012;32(8):1777-83.
31. Dyer MR, Chen Q, Haldeman S, et al. Deep vein thrombosis in mice is regulated by platelet HMGB1 through release of neutrophil-extracellular traps and DNA. *Sci Rep*. 2018;8(1):2068.
32. Zucoloto AZ, Jenne CN. Platelet-Neutrophil Interplay: Insights Into Neutrophil Extracellular Trap (NET)-Driven Coagulation in Infection. *Front Cardiovasc Med*. 2019;6:85.
33. Anderson FA, Jr., Spencer FA. Risk factors for venous thromboembolism. *Circulation*. 2003;107(23 Suppl 1):I9-16.
34. Flinterman LE, van Hylckama Vlieg A, Rosendaal FR, et al. Recurrent thrombosis and survival after a first venous thrombosis of the upper extremity. *Circulation*. 2008;118(13):1366-72.
35. Pomp ER, Lenselink AM, Rosendaal FR, et al. Pregnancy, the postpartum period and prothrombotic defects: risk of venous thrombosis in the MEGA study. *J Thromb Haemost*. 2008;6(4):632-7.
36. Heit JA, Spencer FA, White RH. The epidemiology of venous thromboembolism. *J Thromb Thrombolysis*. 2016;41(1):3-14.
37. Ohlsson H, Sundquist J, Sundquist K, et al. Familial risk of venous thromboembolism in first-, second- and third-degree relatives: a nationwide family study in Sweden. *Thrombosis and Haemostasis*. 2013;109(03):458-63.
38. Lipe B, Ornstein DL. Deficiencies of natural anticoagulants, protein C, protein S, and antithrombin. *Circulation*. 2011;124(14):e365-8.
39. Dentali F, Sironi AP, Ageno W, et al. Non-O blood type is the commonest genetic risk factor for VTE: results from a meta-analysis of the literature. *Semin Thromb Hemost*. 2012;38(5):535-48.
40. Bertina RM, Koeleman BP, Koster T, et al. Mutation in blood coagulation factor V associated with resistance to activated protein C. *Nature*. 1994;369(6475):64-7.
41. Li Y, Bezemer ID, Rowland CM, et al. Genetic variants associated with deep vein thrombosis: theF11locus. *Journal of Thrombosis and Haemostasis*. 2009;7(11):1802-8.
42. Uitte de Willige S, de Visser MC, Houwing-Duistermaat JJ, et al. Genetic variation in the fibrinogen gamma gene increases the risk for deep venous thrombosis by reducing plasma fibrinogen gamma' levels. *Blood*. 2005;106(13):4176-83.

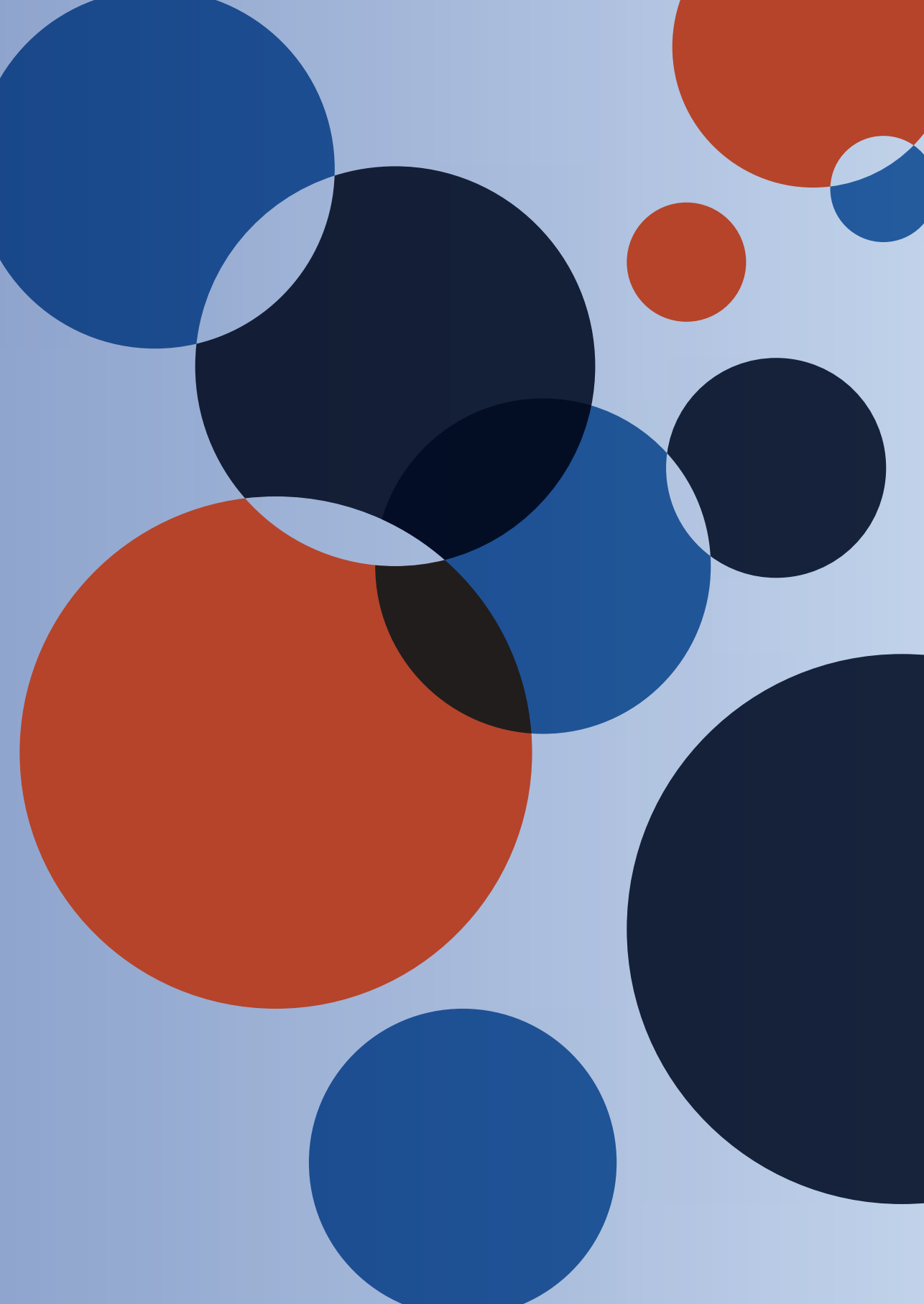
43. Poort SR, Rosendaal FR, Reitsma PH, et al. A common genetic variation in the 3'-untranslated region of the prothrombin gene is associated with elevated plasma prothrombin levels and an increase in venous thrombosis. *Blood*. 1996;88(10):3698-703.
44. Hirschhorn JN, Daly MJ. Genome-wide association studies for common diseases and complex traits. *Nat Rev Genet*. 2005;6(2):95-108.
45. Manolio TA. Genomewide association studies and assessment of the risk of disease. *N Engl J Med*. 2010;363(2):166-76.
46. Samani NJ, Erdmann J, Hall AS, et al. Genomewide association analysis of coronary artery disease. *N Engl J Med*. 2007;357(5):443-53.
47. Erdmann J, Grosshennig A, Braund PS, et al. New susceptibility locus for coronary artery disease on chromosome 3q22.3. *Nat Genet*. 2009;41(3):280-2.
48. Ikram MA, Seshadri S, Bis JC, et al. Genomewide Association Studies of Stroke. *New England Journal of Medicine*. 2009;360(17):1718-28.
49. Ozaki K, Ohnishi Y, Iida A, et al. Functional SNPs in the lymphotoxin-alpha gene that are associated with susceptibility to myocardial infarction. *Nat Genet*. 2002;32(4):650-4.
50. Tregouet DA, Heath S, Saut N, et al. Common susceptibility alleles are unlikely to contribute as strongly as the FV and ABO loci to VTE risk: results from a GWAS approach. 2009;113(21):5298-303.
51. Germain M, Saut N, Greliche N, et al. Genetics of Venous Thrombosis: Insights from a New Genome Wide Association Study. *PLoS ONE*. 2011;6(9):e25581.
52. Germain M, Chasman DI, de Haan H, et al. Meta-analysis of 65,734 individuals identifies TSPAN15 and SLC44A2 as two susceptibility loci for venous thromboembolism. *Am J Hum Genet*. 2015;96(4):532-42.
53. Hinds DA, Buil A, Ziemek D, et al. Genome-wide association analysis of self-reported events in 6135 individuals and 252 827 controls identifies 8 loci associated with thrombosis. *Human Molecular Genetics*. 2016;25(9):1867-74.
54. Buniello A, MacArthur JAL, Cerezo M, et al. The NHGRI-EBI GWAS Catalog of published genome-wide association studies, targeted arrays and summary statistics 2019. *Nucleic Acids Res*. 2019;47(D1):D1005-D12.
55. Caliskan Y, Kiryluk K. Novel biomarkers in glomerular disease. *Adv Chronic Kidney Dis*. 2014;21(2):205-16.
56. Fordyce CB, Roe MT, Ahmad T, et al. Cardiovascular drug development: is it dead or just hibernating? *J Am Coll Cardiol*. 2015;65(15):1567-82.
57. Shu L, Blencowe M, Yang X. Translating GWAS Findings to Novel Therapeutic Targets for Coronary Artery Disease. *Front Cardiovasc Med*. 2018;5:56.
58. Edwards SL, Beesley J, French JD, et al. Beyond GWASs: illuminating the dark road from association to function. *Am J Hum Genet*. 2013;93(5):779-97.
59. Nair TS. Identification and Characterization of Choline Transporter-Like Protein 2, an Inner Ear Glycoprotein of 68 and 72 kDa That Is the Target of Antibody-Induced Hearing Loss. *Journal of Neuroscience*. 2004;24(7):1772-9.
60. Kommareddi PK, Nair TS, Thang LV, et al. Isoforms, Expression, Glycosylation, and Tissue Distribution of CTL2/SLC44A2. *The Protein Journal*. 2010;29(6):417-26.
61. Flesch BK, Wesche J, Berthold T, et al. Expression of the CTL2 transcript variants in human peripheral blood cells and human tissues. 2013;53(12):3217-23.

62. Flesch BK, Reil A. Molecular Genetics of the Human Neutrophil Antigens. *Transfusion Medicine and Hemotherapy*. 2018;45(5):300-9.
63. Bryk AH, Wiśniewski JR. Quantitative Analysis of Human Red Blood Cell Proteome. *Journal of Proteome Research*. 2017;16(8):2752-61.
64. Greinacher A, Wesche J, Hammer E, et al. Characterization of the human neutrophil alloantigen-3a. *Nature Medicine*. 2010;16(1):45-8.
65. Nakamura T, Fujiwara R, Ishiguro N, et al. Involvement of choline transporter-like proteins, CTL1 and CTL2, in glucocorticoid-induced acceleration of phosphatidylcholine synthesis via increased choline uptake. *Biol Pharm Bull*. 2010;33(4):691-6.
66. Iwao B, Yara M, Hara N, et al. Functional expression of choline transporter like-protein 1 (CTL1) and CTL2 in human brain microvascular endothelial cells. *Neurochem Int*. 2016;93:40-50.
67. Storch EK, Hillyer CD, Shaz BH. Spotlight on pathogenesis of TRALI: HNA-3a (CTL2) antibodies. *Blood*. 2014;124(12):1868-72.
68. Reil A, Wesche J, Greinacher A, et al. Geno- and phenotyping and immunogenicity of HNA-3. *Transfusion*. 2011;51(1):18-24.
69. Huvard MJ, Schmid P, Stroncek DF, et al. Frequencies of SLC44A2 alleles encoding human neutrophil antigen-3 variants in the African American population. *Transfusion*. 2012;52(5):1106-11.
70. Xia W, Bayat B, Sachs U, et al. The frequencies of human neutrophil alloantigens in the Chinese Han population of Guangzhou. *Transfusion*. 2011;51(6):1271-7.
71. Keller-Stanislawski B, Reil A, Günay S, et al. Frequency and severity of transfusion-related acute lung injury – German haemovigilance data (2006–2007). *Vox Sanguinis*. 2010;98(1):70-7.
72. Thomas GM, Carbo C, Curtis BR, et al. Extracellular DNA traps are associated with the pathogenesis of TRALI in humans and mice. *Blood*. 2012;119(26):6335-43.
73. Sachs UJ, Hattar K, Weissmann N, et al. Antibody-induced neutrophil activation as a trigger for transfusion-related acute lung injury in an ex vivo rat lung model. *Blood*. 2006;107(3):1217-9.
74. Gilliss BM, Looney MR. Experimental models of transfusion-related acute lung injury. *Transfus Med Rev*. 2011;25(1):1-11.
75. Wiersum-Osselton JC, Middelburg RA, Beckers EA, et al. Male-only fresh-frozen plasma for transfusion-related acute lung injury prevention: before-and-after comparative cohort study. *Transfusion*. 2011;51(6):1278-83.
76. Curtis BR, Cox NJ, Sullivan MJ, et al. The neutrophil alloantigen HNA-3a (5b) is located on choline transporter-like protein 2 and appears to be encoded by an R>Q154 amino acid substitution. *Blood*. 2010;115(10):2073-6.
77. Curtis BR, Sullivan MJ, Holyst MT, et al. HNA-3a-specific antibodies recognize choline transporter-like protein-2 peptides containing arginine, but not glutamine at Position 154. *Transfusion*. 2011;51(10):2168-74.
78. Kommareddi PK, Nair TS, Vallurupalli M, et al. Autoantibodies to recombinant human CTL2 in autoimmune hearing loss. *Laryngoscope*. 2009;119(5):924-32.
79. Lim DJ. Functional structure of the organ of Corti: a review. *Hear Res*. 1986;22:117-46.
80. Kommareddi P, Nair T, Kakaraparthi BN, et al. Hair Cell Loss, Spiral Ganglion Degeneration, and Progressive Sensorineural Hearing Loss in Mice with Targeted Deletion of Slc44a2/Ctl2. *J Assoc Res Otolaryngol*. 2015;16(6):695-712.

81. Kommareddi PK, Nair TS, Raphael Y, et al. Cochlin isoforms and their interaction with CTL2 (SLC44A2) in the inner ear. *J Assoc Res Otolaryngol*. 2007;8(4):435-46.
82. Robertson NG, Skvorak AB, Yin Y, et al. Mapping and characterization of a novel cochlear gene in human and in mouse: a positional candidate gene for a deafness disorder, DFNA9. *Genomics*. 1997;46(3):345-54.
83. Bayat B, Tjahjono Y, Berghofer H, et al. Choline Transporter-Like Protein-2: New von Willebrand Factor-Binding Partner Involved in Antibody-Mediated Neutrophil Activation and Transfusion-Related Acute Lung Injury. *Arterioscler Thromb Vasc Biol*. 2015;35(7):1616-22.
84. Hogan KA, Weiler H, Lord ST. Mouse models in coagulation. *Thromb Haemost*. 2002;87(4):563-74.
85. Mouse Genome Sequencing C, Waterston RH, Lindblad-Toh K, et al. Initial sequencing and comparative analysis of the mouse genome. *Nature*. 2002;420(6915):520-62.
86. Young NS. Mouse medicine and human biology. *Semin Hematol*. 2013;50(2):88-91.
87. Diaz JA, Obi AT, Myers DD, Jr., et al. Critical review of mouse models of venous thrombosis. *Arterioscler Thromb Vasc Biol*. 2012;32(3):556-62.
88. Bonnard T, Hagemeyer CE. Ferric Chloride-induced Thrombosis Mouse Model on Carotid Artery and Mesentery Vessel. *J Vis Exp*. 2015(100):e52838.
89. Atkinson BT, Jasuja R, Chen VM, et al. Laser-induced endothelial cell activation supports fibrin formation. *Blood*. 2010;116(22):4675-83.
90. Denis CV, Andre P, Saffaripour S, et al. Defect in regulated secretion of P-selectin affects leukocyte recruitment in von Willebrand factor-deficient mice. *Proc Natl Acad Sci U S A*. 2001;98(7):4072-7.
91. Myers D, Jr., Farris D, Hawley A, et al. Selectins influence thrombosis in a mouse model of experimental deep venous thrombosis. *J Surg Res*. 2002;108(2):212-21.
92. Payne H, Brill A. Stenosis of the Inferior Vena Cava: A Murine Model of Deep Vein Thrombosis. *J Vis Exp*. 2017(130).
93. Cui J, Eitzman DT, Westrick RJ, et al. Spontaneous thrombosis in mice carrying the factor V Leiden mutation. *Blood*. 2000;96(13):4222-6.
94. Westrick RJ, Bodary PF, Xu Z, et al. Deficiency of tissue factor pathway inhibitor promotes atherosclerosis and thrombosis in mice. *Circulation*. 2001;103(25):3044-6.
95. Ishiguro K, Kojima T, Kadomatsu K, et al. Complete antithrombin deficiency in mice results in embryonic lethality. *J Clin Invest*. 2000;106(7):873-8.
96. Jalbert LR, Rosen ED, Moons L, et al. Inactivation of the gene for anticoagulant protein C causes lethal perinatal consumptive coagulopathy in mice. *J Clin Invest*. 1998;102(8):1481-8.
97. Huang ZF, Higuchi D, Lasky N, et al. Tissue factor pathway inhibitor gene disruption produces intrauterine lethality in mice. *Blood*. 1997;90(3):944-51.
98. Safdar H, Cheung KL, Salvatori D, et al. Acute and severe coagulopathy in adult mice following silencing of hepatic antithrombin and protein C production. *Blood*. 2013;121(21):4413-6.
99. Heestermans M, Salloum-Asfar S, Streef T, et al. Mouse venous thrombosis upon silencing of anticoagulants depends on tissue factor and platelets, not FXII or neutrophils. *Blood*. 2019.
100. Mackman N. Mouse models of venous thrombosis are not equal. *Blood*. 2016;127(21):2510-1.
101. Diaz JA, Saha P, Cooley B, et al. Choosing a mouse model of venous thrombosis: a consensus assessment of utility and application. *J Thromb Haemost*. 2019;17(4):699-707.
102. Diaz JA, Saha P, Cooley B, et al. Choosing a Mouse Model of Venous Thrombosis. *Arterioscler Thromb Vasc Biol*. 2019;39(3):311-8.

103. Falati S, Gross P, Merrill-Skoloff G, et al. Real-time in vivo imaging of platelets, tissue factor and fibrin during arterial thrombus formation in the mouse. *Nature Medicine*. 2002;8(10):1175-80.
104. Darbousset R, Thomas GM, Mezouar S, et al. Tissue factor-positive neutrophils bind to injured endothelial wall and initiate thrombus formation. *Blood*. 2012;120(10):2133-43.
105. Dubois C, Panicot-Dubois L, Merrill-Skoloff G, et al. Glycoprotein VI-dependent and -independent pathways of thrombus formation in vivo. *Blood*. 2006;107(10):3902-6.
106. Marx I, Christophe OD, Lenting PJ, et al. Altered thrombus formation in von Willebrand factor-deficient mice expressing von Willebrand factor variants with defective binding to collagen or GPIIbIIIa. *Blood*. 2008;112(3):603-9.
107. Vandendries ER, Hamilton JR, Coughlin SR, et al. Par4 is required for platelet thrombus propagation but not fibrin generation in a mouse model of thrombosis. 2007;104(1):288-92.
108. Sun WY, Abeynaike LD, Escarbe S, et al. Rapid histamine-induced neutrophil recruitment is sphingosine kinase-1 dependent. *Am J Pathol*. 2012;180(4):1740-50.
109. Asako H, Kurose I, Wolf R, et al. Role of H1 receptors and P-selectin in histamine-induced leukocyte rolling and adhesion in postcapillary venules. *J Clin Invest*. 1994;93(4):1508-15.
110. Esposito B, Gambara G, Lewis AM, et al. NAADP links histamine H1 receptors to secretion of von Willebrand factor in human endothelial cells. *Blood*. 2011;117(18):4968-77.
111. Brill A, Fuchs TA, Chauhan AK, et al. von Willebrand factor-mediated platelet adhesion is critical for deep vein thrombosis in mouse models. *Blood*. 2011;117(4):1400-7.
112. Yago T, Liu Z, Ahamed J, et al. Cooperative PSGL-1 and CXCR2 signaling in neutrophils promotes deep vein thrombosis in mice. *Blood*. 2018;132(13):1426-37.
113. Heestermans M, Salloum-Asfar S, Streef T, et al. Mouse venous thrombosis upon silencing of anticoagulants depends on tissue factor and platelets, not FXII or neutrophils. *Blood*. 2019;133(19):2090-9.
114. Fest J, Ruiter R, Ikram MA, et al. Reference values for white blood-cell-based inflammatory markers in the Rotterdam Study: a population-based prospective cohort study. *Sci Rep*. 2018;8(1):10566.
115. Agarwal R, Light RP. Patterns and prognostic value of total and differential leukocyte count in chronic kidney disease. *Clin J Am Soc Nephrol*. 2011;6(6):1393-9.
116. Smock KJ, Perkins SL. Thrombocytopenia: an update. *Int J Lab Hematol*. 2014;36(3):269-78.
117. Farrah T, Deutsch EW, Omenn GS, et al. A high-confidence human plasma proteome reference set with estimated concentrations in PeptideAtlas. *Mol Cell Proteomics*. 2011;10(9):M110 006353.
118. Zhang Q, Menon R, Deutsch EW, et al. A mouse plasma PeptideAtlas as a resource for disease proteomics. 2008;9(6):R93.
119. Geyer PE, Holdt LM, Teupser D, et al. Revisiting biomarker discovery by plasma proteomics. *Molecular Systems Biology*. 2017;13(9):942.
120. Anderson NL. The clinical plasma proteome: a survey of clinical assays for proteins in plasma and serum. *Clin Chem*. 2010;56(2):177-85.
121. Sun BB, Maranville JC, Peters JE, et al. Genomic atlas of the human plasma proteome. *Nature*. 2018;558(7708):73-9.
122. Marx V. Finding the right antibody for the job. *Nat Methods*. 2013;10(8):703-7.
123. Berglund L, Bjorling E, Oksvold P, et al. A genecentric Human Protein Atlas for expression profiles based on antibodies. *Mol Cell Proteomics*. 2008;7(10):2019-27.

124. Pernemalm M, Lehtio J. Mass spectrometry-based plasma proteomics: state of the art and future outlook. *Expert Rev Proteomics*. 2014;11(4):431-48.
125. Ignjatovic V, Geyer PE, Palaniappan KK, et al. Mass Spectrometry-Based Plasma Proteomics: Considerations from Sample Collection to Achieving Translational Data. *J Proteome Res*. 2019;18(12):4085-97.
126. Gillette MA, Carr SA. Quantitative analysis of peptides and proteins in biomedicine by targeted mass spectrometry. *Nat Methods*. 2013;10(1):28-34.
127. Picotti P, Aebersold R. Selected reaction monitoring-based proteomics: workflows, potential, pitfalls and future directions. *Nat Methods*. 2012;9(6):555-66.
128. Brun V, Masselon C, Garin J, et al. Isotope dilution strategies for absolute quantitative proteomics. *J Proteomics*. 2009;72(5):740-9.
129. Marx V. Targeted proteomics. *Nat Methods*. 2013;10(1):19-22.
130. Doerr A. Mass spectrometry-based targeted proteomics. *Nat Methods*. 2013;10(1):23.
131. Keshishian H, Addona T, Burgess M, et al. Quantitative, multiplexed assays for low abundance proteins in plasma by targeted mass spectrometry and stable isotope dilution. *Mol Cell Proteomics*. 2007;6(12):2212-29.
132. Parker CE, Domanski D, Percy AJ, et al. Mass spectrometry in high-throughput clinical biomarker assays: multiple reaction monitoring. *Top Curr Chem*. 2014;336:117-37.
133. Mohammed Y, van Vlijmen BJ, Yang J, et al. Multiplexed targeted proteomic assay to assess coagulation factor concentrations and thrombosis-associated cancer. *Blood Adv*. 2017;1(15):1080-7.
134. Percy AJ, Michaud SA, Jardim A, et al. Multiplexed MRM-based assays for the quantitation of proteins in mouse plasma and heart tissue. *Proteomics*. 2017;17(7).
135. Michaud SA, Sinclair NJ, Petrosova H, et al. Molecular phenotyping of laboratory mouse strains using 500 multiple reaction monitoring mass spectrometry plasma assays. *Commun Biol*. 2018;1:78.



CHARACTERIZATION OF HEMOSTASIS IN MICE LACKING THE NOVEL THROMBOSIS SUSCEPTIBILITY GENE *SLC44A2*

Julia Tilburg*, Raymond Adili*, Thankam S. Nair, Megan E. Hawley, David C. Tuk, Madeline Jackson, Henri M. Spronk, Henri H. Versteeg, Thomas E. Carey, Bart J.M. van Vlijmen, Chrissta X. Maracle**, Michael Holinstat**

* / **: These authors contributed equally

Thromb Res. 2018 Nov;171:155-159.

2

Abstract

Introduction

Recent genome wide association studies (GWAS) identified a novel susceptibility locus for thrombosis, harbouring the *SLC44A2* gene which encodes the Solute Carrier Family 44 Member 2 protein (SLC44A2). Thus far, SLC44A2 has not been studied in the context of thrombosis and may be a unique contributor to thrombotic disease. Here we utilize mice lacking SLC44A2 (*Slc44a2-/-*) to evaluate a possible role of SLC44A2 in hemostasis.

Methods

Slc44a2-/- mice were evaluated in key aspects of normal hemostasis including a challenge of vascular damage by applying laser induced injury to the cremaster muscle arteriole.

Results

Slc44a2-/- mice had comparable levels of thrombin generation and gene expression of coagulation related genes, as compared to littermate wild type controls. Lower levels of circulating plasma von Willebrand factor (VWF) were measured in *Slc44a2-/-* mice, while no difference in VWF multimerization or vascular localization was detected. Upon *in vivo* laser injury of the cremaster arterioles, we detected an impairment of clot formation for *Slc44a2-/-* mice.

Conclusions

Although mice lacking SLC44A2 are normal for several hemostasis parameters, we do observe a reduction of plasma VWF levels and an altered response upon vascular damage, which suggests that SLC44A2 contributes to hemostasis upon injury. These findings are in line with the reported GWAS data and support further research on SLC44A2 in thrombosis.

Introduction

Thrombosis is a major contributor to the global health burden, with genetic predisposition being an important underlying element (1). Recently, a genome wide association study (GWAS) aimed at identifying novel genetic risk factors for venous thromboembolism (VTE, i.e. deep vein thrombosis (DVT) and pulmonary embolism (PE)), identified a susceptibility locus containing *SLC44A2* (2). Interestingly, unlike the loci previously known to associate with VTE (*ABO, F2, F5, F11, FGG, and PROCR*), the *SLC44A2* locus did not associate with hemostasis phenotypes included in the GWAS, such as enhanced thrombin generation, platelet counts and von Willebrand factor (VWF) levels (2). Moreover, a second, independent GWAS detected an association between *SLC44A2* and self-reported blood clotting events (DVT, PE, ischemic stroke), strengthening the implication that *SLC44A2* is linked to thrombosis (3). Therefore, it is plausible that SLC44A2 plays a role in the pathophysiology of thrombosis.

SLC44A2 encodes Solute Carrier Family 44 Member 2 (SLC44A2) (4), a presumed choline transporter based on its homology to other transport proteins (5). Notably, an SLC44A2 polymorphic site forms the human neutrophil antigen 3, an epitope for alloantibodies that mediate transfusion related acute lung injury (TRALI) (6, 7). TRALI, like thrombosis, has a central role in its pathogenesis for endothelial cells and neutrophils, both of which express SLC44A2, in addition to several other tissues (4). Furthermore, a recent TRALI study described SLC44A2 to be a binding partner of VWF, a key molecule in hemostasis (8). Additionally, SLC44A2 has been associated with autoimmune hearing loss, due to its importance in hair cell viability (9).

As the GWAS show an association between SLC44A2 and thrombosis, but not a mechanistic insight, further investigation of SLC44A2 with respect to its role in thrombosis is warranted. Here we utilize mice lacking SLC44A2 (*Slc442-/-*) to gain insight into the role of SLC44A2, if any, in hemostasis as a precursor to further thrombosis studies. To this end we characterized *Slc44a2-/-* mice for several parameters of hemostasis under normal conditions including a challenge of vascular injury.

Material and Methods

Slc44a2-/- mice were previously generated from mice with *Slc44a2* exons 3-10 flanked with LoxP sites (*Slc44a2fl/fl* mice) and deleter EIIa-Cre transgenic mice (9, 10). The resulting *Slc44a2-/-* mice were subsequently backcrossed to FVB/NJ (FVB) (7 generations) to form a FVB line at University of Michigan, USA. FVB*;Slc44a2+/-* mice were used to generate *Slc44a2-/-* mice used for experiments, and *Slc44a2*+/+ littermates were used as controls. At Leiden University Medical Center (LUMC), In the Netherlands, a colony of *Slc44a2-/-* mice on an C57BL/6J (B6) background was established starting from frozen B6;129Sv-*Slc44a2*$^{fl/+F2\text{-}N2}$ embryos obtained from the University of Michigan. After cryorecovery, genotyping (9) and backcross with B6 mice (Charles River, The Netherlands), *Slc44a2*fl/+ mice were again

combined with in house B6;EIIa-Cre transgenic mice ((10), originally obtained from Jackson Laboratories, Bar Harbor, USA). The resulting EIIa-Cre positive *Slc44a2*+/- mice were used to generate the *Slc44a2-/-* and control *Slc44a2*+/+ littermates (backcrossed total 5 generations to B6). Mice of both sexes were used unless indicated otherwise. Apart from previously described age related (>6 months of age) progressive hearing impairment in FVB;*Slc44a2*$^{-/-}$, no other abnormalities in *Slc44a2-/-* mice were reported (9). All experimental procedures were approved by local institutional animal welfare committees.

Sodium-citrated blood was collected directly from inferior caval vein of mice anesthetized by intraperitoneal injection of ketamine/xylazine (100 mg/kg). Plasma thrombin generation assays were performed using 10 or 20µg/mL ellagic acid (Sigma, USA) or 1pM tissue factor (Stago BNL, The Netherlands) (11). Coagulation gene profiling of lung and liver were determined by quantitative polymerase chain reaction (12). Primers are listed in Table S1. Lung and liver fibrin deposition are determined by immunoblotting with 59D8 antibody (13).

Plasma VWF levels were determined by ELISA and multimerization by immunoblot with anti-human VWF (DAKO A082, USA) as described (14), except 10-fold higher plasma concentration was used compared to VWF ELISA using human plasma. 4µM cryosections of hind leg muscle (including femoral vein and artery) and left lung lobule, immunostained for VWF (DAKO A082, USA), were imaged by confocal microscopy (Leica SP8, Germany) at 63x magnification.

Blood cell counts were assessed by Hemavet (Hemavet950FS, USA) or Sysmex (SysmexXT-2000iV, Sysmex Europe GMBH, Germany). For platelet analysis, citrated blood was drawn via orbital sinus puncture of anesthetized mice. Pooled washed platelets were obtained from blood as described before (15). The presence of SLC44A2 protein in platelets was determined by immunoblot with anti-SLC44A2 antibody as previously described (9). Platelet count was adjusted to $2.4x10^8$ platelets/mL and thrombin (0.1, 0.25, 0.5, 1.0 nM) induced platelet aggregation was measured as described before (15).

The *in vivo* response to vascular injury in mice was evaluated using a cremaster muscle arteriole injury model as described (15). Briefly, adult mice were anesthetized by intraperitoneal injection of ketamine/xylazine (100 mg/kg) and the cremaster muscle was prepared. DyLight 488-conjugated anti-GP1bβ antibody and Alexa Fluor 647-conjugated anti-fibrin antibody were administered prior to vascular injury via the jugular vein. Multiple independent injuries were induced in the arterioles of the cremaster muscle in each mouse by a laser ablation system. The dynamic accumulation of platelets and fibrin was monitored in real-time using a fluorescent microscope (Zeiss Axio Examiner Z1 fluorescent microscope with a ×63 objective and a high-speed sCMOS camera) and the data was analysed as previously described (15-18). Injury experiments for both FVB and B6 background mice were performed and analysed by one operator in a blinded fashion at the University of Michigan.

Results and Discussion

Mice deficient for SLC44A2 were originally generated for studies characterizing the role of SLC44A2 in autoimmune hearing loss and required FVB as the strain background (9). Here, we use these FVB;*Slc44a2-/-* mice and their wild type (*Slc44a2*+/+) littermates to further characterize the mice with regards to hemostasis under normal and challenging conditions (Figure 1). Additionally, elements of this characterization were repeated for *Slc44a2-/-* mice and their wild type (*Slc44a2*+/+) littermates present on a B6 background (Figure S1), as this is the preferred background in cardiovascular research.

Thrombin generation, induced both by tissue factor and ellagic acid, was unaltered in *Slc44a2-/-* mice as compared to *Slc44a2*+/+ littermate controls (Figure 1A/S1A). Changes in coagulation were also examined through transcriptional profiling of lung and liver genes (Figure 1B/1SB). As expected, *Slc44a2* was not detectable in *Slc44a2-/-* mice, confirming the genotype. Additionally, we did not observe a compensatory effect within the gene family in either line, as transcript levels of *Slc44a* family members (*Slc44a1, Slc44a3* and *Slc44a4)* remained unchanged (Figure S2), with *Slc44a5* being undetectable. In FVB *Slc44a2-/-* mice, a 12% increase in lung transcript of tissue plasminogen activator (*Plat*) was detected (p=0.018), when compared to *Slc44a2*+/+ littermates, whereas the levels remained comparable between B6 mice. Additionally, in the lung, transcript levels of *F3*, *Vwf*, *F2r*, *F8*, *Thbd*, *Tfpi* and *Serpine1* were not different and no variation in *Fga*, *F2*, *F5*, *F11* or *Proc* expression in the liver was found in either background. Furthermore, there was no detectable fibrin deposition (<2µg/mg tissue) in these tissues (Figure S3) of either background. These findings indicate that *Slc44a2-/-* mice do not display abnormalities in general coagulation, which is in line with the reported GWAS linking *SLC44A2* to VTE, but not to coagulation parameters (2).

As it was previously described that HEK293 cells overexpressing SLC44A2 bind VWF *in vitro,* we sought to determine whether VWF could be altered in *Slc44a2-/-* mice (8). In the FVB line, a non-significant 27% decrease in median plasma levels of VWF was observed in *Slc44a2-/-* mice (p=0.1996) (Figure 1C). In B6 *Slc44a2-/-* mice, median VWF plasma levels were significantly reduced by 20% (p=0.0442) (Figure S1C). SLC44A2 status did not affect VWF multimerization (Figure 1D/S1D). To visualize possible changes in VWF localization, femoral veins and arteries as well as microvessels of the lung, were stained for VWF (Figure 1E/S3/S4/S5). Although intensity of VWF was variable, we did not observe any differences in localization on the luminal side of the endothelial lining of the vessel walls nor in the microvasculature of the lung. Together these data suggest that VWF is lowered in the plasma of *Slc44a2-/-* mice, whereas multimerization and localization is unaltered.

Prior RNA-sequencing data confirmed that SLC44A2 is expressed by human platelets (19), and here we demonstrate that it is also present on murine platelets (Figure 1F). Moreover, loss of SLC44A2 does not impact platelet counts, nor amounts of other blood cells (Figure 1F/Table S2). To determine if SLC44A2 influences platelet function, we measured *ex vivo* platelet

aggregation induced both by thrombin (Figure 1G) and collagen (Figure S6), and although a trend towards accelerated thrombin induced platelet aggregation in *Slc44a2-/-* mice was visible, no significant differences between genotypes were observed.

To determine whether *Slc44a2* status could affect clot formation *in vivo*, platelet and fibrin accumulation was measured upon laser-induced injury of the cremaster arteriole using intravital microscopy (Figure 1H). Compared to control mice, clots grew to similar size in *Slc44a2-/-* mice on FVB background; however, clots in *Slc44a2-/-* mice were visually more unstable. There was no significant difference found in dynamics of platelet accumulation, although fibrin accumulation was significantly impaired in *Slc44a2-/-* mice ($p<0.0001$), which may be responsible for clot instability (Figure 1I). Interestingly, the response following laser injury in *Slc44a2-/-* mice on B6 background was also impaired with platelet accumulation significantly decreased as compared to control mice ($p<0.05$) (Figure S1E). Although the background of the mice was different, the impairment of clot formation seemed consistent across backgrounds.

We conclude that mice deficient for SLC44A2 are normal for the several hemostasis parameters that we evaluated; apart from the elevated lung *Plat* transcripts observed for Slc44a2-/- mice with an FVB background, and the reduced levels of circulating plasma VWF. Of note, a lower amount of plasma VWF was again observed for a third independent group of Slc44a2-/- mice (B6 background, -17% as compared to littermate controls, n=12, $p=0.0211$), highlighting that this observation is reproducible. Since SLC44A2 was reported to interact with VWF *in vitro*, at least in the context of TRALI (7), the observed modest lowering of plasma VWF upon SLC44A2 deficiency warrants further investigation, including VWF dependent models of thrombosis. Of note the cremaster laser injury model clot formation was previously shown to be independent of plasma VWF levels (20). Regardless, this observation, in addition to the recorded impact of SLC44A2 deficiency upon vascular challenge, suggests that SLC44A2 contributes to hemostasis in response to injury, however, whether this effect is direct or indirect remains to be determined. Nonetheless, these findings are in line with the reported GWAS (2, 3) and encourage further investigation of the role of SLC44A2 under pathological conditions i.e. thrombosis and, if any, the underlying mechanism.

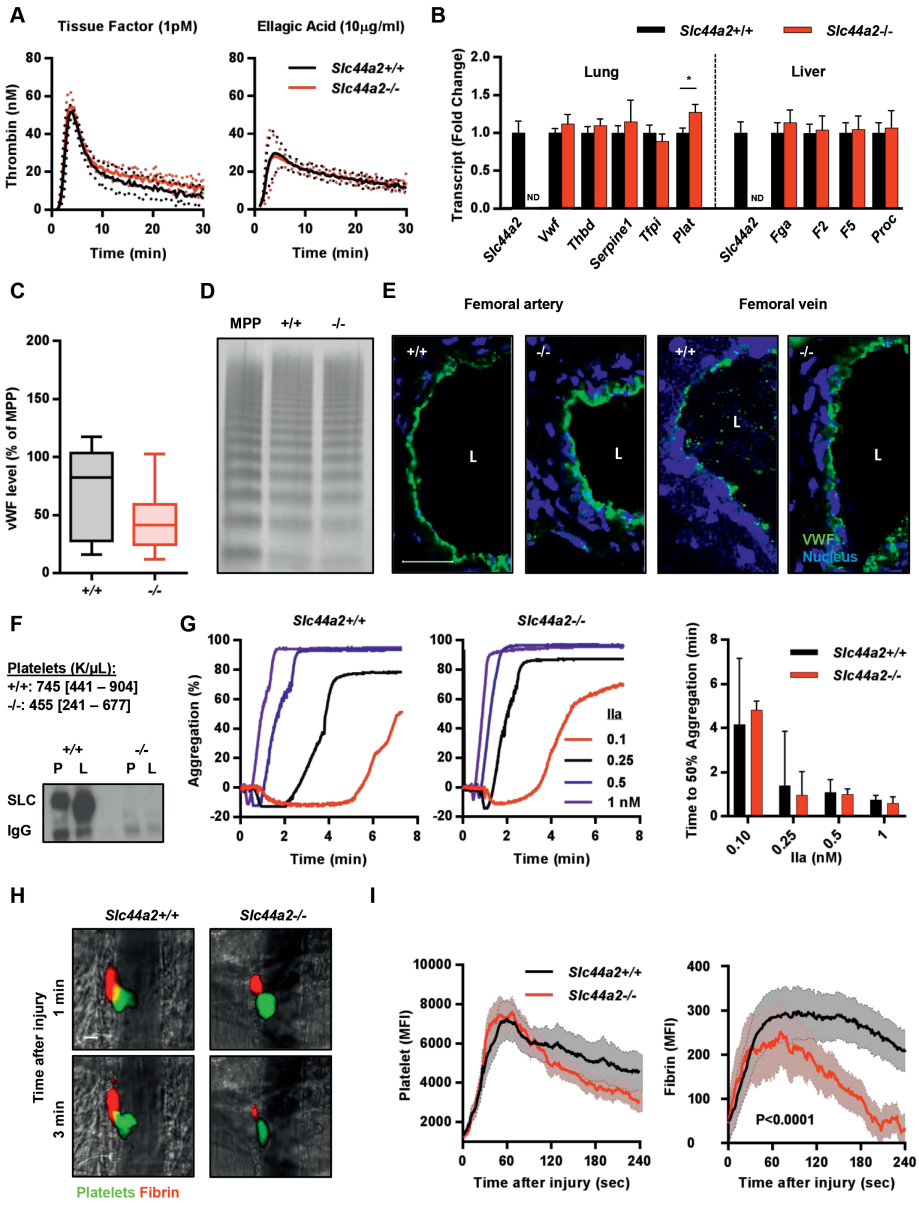


Figure 1. Characterization of hemostasis in *Slc44a2* deficient mice on an FVB background: (A) Thrombin generation in plasma from mice induced either by 1pM Tissue Factor (n=7 both groups) or 10 µg/mL ellagic acid (n=4 *Slc44a2*+/+; n=7 *Slc44a2-/-*). Solid lines represent the mean value and dotted lines the standard deviation (SD). **(B)** Gene transcript levels of *Slc44a2* and coagulation related genes in lung (n=11 *Slc44a2*+/+; n=7 *Slc44a2-/-*) and liver (n=7 both groups). The comparative threshold cycle method with β-actin as internal control was used for quantification and normalization. The mean is represented as fold change compared to *Slc44a2*+/+mice. Error bars represent the difference between

2 POWER of upper range of the mean ΔΔCt. ND; non detectable. **(C)** Level of plasma vWF expressed as a percentage (%) of the wild type controls; represented as Tukey whisker plot. **(D)** Immunoblot of VWF multimerization in plasma of *Slc44a2*+/+and *Slc44a2-/-* mice (n=7). **(E)** Confocal microscopic images of vWF (green) in femoral vein and artery. (Images representative of 5 mice per group; scale bar 30µm). L: Luminal side. **(F)** Top: Total platelet counts of *Slc44a2*+/+and *Slc44a2-/-* mice quantified as the median with range (n=5, female). Bottom: Immunoblot of *SLC44A2* (SLC) protein expression in pooled platelets (P) (n=3) and lung tissues (L) from *Slc44a2*+/+and *Slc44a2-/-* mice compared to control immunoglobulinG (IgG). **(G)** Thrombin (IIa) induced platelet aggregation using pooled platelets from *Slc44a2*+/+(left graph) and *Slc44a2-/-* (middle graph) mice. Concentrations of thrombin indicated in red (0.1nM), black (0.25nM), blue (0.5nM) and purple (1.0nM) (Representative of n=3 platelet pools of 5 mice per pool, female). Quantification (right graph) represented as time to 50% aggregation in minutes (min) as median±range; (n=3 platelet pools of 5 mice per pool, female). **(H)** Representative images of laser-induced injury of the cremaster arterioles with stained platelets (green) and fibrin (red) (n=3 male mice per group, 9-10 injuries per mouse, scale bar 10µm). Images taken one and three minutes after injury. **(I)** Dynamics of platelet accumulation and fibrin formation in clots in the cremaster arterioles in *Slc44a2*+/+and *Slc44a2-/-* mice. The kinetic curves represent the mean fluorescence intensity (after subtracting the background) and the shaded regions are representative of the standard error (SEM). Platelets accumulation into the clot (left) and fibrin contents within clot (right) (8-10 independent injury per mouse, 3 mice in each group). Data represents mean±SEM; statistical analysis using 2-way ANOVA. This figure represents data from mice on a FVB background. Figure S1 provides data from mice with a C57BL/6J background corresponding to Figure 1A, B, C, D and I. Data were analyzed with the Instat software (GraphPad, San Diego, USA). Statistical differences between *Slc44a2*+/+and *Slc44a2-/-* were evaluated using a Mann-Whitney Rank sum test unless indicated otherwise. p-values<0.05 were regarded as statistically significant. Abbreviations: Vwf; von Willebrand Factor, Thbd; thrombomodulin, Tfpi; tissue factor pathway inhibitor, Serpine1; serine protease inhibitor E 1, Plat; tissue-type plasminogen activator; Fga; Fibrinogen Alpha Chain, F2; Thrombin, F5; Coagulation Factor V, Proc; Protein C, *Slc44a2*+/+; *Slc44a2* wild-type mice, *Slc44a2-/-*; *Slc44a2* deficient mice.

Acknowledgments

The authors thank Charles Esmon (University of Oklahoma Health Sciences Center, Oklahoma City, OK) for providing 59D8 antibody and Annika de Jong and Richard Dirven for their expertise concerning VWF. Also, we thank the University of Michigan Transgenic core for shipping the transgenic embryos to Leiden. This work was supported by Trombosestichting Nederland (#2015-4), Landsteiner Foundation for Blood Transfusion Research (#1503), travel grant by Boehringer Ingelheim Fonds, NIDCD R01 DC003686, NIGMS R01 GM105671, NHLBI R01 HL114405.

Authorship Contributions

Experimental design: JT, TEC, BJMvV, CXM, MH. Performed experiments and analyzed data: JT, RA, TSN, MEH, DCT, MJ, HMS, CXM. Wrote the paper: JT, BJMvV, CXM. BJMvV supervised the project. All authors commented on manuscript drafts and approved manuscript.

Disclosure of Conflicts of Interest

The authors declare no competing financial interests.

References

1. Day ISCfWT. Thrombosis: a major contributor to the global disease burden. *J Thromb Haemost*. 2014;12(10):1580-90.
2. Germain M, Chasman DI, de Haan H, et al. Meta-analysis of 65,734 individuals identifies TSPAN15 and SLC44A2 as two susceptibility loci for venous thromboembolism. *Am J Hum Genet*. 2015;96(4):532-42.
3. Hinds DA, Buil A, Ziemek D, et al. Genome-wide association analysis of self-reported events in 6135 individuals and 252 827 controls identifies 8 loci associated with thrombosis. *Hum Mol Genet*. 2016;25(9):1867-74.
4. Nair TS, Kozma KE, Hoefling NL, et al. Identification and characterization of choline transporter-like protein 2, an inner ear glycoprotein of 68 and 72 kDa that is the target of antibody-induced hearing loss. *J Neurosci*. 2004;24(7):1772-9.
5. Iwao B, Yara M, Hara N, et al. Functional expression of choline transporter like-protein 1 (CTL1) and CTL2 in human brain microvascular endothelial cells. *Neurochem Int*. 2016;93:40-50.
6. Greinacher A, Wesche J, Hammer E, et al. Characterization of the human neutrophil alloantigen-3a. *Nat Med*. 2010;16(1):45-8.
7. Curtis BR, Cox NJ, Sullivan MJ, et al. The neutrophil alloantigen HNA-3a (5b) is located on choline transporter-like protein 2 and appears to be encoded by an R>Q154 amino acid substitution. *Blood*. 2010;115(10):2073-6.
8. Bayat B, Tjahjono Y, Berghofer H, et al. Choline Transporter-Like Protein-2: New von Willebrand Factor-Binding Partner Involved in Antibody-Mediated Neutrophil Activation and Transfusion-Related Acute Lung Injury. *Arterioscler Thromb Vasc Biol*. 2015;35(7):1616-22.
9. Kommareddi P, Nair T, Kakaraparthi BN, et al. Hair Cell Loss, Spiral Ganglion Degeneration, and Progressive Sensorineural Hearing Loss in Mice with Targeted Deletion of Slc44a2/Ctl2. *J Assoc Res Otolaryngol*. 2015;16(6):695-712.
10. Lakso M, Pichel JG, Gorman JR, et al. Efficient in vivo manipulation of mouse genomic sequences at the zygote stage. *Proc Natl Acad Sci U S A*. 1996;93(12):5860-5.
11. Hemker HC, Giesen P, AlDieri R, et al. The calibrated automated thrombogram (CAT): a universal routine test for hyper- and hypocoagulability. *Pathophysiol Haemost Thromb*. 2002;32(5-6):249-53.
12. Cleuren AC, Van der Linden IK, De Visser YP, et al. 17alpha-Ethinylestradiol rapidly alters transcript levels of murine coagulation genes via estrogen receptor alpha. *J Thromb Haemost*. 2010;8(8):1838-46.
13. Visser YP, Walther FJ, Laghmani el H, et al. Apelin attenuates hyperoxic lung and heart injury in neonatal rats. *Am J Respir Crit Care Med*. 2010;182(10):1239-50.
14. Tjernberg P, Vos HL, Castaman G, et al. Dimerization and multimerization defects of von Willebrand factor due to mutated cysteine residues. *J Thromb Haemost*. 2004;2(2):257-65.
15. Yeung J, Tourdot BE, Adili R, et al. 12(S)-HETrE, a 12-Lipoxygenase Oxylipin of Dihomo-gamma-Linolenic Acid, Inhibits Thrombosis via Galphas Signaling in Platelets. *Arterioscler Thromb Vasc Biol*. 2016;36(10):2068-77.

16. Adili R, Tourdot BE, Mast K, et al. First Selective 12-LOX Inhibitor, ML355, Impairs Thrombus Formation and Vessel Occlusion In Vivo With Minimal Effects on Hemostasis. *Arterioscler Thromb Vasc Biol*. 2017;37(10):1828-39.
17. Adili R, Voigt EM, Bormann JL, et al. In vivo modeling of docosahexaenoic acid and eicosapentaenoic acid-mediated inhibition of both platelet function and accumulation in arterial thrombi. *Platelets*. 2017:1-9.
18. Tourdot BE, Adili R, Isingizwe ZR, et al. 12-HETrE inhibits platelet reactivity and thrombosis in part through the prostacyclin receptor. *Blood Adv*. 2017;1(15):1124-31.
19. Simon LM, Edelstein LC, Nagalla S, et al. Human platelet microRNA-mRNA networks associated with age and gender revealed by integrated plateletomics. *Blood*. 2014;123(16):e37-45.
20. Marx I, Christophe OD, Lenting PJ, et al. Altered thrombus formation in von Willebrand factor-deficient mice expressing von Willebrand factor variants with defective binding to collagen or GPIIbIIIa. *Blood*. 2008;112(3):603-9.

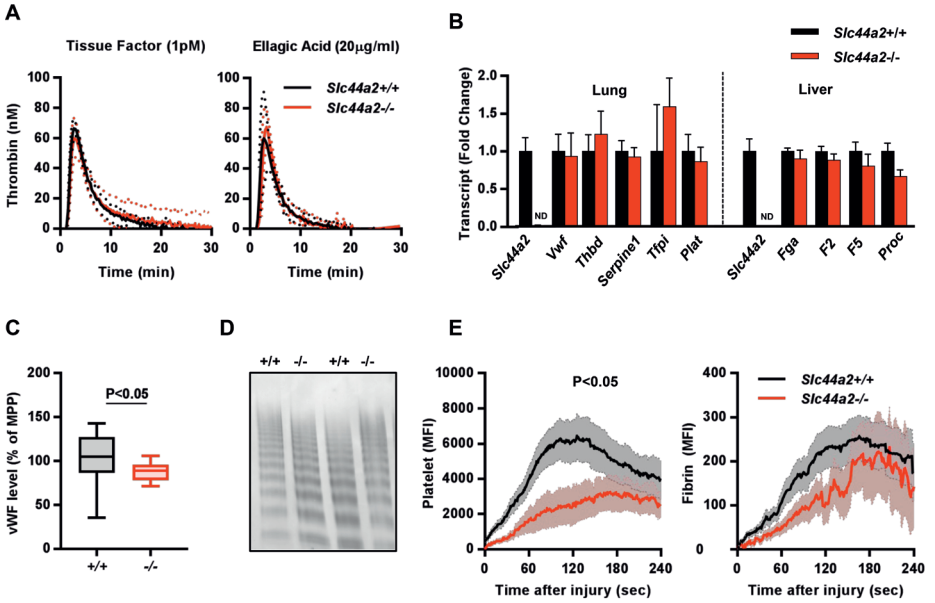


Figure S1. Characterization of hemostasis in Slc44a2 deficient mice on a C57BL/6J (B6) background (A) Thrombin generation in plasma from mice induced either by 1pM Tissue Factor (n=10 for Slc44a2+/+; n=9 for Slc44a2-/-) or 20 µg/mL ellagic acid (n=11 for Slc44a2+/+; n=9 for Slc44a2-/-). Solid lines represent the mean value and dotted lines the standard deviation (SD). (B) Gene transcript levels of Slc44a2 and coagulation related genes in lung and liver (n=15 for Slc44a2+/+; n=11 for Slc44a2-/-). The comparative threshold cycle method with β-actin as internal control was used for quantification and normalization. The mean is represented as fold change compared to Slc44a2+/+ mice. Error bars represent the difference between 2 POWER of upper range of the mean ΔΔCt. ND; non detectable. (C) Levels of plasma vWF expressed as a percentage (%) of (normal) mouse pool plasma (n=14 Slc44a2+/+; n=11 Slc44a2-/-); represented as whisker plot with Tukey. (D) Immunoblot of vWF multimerization in plasma of Slc44a2+/+ and Slc44a2-/- mice (representative of Slc44a2+/+ (n=15) and Slc44a2-/- mice (n=11)). (E) Dynamics of platelet accumulation and fibrin formation in clots in the cremaster arterioles in Slc44a2+/+ and Slc44a2-/- mice. The kinetic curves represent the mean fluorescence intensity (after subtracting the background) and the shaded regions are representative of the standard error (SEM). Platelets accumulation into the clot (left) and fibrin contents within clot (right) (8-10 independent injuries per mouse, 3 mice in each group). Data represents mean±SEM; statistical analysis using 2-way ANOVA. Abbreviations: Vwf; Von Willebrand Factor, Thbd; thrombomodulin, Tfpi; tissue factor pathway inhibitor, Serpine1; serine protease inhibitor E 1, Plat; tissue-type plasminogen activator; Fga; Fibrinogen Alpha, F2; Prothrombin, F5; Coagulation Factor V, Proc; Protein C. *p<0.05.

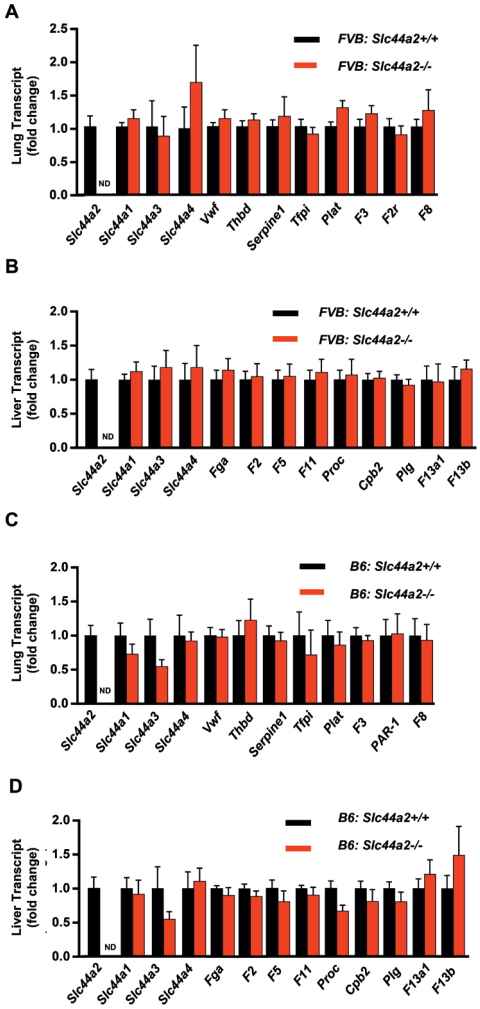


Figure S2. Gene transcript level of *Slc44a* gene family members and coagulation-related genes in liver and lung (A) Lung gene transcript levels in FVB mice (n=11 *Slc44a2*$^{+/+}$; n=7 *Slc44a2*$^{-/-}$). **(B)** Liver gene transcript levels in FVB mice (n=11 *Slc44a2*$^{+/+}$; n=7 *Slc44a2*$^{-/-}$). **(C)** Lung gene transcript levels in B6 mice (n=15 *Slc44a2*$^{+/+}$; n=11 *Slc44a2*$^{-/-}$). **(D)** Liver gene transcript levels in B6 mice (n=15 *Slc44a2*$^{+/+}$; n=11 *Slc44a2*$^{-/-}$). The comparative threshold cycle method with β-actin as internal control was used for quantification and normalization. The mean is represented as fold change compared to *Slc44a2*$^{+/+}$ mice. Error bars represent the difference between 2 POWER of upper range of the mean ΔΔCt. ND; not detectable. Abbreviations: *F3*; tissue factor, *Vwf*; Von Willebrand Factor, *F2r*; coagulation factor II (thrombin) receptor, *F8*; coagulation factor VIII, *Thbd*; thrombomodulin, *Tfpi*; tissue factor pathway inhibitor, *Serpine1*; serine protease inhibitor E 1, *Plat*; tissue-type plasminogen activator, *Fga*; Fibrinogen Alpha , *F2*; Prothrombin, *F5*; Coagulation Factor V, *F11*; Coagulation Factor XI, *Proc*; Protein C, *Cpb2*; thrombin-activatable fibrinolysis inhibitor, *Plg*; Plasminogen, *F13a1*: coagulation factor XIIIa, *F13b*: coagulation factor FXIIIb.

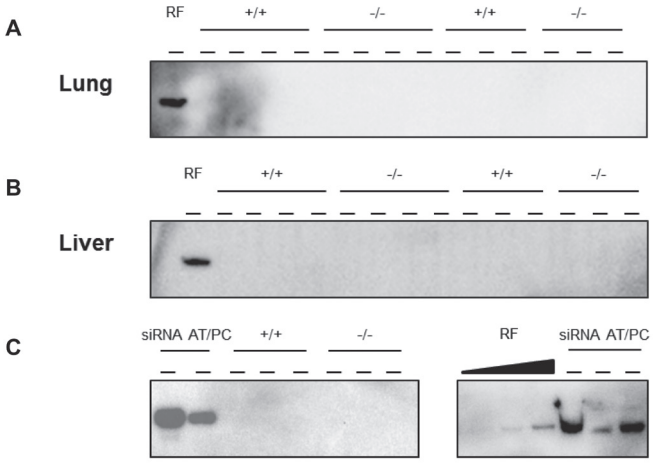


Figure S3. Fibrin deposition in lung and liver. Immunoblot for fibrin in FVB;*Slc44a2*$^{+/+}$ (+/+) and FVB;*Slc44a2*$^{-/-}$ (-/-) mouse lung (A) and liver (B). Each lane represents tissue from 1 mouse per genotype (n=7). RF: positive control; purified rat fibrinogen converted fibrin and processed for immunoblot identical to mouse tissue samples. (C) Immunoblot with additional fibrin positive liver control samples from C57BL/6J mice injected with siRNA targeting *Serpinc1* and *Proc* (siRNA AT/PC) (N=2). These mice were previously established to exhibit fibrin deposition (Safdar et al. Blood 2013) (left panel). Immunoblot with the two positive controls: fibrin converted from rat fibrinogen, that is used throughout the procedure for calibration, and material from mice treated with siRNA AT/PC (right panel). Results for liver and lung of B6;*Slc44a2*$^{+/+}$ and B6;*Slc44a2*$^{-/-}$ animals are comparable (no fibrin detectable, not shown).

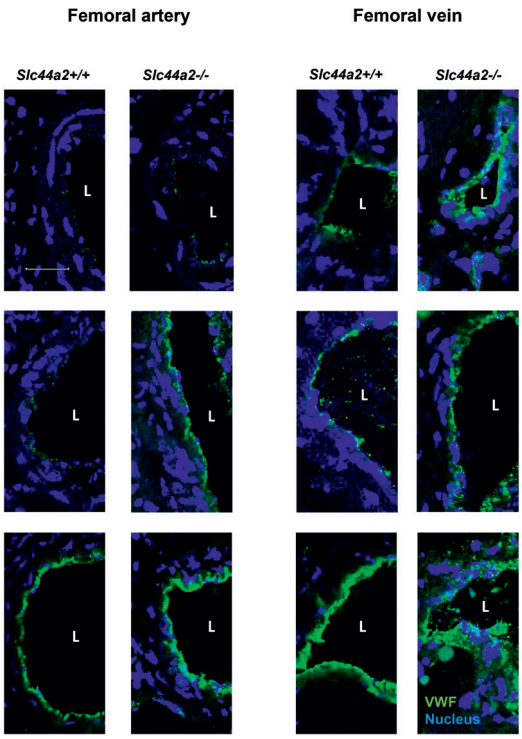


Figure S4. Confocal microscopic images of VWF in the femoral vein and artery. Von Willebrand Factor (green) staining of the femoral artery (left panels) and vein (right panels) from FVB,*Slc44a2*$^{+/+}$ and FVB,*Slc44a2*$^{-/-}$ mice. L; Lumen. (Representative images for 5 mice per genotype that have low, moderate or abundant signal for VWF immunostain. Note: Images shown for each mouse represent one out of the 8 to 9 stacks available per imaged section; Scale bar 30μM). VWF; Von Willebrand Factor.

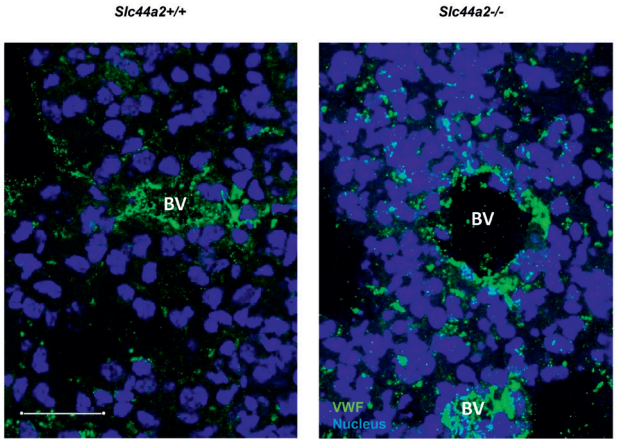


Figure S5. Confocal microscopy images of VWF in microvasculature of the lung. Von Willebrand Factor (green) staining of lung tissue from FVB,*Slc44a2*$^{+/+}$ and FVB,*Slc44a2*$^{-/-}$ mice. Lungs were snap frozen in liquid nitrogen making the architecture of the lung alveolar no longer clearly visible, BV; blood vessel. (Representative images for 5 mice per genotype. Note, Images shown for each mouse represents one out of the 8 to 9 stacks available per imaged section; Scale bar 30µM). VWF; Von Willebrand Factor.

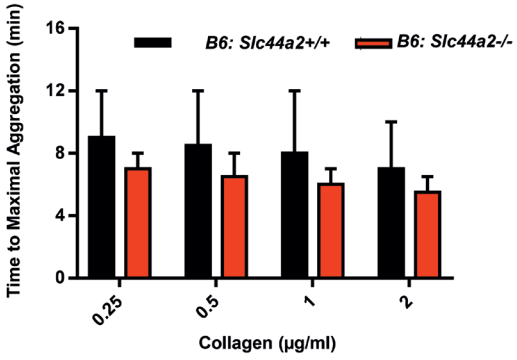


Figure S6. Ex-vivo platelet aggregation Collagen induced platelet aggregation using pooled platelets from *Slc44a2*$^{+/+}$ and *Slc44a2*$^{-/-}$ mice with different concentrations of collagen, represented as time in minutes (min) to maximal aggregation as median±range; (n=2 platelet pools of 5 mice per pool, female).

Table S1 qPCR primer sequences used for (coagulation) gene profiling of lung and liver

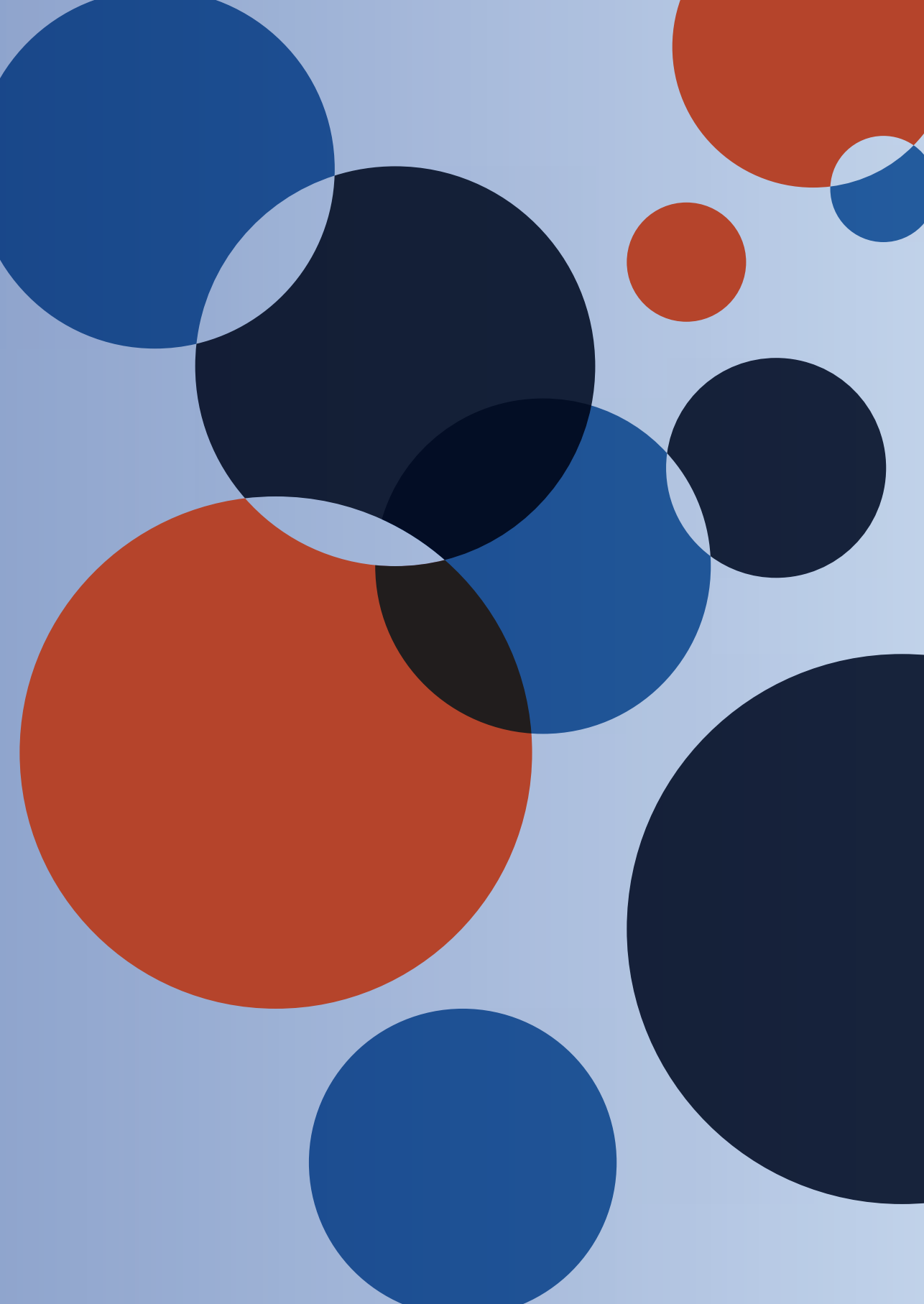
Gene	Forward primer	Reverse primer
Actb Reference	AGGTCATCACTATTGGCAACGA	CCAAGAAGGAAGGCTGGAAAA
Slc44a1	ACCCACCGGAAGTATGTGTTC	GCTGCTACGCACAGTGCTA
Slc44a2	CGGAAGGACGCAGTCTATGG	AGGAAGAGCAACACACAGCA
Slc44a3	ATGAATGCCTGCAATCTTGAAGT	GACCTCTTCCAGAGTGTCCAG
Slc44a4	AGAATGAGAACGAGGCTCACG	CCCCACTATGATGTAACCCAAAA
Slc44a5	ATGATGCTCCGGCTACAGTG	TCCAAGTAGGTGAGGAATCTCTC
F3	ACCAAAATAGCCCAGGAAGC	CCAGGAAACTCTTCCATTGC
Vwf	AGCTGTCAGCCAGGTTTTTCTT	GCAGAGGGCAGGCACCTT
F2r	TGCTGGGAGGTATCACCCTTC	GCTGGGTTTCTAATCTGCCAAT
F8	CTTCACCTCCAGGGAAGGACTA	TCCACTTGCAACCATTGTTTTG
Thbd	CACAGGCAGTCAATGCGTG	GAGCGCACTGTCATCAAATGT
Tfpi	GGCTTCGCCTTTCAGAGTG	GAGAACGACCTCATACGTTGTAG
Serpine1	CCCTGGCCGACTTCACAA	TTTTGCAGTGCCTGTGCTACA
Plat	AGATGAGCCAACGCAGACAA	AACTTCGGACAGGCACTGAG
Fga	TGCTGCCTGCTTTTACTGTTCTC	TCTAGGATGCAACAGTTATCTCTGGTA
F2	GGACGCTGAGAAGGGTATCG	CCCCACACAGCAGCTCTTG
F5	CATGGAAACCTTACCGACAGAAA	CATGTGCCCCTTGGTATTGC
F11	GAAGGATACGTGCAAGGGAGATT	CAAGTGCCAGACCCCATTGT
Proc	GCGTGGAGGGCACCAA	CCCTGCGTCGCAGATCAT
Cpb2	GGCTTCGCCTTTCAGAGTG	GAGAACGACCTCATACGTTGTAG
Plg	GGAGGTGTCTCGGACTGTTTG	GATGCCGGTCTTACATTCTGAC

Table S2 Blood cell counts and *Slc44a2* status

FVB*	*Slc44a2*+/+ Median [range]	*Slc44a2*-/- Median [range]
Platelets (K/μL)	745 [441-904]	455 [241-677]
Erythrocytes (K/μL)	8.62 [7.62-10.49]	8.53 [7.08-10.74]
White Blood Cells (K/μL)	8.92 [6.26-14.04]	10.99 [6.26-12.4]
B6[#]	*Slc44a2*+/+ Median [range]	*Slc44a2*-/- Median [range]
Platelets (K/μL)	601 [466-856]	626 [328-972]
Erythrocytes (K/μL)	8.00 [6.94-8.70]	7.96 [3.48-8.58]
White Blood Cells (K/μL)	5.2 [3.4-11.0]	4.6 [2.4-6.8]

*Analyzed using Hemavet950FS (N=5), analysis only performed for mice used in platelet aggregation experiments (Figure 1G).

[#]Analyzed using SysmexXT-2000iV (N=12).



SLC44A2 DEFICIENT MICE HAVE A REDUCED RESPONSE IN STENOSIS BUT NOT IN HYPERCOAGULABILITY DRIVEN VENOUS THROMBOSIS

Julia Tilburg, Daniëlle M. Coenen, Gaia Zirka, Sophie Dólleman, Annemarie M. van Oeveren-Rietdijk, Mieke F.A. Karel, Hetty C. de Boer, Judith M.E.M. Cosemans, Henri H. Versteeg, Pierre E. Morange, Bart J.M. van Vlijmen, Chrissta X. Maracle*, Grace M. Thomas*
*: These authors contributed equally

J Thromb Haemost. 2020;July;18:1714–1727

3

Abstract

Background

Genome wide association studies (GWAS) identified *SLC44A2* as a novel susceptibility gene for venous thrombosis (VT) and previous work established that SLC44A2 contributed to clot formation upon vascular injury.

Objective

To further investigate the role of SLC44A2 in VT by utilizing SLC44A2 deficient mice (*Slc44a2-/-*) in two representative disease models.

Methods

Mice were included in a hypercoagulability model driven by siRNA-mediated hepatic gene silencing of anticoagulants *Serpinc1* (Antithrombin) and *Proc* (Protein C) and a flow restriction (stenosis) model induced by partial ligation of the inferior vena cava.

Results

In the hypercoagulability model, no effect in onset was observed in *Slc44a2-/-* animals, however a drop in plasma fibrinogen and VWF coinciding with an increase in blood neutrophils was recorded. In the neutrophil dependent stenosis model after 48 hours, *Slc44a2-/-* mice had significantly smaller thrombi both in length and weight with less platelet accumulation as a percentage of the total thrombus area. During the initiation of thrombosis at 6 hours post-stenosis, *Slc44a2-/-* mice also had smaller thrombi both in length and weight, with circulating platelets remaining elevated in *Slc44a2-/-* animals. Platelet activation and aggregation under both static- and venous and arterial shear conditions were normal for blood from *Slc44a2-/-* mice.

Conclusions

These studies corroborate the original GWAS findings and establish a contributing role for SLC44A2 during the initiation of VT, with indications that this may be related to platelet-neutrophil interaction. The precise mechanism however remains elusive and warrants further investigation.

Introduction

Venous thrombosis (VT) is a major contributor to the global health burden with a number of well-characterized genetic determinants identified, that are all linked to coagulation pathways (1). A recent meta-analysis of 12 genome wide association studies (GWAS) identified a novel susceptibility locus for VT within the *SLC44A2* gene which had never been linked to coagulation and/or hemostasis before (2). The association between *SLC44A2* and thrombotic events has been next reported in a second GWAS study, confirming *SLC44A2* as being a unique contributor to thrombotic disease (3).

The solute carrier family 44 member 2 protein (SLC44A2) (4) is a presumed choline transporter based on its sequence; however, functional evidence remains limited (5). We previously characterized SLC44A2 deficient mice (*Slc44a2-/-*) by evaluating several parameters of hemostasis including thrombin generation, transcriptional profiling of coagulation related genes, plasma levels of coagulation factors, von Willebrand factor (VWF) antigen plasma levels, multimerization, and localization within vessels, in addition to recording responses to vascular injury (6, 7). We established that *Slc44a2-/-* have relatively normal hemostasis with the exception of a reduced level of circulating plasma VWF (~20%). These mice have also an impaired response to laser injury of the cremaster arterioles, with significantly less platelet accumulation measured at the site of injury in the C57BL/6J background.

In the present study we delineate the importance of SLC44A2 in VT by utilizing *Slc44a2-/-* mice in two different VT models; the hypercoagulability small interfering ribonucleic acid (siRNA)-induced model and the flow restriction (stenosis) model. In the first model, mice are injected with siRNA targeting hepatic expression of the anticoagulants *Proc* (Protein C) and *Serpinc1* (Antithrombin), thereby creating a state of hypercoagulability and resulting in the formation of pronounced blood clots within the large veins in and around the mandibular area of the head (8). In the second model thrombus formation is induced by reduction in blood flow of the inferior vena cava (IVC) by approximately 90%, thereby activating the local endothelium and the recruitment of immune cells (9).

Material and methods

Mice

Mice deficient for SLC44A2 (*Slc44a2-/-*) were previously generated (10) and introduced on a C57BL/6J background (6, 10). *Slc44a2-/-* and littermate controls (*Slc44a2*$^{+/+}$) were genotyped using ear biopsy DNA as described [10]. Experimental animal procedures were approved by local animal welfare committees at the Leiden University Medical Center and Aix-Marseille University. All experiments were performed blinded for genotype.

Spontaneous thrombosis following silencing of antithrombin and protein C

Female *Slc44a2-/-* and *Slc44a2*$^{+/+}$ mice 6 weeks of age were intravenously injected with siRNAs targeting antithrombin (si*Serpinc1*: #S62673; Ambion, Carlsbad, CA, USA) and protein C (si*Proc*: #S72192) complexed with invivofectamine 3.0 (Invitrogen, Carlsbad, CA, USA) as previously described (8). A dose of 80 nmol of si*Serpinc1* and si*Proc* per kg of body weight in study one and 60 nmol in study two was used. The endpoint was reached once 50% of all mice displayed previously described typical clinical features (8). Blood was collected 24 hours pre-injection via tail cut using dipotassium ethylenediaminetetraacetic acid (K_2EDTA) coated vials (Sarstedt, The Netherlands). Blood was also collected from the IVC with 11 µmol/L sodium citrate upon sacrifice and under anesthesia induced by subcutaneous injection of ketamine (100 mg/kg), xylazine (12.5 mg/kg) and atropine (125 µg/kg). Cell counts were assessed by SysmexXT-2000iV (Sysmex Europe GMBH, Germany).

Thrombosis following stenosis of the IVC

Male *Slc44a2-/-* and *Slc44a2*$^{+/+}$ mice 11 to 12 weeks of age underwent partial ligation of the IVC as previously described (9, 11), with all side branches below the renal veins completely ligated. A 50 µl blood sample was collected from the periorbital eye plexus directly before the collection surgery and stabilized with 0.5 mol/L K_2EDTA. Cell counts were assessed by Sysmex XN 3000 instrument.

Plasma analysis

VWF antigen levels were determined by enzyme-linked immunosorbent assay (ELISA) with anti-human VWF (DAKO A082, Santa Clara, CA, USA) as described (12). Fibrinogen levels were measured by ELISA according to the manufacturer's protocol, with the exception of using 1mol/L H_2SO_4 and half the reaction volume (MGF-EIA, Stago, The Netherlands). Extracellular DNA was quantified using the Quant-iT PicoGreen DNA Assay Kit (ThermoFisher Scientific, Waltham, MA, USA).

Liver analysis

RNA was isolated from liver using RNA-Bee (Tel-Test, Inc, Friendswood, TX, USA) and subsequently cDNA was synthesized according to manufacturer's protocol (SuperScript II Reverse Transcriptase, Thermofischer, USA). Liver transcript levels of *Slc44a2, Serpinc1* and *Proc* were determined by quantitative polymerase chain reaction (qPCR) (13). IVC RNA was isolated using the RNeasy microkit (Qiagen 74034, Hilden, Germany). cDNA was synthesized and transcript levels of *Slc44a2, Ccl2*, *Cxcl1*, *Cxcl5*, *Il6*, *Selplg* and *Vcam1* were quantified by qPCR. ß-actin (*Actb)* was used as reference gene (primers TableS1). Fibrin in liver (and also lungs) was determined by immunoblotting using the mouse monoclonal 59D8 anti-fibrin antibody as previously described (14).

Histology

Following removal, thrombi were measured, weighed and frozen in optimum cutting temperature (OCT; Tissue Tek, Alphen a/d Rijn, The Netherlands). Serial cryo sections from

the medial region of the thrombi were made at 10µm. Immunohistochemical staining was performed as described (11) using anti-Ly6G (Biolegend #127602, San Diego, CA, USA; 1:1000 dilution), anti--citrullinated histone H3 (CitH3; Abcam #ab5103, Cambridge, UK; 1:300 dilution), anti-VWF (DAKO #A0082, Santa Clara, CA, USA; 1:4000 dilution; Abcam #ab11713, Cambridge, UK; 1:50 dilution), anti- glycoprotein Ib (GPIb; Emfret #R300, Eibelstadt, Germany; 1:2000 dilution) and anti-tissue factor (TF; in-house resource, 1:2000 dilution) antibodies. The corresponding secondaries were anti-Rat IgG horseradish peroxidase (HRP) conjugated (Abcam #ab205720; 125 µg/mL) or anti-Rabbit IgG HRP conjugated (DAKO #P039901-2, Santa Clara, CA, USA; 125µg/mL) and signal was visualized using Vector NovaRED (Vector Laboratories #SK4800, Burlingame, CA, USA). Immunofluorescence staining was performed as before (11) using the fluorophore-conjugated secondaries anti-rabbit 488 (#A-11008), anti-rat 568 (#A-11077) anti-sheep 647 (#A-21448) (Invitrogen, Waltham, MA, USA, all at 1:750 dilution). Microscopic images were taken using the Panoramic MIDI Slide Scanner and Caseviewer software (3Dhistech, Budapest, Hungary). Quantifications were calculated using the Fiji ImageJ program (15). Per mouse, when a thrombus was available, one stained section from the medial region was used for comparison.

Reactive oxygen species production

Citrated blood was collected via tail cut and leukocyte activation was measured *ex vivo* in 25µl blood incubated with anti-CD11b (BD Pharmingen; clone M1/70), anti-B220 (eBioscience; clone RA3-6B2, San Diego, CA, USA), and anti-Ly6G (eBioscience, clone 1A8) for 30 minutes on ice. Erythrocytes were then lysed using 0.155 mol/L NH_4Cl, 0.01 mol/L $KHCO_3$, 0.1 mmol/L ethylenediaminetetraacetic acid (EDTA) for 10 minutes 20°C and remaining cells were incubated with DHR-123 (ThermoFischer, #D23086, Waltham, MA, USA, 1:1000, 10 minutes, 37°C) and stimulated or not with phorbol myristate acetate (PMA) (2 µg/mL, Sigma P8139, 10 minutes, 37°C). Fluorescence was measured on an LSR II flow cytometer (BD Bioscience, San Francisco, CA, USA).

Platelet aggregation

Citrated-blood was collected via IVC and centrifuged at 313 g for 3 minutes at room temperature using a soft break. Platelet rich plasma layer (PRP) and one third of erythrocytes layer was collected and separately centrifuged at 704 g for 15 seconds using soft break. Platelet counts were determined by Sysmex and adjusted with platelet poor plasma (PPP). PRP was further diluted into HEPES:Tyrode pH 7.3 and rested for 30 minutes before measurements. PRP was then incubated with 1.2mmol/L thrombin receptor activating peptide 4 (TRAP4; Bachem, #4035529-005, Bubendorf, Switzerland) or 24 µM adenosine diphosphate (ADP; HART biological, Hartlepool, UK). Aggregation was measured for 15 minutes on a Thrombo-Aggregometer (SD Medical, #TA-8V, Frouard, France) against PPP.

Platelet perfusion

Platelet adhesion and activation following perfusion over coverslip coated with VWF-binding peptide (50 µg/mL, Dept. of Biochemistry, Cambridge University, UK) or collagen type I (50

µg/ml, HORM collagen, Takeda, Tokyo, Japan) was assessed as described before (16). Citrated whole blood was re-calcified with 7.5 mmol/L $CaCl_2$ and 3.75 mmol/L $MgCl_2$ in the presence of D-phenylalanyl-prolyl-arginyl chloromethyl ketone (PPACK) (53µmol/L, Calbiochem, Darmstadt, Germany) and heparin (5 U/mL), labelled with 0.5 µg/mL $DiOC_6$ (AnaSpec, Fremont, CA, USA). Analysis of fluorescence images was performed with pre-defined scripts in Fiji software (15, 17).

Platelet activation by flow cytometry

Citrated tail blood was diluted 25 times in Tyrode HEPES pH 7.45 (5 mmol/L HEPES, 136 mmol/L NaCl, 2.7 mmol/L KCl, 0.42 mmol/L NaH_2PO_4, 2 mmol/L $MgCl_2$, 0.1% glucose and 0.1% bovine serum albumin) in the presence of PPACK (20 µmol/L) and fragmin (20 U/mL, Pfizer, New York, NY, USA). The blood was activated for 10 minutes with various concentrations of cross-linked collagen-related peptide (CRP-XL, from Cambridge University), 2-methylthio-adenosine-5′-diphosphate (2-MeSADP, BioConnect, Toronto, Canada), or the protease activated receptor 4 (PAR4) agonist AYPGKF (Bachem Bioscience, Bubendorf, Switserland). Platelets were labelled with anti-GPIIbIIIa (JON/A) (Emfret, PE, 1:10 dilution) and anti-P-selectin (CD62P; Emfret, Eibelstadt, Germany, FITC, 1:10 dilution), and activation measured with an Accuri C6 flow cytometer (Becton Dickinson, San Francisco, CA, USA).

Statistics

For phenotype free survival, differences were calculated using the Mantel-Cox log rank test method. Spearman's correlation was used to compute r and determine correlation between immunohistochemical stains. Reactive oxygen species (ROS) production and platelet aggregation were evaluated by t-test. Changes in platelet binding under perfusion and platelet activation with flow cytometry were determined by two-way analysis of variance. Statistical testing for the remaining readouts were calculated using the Mann-Whitney rank-sum test. All calculations were performed using the Prism statistical program, version 8 (GraphPad, San Diego, CA, USA).

Results

SLC44A2 does not alter onset in a model of hypercoagulability driven VT

In order to determine whether SLC44A2 had an effect on thrombus formation driven by hypercoagulability, we induced a hypercoagulable state in SLC44A2 deficient mice (*Slc44a2-/-*) and wild type control (*Slc44a2*$^{+/+}$) through siRNA-mediated knockdown of hepatic expression of the anticoagulants Antithrombin (*Serpinc1*) and Protein C (*Proc*). Venous thrombosis and related features in this model are same for male and female mice, but well-characterized particularly for female mice (8, 18). We thus used female mice here. After 24 hours, mice from both groups began to present typical features coinciding with thrombotic coagulopathy i.e. oedema of mandibular area and bleeding around the eye. At the time of sacrifice, 32 hours post-siRNA treatment, 50% of *Slc44a2*$^{+/+}$ (6/12) and 92% of *Slc44a2-/-* mice (11/12) had developed the observable phenotype (Figure 1A), but this difference in onset was not

significant. Both groups lost approximately 8% of their original body weight (Figure S1). To validate the incidence over a more protracted timeline, we repeated the study using a lower dose of siRNA. Again no significant difference could be observed with 43% of *Slc44a2*$^{+/+}$ (3/7) and 29% of *Slc44a2-/-* mice (2/7) developing the phenotype 32 hours post injection (Figure 1B). All mice were affected at the collection point of 46 hours. Upon sacrifice, knockdown of hepatic *Serpinc1* and *Proc* was confirmed and was 70% and 98% lower, respectively, as compared to untreated control mice. This was comparable between genotypes (Figure S2), although *Proc* levels were lower (p=0.0024) in *Slc44a2-/-*, measured at 1% of control versus 3.6% in *Slc44a2*$^{+/+}$.

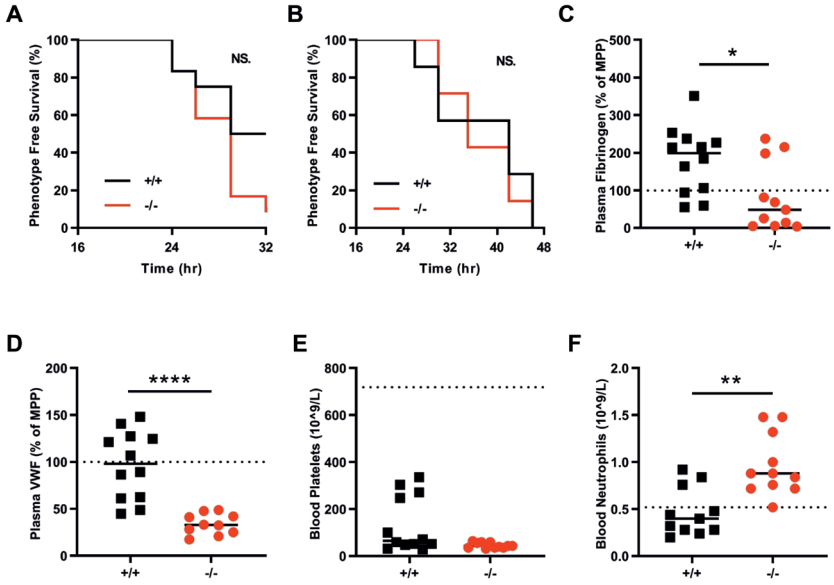


Figure 1. Hypercoagulability mediated venous thrombosis through siRNAs targeting *Serpinc1* and *Proc* in SLC44A2 deficient mice. (A) Phenotype free survival in SLC44A2 deficient mice (*Slc44a2-/-*, -/-) and littermate wild type controls (*Slc44a2*$^{+/+}$, +/+) shown as percentage following injection with 80nmol/kg siRNA. (n=12 per group) **(B)** Phenotype free survival following injection with 60nmol/kg siRNA. (n=6 per group). The following blood parameters were measured after treatment with 80nmol/kg siRNA: **(C)** plasma fibrinogen levels 32 hours post-treatment expressed as a percentage of MPP (mouse pool plasma) **(D)** plasma VWF (von Willebrand factor) levels 32 hours post-treatment expressed as a percentage of MPP (mouse pool plasma) **(E)** blood platelet counts at time of sacrifice. For reference platelet levels of *Slc44a2*$^{+/+}$ before siRNA treatment are represented by the dotted line (mean cell counts). **(F)** Circulating neutrophil levels at time of sacrifice. For reference platelet levels of *Slc44a2*$^{+/+}$ mice before siRNA treatment are represented by the dotted line (mean cell counts). Statistical analysis for phenotype free survival determined using Mantel-Cox test. Solid line represents median value. Statistical differences were evaluated using Mann-Whitney rank-sum test (NS=non-significant; * signifies p<0.05; ** signifies p<0.01; **** signifies p<0.0001).

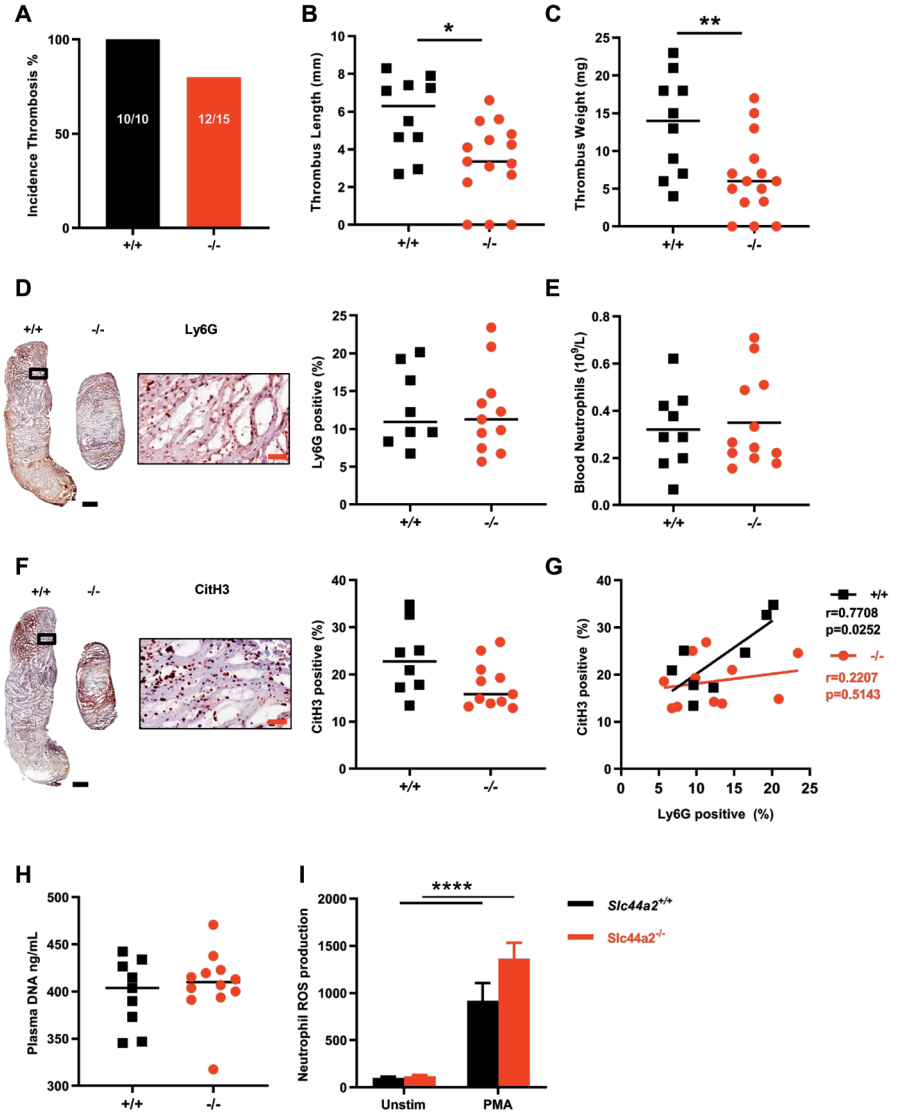


Figure 2. Venous thrombosis in SLC44A2 deficient mice following 48 hour stenosis of the inferior vena cava (IVC). (A) Incidence of thrombosis after 48 hours in wild type (*Slc44a2*$^{+/+}$, +/+) (n=10) or SLC44A2 deficient mice (*Slc44a2-/-*, -/-) (n=15), shown as percentage (%). **(B)** Length and **(C)** weight of thrombi formed at 48 hours. **(D)** Immunohistochemical (IHC) staining of neutrophil marker Ly6G in a representative thrombus from a *Slc44a2*$^{+/+}$ and *Slc44a2-/-*, with high magnification from *Slc44a2*$^{+/+}$ (location is indicated by the black box) (left) and quantification of positive area as a percentage of total thrombus area (right, +/+ n=8, -/- n=11) **(E)** Blood neutrophil counts at time of sacrifice (48 hours). (+/+ n=9, -/- n=12) **(F)** IHC staining of the NETosis marker citrullinated histone H3 (CitH3) in a representative thrombus of a *Slc44a2*$^{+/+}$ and *Slc44a2-/-*, with high magnification from *Slc44a2*$^{+/+}$ (location is indicated

by the black box) (left) and quantification of positive area as a percentage of total thrombus area (right, +/+ n=8, -/- n=11). **(G)** Correlation plot between LY6G and CitH3 staining (+/+, n=8; -/-, n=11) **(H)** Plasma DNA level at time of sacrifice (48 hours; ng/mL) (+/+, n=9; -/-, n=11). **(I)** Reactive oxygen species (ROS) produced by *Slc44a2*$^{+/+}$ or *Slc44a2-/-* neutrophils *ex vivo* following activation of whole blood with 2µg/mL phorbol 12-myristate 13-acetate (PMA), quantified by FACS analysis, expressed in Median Fluorescence Intensity (MFI). (n=5). (Note on numbers: blood samples that became coagulated or thrombi that were damaged during sectioning were not included for subsequent analysis.) Black bars equal 500 µm. Red bars equal 50 µm. Solid line represents median value. Statistical differences for ROS production were evaluated by t-test and for remaining biological readouts, the Mann-Whitney rank-sum test (* signifies p<0.05; ** signifies p<0.01; **** signifies p<0.0001).

In additional to macrovascular thrombosis in the head the deposition of fibrin in the lungs and liver typically occurs in this model (8, 18). Accordingly, fibrin was detected in both the lungs and liver of the *Slc44a2*$^{+/+}$ mice and was comparable to *Slc44a2-/-* mice (Figure S3). Fibrinogen levels in the plasma were lowered in the *Slc44a2-/-* mice as compared to *Slc44a2*$^{+/+}$ (p=0.0129, Figure 1C). We confirmed the previously described reduction in circulating VWF of ~20% in *Slc44a2-/-* mice before siRNA treatment (p=0.0211, Figure S4) (6). Remarkably, upon sacrifice following thrombosis, this difference in VWF was even more pronounced as measured antigen levels were 66% lower in *Slc44a2-/-* mice as compared to *Slc44a2*$^{+/+}$ (p<0.0001, Figure 1D). No differences in blood cell counts prior to injection and following siRNA treatment were observed. Platelet consumption is associated with thrombosis in this model and even though four *Slc44a2*$^{+/+}$ mice did not develop an observable thrombus, corresponding with higher amounts of blood platelets, there was no significant difference in platelet levels following treatment between genotypes (Figure 1E). Interestingly, a significant increase in blood neutrophils (p=0.0017, Figure 1F) was recorded in the *Slc44a2-/-* mice upon sacrifice. However the formation of thrombi in this model was previously demonstrated to occur independently of VWF or neutrophils (18). Thus, even with such changes, SLC44A2 does not affect thrombosis incidence in this model.

Slc44a2-/- mice have reduced thrombosis following 48 hours of stenosis

We continued by using a model demonstrated to be dependent on neutrophils and VWF: the flow restriction (stenosis) model of deep vein thrombosis (DVT) (11, 19, 20). Male mice, littermates of the female mice used in the previous model were used in respect of the "3R's" rule for more ethical use of animals and to maintain the same environmental exposure and breeding sources for mice included in the different VT models (21). In this model the blood flow was reduced by approximately 90%, with blood stasis activating the local endothelium and driving inflammation-mediated thrombosis (9). Following 48 hours, 100% of the *Slc44a2*$^{+/+}$ mice (10/10) and 80% of the *Slc44a2-/-* mice (12/15) developed a thrombus (Figure 2A). The thrombi formed in *Slc44a2-/-* mice were significantly smaller both in length (-43%, p=0.0120) and weight (-52%, p=0.0099) (Figure 2B-C). Mice heterozygous for SLC44A2 (*Slc44a2*$^{+/-}$) were found to have 100% incidence (7/7) with median thrombus measurements for length and weight falling between those of the *Slc44a2*$^{+/+}$and *Slc44a2-/-* groups (Figure

S5), suggesting a dose-dependent effect of SLC44A2 on VT. No differences in thrombi neutrophil density were visible (Ly6G staining, Figure 2D) and the levels of circulating blood neutrophils at the time of sacrifice were also similar (Figure 2E). To determine whether neutrophil extracellular trap release (NETosis) was affected, we evaluated CitH3 into the obtained thrombi. A trend was observed for lower CitH3 in the *Slc44a2-/-* mice (p=0.0908) (Figure 2F) and the positive correlation found between the neutrophil and CitH3 staining (r=0.7708; p=0.0252) in *Slc44a2*$^{+/+}$ was absent in *Slc44a2-/-* animals (r=0.2207; p=0.5143) (Figure 2G) suggesting reduced NETosis within thrombi in absence of SLC44A2. However no signs of systemic decrease in plasma DNA levels could be found 48 hours after stenosis (Figure 2H). Additionally, *ex vivo* production of ROS by stimulated neutrophils was not different between neutrophils deficient or not for SLC44A2 (Figure 2I). Together these data demonstrate a role for SLC44A2 in stenosis driven thrombosis and suggest a possible effect on NETosis at the site of thrombosis.

Slc44a2-/- mice have less platelet accumulation after 48 hours stenosis

Previously, we determined that *Slc44a2-/-* have a reduced level of circulating plasma VWF antigen when compared to *Slc44a2*$^{+/+}$ (6). To investigate whether the VWF release from the endothelium was reduced in SLC44A2 deficient mice, this discharge was stimulated using intraperitoneal injection of 2 mg/kg lipopolysaccharides (LPS), a dose inducing Weibel-Palade body release. VWF plasma levels were increased following LPS injection, however, in time we observed no differences in VWF levels between *Slc44a2*$^{+/+}$ and *Slc44a2-/-* mice (Figure S6). This suggests that smaller thrombi in *Slc44a2-/-* mice are not likely due to reduced levels of available VWF following stenosis. We also found that VWF distribution within thrombi was comparable between the two genotypes by constituting approximately 30% of the thrombus area (Figure 3A) and that plasma VWF at 48 hours post-stenosis was not significantly different between groups (P=0.2030) (Figure 3B). When we focused on platelets, platelet counts could be correlated to thrombus size both in *Slc44a2*$^{+/+}$ and *Slc44a2-/-* mice as platelet accumulation is a major determinant of thrombus size at 48 hour-stenosis (Figure 3D). Remarkably though, the proportion of platelet marker GPIb-positive area was significantly reduced (p=0.0259) in thrombi from *Slc44a2-/-* mice (Figure 3C). As VWF and GPIb are established binding partners (22), we evaluated the relationship of the two proteins on serial sections. VWF was strongly associated with GPIb in *Slc44a2*$^{+/+}$ mice (r=0.9004; p=0.0023), however this association was absent in *Slc44a2-/-* (r=-0.3471; p=0.2956) (Figure S7). We then verified these relationships on the same thrombus section by confocal microscopy. We measured a clear association between VWF and GPIb in the *Slc44a2*$^{+/+}$ group (r=0.9048; p=0.0046) and none within the *Slc44a2-/-* (r=0.2818; p=0.4023) (Figure 3E). Moreover, the area of VWF that co-localized with GPIb was reduced in the *Slc44a2-/-* animals (-36%, p=0.0506) (Figure 3F). As this indicated a possible altered interaction between GPIb and VWF, we evaluated the binding potential of platelets to VWF under venous flow (150s^{-1}) *ex vivo* using slides coated with a murine VWF binding peptide and perfused with whole blood. We observed a comparable increase of platelet binding with a final mean surface area coverage of 15.4% (5.6%-22.2%) by *Slc44a2*$^{+/+}$ platelets and 19.7% (17.2%-25.6%) by *Slc44a2-/-* platelets after 6 minutes (p=0.9122) (Figure

3G). When we further dissect between firmly adherent and translocating platelets we also did not observe differences, indicating that also stable binding of platelets is unaffected by SLC44A2 (Figure 3H). To evaluate whether platelets under arterial flow have altered adherence, whole blood was perfused over collagen at 1000s^{-1}, also here no differences were observed (Figure S8). Based on these findings, platelet accumulation is reduced in thrombi from *Slc44a2-/-* mice at 48 hours and this is not related to VWF availability. Additionally, perfusion studies revealed that platelet-VWF interactions did not seem to be affected in *Slc44a2-/-* mice.

Thrombosis in Slc44a2-/- mice is reduced at 6 hours post-stenosis

To gain further insight into the role of SLC44A2 during the initiation phase of thrombosis, thrombosis was measured 6 hours post IVC ligation. At this timepoint 100% of the *Slc44a2*$^{+/+}$ (6/6) and 62.5% of the *Slc44a2-/-* mice formed a thrombi (5/8) (Figure 4A). The thrombi from the *Slc44a2-/-* mice were again smaller both in length (-83%, p=0.0007) and weight (-99%, p=0.0013) (Figure 4B-C). As before, we observed that *Slc44a2*$^{+/-}$ mice (incidentally included) fell in between with 75% incidence (3/4) and median values of length and weight halfway in between those of the *Slc44a2*$^{+/+}$ and *Slc44a2-/-* (Figure S9). An independent experiment executed by a different operator, in a different facility substantiated these findings, with significant effects of genotype on thrombus weight (p=0.0020) and length (p=0.0010), and again no effect on incidence (Figure S10). Evaluation of the thrombi revealed large variability within each group for GPIb staining with high and low subsets for both *Slc44a2*$^{+/+}$ and *Slc44a2-/-*, leading to no significant differences with regard to platelet density (Figure S11A). Similarly, no differences could be detected with regard to VWF staining (Figure S11B). We found again a correlation between the VWF and GPIb staining in *Slc44a2*$^{+/+}$ mice (r=0.8857; p=0.0333) that persisted this time in *Slc44a2-/-* (r=0.9000; p=0.0833) (Figure 4D). The percentage of VWF that colocalized with GPIb was also comparable between the groups (Figure 4E). These data indicate that the early binding of platelets to VWF is unaltered. Additional quantification determined no differences in thrombus density in neutrophils (Ly6G staining) and NETs (CitH3 staining) (Figure S11C-D). The CitH3 positive area was found to be strongly correlated with GPIb levels in *Slc44a2*$^{+/+}$ mice (r=0.9429; p=0.0167), but not in the *Slc44a2-/-* animals (r=0.5000; p=0.4500) (Figure 4F) which was not observed at the 48 hour-timepoint (Figure S12).

Stenosis is followed by an acute response from the local endothelium marked by upregulation of inflammatory cytokines and adhesion markers (9). Transcript levels of cytokines CCL2, CXCL1, CXCL5 and IL-6 in the IVC 6 hours post-stenosis were increased compared to control untreated IVC ($p<0.05$), which was in line with previous reports (9). However, there were no differences in transcript levels between genotypes (Figure 4G). The same observations were made for the transcripts coding for the adhesion molecules P-selectin and VCAM-1, which are central to immune cell interactions with the endothelium ($p<0.05$) (Figure 4H). These data indicate a normal inflammatory response by the endothelium in *Slc44a2-/-* mice after stenosis.

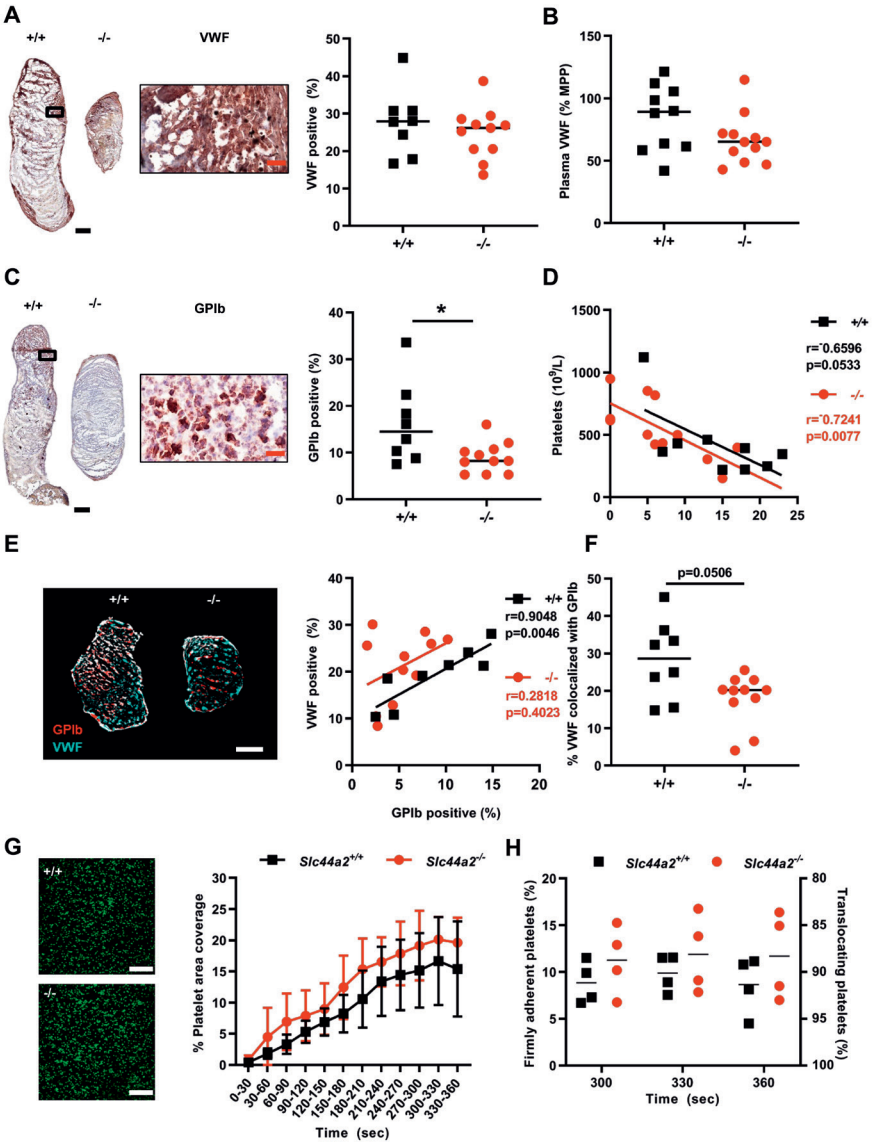


Figure 3. von Willebrand factor and platelet characteristics of SLC44A2 deficient mice following 48 hours stenosis and *ex vivo* under flow conditions. (A) Immunohistochemical (IHC) staining of von Willebrand Factor (VWF) in thrombus of a representative wild type (*Slc44a2*$^{+/+}$, +/+) and SLC44A2 deficient mice (*Slc44a2-/-, -/-),* with high magnification from *Slc44a2*$^{+/+}$ (location is indicated by the black box) (left) and quantification (right) of positive area as a percentage of total thrombus area in *Slc44a2*$^{+/+}$ (n=8) or *Slc44a2-/-* mice (n=11) **(B)** Plasma VWF levels after 48 hours stenosis expressed as a percentage of MMP (mouse pool plasma). (+/+ n=9, -/- n=12) **(C)** IHC staining of glycoprotein Ib (GPIb) in thrombus of a representative *Slc44a2*$^{+/+}$ and *Slc44a2-/-*, with high magnification from *Slc44a2*$^{+/+}$ (location

is indicated by the black box) (left) and quantification (right) of positive area as a percentage of total thrombus area. (+/+ n=8, -/- n=11) **(D)** Correlation plot between thrombus weight and circulating blood platelets. ((+/+ n=9, -/- n=12). **(E)** Immunofluorescent co-stain of GPIb (red) and VWF (cyan) on thrombus sections (left) with correlation plot (right) (n=8 +/+; 11 -/-). **(F)** Percentage of VWF positive area colocalized with GPIb. **(G)** Representative images of $DiOC_6$-labeled platelets of a wild type (*Slc44a2*$^{+/+}$, +/+) control (up) and a SLC44a2 deficient mouse (*Slc44a2-/-*, -/-) (down) on a surface coated with VWF-binding peptide. Scale bar is 20 µm. **(H)** Percentage of stable platelet area coverage over a 30 second time period in field view within heparinized and D-phenylalanyl-prolyl-arginyl chloromethyl ketone (PPACK) treated whole blood flowing over slides coated with a murine VWF binding peptide at venous shear rate ($150s^{-1}$) over time (n=5 per group). (Note on numbers: blood samples that became coagulated or thrombi that were damaged during sectioning were not included for subsequent analysis.) **(I)** Percentage platelets displaying a firm or transient interaction with VWF-binding peptide determined by a method described by Meyer dos Santos et al. Platelets 2010. Black and white bars equal 500 µm. Red bar equals 50 µm. Statistical differences between for platelet perfusion were evaluated by two-way analysis of variance and for remaining biological readouts, the Mann-Whitney rank-sum test. Coefficient r calculated using Spearman's correlation (* signifies $p<0.05$).

In this model endothelial activation is followed by recruitment of immune cells to the site of stenosis. Leukocytes incorporated into the thrombi can be visualized using a nuclear stain becuse platelets and erythrocytes are enucleated cells. Interestingly, when the thrombi were stained with 4',6-diamidino-2-phenylindole (DAPI), the density of DAPI-positive leukocytes was significantly elevated in the *Slc44a2-/-* mice (%, p=0.0303) (Figure 4I). This was not observed at 48 hours post-stenosis (Figure S13). As we established there was no difference in Ly6G positive cell composition (Figure S11C), this observation suggests that the increased leukocytes are likely not neutrophils. Tissue Factor (TF) production by leukocytes is another critical step in this model and we observed a two-fold increase in TF immunostaining density in thrombi from the *Slc44a2-/-* animals (p=0.0043) (Figure 4J). Interestingly, the nucleated cells that co-localized with TF were mainly Ly6G negative (Figure 4J) while all nucleated cells were Ly6C positive (Figure S14) indicating that these are likely monocytes, which was previously reported to be the main source of TF in this model (9). Together these data demonstrate that SLC44A2 is important during the initiation of thrombosis, but not for endothelial activation in this VT model.

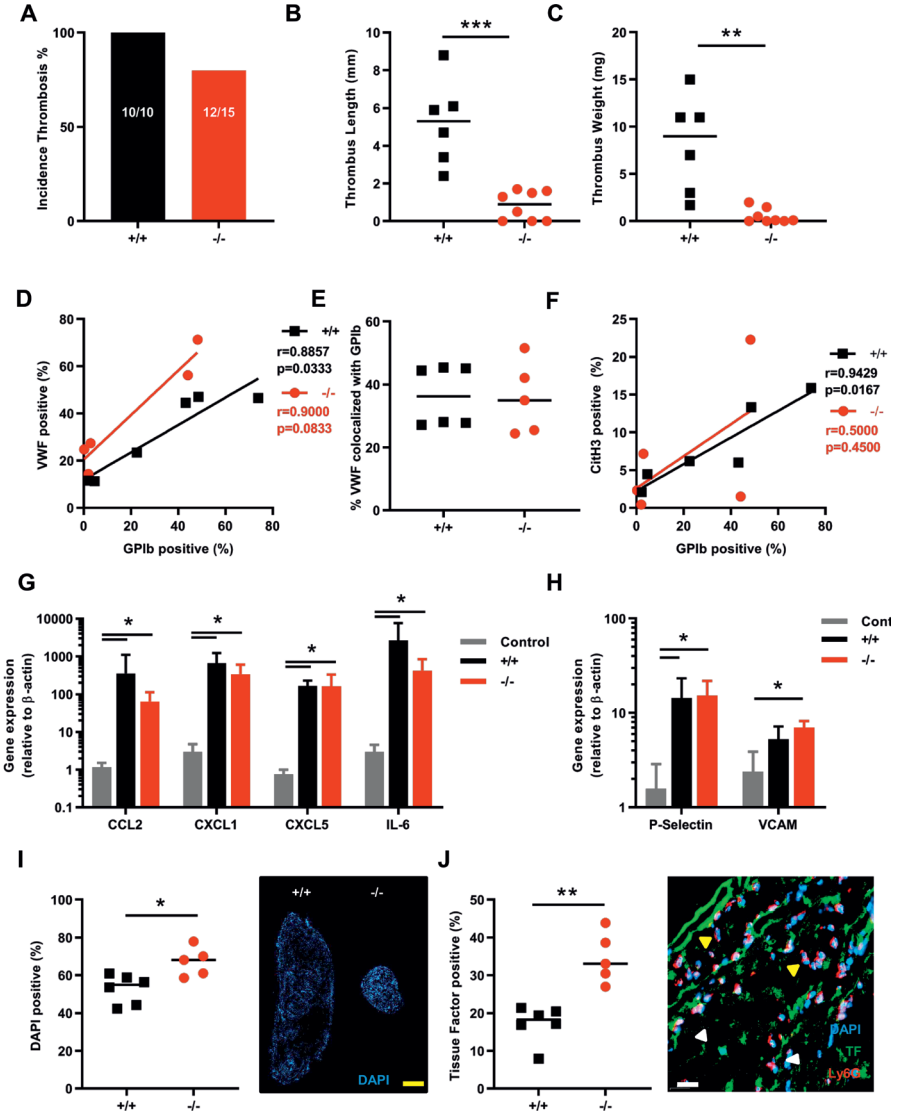


Figure 4. Thrombosis in SLC44A2 deficient mice following 6 hours stenosis of the inferior vena cava (IVC). (A) Incidence of thrombosis after 6 hours in mice wild type (+/+, n=6) or SLC44A2 deficient mice (-/-, n=8), shown as percentage. **(B)** Length and **(C)** weight of thrombi formed at 6 hours. **(D)** Correlation plot of GPIb and VWF immunostaining on thrombus sections (+/+, n=6; -/-, n=5). **(E)** Percentage of VWF positive area colocalized with GPIb. **(F)** Correlation plot of GPIb and citrullinated histone H3 immunostaining on thrombus sections. **(G)** Transcript levels of inflammatory molecules produced by the local IVC in *Slc44a2*$^{+/+}$ (+/+, n=6) or *Slc44a2-/-* (-/-, n=5) for SLC44A2 collected at 6 hours post-stenosis as compared to non-ligated control C57BL/6J mice (n=3); chemokine (C-C motif) ligand 2 (*Ccl2*), chemokine (C-X-C motif) ligand 1 (*Cxcl1*), *Cxcl5*, interleukin-6 (*Il6*). **(H)** IVC expression of mRNA

transcripts encoding adhesion molecules; P-Selectin and vascular cell adhesion molecule 1 (VCAM1) following 6 hours stenosis. Bars represent mean values with standard deviation (error bars). **(I)** Nuclear stain (DAPI) of leukocytes in thrombi from *Slc44a2*$^{+/+}$ and *Slc44a2-/-* mice (top left) with quantification as a percentage of total thrombus area (n=6 +/+; 5 -/-). **(J)** Quantification of immunofluorescent (IF) staining of tissue factor (TF) (left) as a percentage of total thrombus area. Representative image of IF co-stain by confocal microscopy of neutrophil marker Ly6G, TF and nuclear stain (DAPI; right panel). Yellow arrows indicate Ly6G positive cells and white arrows indicate TF positive cells. Yellow bar equals 500 µm and white bar equals 20 µm. Statistical differences were evaluated using Mann-Whitney rank-sum test (* signifies p<0.05; ** signifies p<0.01; *** signifies p<0.001).

Platelet activation, aggregation and neutrophil interactions is unaltered in Slc44a2-/- platelets

We established that SLC44A2 deficiency has a pronounced effect on stenosis-driven thrombosis, coinciding with reduced platelet accumulation after two days without any noticeable effect on platelet/VWF colocalization. We hypothesized that SLC44A2 may be involved after platelet adhesion to the vessel wall in subsequent stages of platelet activation. We observed that the consumption of platelets from circulation had not yet occurred in the *Slc44a2-/-* mice at 6 hours post-stenosis. As a result the levels of circulating platelets differ between *Slc44a2*$^{+/+}$ and *Slc44a2-/-* after stenosis (p=0.0061) (Figure S15). The upregulation of membrane protein P-selectin (CD62P) is a key step during platelet activation (23), whereas a feature of later stages of platelet activation is the binding of platelets to fibrinogen via the αIIbβ3 integrins. When we look at the percentage positive platelets for CD62P exposure as well as αIIbβ3 activation after stimulation with different concentrations of ADP, PAR4 agonist and collagen-related peptide CRP-XL, we observed a significantly lowered exposure in *Slc44a2-/-* platelets under some conditions (Figure S16). When we however analyzed the median fluorescence intensity of both CD62P and αIIbβ3 we did not find an effect of SLC44A2 (Figure 5A-B). To determine if SLC44A2 had an effect on platelet-platelet interactions, we measured platelet aggregation using PRP following activation using TRAP-4 (strong stimulus) and ADP (weak stimulus). We did not detect any significant differences in platelet aggregation in *Slc44a2-/-* (Figure 5C-D). This is in line with our previous observation, using washed platelets, in which platelet aggregation induced by thrombin or collagen was unaffected (6). Together, this is suggestive of a normal response by *Slc44a2-/-* platelets.

In addition to the primary role of platelets in hemostasis, they can also activate neutrophils and stimulate NETosis (24) as neutrophils and NETs can activate and recruit platelets (20, 25, 26). To evaluate whether SLC44A2 influenced murine platelet-neutrophil interactions, we perfused recalcified whole blood at venous shear rates (150s^{-1}) over slides coated with a VWF capturing peptide. Under these conditions, we did not observe neutrophil binding to the platelets that adhered to the slides, however the rapid formation of fibrin and coagulation of the blood also made the analysis challenging. We then used a different approach and analyzed platelet-leukocyte interactions within the thrombi of the mice obtained 6 hours after stenosis.

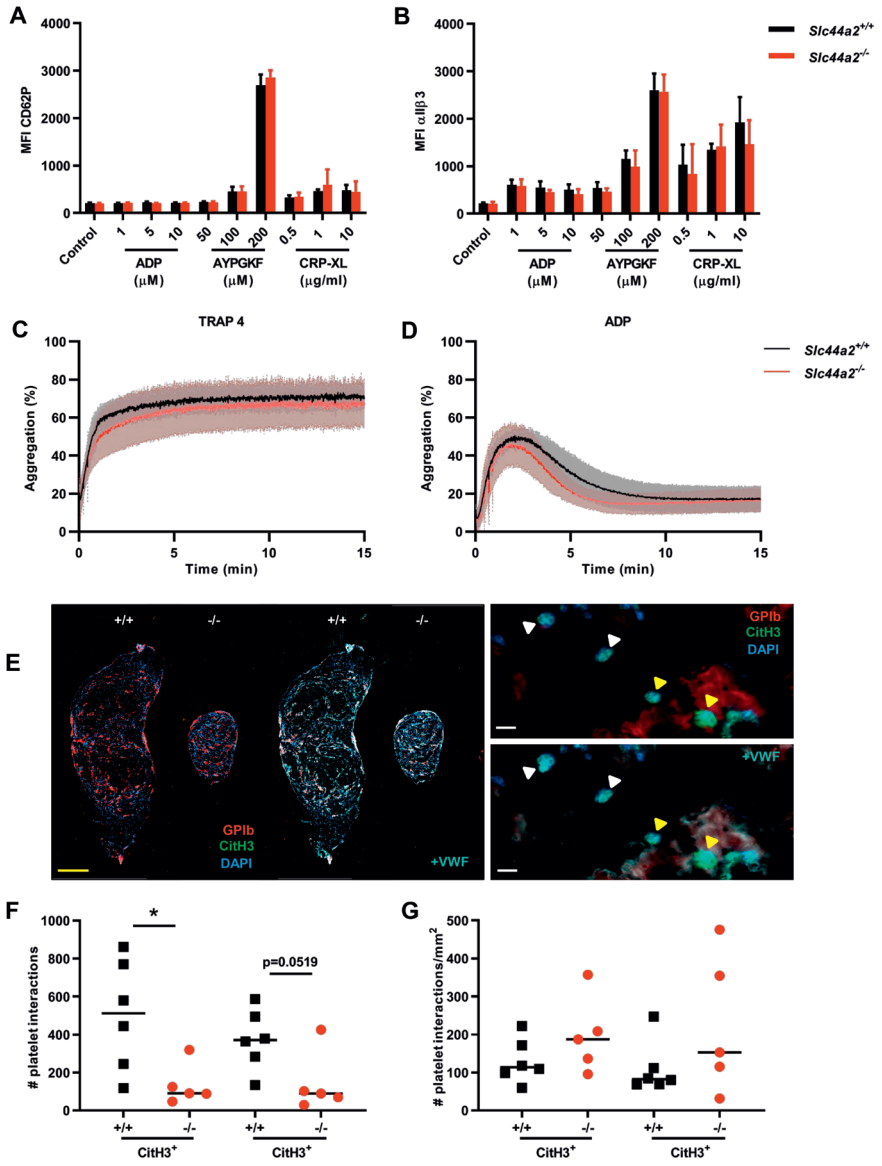


Figure 5. Characterization of platelets in SLC44A2 deficient mice. Percentage of cells positive for **(A)** exposed P-selectin (CD62P) or **(B)** activated integrin αIIbβ3 following activation with adenosine diphosphate (ADP; 1, 5, 10μmol/L), protease-activated receptor 4 (PAR4) agonist AYPGKF (50, 100, 200μmol/L) or collagen related peptide (CRP-XL; 0.5, 1 or 10 μg/mL) as determined by flow cytometry and quantified as the percentage of cells staining positive (%) in wild type (*Slc44a2*$^{+/+}$, N=5) or SLC44A2 deficient mice (*Slc44a2-/-* N=5). Platelet aggregation following stimulation with **(C)** 1.2 mmol/L thrombin receptor activating peptide 4 (TRAP-4) or **(D)** 24 μmol/L ADP in *Slc44a2*$^{+/+}$ and *Slc44a2-/-*

(E) Immunofluorescent co-stain of thrombi from *Slc44a2*$^{+/+}$ and *Slc44a2-/-* of nuclei (DAPI; blue), platelet marker glycoprotein Ib (GPIb; red) and citrullinated histone H3 (CitH3; green) with and without additional visualization of staining with VWF (cyan) (left). Higher magnification indicate leukocyte-platelet interactions (yellow triangles) and leukocytes positive for CitH3 without platelet interactions (white triangles) with (right bottom) and without (right top) additional visualization of VWF. Yellow bar represents 500 µm, white bar represents 10 µm. **(F)** Quantification of nucleated cells in contact with platelets either positive or negative for CitH. **(G)** Number of platelet interactions with leukocytes per mm^2 of thrombus. Statistical differences for flow cytometry were calculated using two-way analysis of variance (shown as mean with standard deviation (SD)) and for aggregometry, t-test (shown with mean and SD). For platelet-leukocyte quantifications, statistical differences were evaluated using Mann-Whitney rank-sum test (* signifies $p<0.05$; ** signifies $p<0.01$).

Here we could clearly distinguish leukocytes adjacent to platelets and record if they were either positive or negative for CitH3 (Figure 5E, left panel). We noticed that areas positive for GPIb strongly overlapped with VWF expression (Figure 5E, right panel) as we saw earlier (Figure 4D). Quantification of the total number of platelet-leukocyte interactions revealed that more platelets were found interacting with CitH3 positive cells in *Slc44a2*$^{+/+}$ mice than in *Slc44a2-/-* mice (Figure 5F), however this difference was not significant when thrombus size was taken into account (Figure 5G).

Discussion

Genomic studies can be a powerful tool for identifying novel factors that contribute to pathophysiology (27, 28). *SLC44A2* is the first gene outside of the coagulation cascade found to be associated with VT risk (2, 3). VT is influenced both by inflammation and coagulation (29). During inflammation, endothelial cells and neutrophils will play a major role in the initiation phase of thrombosis, whereas hypercoagulability will mostly influence the propagation phase (9). Here we used SLC44A2 deficient mice in two independent models of VT. We have substantiated the genomic data from the GWAS and established a functional role for SLC44A2 in stenosis-, but not in hypercoagulability, driven thrombosis. The absence of a role for SLC44A2 in thrombosis driven by hypercoagulability supports the notion that SLC44A2 does not interfere with the coagulation system. This is in agreement with our previous finding that SLC44A2 does not influence mouse hemostasis (including coagulation) under normal conditions (6) and also with the observation that variation in SLC44A2 did not associate with hemostasis phenotypes included in the GWAS (2). For stenosis driven thrombosis we observed that SLC44A2 deficiency affects thrombus size after 6 and 48 hours of blood flow restriction in mice. This is interesting because in contrast to the hypercoagulability model, the stenosis model is inflammation driven, indicating a role for SLC44A2 in inflammation regulated thrombosis. This suggests that neutrophil recruitment and/or activation could be altered in *Slc44a2-/-* mice. Our data do not permit us to conclude on a possible reduction in neutrophil adhesion to the vessel wall in absence of SLC44A2 but they could still suggest a possible reduction in NETosis and platelet accumulation in this model.

Moreover, aggregation and thrombus formation *in vitro/ex vivo* was found to be normal for blood from SLC44A2 deficient mice, which is suggestive of normal hemostatic function of *Slc44a2-/-* platelets. Despite the normal hemostatic function of platelets, altogether, these studies establish a contributing role for SLC44A2 during the initiation of VT.

The function of SLC44A2 is poorly understood, although there is emerging data that describe ways it may be modulating thrombosis. SLC44A2 is suggested to be a binding partner of VWF and this interaction on neutrophils led to agglutination when in the presence of plasma containing anti-SLC44A2 antibodies (HNA3A), thereby inducing transfusion related acute lung injury (TRALI) (30). Additionally, findings presented at the European Congress on Thrombosis and Hemostasis 2018 demonstrated that a specific allelic variant of SLC44A2, also associated with VT, plays a role in neutrophil binding to VWF which leads to NETosis after priming with TNFα (31). Most recently, it was shown that platelets primed by VWF display activated integrin αIIbβ3 (but not CD62P), which can then bind neutrophil SLC44A2 and mediate NETosis under venous flow (32). Based on these findings, the role of SLC44A2 is supposedly limited to neutrophil biology and NET release, however the suggested binding partner differs. One theory suggests a direct interaction with VWF and the other with platelet integrin αIIbβ3 following adherence to VWF. Combining all these findings would implicate SLC44A2 as a binding partner of two elements involved in thrombosis, one being VWF and the other platelet integrin αIIbβ3, with both binding to SLC44A2 on neutrophils.

Neutrophils are known to be a major driver of venous thrombosis in the stenosis model (9). Therefore it is tempting to speculate that SLC44A2 on neutrophils is responsible for the underlying effects of this protein on thrombus formation. In the current study, upon stenosis we observe a trend for less CitH3 within the *Slc44a2-/-* thrombi at 48 hours which is in line with the notion that SLC44A2 deficient neutrophils are less active in the production of NETs. However, we demonstrated that neutrophil activation is still occurring in these mice both *in vivo* and *ex vivo,* as determined by CitH3 staining, plasma DNA levels and ROS production. It is possible that the observed reduced platelet incorporation into *Slc44a2-/-* thrombi at 48 hours is due to slightly less NETosis as this process promotes platelet aggregation through the interaction of NET bound cathepsin G with platelet $P2Y_{12}$ and αIIbβ3 receptors (26, 33).

Alternatively, platelet activation can also drive NET production through the presentation of high mobility group box 1 (HMGB1) (34) or CD62P (35). This would support our observation of increased CitH3 expression with increasing platelet levels in thrombi following 6 hours stenosis in the *Slc44a2*$^{+/+}$ mice. Importantly though, we did observe direct contact of platelets with CitH3 positive leukocytes within the thrombi of both groups at 6 hours, implying that platelets deficient for SLC44A2 can still activate neutrophils, even when they are also lacking SLC44A2. Interestingly, the lost correlation of GPIb and VWF at 48 hours is in line with the previous finding of reduced platelet accumulation following laser injury of the cremaster arterioles (6). This may however still be related to neutrophil activation as it was demonstrated to also contribute to clot formation in this model (36).

To better address the importance of SLC44A2 in platelets versus neutrophils, a more dynamic system would be useful such as intra-vital microscopy combined with live cell imaging of the cell types following stenosis (9). Furthermore, as SLC44A2 is expressed by many cell types central to thrombosis including endothelial cells, leukocytes, platelets and erythrocytes, cell transfer experiments or cell-specific knock-outs may also be necessary when dissecting out the contributions of certain compartments or cell types. In particular neutrophil and platelet specific *Slc44a2* knock-outs would be of interest for future investigations as our data, in addition to the findings from others (30-32), points toward SLC44A2 involvement on these two cell types as being relevant to VT pathophysiology. With the existence of mice carrying a conditional allele for *Slc44a2,* these studies are certainly feasible. We do not find evidence that SLC44A2 is important for endothelial activation following stenosis. Notably, in the present study we used female mice for the hypercoagulability model and male mice for the stenosis model, which was in part because it allowed comparison with previous published studies using these models. Future work using a cell-specific approach may include both sexes, allowing detection of possible sex-specific effects, which was not possible in the present study.

In conclusion, by utilizing a murine representation of DVT, we were able to corroborate the recent genomic studies identifying SLC44A2 as a susceptibility gene for VT and establish that SLC44A2 is key during the initiation of thrombosis with indications that this may be related to platelet-neutrophil interaction, either directly and/or indirectly. The precise mechanism however remains elusive and warrants further investigation.

Acknowledgments

The authors thank Dr Pavan K. Kommareddi, Thankam S. Nair and Dr Thomas E. Carey and (Kresge Hearing Research Institute, Department of Otolaryngology/Head and Neck Surgery, University of Michigan, Ann Arbor, MI, USA) for the floxed *Slc44a2* mouse embryos used to generate the mice on a C57BL/6J background and Dr Charles Esmon (University of Oklahoma Health Sciences Center, Oklahoma City, OK, USA) for providing the 59D8 fibrin antibody. Also, we thank Lieke van den Heijekant for assisting with the hypercoagulability model.

Sources of Funding

This work was supported by Trombosestichting Nederland (#2015-4), the Landsteiner Foundation for Blood Transfusion Research (#1503), the Dutch Heart Foundation (2015T79), the Netherlands Organization for Scientific Research (NWO Vidi 91716421), a European Molecular Biology Organization Short-Term Fellowship (EMBO #7468), a European Society of Cardiology First Contact Initiative grant and by a French ANR grant (ANR-17-CE14-0003-01).

Authorship Contributions

Experimental design: JT, DMC, GZ, SD, HCdB, JMEMC, HHV, PEM, BJMvV, CXM, GMT. Performed experiments and analyzed data: JT, DMC, GZ, SD, MFAK, HCdB, JMEMC, BJMvV, CXM, GMT. Wrote the paper: JT, BJMvV, CXM, GMT. All authors commented on manuscript drafts.

Disclosure of Conflicts of Interest

The authors declare no competing financial interests.

References

1. Raskob GE, Angchaisuksiri P, Blanco AN, et al. Thrombosis: a major contributor to global disease burden. *Arterioscler Thromb Vasc Biol*. 2014;34(11):2363-71.
2. Germain M, Chasman DI, de Haan H, et al. Meta-analysis of 65,734 individuals identifies TSPAN15 and SLC44A2 as two susceptibility loci for venous thromboembolism. *Am J Hum Genet*. 2015;96(4):532-42.
3. Hinds DA, Buil A, Ziemek D, et al. Genome-wide association analysis of self-reported events in 6135 individuals and 252 827 controls identifies 8 loci associated with thrombosis. *Hum Mol Genet*. 2016;25(9):1867-74.
4. Nair TS, Kozma KE, Hoefling NL, et al. Identification and characterization of choline transporter-like protein 2, an inner ear glycoprotein of 68 and 72 kDa that is the target of antibody-induced hearing loss. *J Neurosci*. 2004;24(7):1772-9.
5. Iwao B, Yara M, Hara N, et al. Functional expression of choline transporter like-protein 1 (CTL1) and CTL2 in human brain microvascular endothelial cells. *Neurochem Int*. 2016;93:40-50.
6. Tilburg J, Adili R, Nair TS, et al. Characterization of hemostasis in mice lacking the novel thrombosis susceptibility gene Slc44a2. *Thromb Res*. 2018;171:155-9.
7. Tilburg J, Michaud SA, Maracle CX, et al. Plasma Protein Signatures of a Murine Venous Thrombosis Model and Slc44a2 Knockout Mice Using Quantitative-Targeted Proteomics. *Thromb Haemost*. 2020;120(3):423-36.
8. Safdar H, Cheung KL, Salvatori D, et al. Acute and severe coagulopathy in adult mice following silencing of hepatic antithrombin and protein C production. *Blood*. 2013;121(21):4413-6.
9. von Bruhl ML, Stark K, Steinhart A, et al. Monocytes, neutrophils, and platelets cooperate to initiate and propagate venous thrombosis in mice in vivo. *J Exp Med*. 2012;209(4):819-35.
10. Kommareddi P, Nair T, Kakaraparthi BN, et al. Hair Cell Loss, Spiral Ganglion Degeneration, and Progressive Sensorineural Hearing Loss in Mice with Targeted Deletion of Slc44a2/Ctl2. *J Assoc Res Otolaryngol*. 2015;16(6):695-712.
11. Brill A, Fuchs TA, Savchenko AS, et al. Neutrophil extracellular traps promote deep vein thrombosis in mice. *J Thromb Haemost*. 2012;10(1):136-44.
12. Tjernberg P, Vos HL, Castaman G, et al. Dimerization and multimerization defects of von Willebrand factor due to mutated cysteine residues. *J Thromb Haemost*. 2004;2(2):257-65.
13. Cleuren AC, Van der Linden IK, De Visser YP, et al. 17alpha-Ethinylestradiol rapidly alters transcript levels of murine coagulation genes via estrogen receptor alpha. *J Thromb Haemost*. 2010;8(8):1838-46.
14. Visser YP, Walther FJ, Laghmani el H, et al. Apelin attenuates hyperoxic lung and heart injury in neonatal rats. *Am J Respir Crit Care Med*. 2010;182(10):1239-50.
15. Schindelin J, Arganda-Carreras I, Frise E, et al. Fiji: an open-source platform for biological-image analysis. *Nat Methods*. 2012;9(7):676-82.
16. de Witt SM, Swieringa F, Cavill R, et al. Identification of platelet function defects by multi-parameter assessment of thrombus formation. *Nat Commun*. 2014;5:4257.

17. Meyer dos Santos S, Klinkhardt U, Schneppenheim R, et al. Using ImageJ for the quantitative analysis of flow-based adhesion assays in real-time under physiologic flow conditions. *Platelets*. 2010;21(1):60-6.
18. Heestermans M, Salloum-Asfar S, Streef T, et al. Mouse venous thrombosis upon silencing of anticoagulants depends on tissue factor and platelets, not FXII or neutrophils. *Blood*. 2019.
19. Brill A, Fuchs TA, Chauhan AK, et al. von Willebrand factor-mediated platelet adhesion is critical for deep vein thrombosis in mouse models. *Blood*. 2011;117(4):1400-7.
20. Martinod K, Demers M, Fuchs TA, et al. Neutrophil histone modification by peptidylarginine deiminase 4 is critical for deep vein thrombosis in mice. *Proc Natl Acad Sci U S A*. 2013;110(21):8674-9.
21. Alvarado CM, Diaz JA, Hawley AE, et al. Male mice have increased thrombotic potential: sex differences in a mouse model of venous thrombosis. *Thromb Res*. 2011;127(5):478-86.
22. Bockenstedt P, Greenberg JM, Handin RI. Structural basis of von Willebrand factor binding to platelet glycoprotein Ib and collagen. Effects of disulfide reduction and limited proteolysis of polymeric von Willebrand factor. *J Clin Invest*. 1986;77(3):743-9.
23. Stenberg PE, McEver RP, Shuman MA, et al. A platelet alpha-granule membrane protein (GMP-140) is expressed on the plasma membrane after activation. *J Cell Biol*. 1985;101(3):880-6.
24. Zucoloto AZ, Jenne CN. Platelet-Neutrophil Interplay: Insights Into Neutrophil Extracellular Trap (NET)-Driven Coagulation in Infection. *Front Cardiovasc Med*. 2019;6:85.
25. Darbousset R, Thomas GM, Mezouar S, et al. Tissue factor-positive neutrophils bind to injured endothelial wall and initiate thrombus formation. *Blood*. 2012;120(10):2133-43.
26. Fuchs TA, Brill A, Duerschmied D, et al. Extracellular DNA traps promote thrombosis. *Proc Natl Acad Sci U S A*. 2010;107(36):15880-5.
27. Visscher PM, Wray NR, Zhang Q, et al. 10 Years of GWAS Discovery: Biology, Function, and Translation. *Am J Hum Genet*. 2017;101(1):5-22.
28. Tregouet DA, Morange PE. What is currently known about the genetics of venous thromboembolism at the dawn of next generation sequencing technologies. *Br J Haematol*. 2018;180(3):335-45.
29. Branchford BR, Carpenter SL. The Role of Inflammation in Venous Thromboembolism. *Front Pediatr*. 2018;6:142.
30. Bayat B, Tjahjono Y, Berghofer H, et al. Choline Transporter-Like Protein-2: New von Willebrand Factor-Binding Partner Involved in Antibody-Mediated Neutrophil Activation and Transfusion-Related Acute Lung Injury. *Arterioscler Thromb Vasc Biol*. 2015;35(7):1616-22.
31. Zirka G, Robert P, Legendre P, et al. HNA-3a Expressed by CTL-2 is a Crucial Epitope for Neutrophil Adhesion and Activation on VWF European Congress on Thrombosis and Haemostasis (ECTH); Marseille, France2018.
32. Adela Constantinescu-Bercu LG, Mattia Frontini, Isabelle I. Salles-Crawley, Kevin J Woollard, James T.B. Crawley. Activated αIIbβ3 on platelets mediates flow-dependent NETosis via SLC44A2 *bioRxiv 373670*. 2019.
33. Elaskalani O, Abdol Razak NB, Metharom P. Neutrophil extracellular traps induce aggregation of washed human platelets independently of extracellular DNA and histones. *Cell Commun Signal*. 2018;16(1):24.
34. Maugeri N, Campana L, Gavina M, et al. Activated platelets present high mobility group box 1 to neutrophils, inducing autophagy and promoting the extrusion of neutrophil extracellular traps. *J Thromb Haemost*. 2014;12(12):2074-88.

35. Etulain J, Martinod K, Wong SL, et al. P-selectin promotes neutrophil extracellular trap formation in mice. *Blood*. 2015;126(2):242-6.
36. Wang Y, Gao H, Shi C, et al. Leukocyte integrin Mac-1 regulates thrombosis via interaction with platelet GPIbalpha. *Nat Commun*. 2017;8:15559.

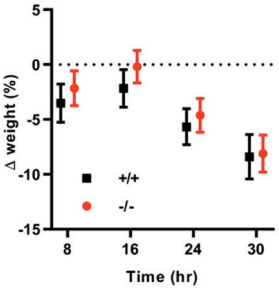


Figure S1. Comparable levels of weight loss in the hypercoagulability model of thrombosis. Weight loss over time following treatment with siRNA targeting the anticoagulants antithrombin and protein C as a percentage of total weight of SLC44A2 deficient (-/-) and wildtype control mice (+/+) represented as mean with SD (n=12 per group).

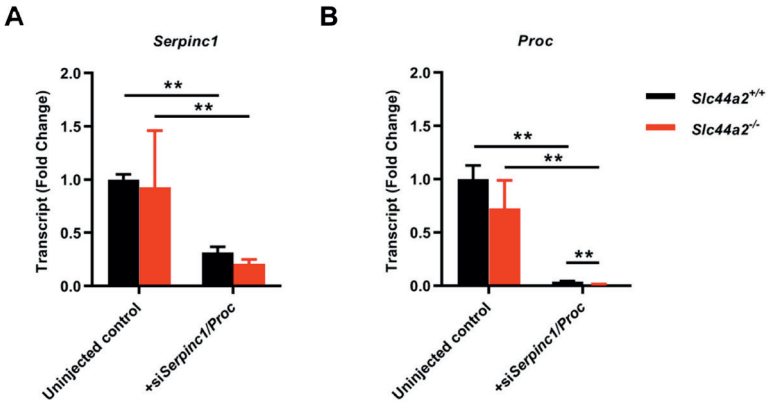


Figure S2. Confirmation of knockdown of *Serpinc1* and *Proc* at the transcriptional level. Liver gene transcript levels of **(A)** *Serpinc1* and **(B)** *Proc* after siRNA-mediated hepatic knockdown of *Serpinc1* and *Proc* (n=12 per group) and uninjected controls (n=4) in SLC44A2 deficient *(Slc44a2-/-)* and wildtype control mice *(Slc44a2$^{+/+}$)*. The comparative threshold cycle method with β-actin as internal control was used for quantification and normalization. The mean is represented as fold change compared to uninjected *Slc44a2-/-* and *Slc44a2$^{+/+}$* mice. Error bars represent the difference between 2^(ΔΔCt). Statistical differences were evaluated using Mann-Whitney rank-sum test (** signifies p<0.01).

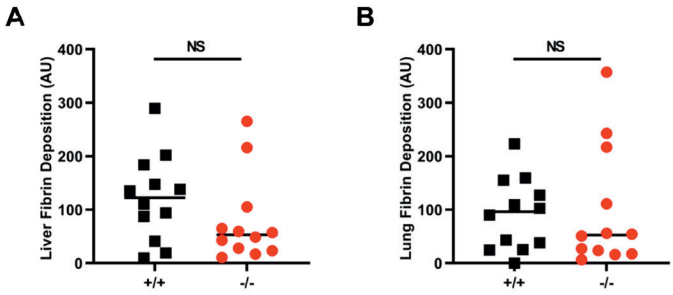


Figure S3. Fibrin deposition in peripheral organs following treatment with siRNA. Deposition of fibrin in arbitrary units (AU) in liver **(A)** and lungs **(B)** of SLC44A2 deficient *(Slc44a2-/-)* and wildtype control mice *(Slc44a2$^{+/+}$)* following treatment with siRNA targeting the anticoagulants antithrombin and protein C (n=12 per group). Black lines represent median value. Statistical differences were evaluated using Mann-Whitney rank-sum test.

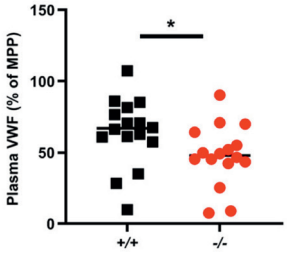


Figure S4. Plasma VWF levels before treatment with siRNA. Plasma VWF (Von Willebrand Factor) levels before siRNA treatment expressed as a percentage of MPP (mouse pool plasma) in SLC44A2 deficient mice (-/-, n=16) and wildtype control mice (+/+, n=16). Statistical differences were evaluated using Mann-Whitney rank-sum test (* signifies $p<0.05$).

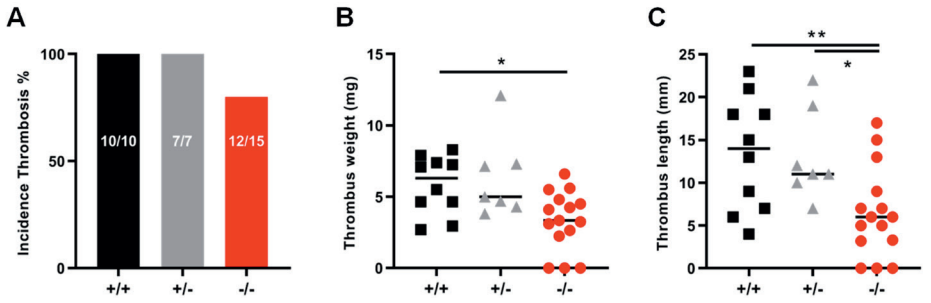


Figure S5. Thrombosis in SLC44A2 deficient mice following 48 hour stenosis of the inferior vena cava. (A) Incidence of thrombosis after 48 hours in-SLC44A2 deficient mice (-/-, n=10), mice heterozygous for SLC44A2 (+/-, n=7) or wildtype control (+/+, n=15) shown as percentage. **(B)** Length and **(C)** weight of thrombi formed after 48 hours. Black lines represent median value. Statistical differences between 3 genotypes were evaluated using ANOVA Kruskal-Wallis test (p=0.0130 for length; p=0.0090 for weight) and Dunn's multiple comparison test. (* signifies p<0.05; ** signifies p<0.01).

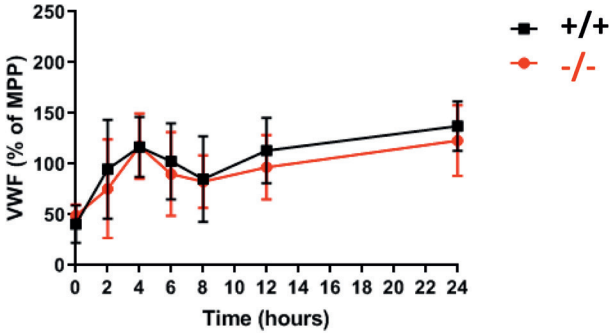


Figure S6. Plasma VWF levels following LPS stimulation. Mice were injected with 2 mg/kg lipopolysaccharides (LPS) and blood samples collected over a time course of 24 hours. Plasma VWF levels were determined by ELISA and compared to a relative standard of mouse pooled plasma (MPP) (n=11 per group).

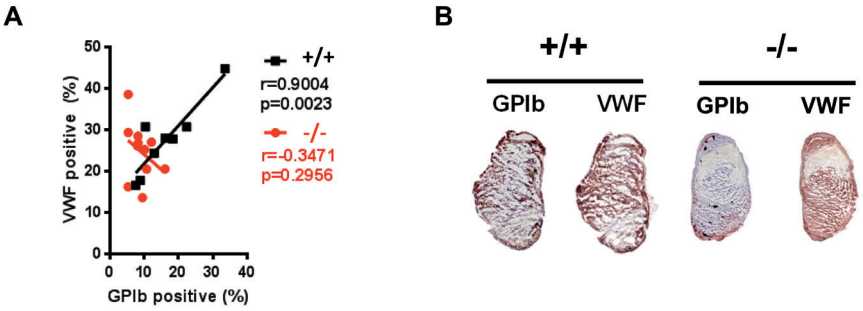


Figure S7. Relationship between VWF and GPIb in thrombi following 48 hour stenosis. **(A)** Correlation plot between GPIb staining and VWF staining on serial thrombus sections after 48 hour stenosis of SLC44A2 deficient *(Slc44a2-/-,* N=11*)* and wildtype control mice *(Slc44a2*$^{+/+}$, N=8*)*. **(B)** Representative images of IHC staining of GPIb and VWF. Coefficient r calculated using Spearman's correlation.

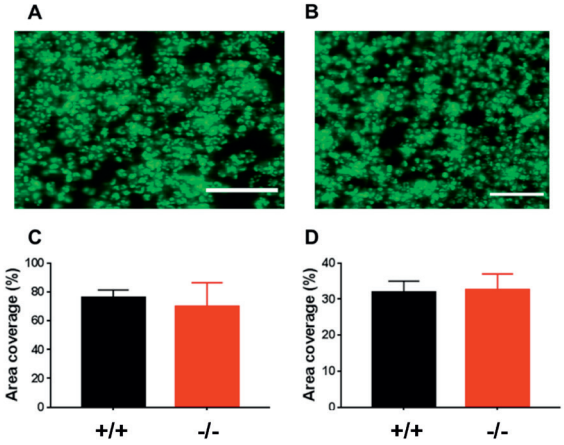


Figure S8. Representative images of platelet adhesion after 3.5 minutes of whole blood perfusion of blood from *Slc44a2*$^{+/+}$ mice **(A)** or *Slc44a2-/-* mice **(B)** at 1000 s-1 over collagen type I. Quantitative analysis of platelet surface area coverage **(C)** and JON/A surface area coverage **(D)**. Scale is 10 µm. Mean + S.D., n = 5-7.

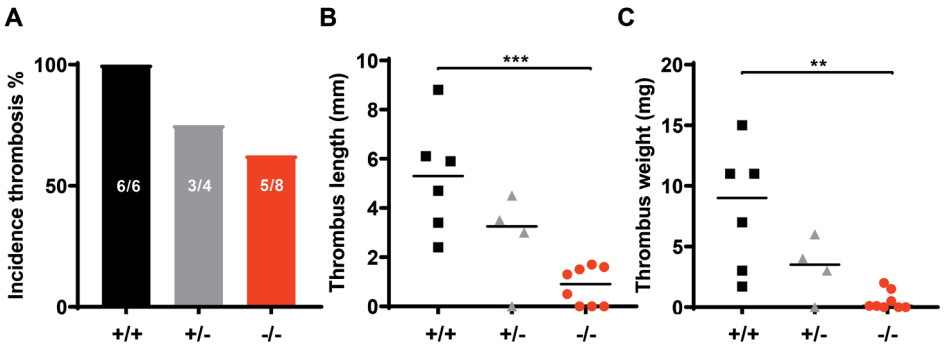


Figure S9. Thrombosis in SLC44A2 deficient mice following 6 hour stenosis of the inferior vena cava. (A) Incidence of thrombosis after 6 hours in mice wild type (*Slc44a2*$^{+/+}$) (n=6), heterozygous (*Slc44a2*$^{+/-}$) (n=4) or knockout (*Slc44a2-/-*) (n=8) for SLC44A2, shown as percentage. **(B)** Length and **(C)** weight of thrombi formed after 6 hours. Black lines represent median value. Statistical differences between genotypes were evaluated using ANOVA Kruskal-Wallis test (p=0.0010 for length; p=0.0020 for weight) and Dunn's multiple comparison test. (** signifies p<0.01; *** signifies p<0.0001).

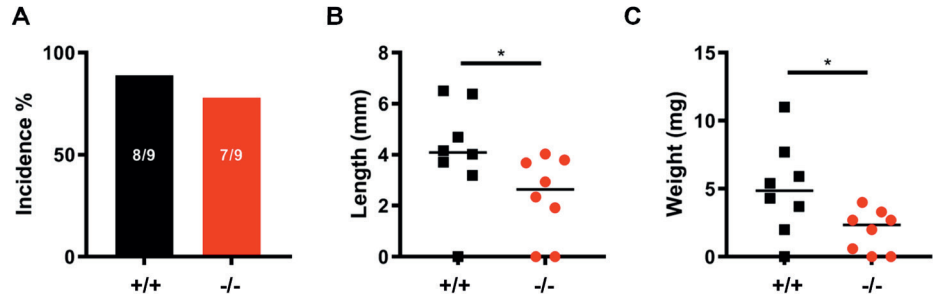


Figure S10. Thrombosis in SLC44A2 deficient mice following 6 hour stenosis of the inferior vena cava. (A) Incidence of thrombosis after 6 hours in mice wild type (*Slc44a2*$^{+/+}$) or knockout (*Slc44a2-/-*) (n=9) for SLC44A2, shown as percentage. **(B)** Length and **(C)** weight of thrombi formed after 6 hours. Black lines represent median value. Statistical differences between genotypes were evaluated using ANOVA Kruskal-Wallis test (p=0.0010 for length; p=0.0020 for weight) and Dunn's multiple comparison test. (* signifies p<0.05).

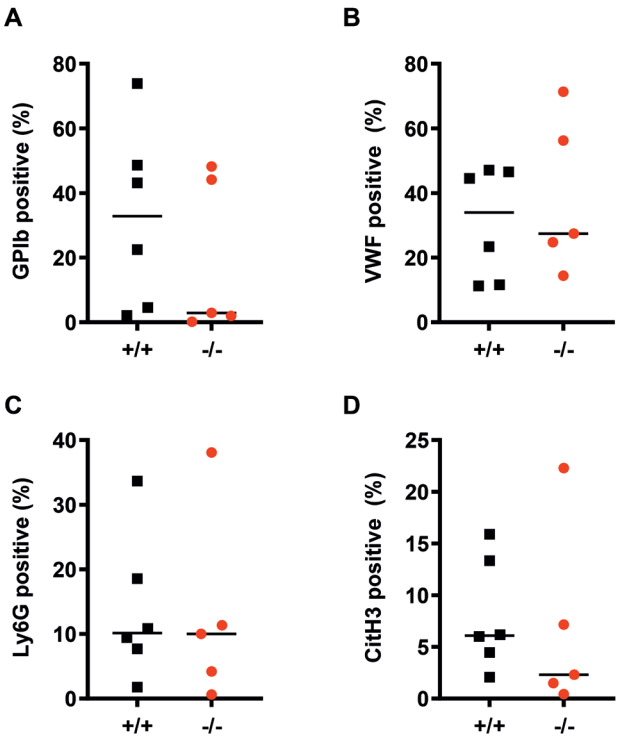


Figure S11. Immunohistochemical characterization of thrombi following 6 hour stenosis. Quantification of immunohistochemical (IHC) staining of **(A)** glycoprotein Ib (GPIb), **(B)** von Willebrand Factor (VWF), **(C)** neutrophil marker Ly6G and **(D)** citrullinated histone H3 (CitH3) as a percentage of total thrombus area (%). (*Slc44a2*$^{+/+}$ (+/+) = 6; *Slc44a2-/-* (-/-) = 5). Black lines represent median value. Statistical differences were evaluated using Mann-Whitney rank-sum test.

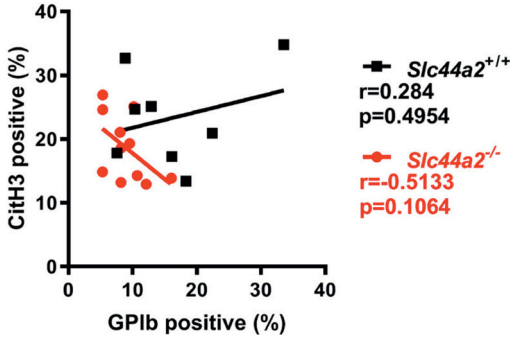


Figure S12. Correlation of platelets and citrullinated histones. Correlation plot of GPIb and citrullinated histone H3 immunostaining on thrombus sections in SLC44A2 deficient (*Slc44a2-/-*, n=11) and wildtype control mice (*Slc44a2*$^{+/+}$, n=8) following 48 hour stenosis of the inferior vena cava.

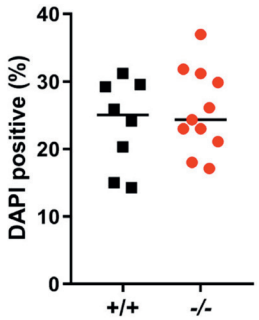


Figure S13. DAPI positive area. Nuclear stain (DAPI) of leukocytes in thrombi from SLC44A2 deficient mice (-/-, n=11) and wildtype control mice (+/+, n=8) as a percentage of total thrombus area following 48 hour stenosis of the inferior vena cava.

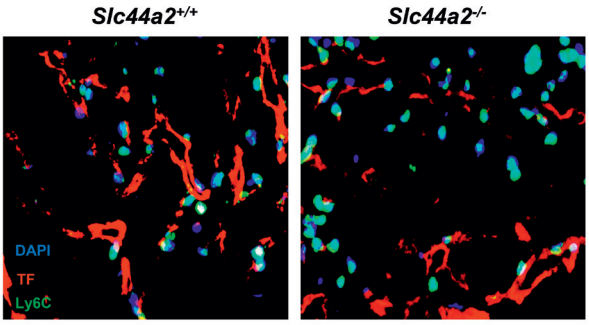


Figure S14 Tissue factor Ly6C staining. Immunofluorescent staining of tissue factor (TF; red), Ly6C (green) and nuclear stain (DAPI; blue) in thrombi from *Slc44a2*$^{+/+}$ and *Slc44a2-/-* mice, light blue signal indicates colocalization of DAPI and Ly6C. 63x magnification.

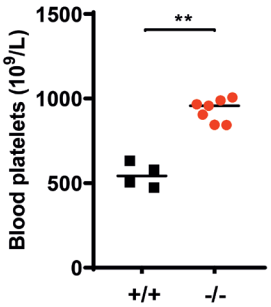


Figure S15. Blood platelet counts at 6 hours post-stenosis of the IVC. Circulating blood platelets counts at sacrifice following 6 hours stenosis procedure. Black lines represent median value. Statistical differences were evaluated using Mann Whitney rank-sum test. (n=4 *Slc44a2*$^{+/+}$; n=5 *Slc44a2-/-*)(** signifies p<0.01).

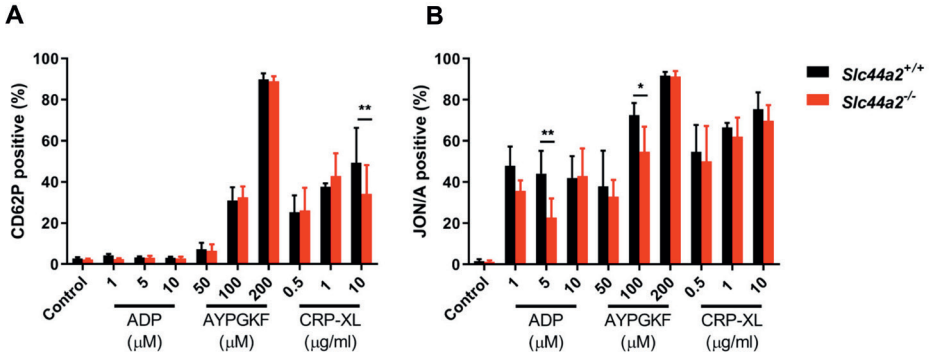
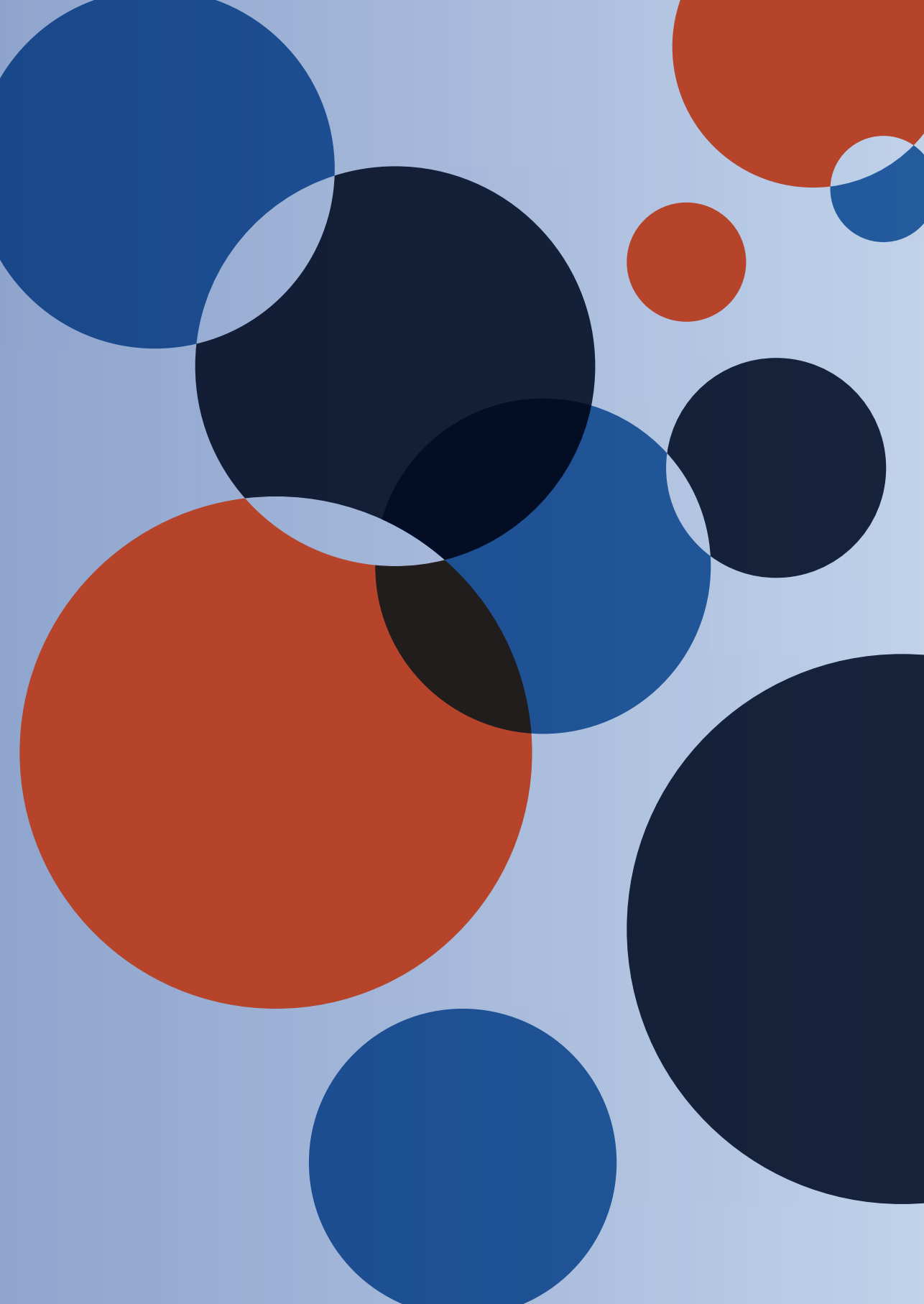


Figure S16. Platelet activation. Percentage of cells positive for **(A)** exposed P-selectin (CD62P) or **(B)** activated integrin αIIbβ3 following activation with adenosine diphosphate (ADP; 1, 5, 10μmol/L), Protease-Activated Receptor 4 (PAR4) agonist AYPGKF (50, 100, 200μmol/L) or collagen related peptide (CRP-XL) (0.5, 1 or 10 μg/mL) as determined by flow cytometry and quantified as the percentage of cells staining positive (%) in platelets from SLC44A2 deficient mice (*Slc44a2-/-*,n =5) and wildtype control mice (*Slc44a2*$^{+/+}$,n =5).

Table S1 qPCR primer sequences used for (coagulation) gene profiling of lung and liver

Gene	Forward Primer	Reverse Primer
Actb	AGGTCATCACTATTGGCAACGA	CCAAGAAGGAAGGCTGGAAAA
Slc44a2	CGGAAGGACGCAGTCTATGG	AGGAAGAGCAACACACAGCA
Serpinc1	CCCTGGCCGACTTCACAA	TTTTGCAGTGCCTGTGCTACA
Proc	GCGTGGAGGGCACCAA	CCCTGCGTCGCAGATCAT
Ccl2	TTAAAAACCTGGATCGGAACCAA	GCATTAGCTTCAGATTTACGGGT
Cxcl1	CTGGGATTCACCTCAAGAACATC	CAGGGTCAAGGCAAGCCTC
Cxcl5	GTTCCATCTCGCCATTCATGC	GCGGCTATGACTGAGGAAGG
Il6	TAGTCCTTCCTACCCCAATTTCC	TTGGTCCTTAGCCACTCCTTC
Selplg	ACCGTGGTCATGCTAGAGAGA	ACTGAGGTTAGACTCCACTGTG
Vcam1	AGTTGGGGATTCGGTTGTTCT	CCCCTCATTCCTTACCACCC



PLASMA PROTEIN SIGNATURES OF A MURINE VENOUS THROMBOSIS MODEL AND SLC44A2 KNOCKOUT MICE USING QUANTITATIVE-TARGETED PROTEOMICS

Julia Tilburg, Sarah A. Michaud, Chrissta X. Maracle, Henri H. Versteeg, Christoph H. Borchers, Bart J.M. van Vlijmen*, Yassene Mohammed*
*: These authors contributed equally

Thromb Haemost. 2020 Mar;120(3):423-436.

4

Abstract

The plasma compartment of the blood holds important information on the risk to develop cardiovascular diseases such as venous thrombosis (VT). Mass spectrometry-based targeted proteomics with internal standards quantifies proteins in multiplex allowing generation of signatures associated with a disease or a condition. Here, to demonstrate the method, we investigate the plasma protein signatures in mice following the onset of VT which was induced by RNA interference targeting the natural anticoagulants antithrombin and protein C. We then study mice lacking SLC44A2 which was recently characterized as a VT-susceptibility gene in human genome-wide association studies. We use a recently developed panel of 375 multiplexed mouse protein assays measured by mass spectrometry. A strong plasma protein signature was observed when VT was induced. Discriminators included acute phase response proteins, and proteins related to erythrocyte function. In mice lacking SLC44A2, protein signature was primarily overruled by the difference between sexes and not by the absent gene. Upon separate analyses for males and females, we were able to establish a signature for *Slc44a2* deficiency, in which glycosylation-dependent cell adhesion molecule-1 and thrombospondin-1 were shared by both sexes. The minimal impact of *Slc44a2* deficiency on the measured plasma proteins suggests that the main effect of SLC44A2 on VT does not lay ultimately in the plasma compartment. This suggests further investigation into the role of this VT-susceptibility gene should perhaps also question the possible involvement in cellular mechanisms.

Introduction

Venous thrombosis (VT), i.e. unwanted clotting of the blood within a vein, is a complex cardiovascular disease and its pathogenesis is not completely understood (1, 2). The plasma compartment of the blood, which provides the clotting factors involved in VT, holds important information on the risk to develop VT (3). Several clotting factors i.e. pro- and anticoagulant proteins, as well as pro- and antifibrinolytic proteins are affected by genetic and acquired risk for VT (4, 5). Plasma levels and activity of these proteins are important in assessing VT risk, and contribute to understanding how genetic and acquired risk factors relate to VT (3, 4). In addition, there is increasing evidence supporting that also proteins not belonging to coagulation and fibrinolytic pathways may play a role in VT, including proteins involved in inflammation, the complement system, or lipoprotein metabolism (6-10).

Recently, a meta-analysis of genome-wide association studies (GWASs) revealed two novel genetic susceptibility loci for VT (5). Interestingly, these loci harbor genes encoding proteins that cannot directly be linked to coagulation. Among these was a VT locus encompassing the *SLC44A2* gene, located on 19p13.2, which was associated with thrombotic events also in a second independent GWAS cohort (11). SLC44A2 encodes the solute carrier family 44 member 2 protein (SLC44A2), a poorly characterized gene, and regarding a mechanism underlying the association between SLC44A2 and VT can, at present, only be speculated. So far no links to coagulation- and fibrinolysis-related pathways could be identified (5) apart from an interaction of SLC44A2 with von Willebrand factor (VWF) as identified in *in vitro* studies (12).

To understand the role of SLC44A2 in VT we previously undertook an animal approach using recently generated *Slc44a2* deficient (*Slc44a2-/-)* mice (13). Compared with their wild type (*Slc44a2+/+)* littermates these *Slc44a2-/-* mice revealed no differences in the measured coagulation related parameters, i.e. thrombin generation, transcriptional profiling of coagulation related genes, multimerization and localization within venous and arterial vessels, with the exception of a modest decrease in plasma VWF level (14). These first observations encourage to further explore the link between SLC44A2 and VT in and outside of coagulation- and fibrinolysis-related pathways using more in depth analysis.

As an alternative to individual activity- or antibody-based plasma protein assays, mass spectrometry(MS)-based proteomics allows deeper investigation of the proteome in relation to health and disease (15-20). The levels of several coagulation proteins can be measured in plasma and serum by MS (21, 22) as well as secreted proteins that are unrelated to the coagulation cascade but associated with VT risk (23). Detection of venous thromboembolism signature in serum using proteomics was previously demonstrated (24) as well as in depth analysis of VT proteomics using *ex vivo* prepared fibrin clots (25). In mouse, various studies demonstrated phenotyping of disease models using proteomics, showing also evidence of an age and sex dependent plasma proteome (26, 27). We recently demonstrated that

MS-based targeted proteomics with stable-isotope-labeled internal standards can be used for rapid, multiplexed, and precise quantification of coagulation- and fibrinolysis-related plasma proteins in human using as small volumes as less than 10 µL of plasma (28, 29). We were able to capture plasma protein signature information on VT, in particular VT and cancer, which was not obvious from single measurements by the conventional assays. Contrary to traditional protein phenotyping techniques, MS-based targeted proteomics can be highly multiplexed without sacrificing specificity nor quantitative precision (30). This allows measuring abundance of hundreds of proteins in hundreds of samples in standardized way facilitating best comparative analysis.

Recently, hundreds of MS-based targeted proteomics assays for various mouse proteins have been developed and validated (26). This opens up the opportunity to measure abundances of many mouse proteins for which traditional techniques like antibody assays are currently not available, nor feasible. In addition, it allows capturing plasma protein signature information associated with genes or disease in an experimental mouse setting using low volumes of samples, which is a limitation in small animals like mice. In the present study, we use these assays to extend our analysis beyond traditional coagulation factors and measure additional plasma proteins.

First, we measured plasma protein levels in mice where VT follows RNA interference-mediated imbalance in natural anticoagulation (31, 32). Although one can question its suitability as best VT model mimicking human disease, we chose to use this model as it presents a strong venous thrombotic phenotype, coincides with clinical signs and changes in clotting tests. As a result, changes in abundance of various plasma proteins are expected. Next, we determined protein levels in plasma samples from seemingly normal *Slc44a2* deficient mice to investigate any possible protein signature for this less-characterized VT-susceptibility gene. Putting the results of both experiments side by side, i.e. changes in plasma protein levels in induced VT and *Slc44a2* knockout mice, can give an indication to the level to which the *Slc44a2* absence affect plasma proteins. A strong signature in plasma protein abundances was observed when VT was induced including acute phase response and erythrocyte-specific proteins. In mice lacking *Slc44a2,* the plasma protein signature was overruled by the sex of the mice and not by the absent gene. When stratifying for sex, we were able to establish a signature for *Slc44a2* deficiency represented in glycosylation-dependent cell adhesion molecule-1 and thrombospondin-1. Both these proteins are associated with cell-cell interactions, which suggests that the role of *Slc44a2* lays outside of the plasma and perhaps question possible involvement of this VT-susceptibility gene in cellular mechanisms.

Materials and Methods

Mice

Female C57BL/6J mice aged 6 weeks were obtained from Charles River, Maastricht, The Netherlands. Mice deficient for solute carrier family 44 member 2 protein (*Slc44a2-/-*, gene

located on mouse chromosome 9) were previously generated by crossing mice with *Slc44a2* exon 3 to 10 flanked by LoxP sites with deleter EIIa-Cre transgenic mice (13, 14). Mice were genotyped for presence of the *Slc44a2* knockout allele using ear biopsy DNA as previously described (14). Offspring, heterozygous for the *Slc44a2* knockout allele (*Slc44a2*+/-), was used for backcrossing to C57BL/6J (at least seven generations). Subsequently, interbreeding of the *Slc44a2*+/- mice yielded male and female *Slc44a2*-/- and wild type littermate control *Slc44a2*+/+ mice which were used for blood and tissue collection (at 15 weeks of age, N=8 for female *Slc44a2*+/+ and weight at euthanasia 21.75 ± 2.14 g, N=8 for female *Slc44a2*-/- mice and weight at euthanasia 22.36 ± 1.14 g, N=8 for male *Slc44a2*+/+ and weight at sacrifice 29.82 ± 5.51 g, and N=7 for male *Slc44a2*-/- mice and weight at euthanasia 29.22 ± 1.70 g). All mice in this study were housed under standard conditions with free access to water and food. All experiments were approved by The Netherlands National Animal Welfare Committee, under project license number AVD106002016607.

Induction of venous thrombosis

Small interfering RNAs (siRNAs) targeting mouse antithrombin (siAT, cat. #S62673, Ambion, Life Technologies, CA, USA) and protein C (siPC(31), cat. #S72192) and a negative control siRNA referred to as siControl (cat. #4404020) were complexed with Invivofectamine® 3.0 (Invitrogen, Life Technologies, CA, USA) exactly according to the procedure provided by the manufacture. A mixture of complexed siAT and siPC (siAT/PC) was prepared in PBS with a final concentration of 4.2 nmol per mL for both siAT and siPC (total 8.4 nmol/mL). The complexed siControl was diluted in PBS to a final concentration of 8.4 nmol/mL. The siAT/PC and siControl were injected intravenously (tail vein) of the 6-week-old female C57BL/6J mice (200 µL per mouse i.e., a total of 1.7 nmol siRNA per mouse, N=8 for siAT/PC and weight at injection was 20.77 ± 1.11 g, and N=7 for siControl and weight at injection was 20.19 ± 0.82 g). The spontaneous venous thrombotic phenotype that follows injection of siAT/PC has been described previously (31, 32). As soon as a siAT/PC injected mouse presented the typical externally visible clinical signs that coincide with the VT phenotype, it was euthanized together with one mouse randomly selected from the siControl injected control group.

Blood collection and processing

For euthanasia, animals were anesthetized using a mixture of ketamine (40 mg/mL, A.A.-Vet, Biddinghuizen, The Netherlands), xylazine (5 mg/mL, Dechra, Northwich, United Kingdom), and atropine (0.1 mg/mL, Pharmachemie BV, Haarlem, The Netherlands) in PBS (indicated are end concentrations) injected subcutaneously at a volume of 75 and 125 µL for females and males, respectively. Before euthanasia, 20 µL of water was added to dipotassium ethylenediaminetetraacetic acid (K_2EDTA) coated vials (average of 1mg K_2EDTA/vial, ref: 365975, BD, NJ, USA), vortexed to dissolve the K_2EDTA, and transferred quantitatively into 1-mL syringes with 24-gauge needle. The anesthetized animal's abdomen was opened, the inferior vena cava exposed and 350 (from animals injected with siControl or siAT/PC) or 500 µL of blood (from *Slc44a2*-/- and *Slc44a2*+/+ males and females) was collected using the K_2EDTA-loaded 1-mL syringe within approximately 15 to 30 seconds. Blood was thoroughly

but carefully mixed with the K_2EDTA within the syringe, and transferred to the original K_2EDTA vials (allowing mixture with possible residual K_2EDTA, and kept on ice until centrifugation). Vena cava and abdominal aorta were cut, allowing euthanasia. Ice-cold blood samples were visually inspected for signs of clotting (absent for all samples) and centrifuged for 5 minutes at 10,000 rpm at 4°C in an Eppendorf Centrifuge 5417R. From the plasma fraction, aliquots were snap frozen in liquid nitrogen, stored at -80°C, shipped on dry ice to the University of Victoria, Canada, and stored again at -80°C until use. *Slc44a2* status was confirmed with PCR on tail tip DNA and at transcript level from the liver transcriptome by quantitative PCR using β-actin (*Actb*) as a reference as described previously (14, 33).

Targeted proteomics

We used 375 validated protein assays in a setting of experimental VT and altered VT-susceptibility. These proteins are measured in a multiplexed experiment and are related to various pathways and, besides their biological relevance reported in literature, they were selected after careful validation for detectability and quantifiably in mouse blood plasma (Table S1, Figure S1)(26). Indeed, proteomics as a field offers other approaches like semi-quantitative bottom-up proteomics that allows detection of more proteins (34). We opted for a targeted proteomics with internal standard approach to achieve best specificity and highest precision, using validated assays for predefined limited–yet expandable–number of proteins. This choice is mainly to achieve best possible comparability between samples.

A total of 375 proteins and their surrogate peptides are listed in supplementary Table S1. The assays are highly multiplexed and standardized consisting of 3 panels of 125 assays each running in parallel in multiple reaction monitoring (MRM) mode and cover various pathways and molecular functions (Figure S1 and Table S1). The development and validation of these assays were performed previously as part of the Proteomics Centre at the University of Victoria efforts to build a library of targeted proteomics assays for profiling mouse plasma and tissues (26, 35, 36). The peptides for the MRM assays were selected using PeptidePicker and synthesized at the University of Victoria Proteomics Centre (37). The sample preparation was performed using a Tecan Freedom Evo 150 robot. The urea-based preparation protocol used was developed and applied previously (38).

The samples were separated on-line with an ultra-high performance liquid chromatography column (EclipsePlusC18 RRHD 150 x 2.1 mm i.d., 1.8 µm particle diameter; Agilent) maintained at 50°C. Peptide separation was performed at 0.4 mL/minute over a 56 minute run, using a multi-step LC gradient (1.5-81% to 2-80% mobile phase B; mobile phase B: 0.1% formic acid in acetonitrile). The exact gradient was as follows (time point in min, solution B %): 0 minutes, 2%; 2 minutes, 7%; 50 minutes, 30%; 53 minutes, 45%, 53.5 minutes, 80%; 55.5 minutes, 80%; 56 minutes, 2%. The LC system was interfaced to a triple-quadrupole mass spectrometer Agilent 6495 via a standard-flow electrospray ionization source and operated in the positive ion mode.

Data processing and analysis

We inspected all response peaks using Skyline software (39) to ensure correct retention time, accurate selection and integration, and uniformity of peak shape for the endogenous and internal standard peptide signals. We calculated the relative peak area ratio of the endogenous to the heavy labeled internal standard peptide. Using this ratio and the known concentration of internal standard peptides, we determined the concentration of the endogenous peptides in the sample by comparison to a standard curve generated in pooled sample (29), for which we used 1/x2 regression weighting. For all hierarchical agglomerative clustering, we used Ward's algorithm (40, 41) on the Euclidean's distances of the scaled and centered determined protein concentrations. All data analysis and visualization were performed using own routines written in R statistical language. For the selection of best discriminating proteins, we used Wilcoxon's signed-rank test.

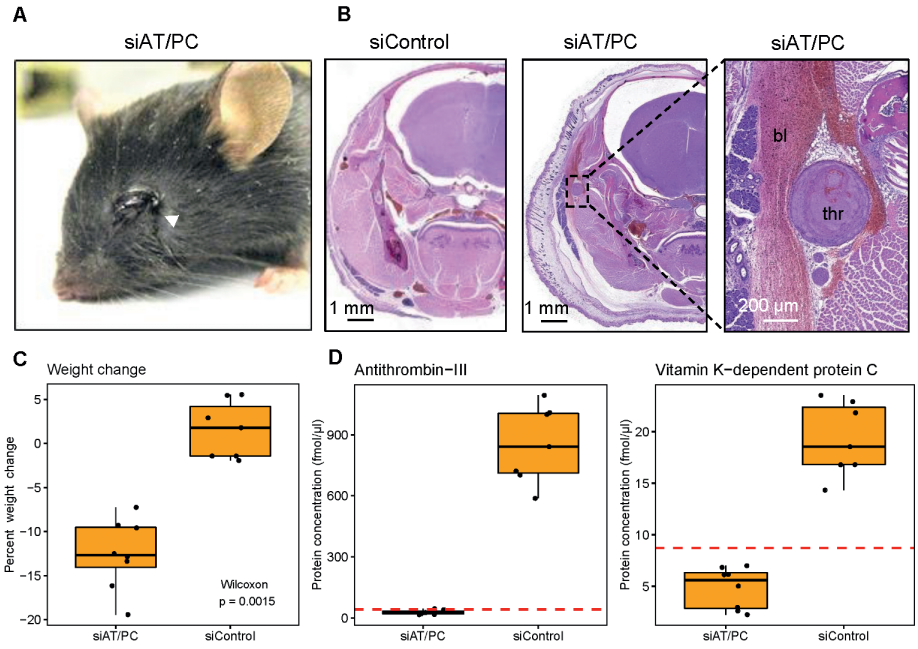


Figure 1. Venous thrombosis in mice 48 to 72 hours after intravenous injection of siRNA targeting antithrombin and protein C (siAT/PC) or control siRNA (siControl). N=8 for siAT/PC and N=7 for siControl. **(A)** Eye of an siAT/PC-treated animal. Unilateral exophthalmos and periocular hemorrhages are shown (arrow head). **(B)** Hematoxylin and eosin staining of coronal head section (5 µm) of mice treated with siAT/PC and siControl, thrombus (thr) and bleeding (bl) are indicated. **(C)** Weight change at euthanasia of mice treated with siAT/PC and siControl relative to weight at siRNA injection (complete information on the weight of all mice are in Table S2 and Table S3). Statistics using Wilcoxon's rank sum test. **(D)** Plasma protein concentration of antithrombin (left) as well as protein C (right) in siAT/PC and siControl mice. PC, protein C; siRNA, small interfering RNA; AT, antithrombin.

Results

Induced venous thrombosis and Slc44a2 deficiency in mice

We applied quantitative targeted proteomics to determine abundance of 375 proteins in plasma samples collected from mice that developed VT following injection of siRNAs targeting antithrombin and protein C (siAT/PC) or control siRNA (siControl). In line with previous observations (31, 32), within 3 days post injection all siAT/PC treated mice developed the typical externally visible clinical signs of VT i.e. unilateral lesions around the eye, edema, and swellings in the head (Figure 1A). Histologically, this presents as a thrombotic coagulopathy (Figure 1B). Additionally, the siAT/PC-treated mice showed expected loss in body weight as compared with their control (P-value=0.0015, Figure 1C). Despite this phenotype, the mice remained lively and did not become lethargic, unresponsive to stimuli, or hypothermic, which may occur upon phenotype progression (31). Effectiveness of antithrombin and protein C silencing was confirmed at the plasma protein level (Figure 1D, described in more detail below). In a parallel experiment, to investigate the effect of the novel thrombosis-susceptibility gene *Slc44a2*, we used *Slc44a2* deficient (-/-) mice and their wild type (+/+) littermates as controls (these mice were all healthy and were not subjected to siAT/PC-induced VT). Upon euthanasia, after *Slc44a2* liver transcript analysis (data not shown), and subsequent re-genotyping at the level of tail tip DNA (data not shown), one knockout male appeared to be heterozygous (*Slc44a2+/-)*. This mouse was included in the plasma proteomics sample measurement, but was later excluded during the data analysis.

Quantification of mouse plasma proteins

In 49 plasma samples (46 mice with 3 measured in duplicate as quality control), we determined the abundance of 375 proteins, which equals a total of 18,375 measurements that were performed on our LC-MS system within a week. The three duplicates were included at origin to control for all aspects of sample handling, shipment, wet laboratory preparation, and measurement. In addition, seven in-house quality controls (pooled mouse plasmas from C57BL/6 mice of both sexes) were included. All measurements were performed in a blinded fashion and the samples were randomized on a 96-well plate to rule out possible batch effects. From the 375 protein assays that were validated and successfully measured in previous mouse experiments (26), 221 proteins passed our stringent quantifiability criteria in the current study, while 154 proteins were below the lower limit of quantification in at least 37 of the 47 samples measured, that is, 80%. This is not necessary a reason to consider these measurements failed. They could still be indicative and the reason to be on the lower side in protein concentration can be related to the experimental intervention, experimental setting, and/or genetics. In addition, our panel includes proteins which are not necessary found in plasma under healthy conditions. For example, the majority of the proteins are not detectable in both male and female control mice cover various molecular functions that are not native to plasma (Figure S1 and Table S1).

Although it was not our main objective to compare the two experimental groups (induced VT and *Slc44a2* deficiency) when looking at all measured samples together using hierarchical clustering (Figure S2), we observed that the strongest discrimination corresponds to the "experimental group". Each experimental group forms its own cluster, the siRNA-treated mice (orange in the first annotation bar, bottom), the *Slc44a2* deficient mice and their controls (green, middle), and the in-house quality controls (blue, top). One single outlier from the female siControl group showed more similarity to wild type *Slc44a2* group from the same sex. Within the siRNA-treated group, a clear distinction was observed between mice treated with siAT/PC, which developed VT and the siControl treated mice, which remained fully healthy, as can be seen in the second annotation bar. In the *Slc44a2* group, we observed a clear distinction between males and females as can be seen in the sex annotation bar, while a clustering based on *Slc44a2*–forth annotation bar–is not observable. The one male *Slc44a2+/-* clusters with the rest of the male mice, but was later removed from the data analysis and interpretation. Including all samples in this comparison allowed a fast check on the data collected and showed that unsupervised clustering on all measured proteins is able to capture clusters based on the presence of VT as well as sex, but not on *Slc44a2* status. In other words, the *Slc44a2* absence does not influence the plasma proteins as strongly as induced VT or sex.

Protein profile (dis)similarities

In order to assess the protein profile similarities in and between groups and samples, we opted to comparing the Pearson's correlation coefficients pairwise between each two samples. When referring to protein profiles, we consider here the proteins that were quantitatively measured in our experiment, although the detectable plasma proteome is indeed larger with over a thousand proteins (42). There were few general observations that stood out. With regard to the three duplicates which were included at origin, a very high correlation of >99% was determined between duplicates (Figure 2A). This confirms the robustness of our method in capturing the similarity in the quantifiable protein profiles. The histogram in Figure 2B shows two distinct distributions of the correlation factors separated around 95%. *Slc44a2-/-* and *Slc44a2+/+* samples were very similar and show a correlation centered around 97%, while those from siAT/PC versus siControl as well as *Slc44a2* knockout were with lower correlation values centered around 92%. This implies that samples from animals with induced VT, that is, siAT/PC are clearly deviating in their profiles from all other samples.

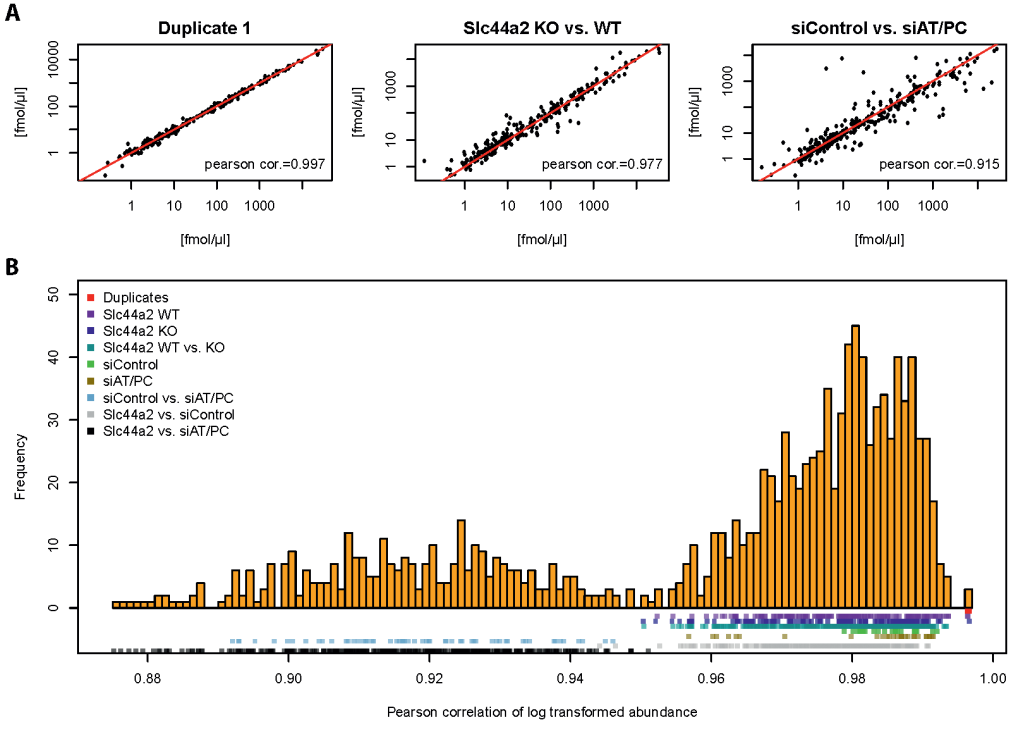


Figure 2. Correlation between samples. N=16 for *Slc44a2+/+* (eight males and eight females), N=15 for *Slc44a2-/-* (six males and eight females), N=8 for siAT/PC, and N=7 for siControl. **(A)** Pairwise correlation between duplicate samples (Duplicate 1), *Slc44a2-/-* and *Slc44a2+/+* (Slc44a2 KO vs. WT), as well as samples from induced VT using siRNA targeting antithrombin and protein C and corresponding controls (siControl vs. siAT/PC) **(B)** Histogram of correlation coefficient values of all pairwise comparisons of samples based on determined protein abundances. PC, protein C; AT, antithrombin; siRNA, small interfering RNA; WT, wild-type; KO, knockout.

Traceable protein changes due to induced venous thrombosis

A clear distinction could be observed between mice treated with siAT/PC, which developed VT, and the siControl treated mice (Figure 2 and Figure S2). Despite developing VT, siAT/PC treated mice remained lively and did not appear sick (i.e. lethargic, unresponsive to stimuli, or hypothermic as may be observed upon progression of the phenotype (31)), nevertheless changes in the plasma proteome appear considerable. The top 10 discriminating plasma proteins are shown in Figure 3A and listed in Table 1A. Principle component analysis (PCA) on these 10 proteins shows a very good separation with principle component (PC) 1 explaining 82% of the variance observed between the two experimental groups (Figure 3E). The log_2 fold changes (log_2 FC) in protein levels also show that the effect on the proteome is substantial with several proteins having more than three times log_2 FC (Figure S3A). As expected antithrombin III is in the list of discriminating proteins with large fold change (log_2 FC of -4.93) which reflects the successful antithrombin gene silencing strategy (Figure 1D). Lower levels of protein C are also expected (32) and were readily observed (log_2 FC of -1.98), although not amongst the top 10 selected most discriminatory proteins. Plasma hemoglobin subunit beta-1 is discriminating and is strongly reduced with log_2 FC of -2.88 upon VT, which is in line with the observed decrease in two other hemoglobulin subunits i.e. alpha and zeta (log_2 FC of -3.94 and -3.97 respectively, Figure S3A).In addition, a strong increase of hemoglobin-binding protein haptoglobin (log_2 FC of 9.20, Figure S3A) is observed. Together these alterations in plasma proteins point toward changes in erythrocyte functioning, which can be explained as erythrocyte trapping and extravasation in the (large veins of the) heads of affected mice is a key feature of this VT model (Figure 1B). Since formation of fibrin-networks (trapping the erythrocytes) is also part of the pathology in this VT model, the decrease in coagulation factor XIIIB (log_2 FC of -1.25) and coagulation factor XIIIA (log_2 FC of -1.91), the two subunits of coagulation factor XIII (FXIII) that is involved in covalent crosslinking of fibrin, is not unexpected either. While consumption of plasma coagulation factors is reported previously in this model (31), this is not supported by the observations in the present study as changes for other coagulation proteins that were included in the current analysis (fibrinogen, coagulation factor II, V, VII, X, XI, XII) were limited (log_2 FC did not exceed -1 or 1). It is important to note that in Safdar et al. (31), the sampling time point is different, i.e. prolonged VT in Safdar et al. versus onset of VT in this study, and the sample collection and handling is different, i.e. normal collection of citrated versus immediate cooling of K_2EDTA plasma which affect the intrinsic proteases activities.

Several proteins among the 10 most discriminating proteins with higher abundance upon VT and number are known as acute phase proteins (APPs) i.e. c-reactive protein (log_2 FC of 1.30), ceruloplasmin (0.80), fibronectin (1.34), alpha-1-acid glycoprotein 2 (3.76), complement C3 (1.01) and complement C8 gamma chain (0.69; (43-45). Various other proteins that increase in their average abundance (Figure S3A), but are not among the top discriminating proteins due to their variance, are also APPs which include serum amyloids (SA) SAa2 (log_2 FC of 11.55), SAa1 (8.91), SAa4 (1.78) and SAp (7.42). Apolipoprotein D was also observed to have a higher abundance in mice with VT (log_2 FC of 0.72), it has however no known role in erythrocyte

function, coagulation, or as an APP. Apolipoprotein D changes upon VT did not coincide with changes in levels of other apolipoproteins included in the analysis (apolipoproteins A-I, A-II, B, C-I, C-II, C-III, C-IV and E).

Plasma proteome influenced by sex group

The (dis)similarities in protein abundance profile according to intervention (Figure 2) as well as the traceable protein changes due to induced VT (Figure S2), demonstrate the capability of the method in capturing protein signatures in experimental VT models. Figure S2 shows further how unsupervised clustering on all data and samples results in perfect discrimination between male and female. We further compared the plasma levels of the wild type (*Slc44a2+/+)* males and females with Figure 3B as well as Table 1 listing the top discriminatory proteins. The $\log_2$ fold changes in plasma protein levels for sex are smaller than those observed upon VT (Figure S3B) and shows that sex has a substantial but more limited impact on the plasma proteome as compared with induced VT. Of note, the protein levels changing mostly do not overlap with the top discriminating proteins for sex. Principal component analysis on the 10 most discriminating proteins shows perfect separation along PC1, which explains 88% of the variance (Figure 3F).

The discriminating proteins are from multiple pathways and include coagulation proteases (vitamin K dependent protein C, $\log_2$ FC of 0.82 and carboxypeptidase B2, $\log_2$ FC of 0.45, a complement protease (C8 alpha and gamma chain, $\log_2$ FC of 2.05 and 1.92 respectively), a protease inhibitor (alpha-1-antitrypsin 1-1, $\log_2$ FC of 4.06), a hormone binding protein (corticosteroid-binding globulin protein, $\log_2$ FC of -1.10), three signaling proteins (adiponectin, $\log_2$ FC of -0.90, epidermal growth factor receptor, $\log_2$ FC of 1.18, interleukin-1 receptor accessory protein, $\log_2$ FC of 0.65) and an immunity-related protein (H-2 class I histocompatibility antigen Q10 alpha chain, $\log_2$ FC of 0.85). For adiponectin and complement C8, an impact of sex on plasma levels was previously reported (46, 47). This observed strong discrimination between the protein profiles of male and female shows that the plasma proteomes for the sexes are different. Subsequently, we performed the analysis of the effect of *Slc44a2* deficiency on the plasma protein levels per sex separately as the anticipated effects of *Slc44a2* deficiency may be more limited.

Table 1. Top 10 discriminating proteins between mice that developed venous thrombosis following injection of small interfering RNA targeting antithrombin and protein C and their controls (siControl) between wild-type male and female mice, and between Slc44a2 -/- (KO) and Slc44a2 +/+ (WT) in male and female mice

					Protein abundancy mean[range] (fmol/µl)					
	Protein names	**Gene names**	**UniprotKB**	**Peptide Sequence**	**siControl**	**siAT/PC**	**WT male**	**WT female**	**KO male**	**KO female**
Top 10 discriminators between siAT/PC and siControl	Alpha-1-acid glycoprotein 2	*Orm2*	P07361	IFADLIVLK	178 [82.2-378]	2410 [1550-4700]	31,1 [13.9-102]	43,7 [27.5-111]	39 [23.8-50.5]	56,3 [29.1-169]
	Antithrombin-III	*Serpinc1*	P32261	DDLYVSDAFHK	851 [588-1090]	27,8 [16.1-45.1]	1040 [725-1440]	1160 [1030-1400]	1100 [782-1240]	1100 [963-1270]
	Apolipoprotein D	*Apod*	P51910	IPASFEK	35 [24.7-38.6]	57,6 [44.4-75]	37,5 [22.6-47.4]	41 [33.7-48.6]	36,8 [17.4-47.8]	46,1 [41.3-52.2]
	Ceruloplasmin	*Cp*	Q61147	DIFTGLIGPMK	340 [269-408]	591 [465-785]	419 [363-504]	448 [398-525]	447 [395-503]	442 [383-516]
	Coagulation factor XIII A chain	*F13a1*	Q8BH61	FQEGQEEER	89,3 [65.8-107]	23,8 [3.87-52.1]	97,8 [73.9-116]	118 [54.9-164]	109 [81.8-164]	87,3 [67.3-141]
	Complement C3	*C3*	P01027	GTLSVVAVYHAK	1240 [896-1710]	2490 [1760-3220]	1170 [923-1360]	1610 [1260-1960]	1210 [1100-1290]	1880 [838-3780]
	Complement component C8 gamma chain	*C8g*	Q8VCG4	FLFQVSR	119 [86.5-153]	192 [167-224]	405 [302-518]	108 [58.3-163]	397 [321-561]	105 [61.4-185]
	C-reactive protein	*Crp Ptx1*	P14847	AFVFPK	59,3 [51.4-68.5]	146 [109-174]	77,9 [59.3-109]	80,3 [61.7-104]	75,5 [53.6-104]	79,3 [64.5-103]
	Fibronectin	*Fn1*	P11276	SYTITGLQPGTDYK	398 [306-519]	1010 [622-1140]	469 [377-588]	548 [380-663]	464 [402-517]	521 [421-632]
	Hemoglobin subunit beta-1	*Hbb-b1*	P02088	VITAFNDGLNHLDSLK	6260 [2930-9130]	853 [422-1540]	4900 [2640-9160]	5290 [3870-7100]	3740 [1170-6610]	4800 [2860-8410]

Table 1 (continued). Top 10 discriminating proteins between mice that developed venous thrombosis following injection of small interfering RNA targeting antithrombin and protein C and their controls (siControl) between wild-type male and female mice, and between Slc44a2 / (KO) and Slc44a2 þ/þ (WT) in male and female mice

	Protein names	Gene names	UniprotKB	Peptide Sequence	Protein abundancy mean[range] (fmol/µl)					
					siControl	siAT/PC	WT male	WT female	KO male	KO female
Top 10 discriminators between female and male in WT	Adiponectin	*Adipoq*	Q60994	SAFSVGLETR	25,3 [16.8-37.7]	18,1 [13-25.3]	16 [12.9-20.1]	29,9 [24.5-37.3]	17,5 [12.2-24.6]	27,2 [20.7-36.4]
	Alpha-1-antitrypsin 1-1	*Serpina1a*	P07758	VINDFVEK	7100 [5400-9700]	6460 [4610-8400]	15400 [13400-18300]	8820 [6850-11000]	15300 [12800-19100]	9170 [7010-11800]
	Carboxypeptidase B2	*Cpb2*	Q9JHH6	YGFLLPER	62,9 [49-84.2]	89,9 [51.9-130]	99,3 [81.9-114]	72,7 [63.2-81.6]	101 [78.8-118]	76,4 [67.8-88.7]
	Complement component C8 beta chain	*C8b*	Q8BH35	GGTSEDITALAYK	129 [90.6-164]	220 [156-299]	478 [415-640]	128 [76.6-185]	516 [391-799]	133 [78.8-246]
	Complement component C8 gamma chain	*C8g*	Q8VCG4	FLFQVSR	119 [86.5-153]	192 [167-224]	405 [302-518]	108 [58.3-163]	397 [321-561]	105 [61.4-185]
	Corticosteroid-binding globulin	*Serpina6*	Q06770	DTPLTLTVLHK	1030 [729-1340]	647 [403-879]	653 [462-1040]	1400 [1240-1490]	819 [394-1090]	1550 [883-2140]
	Epidermal growth factor receptor	*Egfr*	Q01279	IPLENLQIIR	16,8 [11.3-21.4]	28,8 [20.2-46.4]	44,3 [29.2-57.2]	19,6 [10.5-24.5]	37,4 [14.8-52.5]	18,1 [11.1-33.3]
	H-2 class I histocompatibility antigen, Q10 alpha chain	*H2-Q10*	P01898	YFETSVSRPGLGEPR	292 [217-421]	256 [180-331]	623 [458-837]	345 [281-442]	677 [538-973]	374 [326-421]
	Interleukin-1 receptor accessory protein	*Il1rap*	Q61730	VAFPLEVVQK	136 [103-184]	115 [79.3-143]	263 [212-305]	167 [148-185]	258 [195-313]	164 [126-194]
	Vitamin K-dependent protein C	*Proc*	P33587	LGEYDLR	19,2 [14.3-23.5]	4,88 [2.26-7]	38,2 [32.4-45.6]	21,7 [16.8-31.5]	34,8 [25.4-38]	24,1 [19.8-32.7]

Table 1 (continued). Top 10 discriminating proteins between mice that developed venous thrombosis following injection of small interfering RNA targeting antithrombin and protein C and their controls (siControl) between wild-type male and female mice, and between Slc44a2 / (KO) and Slc44a2 þ/þ (WT) in male and female mice

	Protein names	Gene names	UniprotKB	Peptide Sequence	Protein abundancy mean[range] (fmol/µl)					
					siControl	siAT/PC	WT male	WT female	KO male	KO female
Top 10 discriminators between WT and Slc44a2 KO in female	Glycosylation-dependent cell adhesion molecule 1	*Glycam1*	Q02596	DNVVIESTKPENQEAQDGLR	5,14 [2.1-8.32]	4,76 [3.36-8.13]	0,278 [0-0.731]	5,28 [4.37-7.48]	0,666 [0.521-0.944]	8,46 [5.7-11.5]
	Interleukin-18-binding protein	*Il18bp*	Q9Z0M9	ALVLEELSPTLR	5,07 [3.71-6.57]	7,68 [5.76-9.71]	4,98 [3.8-6.96]	5,87 [5.31-6.58]	6,95 [4.61-9.85]	6,93 [6.36-7.85]
	Macrophage colony-stimulating factor 1 receptor	*Csf1r*	P09581	LEIPLNSDFQDNYYK	37,7 [30.7-51.5]	26,5 [18.1-34.4]	39,1 [31.2-50.4]	44,5 [37.6-52.7]	50,2 [37.4-73.5]	49,3 [45.6-53.5]
	Uteroglobin	*Scgb1a1*	Q06318	LVDTLPQETR	5,98 [4.47-8.58]	15,2 [5.87-50]	10,6 [6.98-15.2]	10,9 [7.63-14.9]	9,03 [7.11-12.7]	7,74 [4.76-11.2]
	Thrombospondin-1	*Thbs1*	P35441	FVFGTTPEDILR	4,5 [4.29-4.77]	4,67 [4.35-5.17]	4,84 [4.64-4.98]	5,96 [4.33-13.4]	4,56 [4.4-4.84]	4,5 [4.31-4.82]
	Ubiquitin-like protein ISG15	*Isg15*	Q64339	IGVPAFQQR	16,4 [8.44-23.6]	6,59 [3.64-13]	11,3 [6.94-18.3]	13,6 [9.1-18.4]	15,6 [8.07-22.3]	21,2 [13.9-40.8]
	Collagen alpha-1(XII) chain	*Col12a1*	Q60847	TPDEEFK	8,43 [0-11.6]	8,33 [0-11.8]	11,3 [0-14.9]	7,85 [0-11.3]	7,58 [0-11.9]	11,4 [9.71-14.9]
	Plasma kallikrein	*Klkb1*	P26262	TGAISGHSLK	55 [42.7-70.4]	39,5 [26.5-49.3]	86,8 [72.3-99.7]	68,1 [62.1-81.7]	77,2 [57.7-95.5]	60,5 [52.6-72.3]
	Complement factor H	*Cfh*	P06909	VEYSHGEVVK	10,2 [7.07-14.2]	18 [12.3-23.1]	13,2 [10.1-18.1]	11,7 [8.23-15.7]	13,6 [10.2-16.6]	14,1 [10.9-17.5]
	Ig gamma-3 chain C region	*Ighg3*	P03987	ALPAPIER	300 [9.19-491]	266 [162-373]	838 [452-1670]	1380 [212-3110]	636 [330-819]	660 [334-896]

Table 1 (continued). Top 10 discriminating proteins between mice that developed venous thrombosis following injection of small interfering RNA targeting antithrombin and protein C and their controls (siControl) between wild-type male and female mice, and between Slc44a2 / (KO) and Slc44a2 þ/þ (WT) in male and female mice

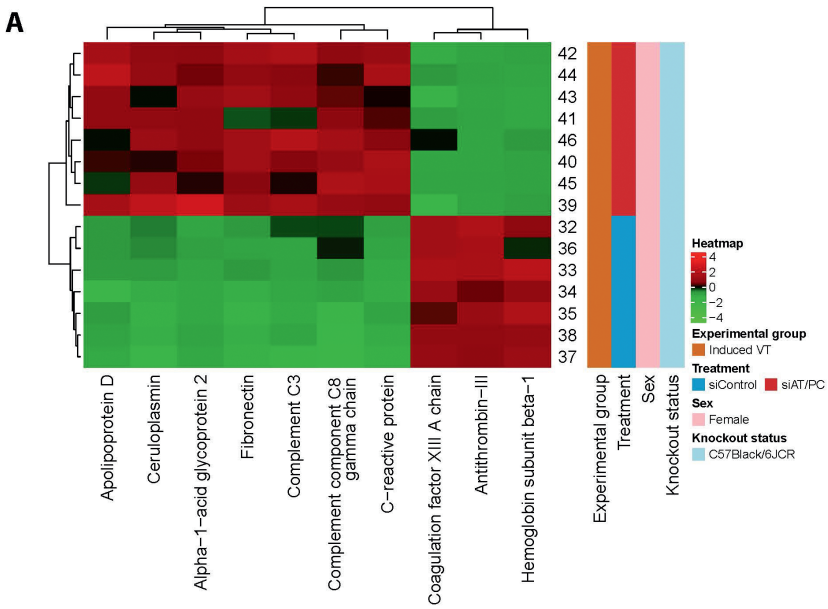
					Protein abundancy mean[range] (fmol/µl)					
	Protein names	**Gene names**	**UniprotKB**	**Peptide Sequence**	**siControl**	**siAT/PC**	**WT male**	**WT female**	**KO male**	**KO female**
Top 10 discriminators between WT and Slc44a2 KO in male	Intercellular adhesion molecule 1	*Icam1*	P13597	GEEILSR	5,87 [4.07-8.25]	7,34 [5.8-10.7]	6,87 [5.27-7.38]	8,22 [7.01-9.03]	8,59 [7.27-9.96]	8,58 [6.77-10.2]
	Glycosylation-dependent cell adhesion molecule 1	*Glycam1*	Q02596	DNVVIESTKPENQEAQDGLR	5,14 [2.1-8.32]	4,76 [3.36-8.13]	0,278 [0-0.731]	5,28 [4.37-7.48]	0,666 [0.521-0.944]	8,46 [5.7-11.5]
	Thrombospondin-1	*Thbs1*	P35441	FVFGTTPEDILR	4,5 [4.29-4.77]	4,67 [4.35-5.17]	4,84 [4.64-4.98]	5,96 [4.33-13.4]	4,56 [4.4-4.84]	4,5 [4.31-4.82]
	Apolipoprotein A-IV	*Apoa4*	P06728	SLEDLNR	2050 [1510-3000]	1800 [1480-2550]	2540 [2260-3150]	2320 [2010-2970]	3060 [2730-3420]	2340 [2040-2690]
	Complement C1s-A subcomponent	*C1sa*	Q8CG14	TTLLENAQR	53,9 [38.8-70.5]	56,1 [43.1-79]	80,7 [69.8-93.3]	57,5 [44-64.9]	68,8 [53-77.6]	64,1 [35.8-80.9]
	Retinoic acid receptor responder protein 2	*Rarres2*	Q9DD06	SLQVALEEFHK	2,27 [1.72-2.79]	1,8 [0-2.61]	3,03 [2.38-4]	2,32 [1.93-3.3]	2,46 [2.19-2.88]	2,59 [1.54-3.33]
	Alpha-1-acid glycoprotein 2	*Orm2*	P07361	IFADLIVLK	178 [82.2-378]	2410 [1550-4700]	31,1 [13.9-102]	43,7 [27.5-111]	39 [23.8-50.5]	56,3 [29.1-169]
	Histidine-rich glycoprotein	*Hrg*	Q9ESB3	FESEFPQISK	340 [251-471]	584 [370-886]	448 [398-535]	407 [274-484]	524 [438-620]	453 [328-575]
	Kunitz-type protease inhibitor 1	*Spint1*	Q9R097	YTSGFDELQNIHFLSDK	3,59 [1.87-4.58]	5,16 [4.27-6.5]	4,61 [3.44-6.42]	4,29 [3.42-5.77]	3,4 [1.63-4.5]	3,85 [2.85-5.23]
	Prenylcysteine oxidase	*Pcyox1*	Q9CQF9	YQSHDYAFSSVEK	4,34 [0-7.73]	5,81 [0-9.22]	7,33 [6.19-8.65]	5,57 [0-7.73]	8,41 [7.17-9.78]	5,64 [0-9.52]

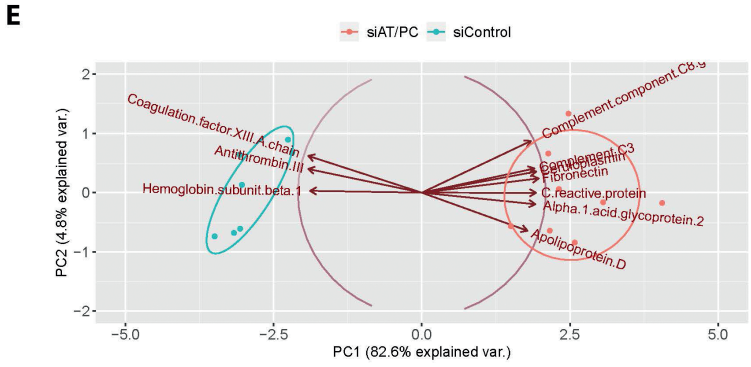
Abbreviations: KO, knockout; PC, protein C; WT, wild type; siRNA, small interfering RNA.

Effect of Slc44a2 on plasma proteome is limited

No obvious discrimination between *Slc44a2-/-* and *Slc44a2*+/+ mice was observed when all proteins were included in the clustering (Figure S2). However, limiting the analysis to the top 10 discriminating proteins between these groups (Table 1), right grouping in Slc44a2-/- and +/+ during cluster analysis for males (Figure 3C) as well as for females (Figure 3D) can be obtained with a single *Slc44a2*+/+ female outlier. PCA on these discriminatory proteins explains 44.6 and 46.2% of variance in male (Figure 3G) and female (Figure 3H), respectively. This is lower compared with the previous PCAs of the VT model as well as the discrimination between female and male. Also, the fold changes in protein levels for *Slc44a2* deficiency are smaller compared with those of VT and sex groups (Figure S3C and S3D). As observed for the male versus female comparison, for *Slc44a2* mice there is no overlap between the proteins that change most in abundance and the proteins that discriminate most for *Slc44a2* status, both in females and males.

The discriminating proteins are from multiple pathways and interestingly, thrombospondin-1 (Tsp-1) and glycosylation-dependent cell adhesion molecule-1 (Glycam-1) are present in the top 10 of both sexes. Tsp-1 is low abundant (Table 1) in plasma and only modestly reduced in plasma of *Slc44a2-/-* as compared to *Slc44a2*+/+ mice (for male and female $\log_2$ FC of -0.09 and -0.41 respectively). This protein functions in platelet signaling and its deficiency was shown to lead to decreased (arterial) thrombus formation in mice (48, 49). Signature protein Glycam-1 is higher in abundancy in *Slc44a2-/-* as compared to *Slc44a2*+/+ mice (Figure S3B, $\log_2$ FC male: 1.26 and female: 0.68). Little is known about the biological function of Glycam-1, though it was shown to be a ligand for L-selectin, expressed on endothelial cells and involved in neutrophil rolling in inflammation (50, 51). In summary, *Slc44a2* deficiency has a smaller impact on the plasma proteome compared to VT and sex, nevertheless we were able to establish a plasma proteome signature for *Slc44a2* for both male and female mice.


A
42
44
43
41
46
40
45
39
32
36
33
34
35
38
37
Heatmap
4
2
0
−2
−4
Experimental group
Induced VT
Treatment
siControl
siAT/PC
Sex
Female
Knockout status
C57Black/6JCR
Apolipoprotein D
Ceruloplasmin
Alpha−1−acid glycoprotein 2
Fibronectin
Complement C3
Complement component C8 gamma chain
C−reactive protein
Coagulation factor XIII A chain
Antithrombin−III
Hemoglobin subunit beta−1
Experimental group
Treatment
Sex
Knockout status


E
siAT/PC
siControl
Coagulation.factor.XIII.A.chain
Antithrombin.III
Hemoglobin.subunit.beta.1
Complement.component.C8.g
Complement.C3
Ceruloplasmin
Fibronectin
C.reactive.protein
Alpha.1.acid.glycoprotein.2
Apolipoprotein.D
PC2 (4.8% explained var.)
PC1 (82.6% explained var.)
2
1
0
−1
−2
−5.0
−2.5
0.0
2.5
5.0

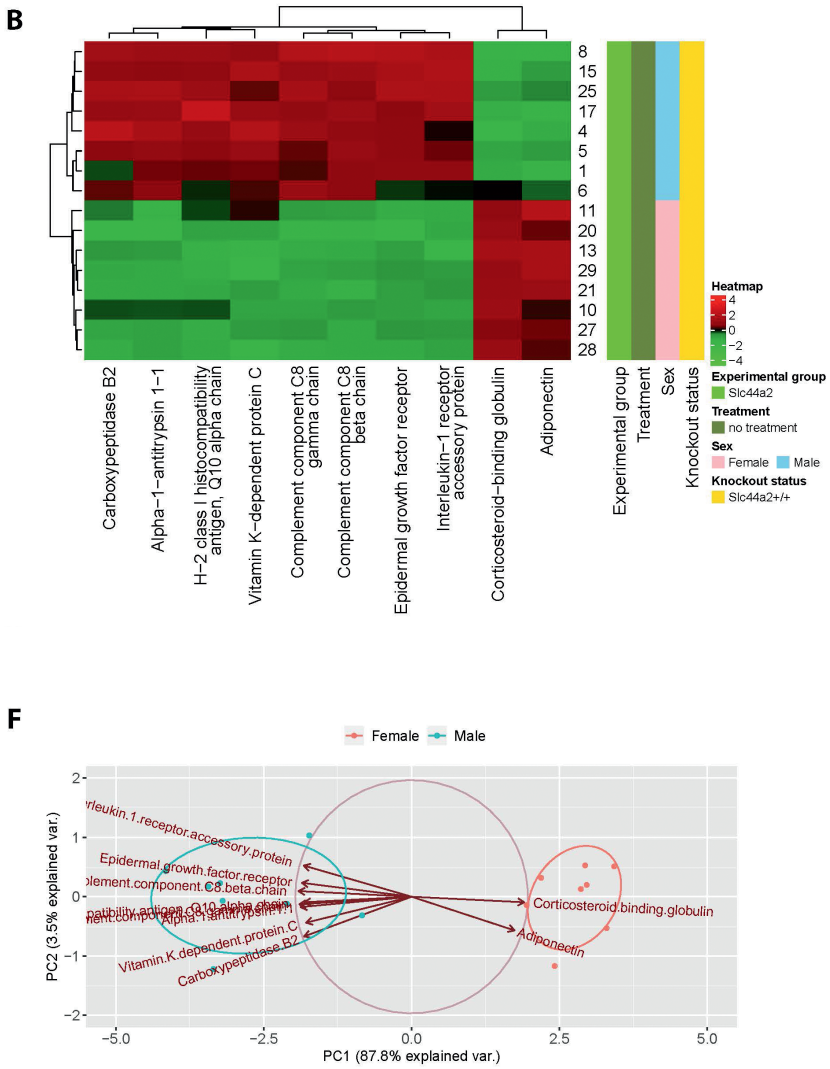
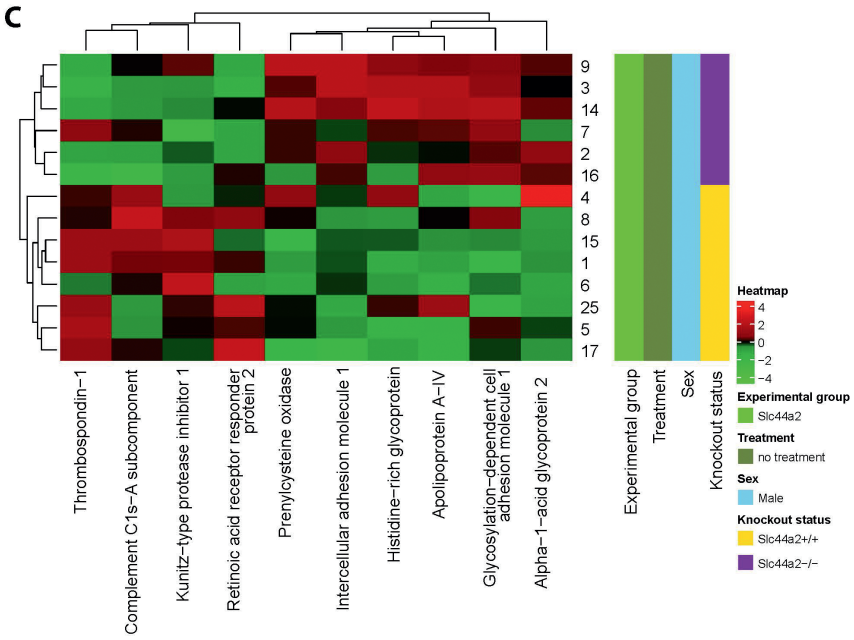
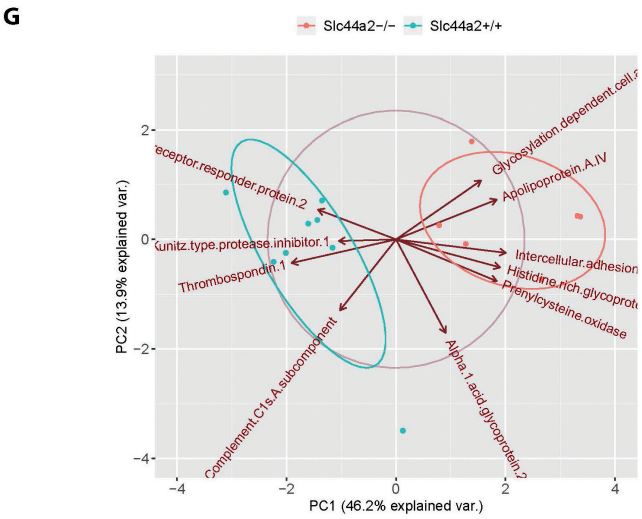


Figure 3. Discrimination between the various study groups based on the plasma abundance of the selected top 10 discriminating proteins in each group (Table 1). Discriminations are illustrated using hieratical clustering and heatmaps **(A-D)** as well as corresponding principle component analysis **(E-H)**. N=8 for female wild-type mice (*Slc44a2*+/+), N=8 for female *Slc44a2* deficient mice (*Slc44a2*-/-), N=8 for male *Slc44a2*+/+, N=6 for male *Slc44a2*-/-, N=8 for siRNA targeting antithrombin and protein C (siAT/PC), and N=7 for siControl. **(A)** and **(E)** show the results for siAT/PC treated mice and their controls (siControl). **(B)** and **(F)** show the discrimination between the wild type male and female mice.


C
9
3
14
7
2
16
4
8
15
1
6
25
5
17
Thrombospondin−1
Complement C1s−A subcomponent
Kunitz−type protease inhibitor 1
Retinoic acid receptor responder protein 2
Prenylcysteine oxidase
Intercellular adhesion molecule 1
Histidine−rich glycoprotein
Apolipoprotein A−IV
Glycosylation−dependent cell adhesion molecule 1
Alpha−1−acid glycoprotein 2
Experimental group
Treatment
Sex
Knockout status
Heatmap
4
2
0
−2
−4
Experimental group
Slc44a2
Treatment
no treatment
Sex
Male
Knockout status
Slc44a2+/+
Slc44a2−/−


G
Slc44a2−/−
Slc44a2+/+
Glycosylation.dependent.cell.a
Apolipoprotein.A.IV
Intercellular.adhesion
Histidine.rich.glycoprote
Prenylcysteine.oxidase
Alpha.1.acid.glycoprotein.2
Complement.C1s.A.subcomponent
Thrombospondin.1
unitz.type.protease.inhibitor.1
eceptor.responder.protein.2
PC2 (13.9% explained var.)
PC1 (46.2% explained var.)
2
0
−2
−4
−4
−2
0
2
4

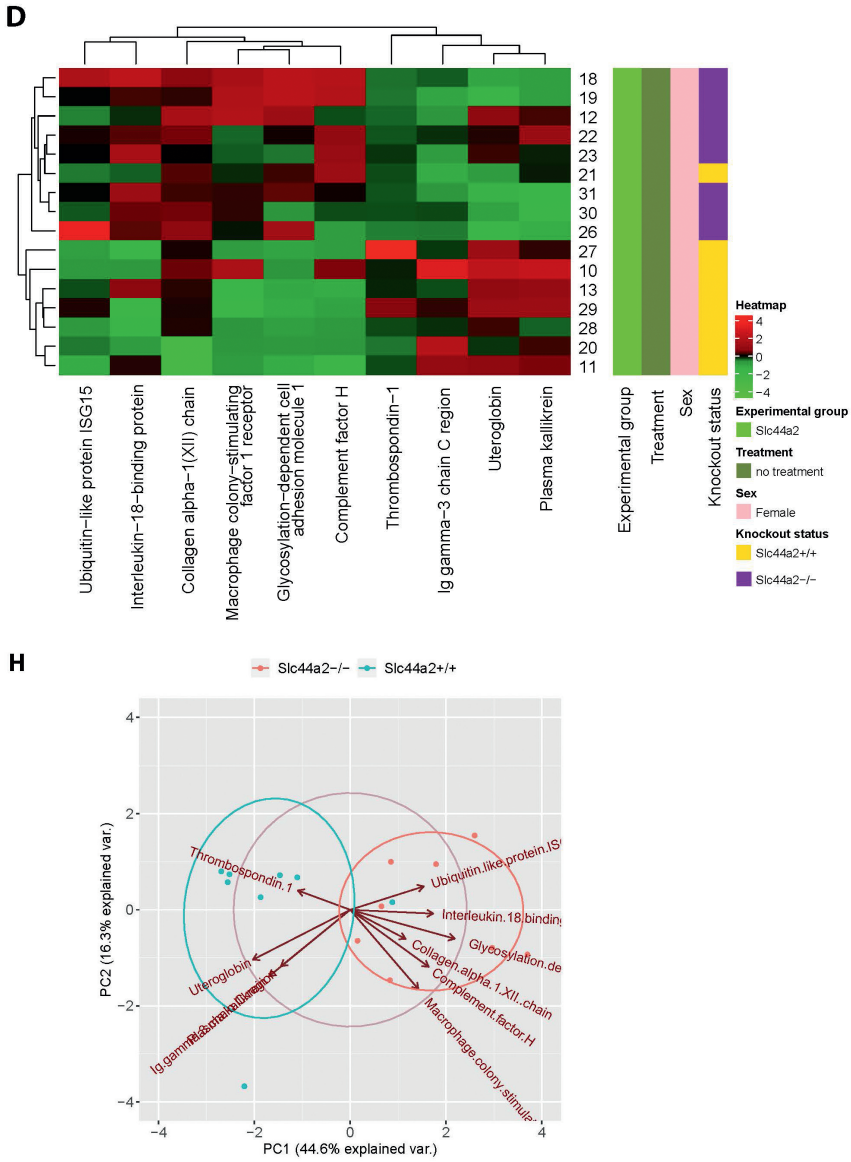


Figure 3 (continued). Discrimination between the various study groups based on the plasma abundance of the selected top 10 discriminating proteins in each group (Table 1). Discriminations are illustrated using hieratical clustering and heatmaps **(A-D)** as well as corresponding principle component analysis **(E-H)**. N=8 for female wild-type mice (*Slc44a2+/+*), N=8 for female *Slc44a2* deficient mice (*Slc44a2-/-*), N=8 for male *Slc44a2+/+*, N=6 for male *Slc44a2-/-*, N=8 for siRNA targeting antithrombin and protein C (siAT/PC), and N=7 for siControl. **(C)** and **(G)**, as well as **(D)** and **(H)** show the discrimination between *Slc44a2+/+* and *Slc44a2-/-* in male and female respectively. PC, protein C; AT, antithrombin; siRNA, small interfering RNA.

Discussion

We investigated the possible plasma protein signatures in mice following the onset of VT and in mice lacking Slc44a2 which was recently characterized as a VT-susceptibility gene in human GWAS. We used 375 validated multiplexed MS-based protein assays to measure the plasma protein levels. The mouse model where VT follows RNA interference mediated silencing of antithrombin and protein C was included as it features a strong VT phenotype, coinciding with strong clinical signs. Upon VT numerous plasma proteins changed yielding a strong protein signature that was easily measurable using our method. Furthermore, profile (dis)similarities according to intervention demonstrated the capability of the method in capturing plasma protein dynamic. In mice lacking *Slc44a2,* the protein signatures were primarily overruled by the differences between male and female and not the absent gene. By looking in each group separately, modest alteration of two proteins was identified in males and females lacking *Slc44a2*. This indicates that the link between SLC44A2 and VT is outside traditional coagulation- and fibrinolysis-related pathways. Possibly, SLC44A2 affects (blood) cell-cell interactions as reflected Glycam1 and L-selectin being part of gene signature.

In addition to serving as validation experiment, the strong signature obtained for the mouse VT model also provided novel insights into this model. The presence of APPs (haptoglobin, fibrinogen, c-reactive protein, ceruloplasmin, fibronectin, alpha-1-acid glycoprotein 2, complement C3, complement C8, SAa2, SAa1, SAa4 and SAp) among the signature for VT indicate that the VT following silencing of natural anticoagulants has a more systemic and acute impact than currently known. The microscopically visible VT is confined to the large veins of the head is characterized among others by a strong recruitment and influx of leukocytes (32). Whether the local recruitment of leukocytes is causing the systemic acute phase response or this is a secondary effect is subject to speculation. Apart from leukocytes, another major constituent of the thrombi in the large veins of the head is trapped and recruited erythrocytes (32). In addition, erythrocytes extravasate upon rupture of the occluded veins. Circulating hemoglobulin and haptoglobin levels (inversely) relate to blood erythrocyte numbers, and may explain why the plasma levels change when erythrocyte-rich thrombi are formed in the head. We expected that the coagulation factors, which were included in the assay, should be among the signature proteins for VT as these may drop in circulating levels being consumed at the expense of thrombus formation. Coagulation factor XIII (FXIII, both FXIIIa and FXIIIb subunits) is the only coagulation protein among the top 10 discriminatory proteins for VT. FXIII is a well-known contributor to fibrin network formation and stabilization (52). In addition, Factor XIII is involved in (fibrin-mediated) erythrocyte retention in venous thrombi (53, 54). The drop in plasma FXIII levels possibly reflects trapping of the FXIII protein in the fibrin-network of the formed thrombi. Hence, it would be interesting to determine the (critical) role of this protein in this model of VT for example by subjecting FXIII knockout mice to the model.

Although the impact of sex overruled the effect *Slc44a2*, we obtained a specific *Slc44a2* signature focusing on most discriminating proteins The proteins involved in these sex-specific signatures have not yet been subject to investigation with respect to control by sex hormones (estrogens and testosterone). Hence, whether these strong male-female differences are a direct result of regulation, or an indirect effect caused by for example differences in body weight, plasma volume, organ size and function can only be speculated. A recent study aimed at determining plasma proteome dynamics in different laboratory mouse strains including C57BL/6J (26) found complement C8 gamma and beta chain, Epidermal growth factor receptor and corticosteroid-binding globulin among the plasma proteins that discriminated males from females, which is in line with our findings using mice of the same background. In a mouse study focusing on sex specific liver gene expression epidermal growth factor receptor and complement factor 8 were found to be different between males and females for liver transcript also in line with our findings in plasma (55). Future studies into the origin of the strong sex-specific plasma protein signature are of interest. For the present study, sex is a major determinant of the plasma proteome and therefore males and females should essentially be considered as two different groups.

Slc44a2 deficient mice appear normal and so far impact on disease (hearing loss, VT) only became apparent upon challenges (13, 14). Hence, the very modest impact of *Slc44a2* deficiency on the plasma proteome supports the concept that SLC44A2 has a limited role in normal physiology, or one that can be compensated for. In the top 10 discriminating proteins for *Slc44a2* two proteins were present in both females and males, i.e. Tsp-1 and Glycam-1. Tsp-1 plasma abundance was lower in *Slc44a2* deficient mice. Tsp-1 is an adhesive glycoprotein that mediates cell-to-cell and cell-to-matrix interactions, first identified as a component of the secreted product of activated platelets (56). Tsp-1 was previously linked to thrombosis, as its absence delays thrombus formation in mice (48, 49). Part of these Tsp-1 effects require interaction with VWF. SLC44A2 also interacts with VWF (12) and we observed a modest decrease in VWF abundance in *Slc44a2* deficient mice before (14). For future studies on the role of SLC44A2 in VT and its possible interaction with VWF it is recommended to investigate Tsp-1. Glycam-1 abundance was higher in Slc44a2 deficient mice. Glycam-1 has not been linked to thrombosis before, it was however shown to be a ligand for L-selectin, expressed on endothelial cells, and involved in neutrophil rolling in inflammation (50, 51). In general, selectins (including also P- and E-selectins) are important in mediating interactions between leukocytes and the vessel wall and P- and E-selectin are well-known player in thrombosis. In future studies on SLC44A2, it is worthwhile to investigate possible roles of Glycam1 and L-selectin. In summary no major effect of *Slc44a2* deficiency in plasma was found. The minimal effect observed involves changes in Glycam-1 and tsp-1 plasma levels, which suggest a mechanism related to cell-cell interactions. Observations regarding the role of SLC44A2 in experimental VT in mice (unpublished work) showed that *Slc44a2* deficiency does not influence VT driven by hypercoagulability (31, 32). *Slc44a2* deficient mice do however display reduced thrombus formation following flow restriction (57) where inflammatory cells from the blood, including neutrophils and platelets, are important

contributors (58, 59). Moreover, it was recently demonstrated that platelets primed by VWF display activated integrin $\alpha_{IIb}\beta_3$ (but not CD62P), which can then bind neutrophil SLC44A2 and mediate NETosis under venous flow (60), suggesting that SLC44A2 is a mediator of cell-cell interactions. Therefore, we suggest incorporating the cellular compartment of the blood in further investigation of the effect of SLC44A2 on VT. To elucidate the contribution of SLC44A2 on the different cell types, cell specific knockouts of *Slc44a2* might be interesting to include.

A strength of MS-based targeted proteomics assays is specificity. Each assay is designed to target a specific peptide with multi-level of assurance. However, the measured endogenous peptide can also be originated from degradation products or inactive forms of the protein. It is possible to design an experiment with multiple peptides per proteins (28) to infer information on the level of protein (in)activity; however, this was not considered in the current study. Nonetheless, quantitative-targeted proteomics allowed detecting subtle changes in abundance of plasma proteins in murine VT research for which currently no traditional (antibody-based) assays are available. Besides unspecificity, the antibody assays that are available for mouse require substantial amounts of plasma making measurement of multiple protein levels from one sample not feasible. For example, when we examined available Tsp-1 antibody assay, these required up to 200 µL plasma, which was unavailable from each mouse, compared with less than 10 µl for MS. The high multiplicity and precision allow determining the abundances of hundreds of proteins with standardized sample processing, producing a sharp snapshot of the targeted proteins in the samples. Using simple data analysis method like correlation, hierarchical clustering, and PCA allow generating clear signatures of conditions and protein signatures were generated for a VT model, sex and a *Slc44a2* deficient mice.

Disclosure of Conflicts of Interest

J.T., C.X.M., H.H.V. and B.J.M.V.V. report grants from Trombosestichting Nederland, grants from Landsteiner Foundation for Blood Transfusion Research, during the conduct of the study. C.H.B. reports grants from Genome Canada and Genome British Columbia, during the conduct of the study; personal fees and other from MRM proteomics, nonfinancial support from Creative Molecules, personal fees from Molecular You, outside the submitted work. C.H.B. is the chief strategy officer of MRM Proteomics, Inc. Y.M. reports grants from Genome Canada; Genome British Columbia, during the conduct of the study.

Acknowledgments

The authors thank Thankam S. Nair, Pavan K. Kommareddi, and Thomas E. Carey (University of Michigan, Ann Arbor, MI, USA) for the development and provision of the *Slc44a2* deficient mice.

Author contributions

Experimental design: J.T, B.J.M.v.V., Y.M. Sample collection J.T., B.J.M.v.V. MRM experiments: S.A.M and Y.M. Data analysis and visualization: J.T. and Y.M., results interpretation and first draft of the manuscript J.T., B.J.M.v.V., Y.M. All authors commented on manuscript drafts and contributed to the text.

References

1. Furie B, Furie BC. Mechanisms of thrombus formation. *N Engl J Med*. 2008;359(9):938-49.
2. Rosendaal FR. Venous thrombosis: the role of genes, environment, and behavior. *Hematology Am Soc Hematol Educ Program*. 2005:1-12.
3. Tripodi A. Levels of coagulation factors and venous thromboembolism. *Haematologica*. 2003;88(6):705-11.
4. Rosendaal FR. Causes of venous thrombosis. *Thromb J*. 2016;14(Suppl 1):24.
5. Germain M, Chasman DI, de Haan H, et al. Meta-analysis of 65,734 individuals identifies TSPAN15 and SLC44A2 as two susceptibility loci for venous thromboembolism. *Am J Hum Genet*. 2015;96(4):532-42.
6. Roumen-Klappe EM, den Heijer M, van Uum SH, et al. Inflammatory response in the acute phase of deep vein thrombosis. *J Vasc Surg*. 2002;35(4):701-6.
7. Fox EA, Kahn SR. The relationship between inflammation and venous thrombosis. A systematic review of clinical studies. *Thromb Haemost*. 2005;94(2):362-5.
8. Conway EM. Reincarnation of ancient links between coagulation and complement. *J Thromb Haemost*. 2015;13 Suppl 1:S121-32.
9. Mosevoll KA, Lindas R, Tvedt TH, et al. Altered plasma levels of cytokines, soluble adhesion molecules and matrix metalloproteases in venous thrombosis. *Thromb Res*. 2015;136(1):30-9.
10. Morelli VM, Lijfering WM, Bos MHA, et al. Lipid levels and risk of venous thrombosis: results from the MEGA-study. *Eur J Epidemiol*. 2017;32(8):669-81.
11. Hinds DA, Buil A, Ziemek D, et al. Genome-wide association analysis of self-reported events in 6135 individuals and 252 827 controls identifies 8 loci associated with thrombosis. *Hum Mol Genet*. 2016;25(9):1867-74.
12. Bayat B, Tjahjono Y, Berghofer H, et al. Choline Transporter-Like Protein-2: New von Willebrand Factor-Binding Partner Involved in Antibody-Mediated Neutrophil Activation and Transfusion-Related Acute Lung Injury. *Arterioscler Thromb Vasc Biol*. 2015;35(7):1616-22.
13. Kommareddi P, Nair T, Kakaraparthi BN, et al. Hair Cell Loss, Spiral Ganglion Degeneration, and Progressive Sensorineural Hearing Loss in Mice with Targeted Deletion of Slc44a2/Ctl2. *J Assoc Res Otolaryngol*. 2015;16(6):695-712.
14. Tilburg J, Adili R, Nair TS, et al. Characterization of hemostasis in mice lacking the novel thrombosis susceptibility gene Slc44a2. *Thromb Res*. 2018;171:155-9.
15. Geyer PE, Kulak NA, Pichler G, et al. Plasma Proteome Profiling to Assess Human Health and Disease. *Cell Syst*. 2016;2(3):185-95.
16. Huttenhain R, Choi M, Martin de la Fuente L, et al. A Targeted Mass Spectrometry Strategy for Developing Proteomic Biomarkers: A Case Study of Epithelial Ovarian Cancer. *Mol Cell Proteomics*. 2019;18(9):1836-50.
17. Niu L, Geyer PE, Wewer Albrechtsen NJ, et al. Plasma proteome profiling discovers novel proteins associated with non-alcoholic fatty liver disease. *Mol Syst Biol*. 2019;15(3):e8793.
18. Pimienta G, Heithoff DM, Rosa-Campos A, et al. Plasma Proteome Signature of Sepsis: a Functionally Connected Protein Network. *Proteomics*. 2019;19(5):e1800389.

19. Wewer Albrechtsen NJ, Geyer PE, Doll S, et al. Plasma Proteome Profiling Reveals Dynamics of Inflammatory and Lipid Homeostasis Markers after Roux-En-Y Gastric Bypass Surgery. *Cell Syst*. 2018;7(6):601-12 e3.
20. Terfve C, Sabido E, Wu Y, et al. System-Wide Quantitative Proteomics of the Metabolic Syndrome in Mice: Genotypic and Dietary Effects. *Journal of proteome research*. 2017;16(2):831-41.
21. Liumbruno GM, Franchini M. Proteomic analysis of venous thromboembolism: an update. *Expert Rev Proteomics*. 2013;10(2):179-88.
22. Lippi G, Favaloro EJ, Plebani M. Proteomic analysis of venous thromboembolism. *Expert Rev Proteomics*. 2010;7(2):275-82.
23. Bruzelius M, Iglesias MJ, Hong MG, et al. PDGFB, a new candidate plasma biomarker for venous thromboembolism: results from the VEREMA affinity proteomics study. *Blood*. 2016;128(23):e59-e66.
24. Ganesh SK, Sharma Y, Dayhoff J, et al. Detection of venous thromboembolism by proteomic serum biomarkers. *PLoS One*. 2007;2(6):e544.
25. Stachowicz A, Siudut J, Suski M, et al. Optimization of quantitative proteomic analysis of clots generated from plasma of patients with venous thromboembolism. *Clin Proteomics*. 2017;14:38.
26. Michaud SA, Sinclair NJ, Petrosova H, et al. Molecular phenotyping of laboratory mouse strains using 500 multiple reaction monitoring mass spectrometry plasma assays. *Commun Biol*. 2018;1:78.
27. Ding J, Berryman DE, Jara A, et al. Age- and sex-associated plasma proteomic changes in growth hormone receptor gene-disrupted mice. *J Gerontol A Biol Sci Med Sci*. 2012;67(8):830-40.
28. Mohammed Y, van Vlijmen BJ, Yang J, et al. Multiplexed targeted proteomic assay to assess coagulation factor concentrations and thrombosis-associated cancer. *Blood Adv*. 2017;1(15):1080-7.
29. Mohammed Y, Pan J, Zhang S, et al. ExSTA: External Standard Addition Method for Accurate High-Throughput Quantitation in Targeted Proteomics Experiments. *Proteomics Clin Appl*. 2018;12(2).
30. Addona TA, Abbatiello SE, Schilling B, et al. Multi-site assessment of the precision and reproducibility of multiple reaction monitoring-based measurements of proteins in plasma. *Nat Biotechnol*. 2009;27(7):633-41.
31. Safdar H, Cheung KL, Salvatori D, et al. Acute and severe coagulopathy in adult mice following silencing of hepatic antithrombin and protein C production. *Blood*. 2013;121(21):4413-6.
32. Heestermans M, Salloum-Asfar S, Streef T, et al. Mouse venous thrombosis upon silencing of anticoagulants depends on tissue factor and platelets, not FXII or neutrophils. *Blood*. 2019;133(19):2090-9.
33. Cleuren AC, Van der Linden IK, De Visser YP, et al. 17alpha-Ethinylestradiol rapidly alters transcript levels of murine coagulation genes via estrogen receptor alpha. *J Thromb Haemost*. 2010;8(8):1838-46.
34. Schwenk JM, Omenn GS, Sun Z, et al. The Human Plasma Proteome Draft of 2017: Building on the Human Plasma PeptideAtlas from Mass Spectrometry and Complementary Assays. *Journal of proteome research*. 2017;16(12):4299-310.
35. Bhowmick P, Mohammed Y, Borchers CH. MRMAssayDB: an integrated resource for validated targeted proteomics assays. *Bioinformatics*. 2018;34(20):3566-71.

36. Mohammed Y, Bhowmick P, Smith DS, et al. PeptideTracker: A knowledge base for collecting and storing information on protein concentrations in biological tissues. *Proteomics*. 2017;17(7).
37. Mohammed Y, Domanski D, Jackson AM, et al. PeptidePicker: a scientific workflow with web interface for selecting appropriate peptides for targeted proteomics experiments. *J Proteomics*. 2014;106:151-61.
38. Percy AJ, Chambers AG, Yang J, et al. Advances in multiplexed MRM-based protein biomarker quantitation toward clinical utility. *Biochim Biophys Acta*. 2014;1844(5):917-26.
39. MacLean B, Tomazela DM, Shulman N, et al. Skyline: an open source document editor for creating and analyzing targeted proteomics experiments. *Bioinformatics*. 2010;26(7):966-8.
40. Ward JH. Hierarchical Grouping to Optimize an Objective Function. *J Am Stat Assoc*. 1963;58(301):236-&.
41. Murtagh F, Legendre P. Ward's Hierarchical Agglomerative Clustering Method: Which Algorithms Implement Ward's Criterion? *J Classif*. 2014;31(3):274-95.
42. Zhang Q, Menon R, Deutsch EW, et al. A mouse plasma peptide atlas as a resource for disease proteomics. *Genome Biol*. 2008;9(6):R93.
43. Scheurer B, Rittner C, Schneider PM. Expression of the human complement C8 subunits is independently regulated by interleukin 1 beta, interleukin 6, and interferon gamma. *Immunopharmacology*. 1997;38(1-2):167-75.
44. Gruys E, Toussaint MJ, Niewold TA, et al. Acute phase reaction and acute phase proteins. *J Zhejiang Univ Sci B*. 2005;6(11):1045-56.
45. Schreiber G, Tsykin A, Aldred AR, et al. The acute phase response in the rodent. *Ann N Y Acad Sci*. 1989;557:61-85; discussion -6.
46. Ohman-Hanson RA, Cree-Green M, Kelsey MM, et al. Ethnic and Sex Differences in Adiponectin: From Childhood to Adulthood. *J Clin Endocrinol Metab*. 2016;101(12):4808-15.
47. Gaya da Costa M, Poppelaars F, van Kooten C, et al. Age and Sex-Associated Changes of Complement Activity and Complement Levels in a Healthy Caucasian Population. *Front Immunol*. 2018;9:2664.
48. Prakash P, Kulkarni PP, Chauhan AK. Thrombospondin 1 requires von Willebrand factor to modulate arterial thrombosis in mice. *Blood*. 2015;125(2):399-406.
49. Bonnefoy A, Daenens K, Feys HB, et al. Thrombospondin-1 controls vascular platelet recruitment and thrombus adherence in mice by protecting (sub)endothelial VWF from cleavage by ADAMTS13. *Blood*. 2006;107(3):955-64.
50. Lasky LA, Singer MS, Dowbenko D, et al. An endothelial ligand for L-selectin is a novel mucin-like molecule. *Cell*. 1992;69(6):927-38.
51. Dwir O, Shimron F, Chen C, et al. GlyCAM-1 supports leukocyte rolling in flow: evidence for a greater dynamic stability of L-selectin rolling of lymphocytes than of neutrophils. *Cell Adhes Commun*. 1998;6(4):349-70.
52. Wolberg AS. Fibrinogen and factor XIII: newly recognized roles in venous thrombus formation and composition. *Curr Opin Hematol*. 2018;25(5):358-64.
53. Byrnes JR, Duval C, Wang Y, et al. Factor XIIIa-dependent retention of red blood cells in clots is mediated by fibrin alpha-chain crosslinking. *Blood*. 2015;126(16):1940-8.
54. Aleman MM, Byrnes JR, Wang JG, et al. Factor XIII activity mediates red blood cell retention in venous thrombi. *J Clin Invest*. 2014;124(8):3590-600.

55. Conforto TL, Waxman DJ. Sex-specific mouse liver gene expression: genome-wide analysis of developmental changes from pre-pubertal period to young adulthood. *Biol Sex Differ*. 2012;3:9.
56. Jurk K, Clemetson KJ, de Groot PG, et al. Thrombospondin-1 mediates platelet adhesion at high shear via glycoprotein Ib (GPIb): an alternative/backup mechanism to von Willebrand factor. *FASEB J*. 2003;17(11):1490-2.
57. von Bruhl ML, Stark K, Steinhart A, et al. Monocytes, neutrophils, and platelets cooperate to initiate and propagate venous thrombosis in mice in vivo. *J Exp Med*. 2012;209(4):819-35.
58. Maracle CX TJ, Zirka G, Morange PE, van Vlijmen BJM, Thomas GM. Slc44a2 deficient mice exhibit less severity of thrombosis in a stenosis model of DVT. *International Society on Thrombosis & Hemostasis: Research and Practice in Thrombosis and Haemostasis Melboure, Australia, 2019*
59. Maracle CX TJ, Zirka G, van den Heijkant L, Morange PE, van Vlijmen BJM, Thomas GM. Slc44a2 deficient mice exhibit less severity of thrombosis in a stenosis model of DVT. *European Congress on Thrombosis and Haemostasis, Marseille, France, 2018*
60. Constantinescu-Bercu A, Grassi L, Frontini M, et al. Activated αIIbβ3 on platelets mediates flow-dependent NETosis via SLC44A2. *bioRxiv*. 2019:373670.

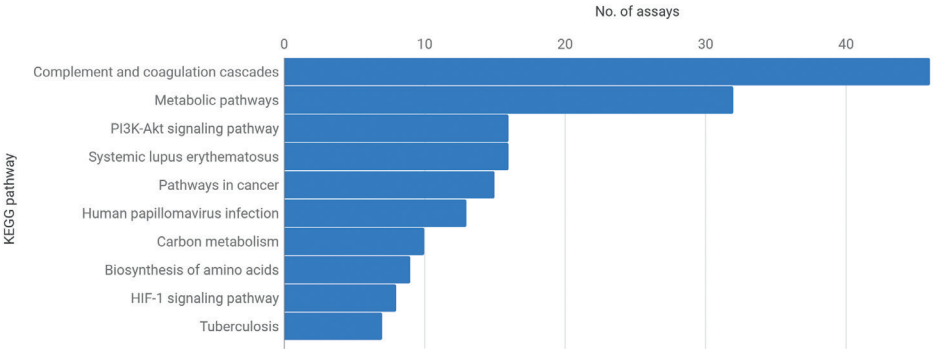


Figure S1. The top 10 biological pathways covered by the used protein assays.

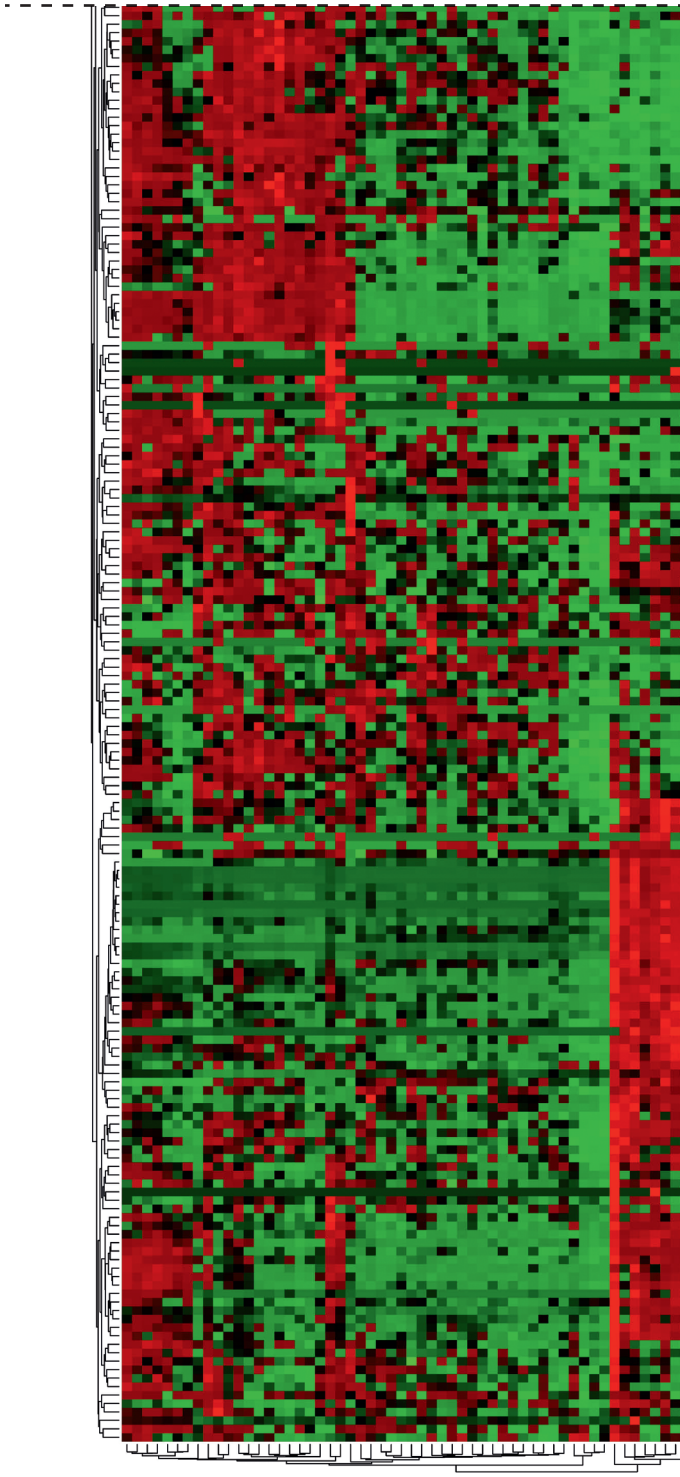


Figure S2. Heatmap showing protein profiles across all included samples annotated with metadata on the experiment, treatment (no treatment, siAT/PC, siControl), sex, and Slc44a2 status (SLC44A2 WT and KO).

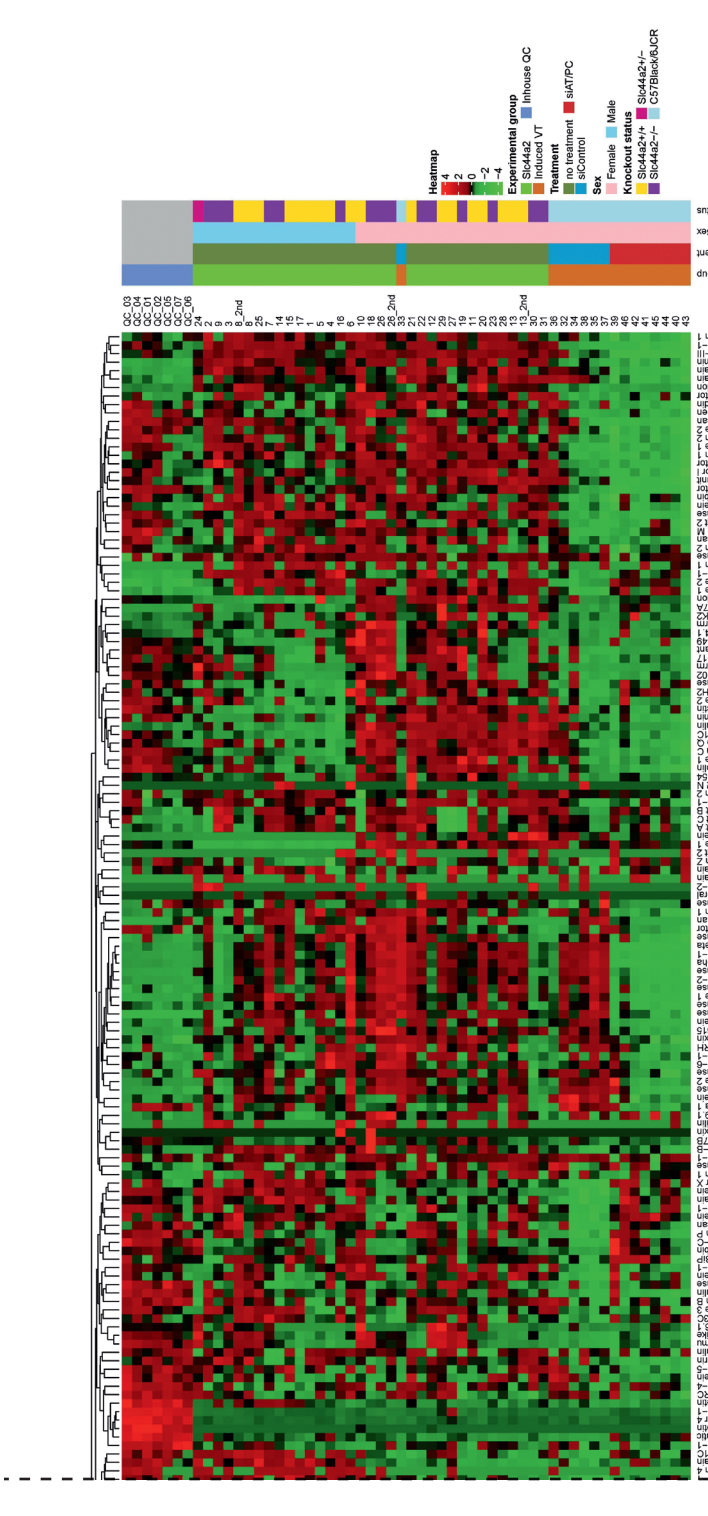


Figure S2 (continued). Heatmap showing protein profiles across all included samples annotated with metadata on the experiment, treatment (no treatment, siAT/PC, siControl), sex, and Slc44a2 status (SLC44A2 WT and KO).

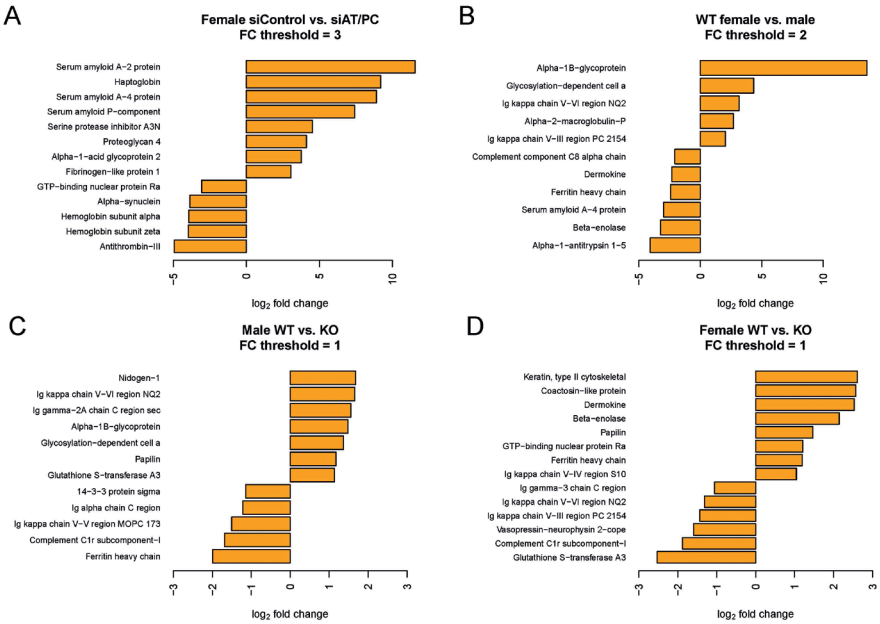


Figure S3. Fold changes in protein abundancy of (A) siAT/PC vs. siControl proteins with higher fold changes than log2 3 are displayed. (B) male vs. female proteins with higher fold changes than log2 2 are displayed. (C) male Slc44a2-/- (KO) vs. male Slc44a12+/+ (WT) proteins with higher fold changes than log2 1 are displayed. (D) female Slc44a2-/- (KO) vs. female Slc44a2+/+ (WT) proteins with higher fold changes than log2 1 are displayed.

Table S1 Proteins and surrogate peptides used in our quantitative targeted proteomics method

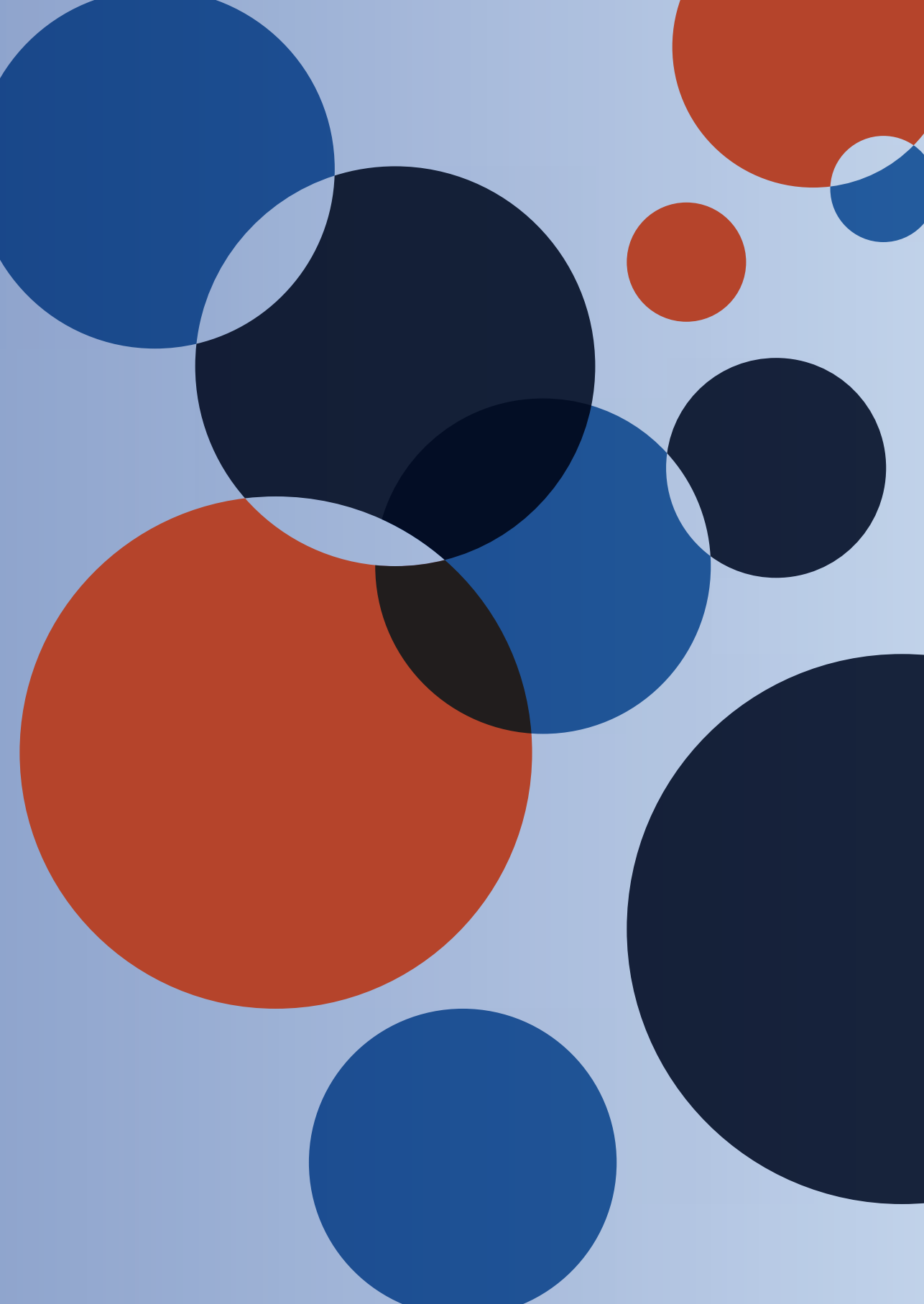
Table is available in online supplement.

Table S2. Weight change of mice treated with siAT/PC and siControl.

					Weigth (gram)					
Mouse #	Strain	Sex	Age (weeks)	Treatment	at siRNA injection	24 hrs post injection	32 hrs post injection	At sacrifice	Delta (injection to sacrifice)	Clinical signs (hr. post injection)
32	C57BLACK/6J	Female	6	siControl	21,4	21,3	21,7	21,1	-0,3	N/A
33	C57BLACK/6J	Female	6	siControl	18,7	19,2	19,7	19,8	1,1	N/A
34	C57BLACK/6J	Female	6	siControl	20,7	21,1	21,4	21,9	1,2	N/A
35	C57BLACK/6J	Female	6	siControl	21,9	22,0	22,0	22,3	0,4	N/A
36	C57BLACK/6J	Female	6	siControl	21,1	20,9	21,3	20,7	-0,4	N/A
37	C57BLACK/6J	Female	6	siControl	21,6	20,5	20,8	21,3	-0,3	N/A
38	C57BLACK/6J	Female	6	siControl	20,0	20,0	20,7	20,6	0,6	N/A
39	C57BLACK/6J	Female	6	siAT/PC	18,7	17,9	17,4	16,1	-2,6	65
40	C57BLACK/6J	Female	6	siAT/PC	20,7	20,4	20,8	18,4	-2,3	65
41	C57BLACK/6J	Female	6	siAT/PC	19,9	19,9	18,9	18,2	-1,7	44
42	C57BLACK/6J	Female	6	siAT/PC	20,9	20,6	20,1	17,5	-3,4	65
43	C57BLACK/6J	Female	6	siAT/PC	19,5	19,5	19,3	17,2	-2,3	65
44	C57BLACK/6J	Female	6	siAT/PC	21,1	20,6	19,3	18,7	-2,4	44
45	C57BLACK/6J	Female	6	siAT/PC	20,7	21,1	21,6	19,3	-1,4	65
46	C57BLACK/6J	Female	6	siAT/PC	20,0	20,0	20,4	18,3	-1,7	66

Table S3. Weight of the *Slc44a2* KO mice as well as wild type littermates at sacrifice.

Mouse #	Age (weeks)	Sex	Genotype	Body weigth at sacrifice (gram)
11	15	Female	WT	24,8
21	15	Female	WT	22,5
10	15	Female	WT	21,2
27	15	Female	WT	18,3
20	15	Female	WT	23,3
13	15	Female	WT	23,5
28	15	Female	WT	20,1
29	15	Female	WT	20,4
22	15	Female	KO	21,3
31	15	Female	KO	22,7
12	15	Female	KO	21,9
18	15	Female	KO	22,5
23	15	Female	KO	22,2
26	15	Female	KO	21,4
19	15	Female	KO	21,9
30	15	Female	KO	24,9
6	15	Male	WT	28,3
17	15	Male	WT	28,9
1	15	Male	WT	27,2
15	15	Male	WT	30,7
25	15	Male	WT	28,4
4	15	Male	WT	29,7
8	15	Male	WT	31,7
5	15	Male	WT	31,1
24	15	Male	HET	27,0
14	15	Male	KO	35,2
16	15	Male	KO	31,2
3	15	Male	KO	30,5
9	15	Male	KO	24,7
2	15	Male	KO	29,6
7	15	Male	KO	27,7



SLC44A2/HNA-3A IS INVOLVED IN NEUTROPHIL ADHESION AND ACTIVATION TO VON WILLEBRAND FACTOR IN HUMANS AND MICE

Gaïa Zirka, Julia Tilburg, Philippe Robert, Chrissta X. Maracle, Bart J.M. van Vlijmen, Paulette Legendre, Marie-Christine Alessi, Peter J. Lenting, Pierre-Emmanuel Morange and Grace M. Thomas

Manuscript under revision.

5

Abstract

Background

Genome wide association studies linked expression of the HNA-3a (human neutrophil antigen-3a) epitope on the solute carrier family 44 member 2 (SLC44A2) protein with venous thrombosis (VT) in humans. Expression of the HNA-3b is associated with a 30% decreased risk of VT. SLC44A2 is a ubiquitous transmembrane protein identified as a receptor for Von Willebrand factor (VWF).

Aims

To explain the link between SLC44A2 and VT we wanted to determine how SLC44A2 expressing either HNA-3a or HNA-3b on neutrophils could modulate their adhesion and activation on VWF under flow.

Methods

Transfected HEK293T cells or neutrophils homozygous for the HNA-3a- or the HNA-3b-coding allele purified from healthy donors were perfused in flow chambers at venous shear rates ($100s^{-1}$). Different matrices including VWF and blocking antibodies were tested. Neutrophil activation by lipopolysaccharide (LPS) was evaluated at various cell concentrations in different flow conditions. Neutrophil mobilization was also measured by intravital microscopy in venules from SLC44A2 deficient mice and wildtype controls after histamine-induced endothelial degranulation and anti-Ly6G staining.

Results

HNA-3a expression was required for SLC44A2-mediated neutrophil adhesion to VWF at $100s^{-1}$. This adhesion could occur independently of beta-2 integrin engagement. We observed that adhesion of HNA-3a-expressing neutrophils was enhanced when they were preactivated with LPS. Moreover, specific shear conditions could act as a "second hit" on those, increasing their activation and inducing the formation of neutrophil extracellular traps. *In vivo*, mice lacking SLC44A2 showed a massive reduction in neutrophil recruitment in inflamed mesenteric venules.

Conclusions

Our results show that SLC44A2/HNA-3a is important in the adhesion and activation process of neutrophils in veins under inflammation and when submitted to specific shears conditions. Neutrophils expressing SLC44A2/HNA-3b not being associated with these observations, these results could thus explain the association between the HNA-3b epitope and the reduced risk for VT in humans.

Introduction

Venous thromboembolic (VT) disease is the third cause of cardiovascular death after myocardial infarction and stroke in industrialized countries. It includes deep vein thrombosis and pulmonary embolisms. Using genome wide association study (GWAS) approaches and transgenic mice our team and others have contributed to the identification of *SLC44A2* as a new gene involved with VT both in humans (1, 2) and in mice (3). In-depth analysis of the *SLC44A2* locus identified rs2288904 (461G>A; Arg154Gln) as the functional variant responsible for the association with VT. This polymorphism corresponds to the expression of the HNA-3a (human neutrophil antigen-3a, Arg154) or HNA-3b antigen (Gln154) expression by the SLC44A2 (4-6). Homozygosity for the HNA-3b-coding allele is associated with a decreased risk of VT of ~30% (2).

SLC44A2 is an ubiquitous transmembrane protein of 70-95kDa (7). It is a choline carrier system proposed to supply choline for the cell membrane phospholipids (8). However, because of alternative splicing, SLC44A2 from blood circulating cells is not able to transport choline, thus suggesting another function in these cells (9). SLC44A2 has been identified in 2015 as a new receptor for Von Willebrand factor (VWF) (10). VT is a multifactorial disease which mechanisms still remained to be fully uncovered. Until recently, pathophysiology of VT was only based on the original cascade model of coagulation. Accumulating data has highlighted mechanisms independent of coagulation cascade on clot formation. These last few years animal studies have shown that neutrophils (11, 12) VWF (13) play a crucial role in the VT process. As the *SLC44A2* gene does not belong to the coagulation/fibrinolytic cascades, dissecting the mechanisms involved in its relation with VT is a powerful strategy to generate new biological knowledge of the underlying pathophysiology and ultimately to develop novel clinical therapies to limit bleeding and prevent recurrent and primary VT.SLC44A2 has been associated with transfusion acute-lung injury (TRALI) which is the leading cause of transfusion-associated mortality in developed countries (Mair and Eastlund, 2010). The most severe cases of TRALI have been associated with alloantibodies reacting against the HNA-3a epitope exposed by SLC44A2, the same antigen associated to VT. We and others have shown that alloantibodies targeting SLC44A2 can lead to neutrophil activation and formation of Neutrophil extracellular traps (NETs) by primed HNA-3a positive neutrophils (14, 15). Neutrophil recruitment to the endothelium and neutrophil activation/NETosis are key steps in TRALI (14, 16) but also in arterial thrombosis (17) and in VT (11, 18, 19). After adhesion to the activated endothelium, neutrophils initiate and propagate VT by interacting with platelets and by exposure and activation of circulating tissue factor and FXII (18). Importantly, mice with impaired NETosis have a decreased incidence of thrombosis in a model of VT (12), and mice treated with DNase-1 (which degrades DNA and NETs) are protected in this model (11). As in mice with thrombosis, outcome of mice with TRALI could be improved by having them inhale DNase-1 (14). The TRALI model, though being different from VT physiopathology may pave the way to understand why SLC44A2 plays a role in VT and why the HNA-3b isoform carrier have a decreased risk of VT. We investigated in this

study whether SLC44A2 could act as an adhesion protein allowing neutrophil adhesion to VWF under flow, and whether SLC44A2 could act as a receptor able to activate neutrophils and stimulate extracellular DNA trap formation.

We demonstrated that SLC44A2 is important in the adhesion and activation process of neutrophils under flow when submitted to inflammation and specific shear conditions. The fact that neutrophils expressing SLC44A2/HNA-3b is not associated with these observations, could thus explain the association between the HNA-3b epitope and the reduced risk for VT in humans.

Material and methods

Cell lines and culture conditions

Human embryonic kidney (HEK)-293T cells non transfected or transfected to overexpress SLC44A2/HNA-3a (R154) or SLC44A2/HNA-3b (Q154) fused with a Green fluorescent protein tag (GFP) were generous gifts from Drs. Daniel Bougie and Brian Curtis from the Bloodcenter of Wisconsin (4, 20). Cells were cultured in Dulbecco's Modified Eagle Medium (DMEM, Gibco) supplemented with 10% Fetal bovine serum (FBS, Gibco), 4mM L-Glutamine (Gibco), 100U/ml penicillin, 100µg/ml streptomycin (Gibco), and 50 µg/mL geneticin (Gibco) when a selection antibiotic was needed. Cells were cultured at 37°C in a humidified atmosphere with 5% CO_2. PBS and Versene (0.48 mM, Gibco) were used for cell dissociation. Single-cell suspensions were obtained after passing the cells through a 70µm cell strainer (Falcon). Cell counts and viability were measured by an automated cell counter after trypan blue staining (EVE™, Nanoentek).

Immunofluorescence staining

Transfected HEK-293 cells were seeded on L-poly-lysine- (0.01%, Gibco) coated coverslips in complete medium. 24 hours later, media was changed. Nonspecific interaction sites were blocked with BSA and cells were incubated with 10µg/ml VWF (LFB) or vehicle control for 1h. Cells were then washed with PBS, fixed with 4% PFA, washed, saturated with Tween/BSA and stained for VWF with 5µg/ml of mouse anti-human VWF antibody (house made monoclonal antibody pool). Secondary antibody staining was done with an Alexa 546-goat anti-mouse IgG (0.4mg/ml, Invitrogen). Nuclei were stained with Dapi (1µg/ml) and f-actin was stained with phalloidin (2µg/ml, invitrogen). Coverslips were then mounted on slides with prolong Gold antifade reagent (Molecular probes). Images were acquired with a Nikon Eclipse E600 microscope with PixelLINKCaptureOEM software. VWF fluorescence per cell was then quantified using ImageJ software.

Human neutrophil isolation

After all participants gave written informed consent, neutrophils were isolated from healthy volunteers' blood at the Timone University Hospital (Marseille, France) who declared that they had not received any medication for at least 2 weeks. Sodium citrate was used as

anticoagulant for blood puncture except if otherwise specified. Neutrophils were prepared as previously described (14). The research was approved by the relevant institutional review boards and ethic committees. The investigation conforms to the principles outlined in the Declaration of Helsinki. After isolation, neutrophils were eventually labeled with the dye of use (Calcein AM 4µM, cell trace red orange 4µM or DiD 2µg/ml). When specified, 1mM $CaCl_2$ and/or blocking antibodies were added to neutrophils before utilization. Concentration was adjusted and only cells at acceptable viability (>75%) were used.

SLC44A2 genotyping

Donors homozygous for the HNA-3a- or HNA-3b-coding allele were identified by SNP genotyping using a taqman 5' exonuclease PCR technology as previously described (21).

Flow chamber assays

Flow chambers µ-slide VI 0.1 ibitreat (Ibidi) were used for cell speed analysis and NETosis experiments, and Vena8 fluoro + microfluidic biochip (Cellix) were used for NETosis experiments. Flow chambers were coated overnight at 4°C with either 70µg/ml VWF (Wilfactin, LFB), VWF recombinant A1-Fc domain (10µg/ml), fibrinogen (10µg/ml), or BSA (10ug/ml, Sigma). After one wash with PBS, saturation was done with PBS/BSA 0.1% 1 hour prior to the assay. If applicable, blocking antibodies (10µg/ml; VWF-A1 blocking Ab 318 clone, anti CD18 TS1/18 clone or irrelevant IgG1 and IgG2) were incubated in the channels 30 minutes before cell perfusion and perfused concomitantly at 25µg/ml for VWF blockade experiments. Continuous flow rate was applied forward using an electrical syringe pump (bioblock scientific) with a 1ml or 5ml syringe (Terumo) connected to the chamber with silicon tubing (Ibidi or Cellix). One chamber was used per condition and the chambers were discarded after each experiment.

Transfected HEK 293 cells (4) or purified neutrophils were labeled 20 minutes under agitation with either Calcein AM (4µM, Life Technologies) or DiD dye (2µg/ml) for activation experiments. Cells were washed once in PBS. When indicated, neutrophils were incubated with lipopolysaccharide (LPS 5 or 25µg/ml) or $MnCl_2$ (1mM) for 1 hour prior to cell perfusion and cells were eventually incubated 5 min prior to perfusion with calcium (1mM). Extracellular DNA was labeled by addition of Sytox green or Sytox red (1µM, Life Technologies) to the neutrophils immediately before perfusion. Cells ($1,5.10^6$ cells/ml) were infused in flow chamber at a wall shear rate of $100s^{-1}$ (or other if specified) at a controlled temperature of 37°C using a thermoregulated thermostatic chamber (Olympus). Cells were allowed to pass through the channel for 5 minutes before acquisition. Acquisition was done with an inverted microscope (IX71, Olympus) and a LED fluorescence lamp for sample excitation (SPECTRA X light engine, Lumencor) in three different fields (1329.4µm wide) during 1 minute at a rate of 20 images/sec. Real-time imaging was performed using a CMOS digital camera (Orca-Flash 4.0 V2 CCD C11440, Hamamatsu).

Flow chamber cell motion analysis

A dedicated program was written in Java (Oracle, USA) as a plug-in for ImageJ (NIH, USA). Cells were detected as bright areas above a chosen threshold over a dark background. Trajectories of individual cells were formed by calculating in a given image the distance between the barycenter of each cell and adding to the forming trajectory the cell of closest barycenter in the next image, while ensuring that cell area would not change above a chosen threshold. Velocities were calculated for each position of each trajectory long the flow axis, as the mean velocity between to positions separated by a user-chosen interval, to form velocity histograms of either individual cells or whole experiment. Cells were categorized in two groups: "adhesion (<10μm/s) and "rolling" (200-500μm/s) to simplify cell behavior analysis.

NET generation in vitro

NET generation was done and quantified as previously described (14). VWF was used at a concentration of 10μg/ml. Imaging was done with the microscope set-up used for flow chamber imaging as described above. Tumor necrosis factor-α (TNFα) was used for cell priming because TNF-α is produced by human neutrophils stimulated by LPS (22) and because commonly used for this assay in other studies.

Mice

11 to 12 week old mice were used. Mice deficient for SLC44A2 (C57BL/6J background) and littermate controls (Slc44a2+/+) were used as previously done (3). Experimental animal procedures were approved by local welfare committees in Aix-Marseille University. Experiments were performed blinded for genotype. For mouse rolling assays, at least 2 venules were recorded for 1 minute each.

Model of endothelial degranulation on mouse mesenteric venules

Intraperitoneal (IP) injection of histamine (13nmol/g of mouse) in 200μl saline or saline alone (control) was injected 30 minutes prior to mouse anesthesia to induce endothelial degranulation. Mice were anesthetized by IP injection of ketamine (100mg/kg) xylazine (20mg/kg). Mice were then infused through the retro-orbital plexus with 2μg/50μl of anti-Ly6g antibody (1A8 clone, eBioscience). After laparotomy the mesentery bed was carefully exposed and kept warm and moist by superfusion of warm saline (~37°C). Neutrophil rolling was recorded in 3 different venules by intravital microscopy and quantified over a 1minute timeframe.

Statistical analysis

Data represents mean ± SEM. Adhesion and rolling experiments were analyzed by Mann-Whitney and Kolmogorov-Smirnov tests. Immunofluorescence experiments were analyzed with one-way ANOVA test. Shapiro-Wilk test was used to check normality. For *in vivo* rolling experiments the population was not normally distributed. As a consequence, data were Log transformed and a test for parametric population was applied. Results were considered significant at $p<0.05$.

Results

The SLC44A2/HNA-3a epitope is necessary for cell adhesion to VWF under flow

We used HEK293T cells transfected to express SLC44A2 with either the HNA-3a epitope (Arg154) or the HNA-3b epitope (Gln154). These cells have been already characterized and express similar levels of SLC44A2 ((4), Figure S1). After incubation of these cells in culture with purified VWF, we observed patches for positive VWF staining 2.6 more intense on HEK293T cells expressing SLC44A2/HNA-3a than on those expressing SLC44A2/HNA-3b (Figure 1, HEK293T/HNA-3a+VWF 65.9±4.2; HEK293T/HNA-3b 38.1±2.2). Then, we wanted to confirm the ability of these cells to bind VWF in presence of flow. We perfused fluorescent HEK293T transfected cells in flow chambers coated with VWF and submitted to a "postcapillary venule" shear rate of $100s^{-1}$. Digital real time imaging at the speed of 1 frame per 50 ms on 1329 µm-wide fields allowed us to digitally extract precise cell speed data from these experiments. We evaluated for each of the 3 different fields the mean velocity of each cell that passed our cut-off parameters. When we plotted the percentage of cells tracked in function of their speed, we observed for both groups a maximum of HEK293T cells passing at around 1400-1600µm/s (Figure 2A). Interestingly we detected also some cells interacting strongly with the matrix (speed <10µm/s) in the HNA-3a-expressing group.

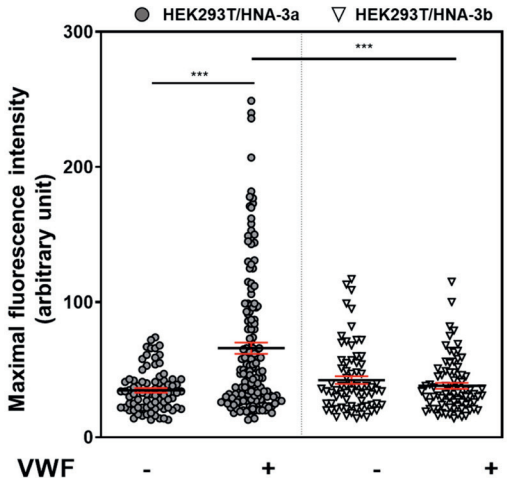


Figure 1. **HEK293T/HNA-3a cells bind more to VWF than HEK293T/HNA-3b cells.** Quantification of maximal fluorescence intensity recorded per cell and representing anti-VWF staining on transfected HNA-3a- (grey circle) or HNA-3b-expressing HEK293T cells (white triangle) (*** p<0.005).

We compiled the recorded cell velocities in 2 different groups: "adhesion (<10µm/s) and "Rolling" (200-500µm/s). We observed that exposure of HNA-3a by HEK293T cells is associated with cell adhesion to the VWF matrix under flow, whereas HEK293T cells

expressing HNA-3b loose this ability (1.32 ± 0.60% against 0% of total tracked cells adhering to the matrix respectively, Figure 2B).

HEK293T cells are not programmed for cell adhesion. We wondered if SLC44A2 could affect VT by modulating neutrophil adhesion to VWF, which is crucial in VT. We genotyped healthy consenting blood donors for the SLC44A2 rs2288904 (R>G154) polymorphism. We purified blood neutrophils only from donors homozygous for the HNA-3a- (R154) or the HNA-3b coding allele (Q154). They were perfused in flow chambers in the same experimental conditions as above. When compared to HEK293T cells, we also observed the majority of the cells going at an approximative speed of 1500-1600s^{-1}, plus others rolling at a speed around 300s^{-1} which is typical for neutrophils (Figure 2C). Here again, we observed that the HNA-3a/3b epitope did not influence "fast rolling" (200-500µm/s) on VWF, whereas HNA-3b-expressing neutrophils showed a significant reduction in cell adhesion on this matrix (Figure 2D). This was not observed in presence of higher shear rates (1000s^{-1}, data not shown) and this adhesion was also inhibited in presence of a specific VWF-A1 domain blocking antibody (Figure 2E).

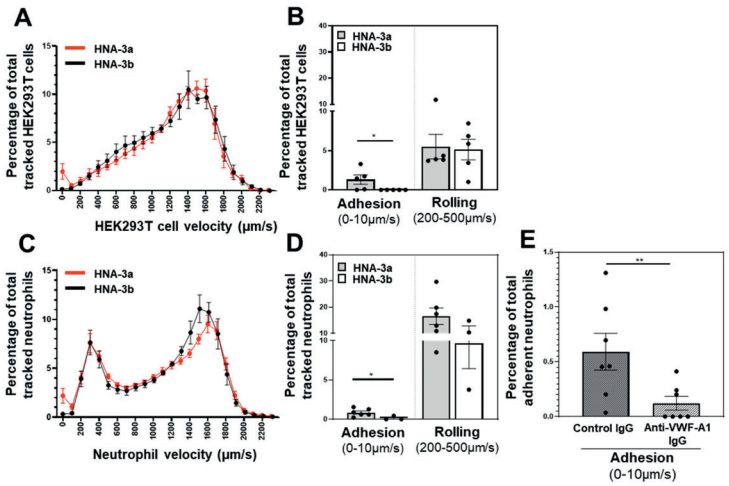


Figure 2. The CTL2/HNA-3a epitope is necessary for cell adhesion to VWF under flow. (A, C) Compiled amount of HEK293T cells **(A)** or neutrophils **(C)** counted in function of their mean velocity (µm/s) on coated VWF when submitted to a 100s^{-1} shear rate. Red: HNA-3a-expressing cells; black: HNA-3b expressing cells (n=5 donors per genotype, 3 fields per donor). **(B, D)** Graphs depicting the adhesion and rolling profiles of HEK293T cells **(B)** and neutrophils **(D)** perfused on a VWF matrix under flow at a 100s^{-1} shear rate. Perfusion of cells at 100s^{-1} resulted in more adhesion and slow rolling of SLC44A2/HNA-3a expressing HEK293T cells (B, n=5 donors per genotype, 3 fields per donor).) and PMN (D, HNA-3a n=6 donors p, 3 fields per donor; HNA-3b n=3 donors, 3 fields per donor) to human VWF coated channels compared to CTL-2/HNA-3b expressing cells. Adhesion and slow rolling of CTL-2/

HNA-3a expressing PMN (E, n=3) to VWF was blocked by VWF-A1 domain blocking monoclonal antibody. (* p<0.05; ** p<0.01; *** p<0.005)

These data suggest that HNA-3a expression is crucial for HEK293T or neutrophil adhesion to VWF in presence of venule shear rate ($100s^{-1}$), and confirm the data from a another team pointing the involvement of the VWF-A1 domain in VWF/SLC44A2 interactions (10).

Neutrophil adhesion on VWF under flow is amplified after an inflammatory first "hit"

Inflammatory-related disorders often follow the two-hit or multiple-hit hypothesis. HNA-3a-associated VT probably follows this pattern, and this may explain why not all the HNA-3a- positive population will suffer from VT. We thus tested if an inflammatory hit mimicking an infection (LPS), could influence SLC44A2-mediated neutrophil adhesion to VWF. For this, we pre-activated neutrophils with LPS (5 or 25µg/ml) for 1 hour before perfusion in flow chambers. Our data show that whereas HNA-3b expressing neutrophils do not adhere more to VWF when activated, LPS does increase adhesion of HNA-3a-expressing neutrophil to VWF at $100s^{-1}$ (Figure 3A). LPS had no effect on "fast rolling" (Figure 3B). The exacerbation of the difference between the HNA-3a and HNA-3b groups in cell adhesion seemed to be present also when lower shear rates were used too (50 and 10s-1, Figure 3C). However, the variations between experiments being higher at lower shear rates, the difficulty to find HNA-3b homozygous donors did not permit us to increase the HNA-3b group size and to conclude for these lower shear rates.

We also observed in the LPS experiment from Figure 3 that the control groups of non-stimulated cells showed higher adhesion rate when compared to the Figure 2 experiments. For LPS experiments, cells received some calcium prior to stimulation in order to replenish their Ca^{2+} intracellular stocks. It is indeed possible that SLC44A2/VWF engagement induces cell and integrin activation that will in return permit the adhesion of neutrophils to VWF under flow.

The fact that the SLC44A2/VWF interaction is followed by the formation of a trimolecular complex composed by SLC44A2, VWF and the $\alpha_M\beta_2$ (Mac-1) integrin (10) supports this hypothesis with the possible existence of a subsequent "outside-in" signaling. Because β_2 integrins are the major integrins involved in neutrophil adhesion, we treated HNA-3a or HNA-3b-expressing neutrophils with either a specific β2- (CD18-) blocking antibody or an irrelevant antibody. We then looked at neutrophil adhesion and rolling on VWF at $100s^{-1}$ (Figure 3D and E). Beta-2 integrin blockade did not abolish neutrophil adhesion to VWF under flow, showing that SLC44A2/HNA-3a mediated neutrophil adhesion to VWF is at least partly beta-2 integrin independent.

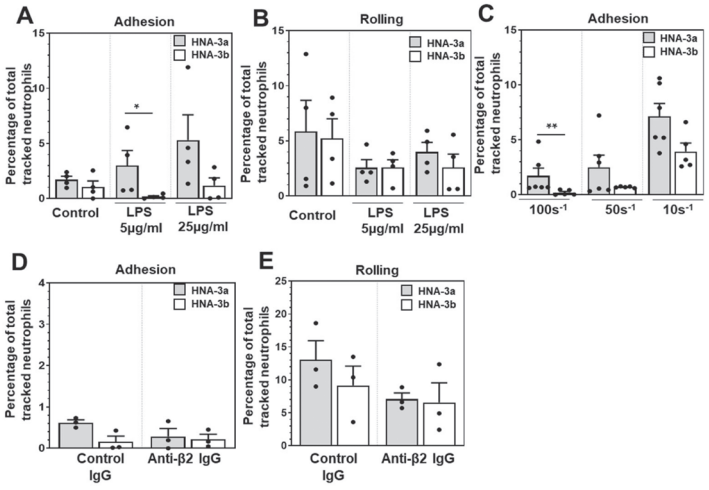


Figure 3. Adhesion of HNA-3a-expressing neutrophils to VWF is amplified by LPS and does not require beta 2 integrins. (A, B) Percentage of total tracked neutrophils qualified as adherent **(A)** and in "fast rolling" **(B)** when perfused at 100s-1 on immobilized VWF after LPS treatment (5 µg/ml or 25µg/ml) prior to perfusion (n=4 donors per genotype, 3 fields per donor). **(C)** Percentage of total tracked neutrophils qualified as adherent or in "slow rolling" when perfused at 100s-1, 50 s-1 and 10s-1 on immobilized VWF (HNA-3a n=5 donors p, 3 fields per donor; HNA-3b n=4 donors, 3 fields per donor). **(D, E)** Percentage of total tracked neutrophils qualified as adherent **(D)** and in "fast rolling" **(E)** when perfused at 100s-1 on immobilized VWF after treatment with a β2 integrin blocking IgG, or a control irrelevant IgG (n=3 donors per genotype, 3 fields per donor). (* p<0.05; ** p<0.01).

SLC44A2/HNA-3a can mediate DNA extracellular trap formation from neutrophils flowing on VWF

The enhanced neutrophil adhesion observed for the SLC44A2/HNA-3a group after LPS treatment suggests that SLC44A2 engagement induce neutrophil activation. NET formation is crucial during VT, and NETosis has been already described in TRALI after antibody binding to SLC44A2/HNA-3a and following a double "hit" scheme.

We chose to reproduce this model here, by stimulating neutrophils with LPS and by modulating a supplemental factor that could predispose to VT. During stasis, local concentrations in leukocytes can increase. We chose to perfuse different concentrations of LPS-pre-stimulated neutrophils trough the VWF-coated flow chamber: equal concentration, concentration increased 5- or 10 times.

Two different brand of flow chambers were used, and fluorescence intensity visualization was set-up to allow focus on cell accumulation and not flowing cells. Cells were flowing as previously observed in the Ibidi chambers at "classic" concentration (Figure 4, upper left panel).

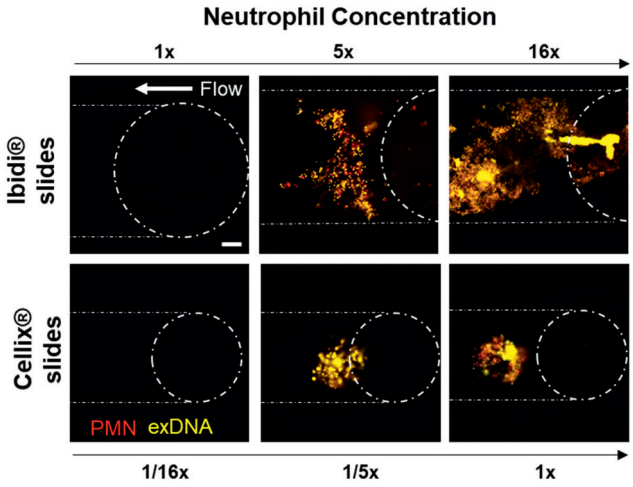


Figure 4. Neutrophils perfused on VWF can form DNA extracellular traps. Visualization of fluorescently-labeled neutrophils (PMN, red) and extracellular DNA (exDNA, yellow) after perfusion ($100s^{-1}$ shear rate) on VWF of different concentrations of neutrophils (1x concentration=$1.5x10^6$ cells/ml) in two different brands of flow chambers (n=2 donors , 3 fields per donor). Scale bar =100 µm. Lines delimit the flow channels and the well entrance.

However, increasing cell concentration induced next to the entry of the chamber (where the rheological conditions are peculiar and where the cells are regaining speed) an accumulation of neutrophils (stained by calcein red orange) sticking together and to the chamber. The additional staining of extracellular DNA by the Sytox green dye suggests that these neutrophils could form NETs (Figure 4, upper middle and right panels) as shown by the presence of DNA fibers escaping from the adhering cells. This phenomenon was also observed when another chamber brand was used (Cellix slides), while ensuring that cell concentrations used are transposed to the rheological conditions and the geometry of the second chamber in order to be comparable (Figure 4, lower panels). We have found that this phenomenon could be amplified by increasing the intensity of the inflammatory stimulus from 5 to 25µg/ml LPS in the two different sets of flow chambers used (Figure S2 and Figure 5A). Interestingly the HNA-3b neutrophils did not react with the VWF matrix as HNA-3a neutrophils did, as they did not form extracellular DNA structures. This HNA-3a-dependent cell accumulation was calcium dependent, showing that extracellular DNA trap formation is an active phenomenon following the adhesion of neutrophils to the immobilized VWF under flow. We tested different matrices such as BSA, fibrinogen and VWF-A1 domain (Figure 5B) and confirmed to be in the presence of a VWF-A1-dependent phenomenon. *In vitro* incubation of TNFα primed-(mimicking LPS activation) HNA-3a-neutrophils with VWF resulted in an increase in the percentage of NET-forming cells (Figure 6) thus supporting the hypothesis that HNA-3a-bearing SLC44A2 can mediate neutrophil activation and NETosis in presence of VWF.

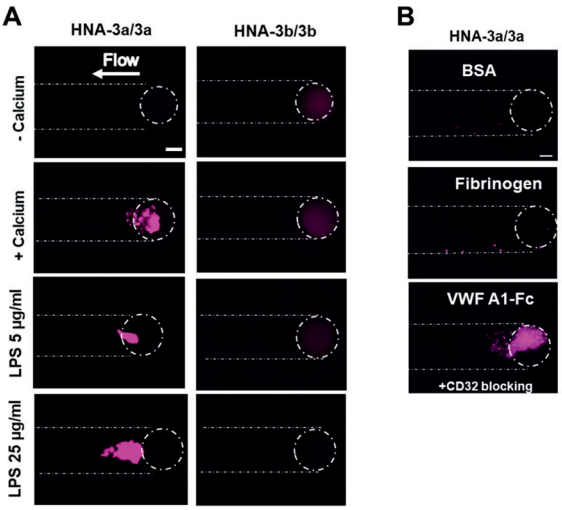


Figure 5. PMN activation on VWF at 100s^{-1} is HNA-3a-, calcium-, VWF A1-domain-dependent, and can be exacerbated by LPS challenge. (A) Visualization of HNA-3a- or HNA-3b neutrophils (anti-Ly6G IgG) submitted to a 100s^{-1} shear rate in absence or presence of calcium, or pre-activated with LPS prior to perfusion (5or 25µg/ml) (Cellix brand flow chambers, n=3 donors per genotype). **(B)** Visualization of HNA-3a neutrophils perfused at a 100s^{-1} shear rate on immobilized BSA, fibrinogen or VWF A1-Fc domain. Neutrophil Fc Receptors were blocked with anti CD32 antibody for A1 dormain experiments. Scale bar=100 µm. Lines delimit the flow channels and the well entrance (n=3 donors per genotype).

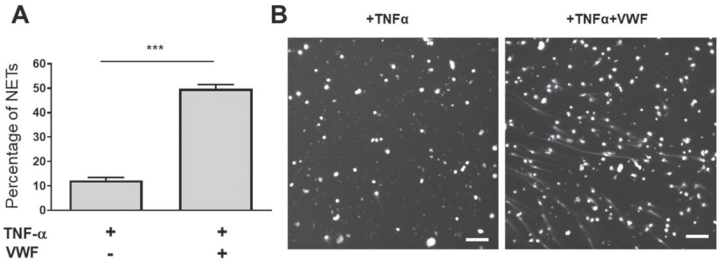


Figure 6. Primed neutrophils can form NETs under VWF challenge (A) Quantification of NETs after VWF challenge by fluorescence microscopy analysis. HNA-3a-positive neutrophils were primed with TNFα and incubated for 180 minutes with PBS (+TNFα) or VWF (+TNFα+VWF). DNA release was visualized after DNA staining with Hoescht 33342. The experiment was independently performed 2 times. **(B)** Example of the fluorescence images quantified in panel (A). Scale bar=100µm (*** p<0.005).

SLC44A2 play a major role in neutrophil recruitment at the vessel wall after endothelial degranulation in vivo

Through the use of human cells expressing either the HNA-3a or the HNA-3b epitope, we demonstrated an effect of SLC44A2 on neutrophil adhesion and activation on VWF under flow. In order to confirm our data *in vivo*, and because mice "knocked-in" for our polymorphism of interest do not exist yet, we used *Slc44a2* deficient mice and submitted them to the model of histamine-induced endothelial degranulation. Endothelial degranulation results in VWF release from the Weibel-Palade bodies. Mouse infusion with fluorescently labeled anti-Ly-6G antibody allowed us to track neutrophil accumulation at the vessel wall in this model. Our data confirmed our *in vitro* hypothesis: we observed a drastic reduction in neutrophil rolling and adhesion at the vessel wall of mesenteric venules (Figure 7, 409 ± 300 cells/min versus 59±26 cells/min).

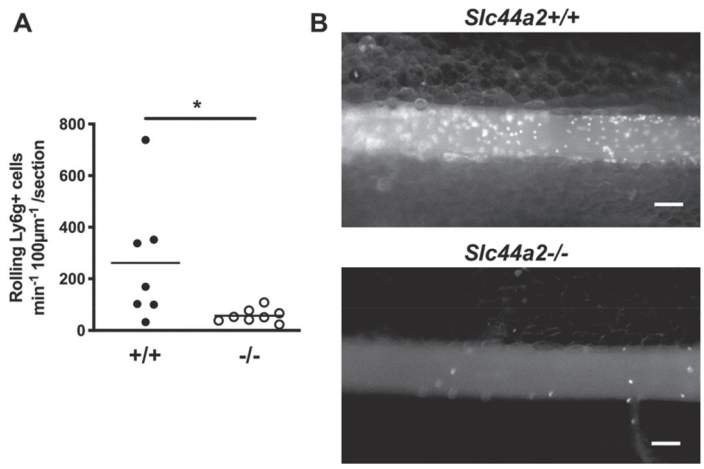


Figure 7. SLC44A2 is essential for neutrophil recruitment at the vessel wall following endothelial activation. Intravital microscopy was performed on mesenteric venules of SLC44A2 deficient mice (*Slc44a2-/-*) and littermate wildtype controls (*Slc44a2+/+)* after IP histamine challenge. **(A)** Quantification of neutrophil rolling on mesenteric venules in wildtype and SLC44A2 deficient mice (*Slc44a2+/+*. n=7 venules in 3 mice; *Slc44a2-/-*, n=8 venules in 3 mice). **(B)** Representative pictures showing reduced neutrophil recruitment in mesenteric venules of SLC44A2 deficient mice and wildtype after staining of endogenous rolling neutrophils by infusion of an Alexa 660-anti-Ly6g antibody. (* $p<0.05$). Scale=100µm.

Discussion

In the present study, we demonstrated that SLC44A2 is involved in the adhesion and activation process of neutrophils on VWF and that this function is HNA 3a/HNA 3b

dependent. SLC44A2-mediated adhesion was VWF-A1 domain-dependent and enhanced under inflammatory stimulus, low shear rates ($100s^{-1}$) or specific rheologic conditions.

Recently, GWAS studies have homogeneously identified that *SLC44A2* was a new gene associated with the risk of VT. This was reinforced by mice data we and our collaborators obtained showing that absence of SLC44A2 is linked to reduced thrombus formation in the stenosis VT model (23). As pathophysiology of VT was mostly based on the original cascade model of coagulation and as *SLC44A2* does not belong to it, it is of major importance to characterize the biological link between this gene and VT. In the current study, we aimed to discover how the *SLC44A2* gene and the lead rs2288904 variant (461G>A; Arg154Gln) could affect SLC44A2 function in thrombosis.

This last decade, neutrophils and VWF have been shown to play a central role in VT. VWF is known to be an important protein in hemostasis by mediating platelet adhesion to the subendothelial matrix, but also in inflammation processes (for review (24)) that are crucial during VT development. SLC44A2 has been shown few years ago as a binding partner for VWF (10). However, how the Arg154Gln polymorphism could modulate this interaction had not been studied before. Because HNA-3b is associated with a decreased risk for VT over HNA-3a in patients (1, 2), we imagined a possible loss of function of SLC44A2 when exposing HNA-3b leading to a reduced binding of SLC44A2 to VWF.

We used HEK293T transfected cells, neutrophils and mice to assess the importance of SLC44A2 in the mechanisms of neutrophil adhesion to VWF *in vitro* and *in vivo*. We observed that the HNA-3a/HNA-3b epitope had no effect on neutrophil rolling when perfused on a VWF-coated matrix. However, SLC44A2/HNA-3a but not SLC44A2/HNA-3b allows cell adhesion to VWF when submitted to venous shear rates. Our *in vivo* data obtained in the mouse model of endothelial degranulation in mesenteric venules done on SLC44A2 deficient mice confirmed our hypothesis that SLC44A2 could be important for neutrophil recruitment at the vessel wall at venous shear rates and during inflammation.

Despite the fact that SLC44A2/HNA-3a-transfected HEK293T cells do not express beta 2 integrins (25), they adhere more on VWF than HEK293T cells expressing the HNA-3b form. This result suggests by itself that SLC44A2 can be sufficient to allow cell adhesion on VWF. However, subsequent integrin activation could potentialize SLC44A2-mediated adhesion of neutrophils as integrins have been described as playing a major role in leukocyte adhesion (26). The utilization of a β_2-blocking antibody on neutrophils or the use of neutrophils purified from EDTA-anticoagulated blood (data not shown, chelation of divalent cations will not allow integrin activation) were not enough to abolish this neutrophil adhesion on VWF. Altogether these observations confirm that SLC44A2 is enough to induce cell adhesion on VWF under flow independently from integrins. However, our results and few hypotheses suggest that VWF/SLC44A2 interaction could also induce neutrophil and integrin activation thus consolidating the cell adhesion process. In TRALI for instance, anti-HNA-3a antibodies have

been shown to activate neutrophils (14). It is indeed possible that VWF has a comparable effect. Bayat and collaborators published evidence that following SLC44A2/VWF engagement VWF, SLC44A2, and Mac-1 ($\alpha_M\beta_2$) form a trimolecular complex at the neutrophil surface (10). This is a process expected to occur after "inside-out" signaling. An old study has also identified the SLC44A2-coding gene as able to activate the NF-κB pathway (27). Interestingly, this pathway is essential for tissue factor expression in VT (28).

We have seen that a second hit can significantly affect SLC44A2-mediated neutrophil adhesion to VWF under flow. Inflammatory stimuli such as TNF-α or LPS, but also special rheologic conditions can in addition to HNA-3a expression stimulate NET formation. NETosis is an active process following neutrophil activation, crucial during VT (12, 18). NETs form a matrix for cell (platelets, red blood cells) or microparticle adhesion and form a thrombogenic surface exposing tissue factor or factor XII.

Our *in vivo* results obtained in the histamine-induced endothelial degranulation model support that SLC44A2 deficiency could delay both neutrophil recruitment and activation on a degranulated endothelium too. This may explain the phenotype of SLC44A2 deficient mice that formed smaller thrombi when submitted to the DVT stenosis model (23).

VWF and NETs are crucial in VT pathogenesis. It is also true for other pathologies linked to inflammation such as stroke or myocardial myocardial ischemia/reperfusion injury (29-32). HNA-3a has been found to be related to stroke too (1). Moreover stroke involves the VWF-A1 domain (33), which is the one important in SLC44A2-mediated adhesion as well. Our work thus suggests that GPIb may not be the only receptor involved when we talk about VWF-A1-associated thrombo-inflammatory pathogenesis. SLC44A2 has to be taken into consideration. VWF is released by endothelial cells through a constitutive pathway and through Weibel-Palade bodies release. VWF released from the storage compartment is of high molecular weight (34) and is released with a relatively high concentrations of calcium ions upon vascular injury or inflammatory stimulation. Our work suggests that SLC44A2 may be involved not only in VT but also in more pathologies than we originally thought in the inflammation field.

HNA-3b homozygous individuals being rare (6% of Caucasians)(21), it is easy to imagine that previous work on neutrophil adhesion and VWF used HNA-3a-positive donors for their work. In this study we point out the necessity to check on the HNA-3a/3b genotype of blood donors before purifying cells that will be used to work with VWF.

In conclusion, we propose here a new mechanism of neutrophil adhesion and activation that connects inflammation to thrombosis in veins. This mechanism involves the VWF-A1 domain and can induce neutrophil activation and NETosis. Other studies are thus warranted to better understand the mechanisms of SLC44A2/VWF molecular interaction and how this interaction can also influence neutrophil activation. Shutting down SLC44A2 function

would allow to target specifically thrombosis without affecting hemostasis, which would reduce the risk of hemorrhagic complications that are associated with actual prophylactic anticoagulant therapies.

Disclosure of Conflicts of Interest

The authors declare no competing financial interests.

Acknowledgments

The authors thank Thomas E. Carey (Kresge Hearing Research Institute, Department of Otolaryngology/Head and Neck Surgery, University of Michigan, Ann Arbor, MI, USA) for the floxed Slc44a2 mouse embryos used to generate the mice on a C57BL/6J background; Matthias Canault and Cécile Denis for helpful discussions; and Brian Curtis, Daniel Bougie for providing us with the HEK293T transfected cells. This work was supported by the ANR (grant ANR-17-CE14-0003-01 to GMT).

Author contributions

Experimental design: GZ, JT, PR, CXM, PL, MCA, PJL, PEM, GMT. Performed experiments and analyzed data: GZ, JT, PR, CXM, PL, MCA, PJL, PEM, GMT. Wrote the paper: GZ, PR, PEM and GMT. All authors commented on manuscript drafts. All authors have approved the final version.

References

1. Hinds DA, Buil A, Ziemek D, et al. Genome-wide association analysis of self-reported events in 6135 individuals and 252 827 controls identifies 8 loci associated with thrombosis. *Human Molecular Genetics*. 2016;25(9):1867-74.
2. Germain M, Chasman DI, de Haan H, et al. Meta-analysis of 65,734 individuals identifies TSPAN15 and SLC44A2 as two susceptibility loci for venous thromboembolism. *Am J Hum Genet*. 2015;96(4):532-42.
3. Tilburg J, Coenen DM, Zirka G, et al. SLC44A2 deficient mice have a reduced response in stenosis but not in hypercoagulability driven venous thrombosis. *J Thromb Haemost*. 2020.
4. Kanack AJ, Peterson JA, Sullivan MJ, et al. Full-length recombinant choline transporter-like protein 2 containing arginine 154 reconstitutes the epitope recognized by HNA-3a antibodies. *Transfusion*. 2012;52(5):1112-6.
5. Greinacher A, Wesche J, Hammer E, et al. Characterization of the human neutrophil alloantigen-3a. *Nature Medicine*. 2010;16(1):45-8.
6. Curtis BR, Sullivan MJ, Holyst MT, et al. HNA-3a-specific antibodies recognize choline transporter-like protein-2 peptides containing arginine, but not glutamine at Position 154. *Transfusion*. 2011;51(10):2168-74.
7. Flesch BK, Wesche J, Berthold T, et al. Expression of the CTL2 transcript variants in human peripheral blood cells and human tissues. 2013;53(12):3217-23.
8. Traiffort E, O'Regan S, Ruat M. The choline transporter-like family SLC44: properties and roles in human diseases. *Mol Aspects Med*. 2013;34(2-3):646-54.
9. Kommareddi PK, Nair TS, Thang LV, et al. Isoforms, Expression, Glycosylation, and Tissue Distribution of CTL2/SLC44A2. *The Protein Journal*. 2010;29(6):417-26.
10. Bayat B, Tjahjono Y, Berghofer H, et al. Choline Transporter-Like Protein-2: New von Willebrand Factor-Binding Partner Involved in Antibody-Mediated Neutrophil Activation and Transfusion-Related Acute Lung Injury. *Arterioscler Thromb Vasc Biol*. 2015;35(7):1616-22.
11. Brill A, Fuchs TA, Savchenko AS, et al. Neutrophil extracellular traps promote deep vein thrombosis in mice. 2012;10(1):136-44.
12. Martinod K, Demers M, Fuchs TA, et al. Neutrophil histone modification by peptidylarginine deiminase 4 is critical for deep vein thrombosis in mice. *Proc Natl Acad Sci U S A*. 2013;110(21):8674-9.
13. Brill A, Fuchs TA, Chauhan AK, et al. von Willebrand factor-mediated platelet adhesion is critical for deep vein thrombosis in mouse models. *Blood*. 2011;117(4):1400-7.
14. Thomas GM, Carbo C, Curtis BR, et al. Extracellular DNA traps are associated with the pathogenesis of TRALI in humans and mice. *Blood*. 2012;119(26):6335-43.
15. Berthold T, Muschter S, Schubert N, et al. Impact of priming on the response of neutrophils to human neutrophil alloantigen-3a antibodies. *Transfusion*. 2015;55(6 Pt 2):1512-21.
16. Caudrillier A, Kessenbrock K, Gilliss BM, et al. Platelets induce neutrophil extracellular traps in transfusion-related acute lung injury. *J Clin Invest*. 2012;122(7):2661-71.
17. Darbousset R, Thomas GM, Mezouar S, et al. Tissue factor-positive neutrophils bind to injured endothelial wall and initiate thrombus formation. *Blood*. 2012;120(10):2133-43.

18. von Bruhl ML, Stark K, Steinhart A, et al. Monocytes, neutrophils, and platelets cooperate to initiate and propagate venous thrombosis in mice in vivo. *J Exp Med*. 2012;209(4):819-35.
19. Fuchs TA, Brill A, Wagner DD. Neutrophil extracellular trap (NET) impact on deep vein thrombosis. *Arterioscler Thromb Vasc Biol*. 2012;32(8):1777-83.
20. Bougie DW, Peterson JA, Kanack AJ, et al. Transfusion-related acute lung injury-associated HNA-3a antibodies recognize complex determinants on choline transporter-like protein 2. *Transfusion*. 2014;54(12):3208-15.
21. Bowens KL, Sullivan MJ, Curtis BR. Determination of neutrophil antigen HNA-3a and HNA-3b genotype frequencies in six racial groups by high-throughput 5' exonuclease assay. *Transfusion*. 2012;52(11):2368-74.
22. Wang P, Wu P, Anthes JC, et al. Interleukin-10 inhibits interleukin-8 production in human neutrophils. *Blood*. 1994;83(9):2678-83.
23. Tilburg J, Michaud SA, Maracle CX, et al. Plasma Protein Signatures of a Murine Venous Thrombosis Model and Slc44a2 Knockout Mice Using Quantitative-Targeted Proteomics. *Thromb Haemost*. 2020;120(3):423-36.
24. Kawecki C, Lenting PJ, Denis CV. von Willebrand factor and inflammation. *J Thromb Haemost*. 2017;15(7):1285-94.
25. Gupta V, Alonso JL, Sugimori T, et al. Role of the beta-subunit arginine/lysine finger in integrin heterodimer formation and function. *J Immunol*. 2008;180(3):1713-8.
26. Kuijpers TW, Van Lier RA, Hamann D, et al. Leukocyte adhesion deficiency type 1 (LAD-1)/variant. A novel immunodeficiency syndrome characterized by dysfunctional beta2 integrins. *J Clin Invest*. 1997;100(7):1725-33.
27. Matsuda A, Suzuki Y, Honda G, et al. Large-scale identification and characterization of human genes that activate NF-kappaB and MAPK signaling pathways. *Oncogene*. 2003;22(21):3307-18.
28. Li YD, Ye BQ, Zheng SX, et al. NF-kappaB transcription factor p50 critically regulates tissue factor in deep vein thrombosis. *J Biol Chem*. 2009;284(7):4473-83.
29. Zhao BQ, Chauhan AK, Canault M, et al. von Willebrand factor-cleaving protease ADAMTS13 reduces ischemic brain injury in experimental stroke. *Blood*. 2009;114(15):3329-34.
30. Hillgruber C, Steingraber AK, Poppelmann B, et al. Blocking von Willebrand factor for treatment of cutaneous inflammation. *J Invest Dermatol*. 2014;134(1):77-86.
31. Savchenko AS, Martinod K, Seidman MA, et al. Neutrophil extracellular traps form predominantly during the organizing stage of human venous thromboembolism development. *J Thromb Haemost*. 2014;12(6):860-70.
32. Dhanesha N, Prakash P, Doddapattar P, et al. Endothelial Cell-Derived von Willebrand Factor Is the Major Determinant That Mediates von Willebrand Factor-Dependent Acute Ischemic Stroke by Promoting Postischemic Thrombo-Inflammation. *Arterioscler Thromb Vasc Biol*. 2016;36(9):1829-37.
33. Denorme F, Martinod K, Vandenbulcke A, et al. The von Willebrand Factor A1 domain mediates thromboinflammation, aggravating ischemic stroke outcome in mice. *Haematologica*. 2020.
34. Wagner DD. Cell biology of von Willebrand factor. *Annu Rev Cell Biol*. 1990;6:217-46.

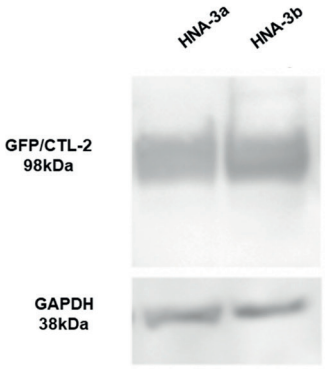


Figure S1. Western blot of transfected HNA-3a- and HNA-3b-expressing HEK293T cell lysates probed with an antibody directed against GFP or GAPDH.

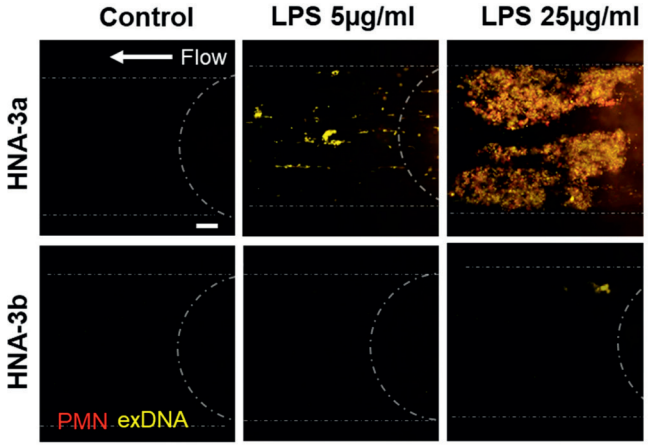
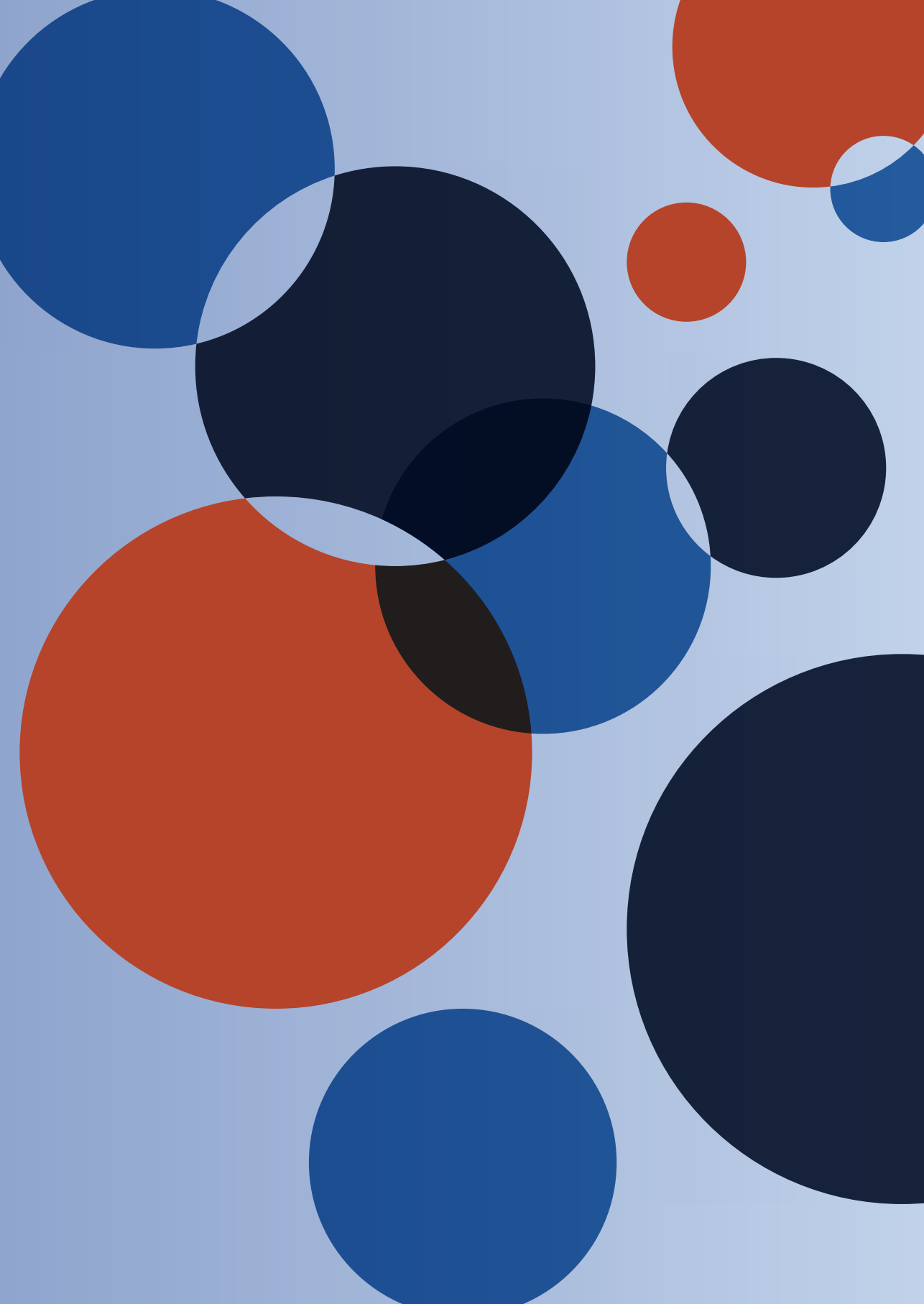


Figure S2. Visualization of fluorescently-labeled HNA-3a- or HNA-3b- neutrophils (PMN, red) stimulated with LPS (5 or 25µg/ml) and extracellular DNA (exDNA, yellow) after perfusion (100s^{-1} shear rate) on VWF-coated flow chambers. (n=3 donors per genotype). Scale bar =100 µm. Lines delimit the flow channels and the well entrance.



GENERAL DISCUSSION AND PERSPECTIVES

Julia Tilburg

6

Venous thrombosis (VT) is a multifactorial disease characterized by the development of an unwanted blood clot. In addition to several environmental risk factors, genetic predisposition contributes to VT development. Genome wide association studies (GWAS) were performed to identify novel VT susceptibility genes and to thereby increase our knowledge on the genetic landscape of VT (1, 2). Besides confirming the associations with known genetic risk factors, two novel loci were revealed, one of them harboring the *SLC44A2* gene. *SLC44A2* encodes the solute carrier family 44 member 2 (SLC44A2), a protein that does not belong to the conventional pathways of thrombosis (3). This is of interest as this association implies that there are undiscovered mechanisms to be revealed regarding the pathophysiology of VT. In addition to functional insights into thrombotic disease, these mechanisms might also present therapeutic targets, potentially without a risk for bleeding. The work described in this thesis aimed to provide functional insights into the mechanism underlying the association between SLC44A2 and VT.

SLC44A2 in hemostasis and thrombosis

We started our investigation into this mechanism by examining the effects of *Slc44a2* gene deletion on hemostasis in mice. Previously, it was shown that the deletion of genes with a crucial function in the hemostatic process may lead to a severe hemophilic or thrombotic phenotype in mice. For instance, it was shown that mice with deletions of the anticoagulant genes tissue factor pathway inhibitor (*Tfpi)* or antithrombin (*Serpinc1*) die during embryonic or gestational days as a consequence of thrombotic features (4, 5). However, mice with a *Slc44a2* gene deletion were fully healthy without clinical phenotype or aberrant development (6). This gave us a first indication that SLC44A2 is not vital to normal hemostasis. Subsequently, we observed that RNA expression (Chapter 2) and plasma protein levels (Chapter 4) of coagulation (related) factors were not altered by SLC44A2 deficiency. This coincided with normal thrombin generation potential in plasma of these mice (Chapter 2), which is indicative of a normally functioning hemostatic system (7). Both these findings are in line with observations from the GWAS, which show that the VT linked small nucleotide polymorphism (SNP) rs2288904 in *SLC44A2* did not affect hemostatic biomarkers included in the GWAS study such as thrombin generation potential and coagulation factor levels (1). The modest drop in von Willebrand factor (VWF) levels in SLC44A2 deficient mice as reported by our group, does not correlate with findings in a human setting that show that VWF levels are unaffected (chapter 2). Together, these observations indicate that SLC44A2 is not involved in normal hemostasis and imply that other mechanisms are underlying the association of this gene with VT.

We took our research a step further and moved from normal hemostasis to pathology to further investigate the mechanism by which SLC44A2 influences thrombosis. To this end, four different murine models representing different elements of thrombosis were used (Chapter 2, 3 and 5). Interestingly, SLC44A2 deficiency resulted in smaller thrombi or reduced neutrophil adhesion in models driven by damage of the cremaster arterioles, inflammation of the mesenteric venules, or stenosis of the inferior vena cava (IVC). In

contrast, the onset of VT was unaffected when *Slc44a2* knockout mice were exposed to VT driven by a hypercoagulable state. The main difference between the various models used is the site of action. The cremaster and stenosis model both have a predefined location of blood clot formation, the site of vessel injury and ligature respectively. The inflammation of the mesentery vein model has a more systemic mode of action but also here, endothelial activation is driving the adhesion of blood cells. In contrast to these three models, endothelial activation or interaction is not the main driver of VT in the hypercoagulability model (although this might occur). Here, it is the imbalance of the pro- and anticoagulant factors in the blood causing the spontaneous development of thrombi. Together, the results from these models provide a compelling argument towards a mediating role for the endothelium, but not coagulation, to drive the effect of SLC44A2 on VT. Interestingly, SLC44A2 is expressed on both the endothelium and on cells that are known to interact with the endothelium in VT, i.e. platelets and neutrophils (8-10). This led us to hypothesize that 1) the endothelium or 2) the interaction between the endothelium and blood cells is involved in the association of SLC44A2 and VT. A systemic (Lipopolysaccharides) and local (ligation of the IVC) stimulus prompting endothelial activation was applied to determine the effect of SLC44A2 in this activation. In both settings activation of the endothelium was found unaffected by SLC44A2 status (Chapter 3). The effect of SLC44A2 on the endothelium was also measured *in vitro* using human umbilical vein cord endothelial cells. Neither overexpression nor knockdown of the *SLC44A2* gene showed an effect on endothelial activation markers measured, including secretion of VWF (unpublished data). Together, these observations in mice and human settings are indicative of a normal endothelial response upon alterations in SLC44A2. Therefore, we focused on our second hypothesis i.e. alterations in the endothelium-blood cell interaction are the contributing factor of SLC44A2 leading to VT.

SLC44A2 mediates Von Willebrand factor neutrophil interaction

SLC44A2 is highly expressed on neutrophils and it is well accepted that neutrophils have a pronounced role in the VT models in which we observe an effect of SLC44A2 (11). In addition, previous studies demonstrated that the A1 domain of endothelial VWF is a SLC44A2 (rs2288904) binding partner (12). These observations, together with our hypothesis that SLC44A2 influences VT through the endothelial-blood cell interaction, piqued our interest. Using flow channel systems, we explored the interaction of neutrophils with VWF. We identified SLC44A2 on neutrophils to be responsible for binding of these cells to VWF resulting in the activation and release of neutrophil extracellular traps (NETs), a process referred to as NETosis (Chapter 5). In addition, we showed that neutrophils homozygous for the minor allele of *SLC44A2* (rs2288904-AA) display a reduction in this adhesion. Our observations thereby form a mechanistical explanation for the reduced VT risk in rs2288904-AA individuals (Odds Ratio (OR): 1.21) (1, 2). Moreover, this possible mechanism also reveals novel insights into the pathophysiology of thrombotic disease itself (Figure 1). It is important to note that for the interaction between VWF and neutrophilic SLC44A2, presence of VWF on the endothelium is required. We therefore envision that this mechanism is augmenting thrombus propagation rather than being a trigger for thrombosis.

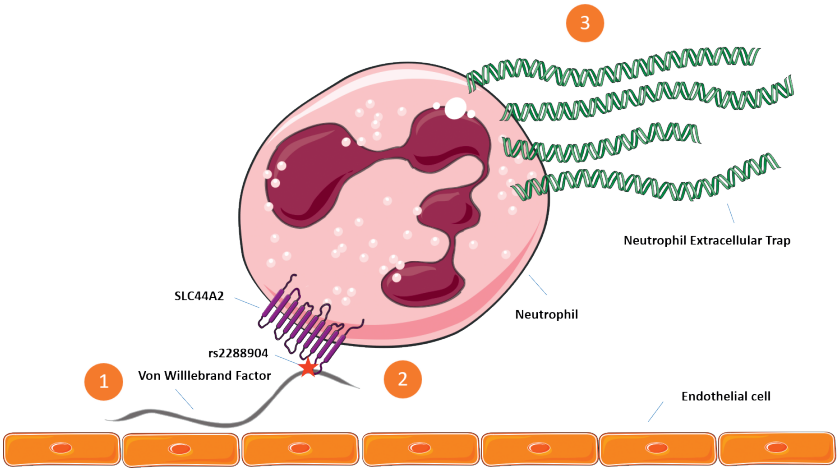


Figure 1 Proposed mechanism underlying the association between SLC44A2 and venous thrombosis.
1) Upon endothelial activation, Von Willebrand Factor is secreted from endothelial cells or captured from circulation and uncoiled, exposing the A1 domain.
2) Neutrophils bind to VWF via the SLC44A2 receptor to the A1 domain on VWF.
rs2288904-G, located within the receptor, has less affinity for this binding compared to rs2288904-A.
3) Neutrophil activation and release of neutrophil extracellular traps propagate thrombosis.

Interestingly, Constantinescu-Bercu and colleagues recently postulated another mechanism by which SLC44A2 contributes to VT involving platelet-neutrophil crosstalk (13). It is well established that platelets and neutrophils bind to each other through P-selectin/P-selectin glycoligand-1 and CD40L/CD40 interactions (14-16). Both these interactions require the activation of platelets to present P-selectin and CD40L on their outer membrane. Remarkably, in low flow microfluidic channel systems, VWF-bound-platelets can bind neutrophils in the absence of full platelet activation. This indicates that alternative mechanisms of platelet-neutrophil interactions are occurring under venous flow. The work of Constantinescu-Bercu and colleagues reveals that upon binding of platelets to VWF, adhesion of neutrophils to these platelets is mediated by platelet integrin αIIbβ3. Interestingly, they identified SLC44A2 as the counter-receptor on neutrophils for the interaction with platelet integrin αIIbβ3. Similar to our observations (Chapter 5), neutrophils with SLC44A2 rs2288904-AA (minor allele) show a reduction in binding and a subsequent reduction in neutrophil activation and NETosis. In contrast to our findings and previous studies by Bayat and colleagues, their experiments do not show a direct interplay between SLC44A2 and VWF (12). One difference in experimental set up is the venous flow applied by Constantinescu-Bercu and colleagues (25 and $50s^{-1}$), which is lower compared to the flow we used ($100s^{-1}$). Possibly, the lower flow does not permit the neutrophils to directly interact with VWF. Overall, these differences observed in SLC44A2-mediated neutrophil vessel wall interplay are of interest and warrant further investigation.

Despite this difference of neutrophil binding, either to VWF or to VWF-bound-platelets, the proposed mechanisms by which *SLC44A2* rs2288904 SNP variants impact VT is similar i.e. altered neutrophil activation and NETosis. Of interest, NETosis is also the driver of another disease with a pronounced role for *SLC44A2* rs2288904; transfusion related active lung injury (TRALI). Evidence for this was previously presented in mice, and disruption of NETs by DNase-1 treatment improved outcome in a TRALI disease model (17). Neutrophil activation and NETosis are also known drivers of immunothrombosis in an experimental mouse model. In the stenosis VT model, both the deletion of peptidyl arginine deiminase 4 (PAD4), a protein crucial in NET formation, and the treatment with DNase-1 resulted in a reduction of thrombus formation (18, 19). The effect we observed of SLC44A2 and the pronounced role of NETs in this model together is therefore supportive of our proposed mechanism by which SLC44A2 influences VT. Interestingly, however, while looking into the composition of the thrombi developed following stenosis of the IVC, we made some observations contradicting NETosis as a driver of the effect of SLC44A2. When neutrophil binding occurs, activation and NETosis is impaired in SLC44A2 knockouts, one would expect that neutrophils and/or NETosis in these thrombi is reduced. Remarkably, we find similar levels of neutrophil and NET markers both at 6 hours (initiation) and 48 hours (propagation) post stenosis (Chapter 3). This raises the question whether the methodology we used to investigate these components is adequate. At 6 hours (thrombosis initiation), we observe variation in neutrophil and NET positivity due to small thrombus size. At 48 hours (thrombosis propagation), the thrombi are fully formed, potentially disallowing us to detect a possible effect occurring in early phases. To overcome these limitations, neutrophil adhesion to the vessel wall upon stenosis can be captured using intravital microscopy of the IVC (11). This is a key experiment to visualize a delay in neutrophil adhesion to the vessel wall, which is expected in SLC44A2 knockout mice. Blocking the integrin αIIbβ3 receptor on platelets will provide answers as to whether SLC44A2 on neutrophils binds VWF directly, via the αIIbβ3 on platelets or perhaps a combination of both. To exclude a role for SLC44A2 on other cell types (for example the endothelium or platelets), follow up murine experiments should preferably be performed using mice deficient for *Slc44a2* specifically in neutrophils. This can be established by crossing mice with a conditional (floxed) *Slc44a2* allele with mice expressing *Cre* recombinase under control of the neutrophil specific Ly6G promotor, which are both available mouse lines (20). These proposed experiments will complement the knowledge we have on the mechanism involving VWF/neutrophil SLC44A2-associated NETosis and determine whether this mechanism is underlying the observed reduction in thrombosis observed in SLC44A2 deficient mice.

Thus far our murine studies have investigated full deficiency of SLC44A2. The GWAS findings however, identified *SLC44A2* rs2288904 as a susceptibility allele for VT and our performed microfluidic flow channel experiments indicate this SNP to be responsible for altered adhesion of neutrophils (Chapter 5). It would be of interest to further study these *SLC44A2* rs2288904 findings in relation to our observations regarding experimental VT in our knockout mice. Laboratory mice are inbred which makes them ideal as experimental

animals as they show little variability in their genetic composition. However, this also means that they do not have allelic variance in *SLC44A2* rs2288904, which would be of interest for our study. Knock in mice expressing human SNP variances of genes involved in coagulation have been previously generated. For instance, mice with the Factor V Leiden variation have been widely used and have led to novel insights into this SNP and its role in thrombosis (21, 22). Development of a 'humanized' *SLC44A2* knock in mouse with the minor *SLC44A2* rs2288904 allele would serve as an interesting tool to further investigate the role of the rs2288904 SNP in VT and, potentially, other diseases such as TRALI.

These knock in mice together with additional flow chamber experiments will enable further dissection of the role of SLC44A2 rs2288904 in NETosis and VT. In addition to these *ex vivo* and *in vivo* experiments, it would be of interest to translate our findings back to the human population. Neutrophil activation and NETosis can be monitored in human plasma by measurement of elastase α1-antitrypsin complexes and circulating nucleosomes, respectively. Interestingly, a previous study detected elevated levels of these markers in VT patients (23). This study did not provide genetic information, hence these levels could not be correlated to *SLC44A2* rs2288904 status. Conversely, the GWAS associating SLC44A2 with VT did not include plasma biomarkers for neutrophils activation or NETosis. A study by Heestermans and colleagues aimed to combine both plasma markers for NETosis and *SLC44A2* rs2288904 data, to see whether there is a relation between SLC44A2 and these levels. In this study, elevated plasma levels of both circulating nucleosomes and elastase α1-antitrypsin complexes were found in VT patients, which is in accordance with previous findings (24). Against expectations however, no association was found between neutrophil/NETosis markers and *SLC44A2* rs2288904 status. One limitation of this study is the grouping of rs2288904-GA and rs2288904-AA (minor allele), which was essential because of the low number of included rs2288904-AA carriers. Our data would argue against this grouping as rs2288904-GA neutrophils still present rs2288904-A, although to a lesser extent. One might expect that the interaction of rs2288904-GA neutrophils with VWF is possibly still occurring to a similar rate as rs2288904-GG because of the presence of this one allele. Overall, the approach presented in the study of Heestermans is of great interest, but an increased sample size and further genotype stratification will be necessary to capture a possible effect of SLC44A2 rs2288904 on NETosis in the human population.

Alternative hypotheses explaining the mechanism underlying the association of SLC44A2 and venous thrombosis

Overall, our research suggests that neutrophilic SLC44A2 is mediating the interaction of neutrophils with VWF. We thereby look at the function of SLC44A2 as a binding partner but overlook two other important features of SLC44A2; the suggested transporter of choline and a protein presenting the human neutrophil antigen-3 (HNA-3). Neutrophils only express the P1 variant of SLC44A2, which is unable to transport choline (10). Therefore, it is not expected that SLC44A2 deficiency or rs2288904 allelic variances will alter choline transport and related functionality of neutrophils. It would be of interest however, to investigate

whether SLC44A2 rs2288904 allelic variances can alter the transport of choline in cells which do express the P2 variant such as endothelial cells. This is of interest, because if alteration in transport capability is observed for the SLC44A2 rs2288904 allelic variants, this might reveal potential insights into VT susceptibility of this SNP. Building on this suggested choline transport function of SLC44A2 is the group of Dr. Lowenstein from Rochester University. Their unpublished research indicated that altered transport of choline by SLC44A2 is affecting acetylcholine levels in platelets (The hemostasis GRC, 2018, poster presentation). Acetylcholine is an endogenous inhibitor of platelets and thereby levels can influence hemostasis (25). Remarkably, their research implies that SLC44A2 on platelet has choline transport capacities. This is in contrast with previous reports showing that platelets do not present the SLC44A2 P2 variant on their membrane (10). In addition, the group of Lowenstein, investigated the effect of SLC44A2 on tail bleeding time in mice, which is an overall measurement of the hemostatic system. Their preliminary data shows elongated tail bleeding time in *Slc44a2* knockout mice, which is in consensus with our observations of SLC44A2 deficient mice showing a reduction in clot formations (Chapter 2 and 3). It would be exciting to see if they can specifically relate the elongated tail bleeding time to platelet SLC44A2 mediated choline uptake. Although multiple aspects of the hemostatic system influence tail bleeding time it should be noted that mice that do not produce NETs, as a result from PAD4 deficiency do not display aberrancies in this hemostatic challenge (18). Therefore, the by Lowenstein and colleagues observed elongated tail bleeding time does not fit the mechanism proposed by us (Figure 1).

Beside the suggested role of SLC44A2 as a choline transporter, SLC44A2 forms the HNA-3 epitope. As the same SNP, rs2288904, and codes this epitope and is associated with VT, an interest is sparked for studying the role of anti-HNA-3 antibodies in thrombotic disease. One might envision similar mechanisms as in TRALI where HNA-3 antibodies bind to SLC44A2 on neutrophils resulting in neutrophil activation and NET release (17, 26). This phenomenon can then result in a higher susceptibility for VT. HNA-3A targeting antibodies are more common than HNA-3B targeting antibodies (27). Also, it is the HNA3A epitope which is associated with elevated VT risk, supporting a potential mechanism involving HNA-3 antibodies in VT (1). Our collaborators at the university of Marseille have started analysis to detect the presence of HNA3 antibodies in VT patients. Results from these studies are awaited with high interest, as elevated levels of these antibodies would reveal a novel element in the pathophysiology of VT.

Clinical implications for SLC44A2

VT has an incidence of 1-2 in 1000 people per year and together with the high rate of recurrence, this results in a large amount of people at high risk for developing VT (28). The anticoagulant treatment often prescribed to these people does not come without a cost, as all currently implemented treatments have a risk of bleeding (29). Because of these side effects, careful consideration of prescribing treatment is necessary, which is achieved by the use of prediction models that combine multiple risk factors (30). These risk prediction

models include, among others, sex, age, D-dimer levels, hormone therapy, body mass index and a history of previous VT (30, 31). Unfortunately, these predictions still suffer from limitations and the discriminating performance is often not optimal. Therefore, further optimization of these models is needed. The findings described in this thesis corroborate the GWAS study and thereby further substantiate the evidence for *SLC44A2* rs2288904 as a genetic risk factor for VT (1). *SLC44A2* rs2288904 status, however, would not make an attractive genetic candidate to be included in prediction algorithms for VT risk. The relatively small OR paired with *SLC44A2* risk (OR 1.21) and the large prevalence of the risk allele in the population (0.785), make SLC44A2 an inefficient discriminating biomarker (1). Moreover, the predictive value of testing for other genetic risk factors for VT is also debatable. Factor V Leiden (rs6025) and variation in prothrombin (rs1799963), both have a larger OR than *SLC44A2* rs2288904, 3.25 and 2.29 respectively, and are also currently not included in VT risk prediction (32). *SLC44A2* rs228904 is therefore not efficient for VT risk prediction. The mechanism by which *SLC44A2* influences VT, however, has potential clinical implications as a target for novel anticoagulant therapies. Our findings show that SLC44A2 does not influence hemostasis, which paves the way for a therapy without bleeding risk. We thereby envision that by blocking SLC44A2 rs2288904, a reduction of VWF/neutrophil SLC44A2-associated NETosis occurs, leading to a protection against VT.

Targeting NETs as a treatment for both arterial and venous thrombosis and other diseases such as TRALI, autoimmune diseases and cancer, has been previously suggested (33). Currently, this is mainly established in mice and *ex vivo* models, but so far, the studies yield promising results. The mode of action of these treatments is comprised of either 1) the degradation of NETs, by DNAse or 2) the blockage of NETosis. Blockage of NETosis can be accomplished in multiple ways, such as through the targeting of PAD4 or Janus kinase 2 (JAK2), another protein involved in NET formation, or by the lowering of reactive oxygen species resulting in a reduction of neutrophil activation (18, 34, 35). As described above, DNAse treatment and PAD4 inhibition have both resulted in a reduction of thrombus formation in the stenosis VT mouse model (11, 18, 19). This is also evident for the JAK2 inhibitor Ruxolitinib, which is an FDA approved drug for myelofibrosis in humans (35). Remarkably, it was observed that patients receiving Ruxolitinib had lower VT incidence in the polycythaemia vera (blood cancer) RESPONSE trial (36). This provides evidence of an anti-NET treatment that results in protection for VT in humans. Of note, this study was not designed for investigations into VT and therefore additional trials are needed (37). In addition to implementation of anti-NET treatment in thromboprophylaxis, the targeting of NETs has also been investigated in thrombolysis as a treatment to disrupt an existing thrombus. The benefits of NET targeting strategies in thrombolysis were recently shown in mouse models for myocardial ischemia and renal ischemia-reperfusion injury (38, 39). Here, the combination of the fibrin degrading protein tissue plasminogen activator (tPA) together with DNAse resulted in improved survival compared to tPA alone, which is the currently used treatment .

Together, these therapies hold a promising future in VT management, but as NETs hold an important biological function in the fight against bacterial infection, implementing these strategies in human can be challenging (40, 41). As follows, it is undesirable to develop novel VT therapies that cause an increased risk for bleeding (as with the current thrombotic therapies), or an increased risk for bacterial infection (as a result of NET inhibition). Therefore, it is important to take into careful consideration this beneficial function of NETs when further exploring NET targeting therapies in VT. A promising recent study in mice showed that PAD4 deficiency did not result in an increased risk of bacterial infection (42). These findings were contradicted, however, by a study that investigated PAD4 in a mouse model for myocardial infarction (43). Here, PAD4 deficiency results in aggravated acute inflammation as a consequence of impaired NET formation. Overall, we may conclude that substantial effort will need to be undertaken to determine safety and efficiency before NET therapies can be implemented for VT (44). Nevertheless, NET targeting therapies form an exciting field with a possible role for SLC44A2. One might speculate that by not blocking NETosis in general, but solely blocking VWF/neutrophil-SLC44A2 mediated NETosis, neutrophils can still exhibit their antibacterial NETosis function, while prothrombotic phenotypes are reduced. This is obviously a speculative assumption, but forms an interesting platform for further investigation into possible therapeutic applications of SLC44A2.

Plasma proteomics in thrombosis research

Plasma protein concentrations hold important information regarding the state of health and disease of an individual. A compelling tool to measure multiple plasma proteins with high precision is mass spectrometry based targeted proteomics. For the work described in this thesis, we have employed this technique to measure 375 proteins in mouse plasma. The experiment provided a wealth of information regarding the effect of the hypercoagulability driven model of VT and *Slc44a2* deficiency on the plasma proteome in mice (Chapter 4). It was observed that the plasma proteome of SLC44A2 deficient mice was weakly affected and the only changes were observed in proteins which are involved in cellular mechanisms. This is in line with the conclusion drawn above, i.e. SLC44A2 influences VT by affecting cellular components and not the coagulation system. Interestingly, we observed that the *Slc44a2* plasma proteome signature was overruled by the effect of sex. Females and males showed distinct plasma profiles which advocates for the careful selection of animals in research or preferably the inclusion of both sexes. It should also be noted that scientific journals currently support the use of both sexes unless arguments for the inclusion of one sex are presented (45). In addition to this observed effect of sex on the plasma proteome, previous reports also showed a variety in plasma proteome signatures in five different mouse strains, commonly used in murine research (46). Interestingly, mouse strain specific effects are also noticeable when looking at their coagulation potential, as differences were observed in coagulation assays such as tail bleeding time (47, 48). Together, the findings by both our group and others further substantiate the importance of taking the plasma proteome into consideration when selecting mouse strains and sex in murine research.

Currently, several initiatives are presented by our department to incorporate mass spectrometry based targeted plasma proteomics in human VT research. Showing the capabilities of this technique, plasma proteome dynamics were determined for patients with VT and the combination of VT and cancer (49). The two groups showed a clear separation based on the plasma proteome and moreover the measured plasma protein levels nicely correlated with levels measured by the conventional assays. Work presented at the International Society of Thrombosis and Hemostasis Congress 2019 described plasma proteomics signatures for patients that developed VT upon a plaster cast or knee arthroscopy (50-52). Findings from these signatures will potentially be incorporated in an expansion of the current prediction models for VT occurrence in these patients. In addition, research is performed to determine the plasma proteome of patients which have major bleeding events during treatment with Vitamin K antagonists. The researchers aim to discover novel biomarkers for bleeding events in these patient group to improve prediction (53). Together, these efforts will expand our knowledge of the plasma proteome in clinical and fundamental VT/bleeding research and further establish a solid mass spectrometry based targeted proteomics workflow (54).

The contribution of the genetic landscape to VT

Within this thesis, we aimed to provide a functional follow-up to the association between *SLC44A2* and VT which was identified by GWAS (1, 2). Moreover, our data successfully corroborated the GWAS and provided insights into the mechanism underlying this finding. In order to give a clinical implication to the GWAS findings, besides solely biomarker discovery, functional follow-ups are necessary. To avoid a discrepancy between the novel gene associations and the gain in functional insights, it is important to keep this overarching goal in mind. For instance, with respect to the other novel VT locus *TSPAN15*, no functional follow up has been published so far and the mechanism by which that gene might influence VT therefore remains elusive (1).

During our functional follow up to the previous GWAS finding, new actions have been undertaken to expand the knowledge on the genomic landscape and VT by Lindström and colleagues. They performed a large meta-analysis of several VT GWAS, which included 30.234 VT cases and 172.122 controls (55), a large increase compared to the previous study, which consisted of 7.507 VT cases and 52.632 controls (1). In addition to the increased population, the included genetic traits (SNPs measured) were increased from 6.751.884 to 12.923.718 SNP variants. Furthermore, this study goes beyond the genome alone by also including a transcriptome-wide association study (TWAS) on liver and whole blood expression data of these subjects. The GWAS and TWAS combined identified a total of 16 novel VT susceptibility loci, in addition to replication of the previously identified loci, including *SLC44A2* (55). This complements our current knowledge and leads to a list of 37 VT susceptibility genes which are summarized in Figure 3 (56). Altogether, the VT GWAS performed over the past decade made enormous contributions to our understanding of the genetic landscape of VT, but this list is still not complete. Together, these 37 genes

are estimated to be responsible for 15% of the VT heritability, while previous twin studies showed that the overall heritability of VT is 40-60%. Two methodologies can be employed to further reveal these genetic contributors; increase the SNPs and number of subjects of GWAS or use genome wide sequencing. The latter is currently used in other research fields and shows promising results (57).

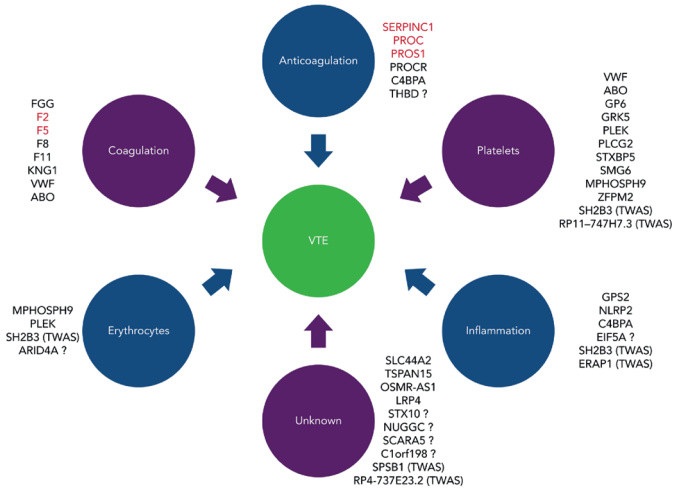


Figure 2 Genes associated with VTE. Genes are grouped according to biological links to VTE: coagulation, anticoagulation, platelets, erythrocytes, inflammation, and unknown. Genes associated with major thrombophilia are marked in red. Question marks denote non-replicated genes. TWAS shows that the gene was identified with transcriptome-wide association study. Adapted from: Zöller, Blood, 2019

The novel VT susceptibility genes identified by the latest GWAS include candidate genes, not related to coagulation. Interestingly, Lindström and colleagues included correlations of these associations with blood cell trait. Several of the novel genetic risk factors were correlated with either platelet or red blood cell traits, indicating that these variances exhibit their contributing role to VT through one of these cell types. From the genes correlating with platelet traits *GP6*, *ZFPM2*, and *VWF* are known, whereas *ABO*, *PLEK*, *GRK5*, *MPHOSPH9*, *PLCG2*, *SMG6*, and *SH2B3* are newly associated loci. Indeed, in line with these GWAS findings are mechanistic insights into the role of platelets in VT. It is suggested that alterations in platelet formation by megakaryocytes, elevated platelet aggregation, platelet derived microparticles, and higher platelet counts and volumes are linked to VT (58). Together, these observations and the presented GWAS findings are indicative of a larger role for platelets than originally thought, which encourages further research into the consideration of antiplatelet therapy in VT. Recent clinical trials are also advocating for the implementation of these therapies in VT, as these trials showed a reduction in VT upon antiplatelet treatment such as aspirin (59-61). In addition to the genes influencing platelet traits, associations were also found with

red blood cell traits. This sparked interest for a role of this cell type in VT risk, which is not unanticipated as they are a major constituent of the venous thrombus. From a mechanistic point of view, red blood cells are suspected to contribute to VT by several mechanisms. This includes altering blood viscosity, formation of platelet aggregates, adhesion to the vessel wall, involvement in the increase of thrombus size and their potential to promote thrombin generation, among others (62-64). The findings of Lindström and colleagues encourages further investigation into the role of red blood cells in the pathophysiology of VT. To summarize, the findings from the most recent VT GWAS hold potential for further functional follow-up studies. Thereby, the overall wealth of genomic data available opens up an opportunity to further dissect the pathophysiology of VT and form a foundation for potential novel therapeutic targets.

Concluding remarks

GWAS identified *SLC44A2* as a novel susceptibility gene for VT and the work in this thesis has corroborated these findings. Moreover, in mice, SLC44A2 deficiency was determined to not affect hemostasis. This is in line with our plasma proteome findings as we did not find an effect of SLC44A2 on plasma protein levels of proteins involved in coagulation. Interestingly, we observed a protective effect of SLC44A2 deficiency in multiple VT mouse models. Furthermore, our research provided evidence that SLC44A2 influences VT by altering the interaction of endothelial-VWF and neutrophils, mediated by SLC44A2. Neutrophils with the *SLC44A2* minor allele, previously identified as a protective SNP for VT, had reduced neutrophil-VWF interaction. Our study thereby revealed a novel mechanism in VT pathophysiology, involving cellular components of the blood. This paves the way for further investigation into novel therapeutics for VT targeting SLC44A2. Furthermore, our research underlines the potential of GWAS to reveal novel genetic contributors to this disease and encourages functional follow-ups to further dissect the pathophysiology of VT.

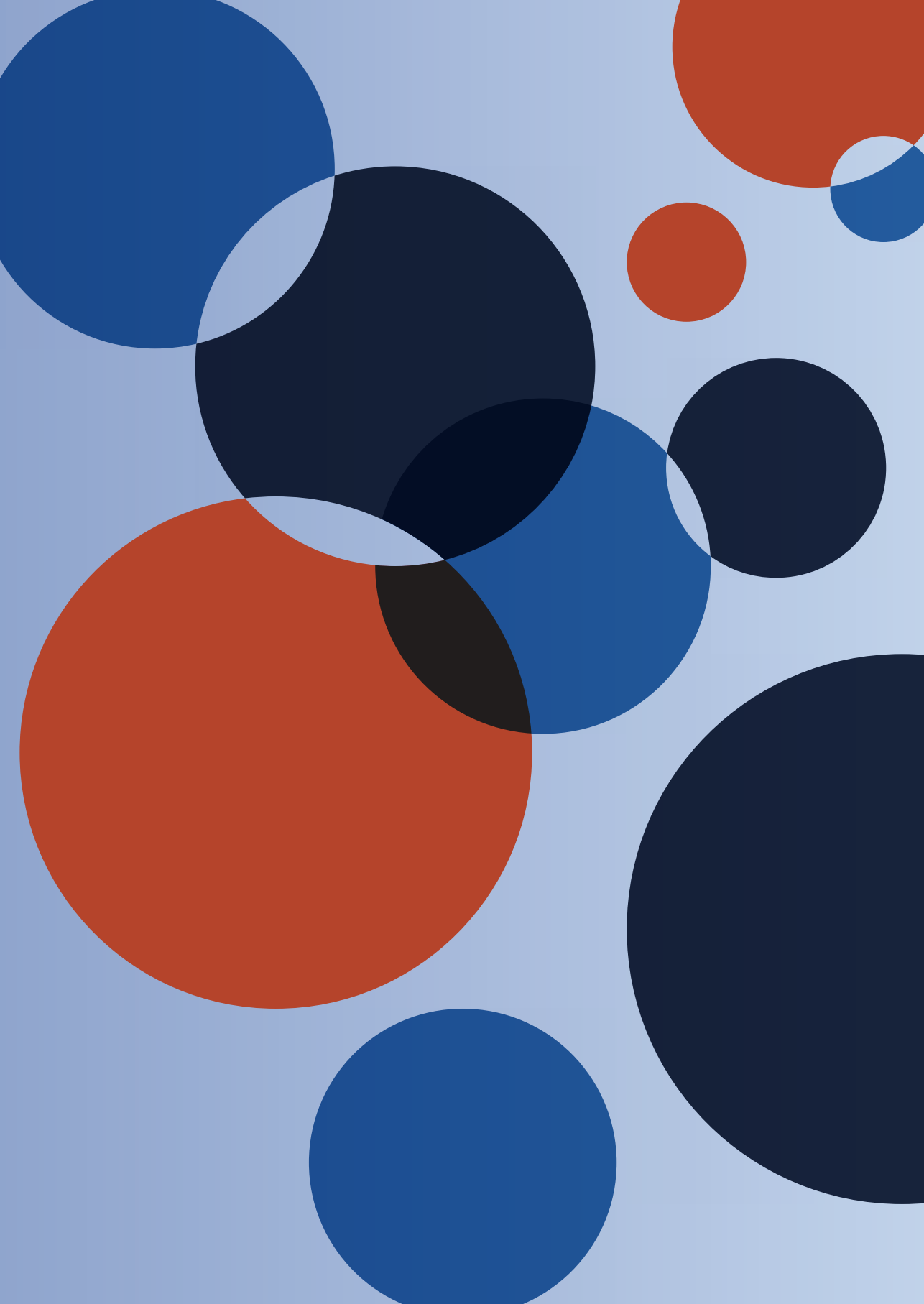
References

1. Germain M, Chasman DI, de Haan H, et al. Meta-analysis of 65,734 individuals identifies TSPAN15 and SLC44A2 as two susceptibility loci for venous thromboembolism. *Am J Hum Genet*. 2015;96(4):532-42.
2. Hinds DA, Buil A, Ziemek D, et al. Genome-wide association analysis of self-reported events in 6135 individuals and 252 827 controls identifies 8 loci associated with thrombosis. *Human Molecular Genetics*. 2016;25(9):1867-74.
3. Nair TS, Kozma KE, Hoefling NL, et al. Identification and characterization of choline transporter-like protein 2, an inner ear glycoprotein of 68 and 72 kDa that is the target of antibody-induced hearing loss. *J Neurosci*. 2004;24(7):1772-9.
4. Huang ZF, Higuchi D, Lasky N, et al. Tissue factor pathway inhibitor gene disruption produces intrauterine lethality in mice. *Blood*. 1997;90(3):944-51.
5. Ishiguro K, Kojima T, Kadomatsu K, et al. Complete antithrombin deficiency in mice results in embryonic lethality. *J Clin Invest*. 2000;106(7):873-8.
6. Kommareddi P, Nair T, Kakaraparthi BN, et al. Hair Cell Loss, Spiral Ganglion Degeneration, and Progressive Sensorineural Hearing Loss in Mice with Targeted Deletion of Slc44a2/Ctl2. *J Assoc Res Otolaryngol*. 2015;16(6):695-712.
7. Duarte RCF, Ferreira CN, Rios DRA, et al. Thrombin generation assays for global evaluation of the hemostatic system: perspectives and limitations. *Rev Bras Hematol Hemoter*. 2017;39(3):259-65.
8. Kommareddi PK, Nair TS, Thang LV, et al. Isoforms, Expression, Glycosylation, and Tissue Distribution of CTL2/SLC44A2. *The Protein Journal*. 2010;29(6):417-26.
9. Greinacher A, Wesche J, Hammer E, et al. Characterization of the human neutrophil alloantigen-3a. *Nature Medicine*. 2010;16(1):45-8.
10. Flesch BK, Wesche J, Berthold T, et al. Expression of the CTL2 transcript variants in human peripheral blood cells and human tissues. 2013;53(12):3217-23.
11. von Bruhl ML, Stark K, Steinhart A, et al. Monocytes, neutrophils, and platelets cooperate to initiate and propagate venous thrombosis in mice in vivo. *J Exp Med*. 2012;209(4):819-35.
12. Bayat B, Tjahjono Y, Berghofer H, et al. Choline Transporter-Like Protein-2: New von Willebrand Factor-Binding Partner Involved in Antibody-Mediated Neutrophil Activation and Transfusion-Related Acute Lung Injury. *Arterioscler Thromb Vasc Biol*. 2015;35(7):1616-22.
13. Constantinescu-Bercu A, Grassi L, Frontini M, et al. Activated αIIbβ3 on platelets mediates flow-dependent NETosis via SLC44A2. 2019:373670.
14. Lievens D, Zernecke A, Seijkens T, et al. Platelet CD40L mediates thrombotic and inflammatory processes in atherosclerosis. *Blood*. 2010;116(20):4317-27.
15. Mayadas TN, Johnson RC, Rayburn H, et al. Leukocyte rolling and extravasation are severely compromised in P selectin-deficient mice. *Cell*. 1993;74(3):541-54.
16. Palabrica T, Lobb R, Furie BC, et al. Leukocyte accumulation promoting fibrin deposition is mediated in vivo by P-selectin on adherent platelets. *Nature*. 1992;359(6398):848-51.
17. Thomas GM, Carbo C, Curtis BR, et al. Extracellular DNA traps are associated with the pathogenesis of TRALI in humans and mice. *Blood*. 2012;119(26):6335-43.

18. Martinod K, Demers M, Fuchs TA, et al. Neutrophil histone modification by peptidylarginine deiminase 4 is critical for deep vein thrombosis in mice. *Proc Natl Acad Sci U S A*. 2013;110(21):8674-9.
19. Brill A, Fuchs TA, Savchenko AS, et al. Neutrophil extracellular traps promote deep vein thrombosis in mice. 2012;10(1):136-44.
20. Stackowicz J, Jonsson F, Reber LL. Mouse Models and Tools for the in vivo Study of Neutrophils. *Front Im139munol*. 2019;10:3130.
21. Snyder LA, Rudnick KA, Tawadros R, et al. Expression of human tissue factor under the control of the mouse tissue factor promoter mediates normal hemostasis in knock-in mice. *J Thromb Haemost*. 2008;6(2):306-14.
22. Cui J, Eitzman DT, Westrick RJ, et al. Spontaneous thrombosis in mice carrying the factor V Leiden mutation. *Blood*. 2000;96(13):4222-6.
23. van Montfoort ML, Stephan F, Lauw MN, et al. Circulating nucleosomes and neutrophil activation as risk factors for deep vein thrombosis. *Arterioscler Thromb Vasc Biol*. 2013;33(1):147-51.
24. Heestermans M, Cunha ML, Reitsma PH, et al. Circulating nucleosomes and elastase alpha1-antitrypsin complexes and the novel thrombosis susceptibility locus SLC44A2. *Thromb Res*. 2016;142:8-10.
25. Bennett JA, Ture SK, Schmidt RA, et al. Acetylcholine Inhibits Platelet Activation. *J Pharmacol Exp Ther*. 2019;369(2):182-7.
26. Sachs UJ, Hattar K, Weissmann N, et al. Antibody-induced neutrophil activation as a trigger for transfusion-related acute lung injury in an ex vivo rat lung model. *Blood*. 2006;107(3):1217-9.
27. Reil A, Wesche J, Greinacher A, et al. Geno- and phenotyping and immunogenicity of HNA-3. *Transfusion*. 2011;51(1):18-24.
28. Raskob GE, Angchaisuksiri P, Blanco AN, et al. Thrombosis: a major contributor to global disease burden. *Arterioscler Thromb Vasc Biol*. 2014;34(11):2363-71.
29. Linkins LA, Choi PT, Douketis JD. Clinical impact of bleeding in patients taking oral anticoagulant therapy for venous thromboembolism: a meta-analysis. *Ann Intern Med*. 2003;139(11):893-900.
30. Timp JF, Braekkan SK, Lijfering WM, et al. Prediction of recurrent venous thrombosis in all patients with a first venous thrombotic event: The Leiden Thrombosis Recurrence Risk Prediction model (L-TRRiP). *PLoS Med*. 2019;16(10):e1002883.
31. Ensor J, Riley RD, Moore D, et al. Systematic review of prognostic models for recurrent venous thromboembolism (VTE) post-treatment of first unprovoked VTE. *BMJ Open*. 2016;6(5):e011190.
32. Segal JB, Brotman DJ, Necochea AJ, et al. Predictive value of factor V Leiden and prothrombin G20210A in adults with venous thromboembolism and in family members of those with a mutation: a systematic review. *JAMA*. 2009;301(23):2472-85.
33. Snoderly HT, Boone BA, Bennewitz MF. Neutrophil extracellular traps in breast cancer and beyond: current perspectives on NET stimuli, thrombosis and metastasis, and clinical utility for diagnosis and treatment. *Breast Cancer Res*. 2019;21(1):145.
34. Martinod K, Wagner DD. Thrombosis: tangled up in NETs. *Blood*. 2014;123(18):2768-76.
35. Wolach O, Sellar RS, Martinod K, et al. Increased neutrophil extracellular trap formation promotes thrombosis in myeloproliferative neoplasms. *Sci Transl Med*. 2018;10(436).
36. Vannucchi AM. Ruxolitinib versus standard therapy for the treatment of polycythemia vera. *N Engl J Med*. 2015;372(17):1670-1.

37. Masciulli A, Ferrari A, Carobbio A, et al. Ruxolitinib for the prevention of thrombosis in polycythemia vera: a systematic review and meta-analysis. *Blood Adv*. 2020;4(2):380-6.
38. Ge L, Zhou X, Ji WJ, et al. Neutrophil extracellular traps in ischemia-reperfusion injury-induced myocardial no-reflow: therapeutic potential of DNase-based reperfusion strategy. *Am J Physiol Heart Circ Physiol*. 2015;308(5):H500-9.
39. Peer V, Abu Hamad R, Berman S, et al. Renoprotective Effects of DNAse-I Treatment in a Rat Model of Ischemia/Reperfusion-Induced Acute Kidney Injury. *Am J Nephrol*. 2016;43(3):195-205.
40. Brinkmann V, Reichard U, Goosmann C, et al. Neutrophil extracellular traps kill bacteria. *Science*. 2004;303(5663):1532-5.
41. Castanheira FVS, Kubes P. Neutrophils and NETs in modulating acute and chronic inflammation. *Blood*. 2019;133(20):2178-85.
42. Martinod K, Fuchs TA, Zitomersky NL, et al. PAD4-deficiency does not affect bacteremia in polymicrobial sepsis and ameliorates endotoxemic shock. *Blood*. 2015;125(12):1948-56.
43. Eghbalzadeh K, Georgi L, Louis T, et al. Compromised Anti-inflammatory Action of Neutrophil Extracellular Traps in PAD4-Deficient Mice Contributes to Aggravated Acute Inflammation After Myocardial Infarction. *Front Immunol*. 2019;10:2313.
44. Laridan E, Martinod K, De Meyer SF. Neutrophil Extracellular Traps in Arterial and Venous Thrombosis. *Semin Thromb Hemost*. 2019;45(1):86-93.
45. Beery AK. Inclusion of females does not increase variability in rodent research studies. *Curr Opin Behav Sci*. 2018;23:143-9.
46. Michaud SA, Sinclair NJ, Petrosova H, et al. Molecular phenotyping of laboratory mouse strains using 500 multiple reaction monitoring mass spectrometry plasma assays. *Commun Biol*. 2018;1:78.
47. Kopic A, Benamara K, Schuster M, et al. Coagulation phenotype of wild-type mice on different genetic backgrounds. *Lab Anim*. 2019;53(1):43-52.
48. Schiviz A, Magirr D, Leidenmuhler P, et al. Influence of genetic background on bleeding phenotype in the tail-tip bleeding model and recommendations for standardization: communication from the SSC of the ISTH. *J Thromb Haemost*. 2014;12(11):1940-2.
49. Mohammed Y, van Vlijmen BJ, Yang J, et al. Multiplexed targeted proteomic assay to assess coagulation factor concentrations and thrombosis-associated cancer. *Blood Adv*. 2017;1(15):1080-7.
50. van Adrichem RA, Nemeth B, Algra A, et al. Thromboprophylaxis after Knee Arthroscopy and Lower-Leg Casting. *N Engl J Med*. 2017;376(6):515-25.
51. Nemeth B, Cannegieter SC. Venous thrombosis following lower-leg cast immobilization and knee arthroscopy: From a population-based approach to individualized therapy. *Thromb Res*. 2019;174:62-75.
52. Y. Mohammed CET, B. Nemeth, B.J.M. van Vlijmen, S.C. Cannegieter. Different Protein Spectrum in Patients with Venous Thrombosis after Lower Leg Plaster Cast Application or Knee Arthroscopy than in Controls International Society of Thrombosis and Hemostasis Congress 20192019.
53. van Rein N, Lijfering WM, Bos MH, et al. Objectives and Design of BLEEDS: A Cohort Study to Identify New Risk Factors and Predictors for Major Bleeding during Treatment with Vitamin K Antagonists. *PLoS One*. 2016;11(12):e0164485.
54. Scheller I, Nieswandt B. Novel Approaches to Unravel Risk Factors and Mechanisms of Venous Thrombosis. *Thromb Haemost*. 2020;120(3):372.

55. Lindstrom S, Wang L, Smith EN, et al. Genomic and Transcriptomic Association Studies Identify 16 Novel Susceptibility Loci for Venous Thromboembolism. *Blood*. 2019:blood.201900043.
56. Zoller B. Genetics of venous thromboembolism revised. *Blood*. 2019;134(19):1568-70.
57. Hoglund J, Rafati N, Rask-Andersen M, et al. Improved power and precision with whole genome sequencing data in genome-wide association studies of inflammatory biomarkers. *Sci Rep*. 2019;9(1):16844.
58. Montoro-Garcia S, Schindewolf M, Stanford S, et al. The Role of Platelets in Venous Thromboembolism. *Semin Thromb Hemost*. 2016;42(3):242-51.
59. Collaborative overview of randomised trials of antiplatelet therapy--III: Reduction in venous thrombosis and pulmonary embolism by antiplatelet prophylaxis among surgical and medical patients. Antiplatelet Trialists' Collaboration. *BMJ*. 1994;308(6923):235-46.
60. Brown GA. Venous thromboembolism prophylaxis after major orthopaedic surgery: a pooled analysis of randomized controlled trials. *J Arthroplasty*. 2009;24(6 Suppl):77-83.
61. Prevention of pulmonary embolism and deep vein thrombosis with low dose aspirin: Pulmonary Embolism Prevention (PEP) trial. *Lancet*. 2000;355(9212):1295-302.
62. Aleman MM, Walton BL, Byrnes JR, et al. Fibrinogen and red blood cells in venous thrombosis. *Thromb Res*. 2014;133 Suppl 1:S38-40.
63. Walton BL, Byrnes JR, Wolberg AS. Fibrinogen, red blood cells, and factor XIII in venous thrombosis. *J Thromb Haemost*. 2015;13 Suppl 1:S208-15.
64. Byrnes JR, Wolberg AS. Red blood cells in thrombosis. *Blood*. 2017;130(16):1795-9.



NEDERLANDSE SAMENVATTING

7

Het bloedstollingssysteem in ons lichaam is van cruciaal belang gezien dit er voor zorgt dat bloedverlies beperkt blijft bij beschadigingen van de vaatwand. De bloedstolling, ook wel hemostase genoemd, is een zeer complex proces waarbij verschillende componenten betrokken zijn waaronder de vaatwand, bloedplaatjes en stollingsfactoren. Een balans tussen pro en anti-stollingsfactoren is hierbij essentieel en een verstoring in deze balans kan zorgen voor bloedingen dan wel overmatige stolling dit laatste wordt ook wel trombose genoemd. Trombose kan in zowel slagaderen als in venen voorkomen, maar dit proefschrift richt zich op veneuze trombose. Deze ziekte heeft een incidentie van 1-2 personen per 1000 mensen per jaar en heeft daarmee een grote weerslag op de gezondheidszorg. Patiënten met veneuze trombose, en ook mensen met een verhoogd risico voor het krijgen van deze ziekte, worden vaak (preventief) behandeld met anticoagulantia. Deze behandelingen zijn echter niet zonder risico, nu deze inspelen op de stolling en daarom kunnen leiden tot bloedingen. Verder onderzoek naar veneuze trombose is nodig, om nieuwe inzichten te verkrijgen in de pathofysiologie en om daarmee te komen tot eventuele nieuwe therapieën zonder bloedingsrisico.

Veneuze trombose kent verschillende omgevingsrisicofactoren zoals leeftijd, overgewicht en co-morbiditeit zoals bijvoorbeeld COVID-19. Daarnaast speelt ook erfelijke belasting een belangrijke rol. Om een beter inzicht te verwerven in de wijze waarop genen bijdragen aan het risico op ziektes met een genetisch element kan men zogenoemde *genome wide association studies* (GWAS) uitvoeren. Binnen deze studies worden genetische variaties vergeleken tussen een aangedane groep en een gezonde controlegroep om zo te kijken of bepaalde varianten geassocieerd zijn met een ziekte. In 2015 zijn de bevindingen van een GWAS-meta-analyse gepubliceerd, waar werd gekeken naar veneuze trombose. Deze bevindingen vormen de basis voor het in dit proefschrift beschreven onderzoek. Variaties op 6.751.884 plekken in het genoom werden gemeten in 7.507 patiënten met veneuze trombose versus 52.632 gezonde controles. Deze studie associeerde negen varianten met dit ziektebeeld. Het merendeel hiervan betreft bekende risicofactoren voor veneuze trombose, zoals factor V Leiden mutatie en bloedgroep O. Echter werden er ook twee varianten in genen gevonden die nog niet eerder geassocieerd zijn met veneuze trombose namelijk TSPAN15 en SLC44A2. SLC44A2 staat voor *solute carrier family 44 member 2* ook wel *choline transport like protein-2* (CTL-2). Gebaseerd op overeenkomsten van SLC44A2 met SLC44A1, wat choline transport faciliteert, wordt er gedacht dat SLC44A2 eenzelfde transportfunctie heeft, echter er ontbreekt hiervoor solide bewijs in de literatuur. SLC44A2 is aanwezig op verschillende weefsels, waaronder ook het endotheel, wat de vaatwand bedekt en daarom een belangrijke speler is in trombose. Ook is dit eiwit aanwezig op verschillende soorten bloedcellen, zoals neutrofielen en bloedplaatjes. Deze bloedcellen worden recentelijk steeds vaker in verband gebracht met de pathofysiologie van veneuze trombose. Verder is er bekend dat SLC44A2 een rol speelt in twee aan veneuze trombose ongerelateerde ziekte namelijk, transfusie gerelateerde acute longschade (TRALI) en gehoorverlies. De variatie in SLC44A2 welke geassocieerd is met veneuze trombose, rs2288904, codeert voor het in TRALI betrokken HNA3-A/B antigen aanwezig op het SLC44A2 eiwit. Het doel van het onderzoek beschreven

in dit proefschrift is om inzichten te verkrijgen in de manier waarop SLC44A2 een rol speelt in veneuze trombose. Dit om de pathofysiologie van dit ziektebeeld verder te ontdekken en, eventueel, nieuwe kandidaten voor therapeutische strategieën te vinden. De belangrijkste bevindingen van het onderzoek zijn hieronder uiteengezet.

Het in dit proefschrift beschreven onderzoek maakt gebruik van zeer recent gegenereerde muis welke deficiënt is voor het *Slc44a2*-gen. Deze zogenaamde *knockout* muismodellen zijn een veelgebruikte strategie in biomedisch onderzoek om de functie van genen te bestuderen. In **hoofdstuk 2** van dit proefschrift wordt dit nieuwe muismodel voor het eerst bekeken vanuit het oogpunt van de bloedstolling, met als doel om een mogelijke rol van dit gen hierin te vinden. Bloedplasma van *Slc44a2*-deficiënte muizen vertoont geen afwijking in de vorming van trombine; een cruciaal eiwit in de stolling. Ook is de genexpressie van stollings (gerelateerde) genen niet verschillend in muizen zonder SLC44A2. Von Willebrand factor (VWF) is een belangrijk stollingseiwit, wat zich bevindt in het plasma, het endotheel en de bloedplaatjes, allemaal belangrijke spelers in de hemostase. Wij vinden een verlaging van VWF-levels in plasma van ~15% in SLC44A2-deficiënte muizen. Het onderzoek laat zien dat SLC44A2 aanwezig is op bloedplaatjes maar dat het de aggregatie van bloedplaatjes niet beïnvloedt. Om naar de interactie tussen bloedplaatjes, stolling en de vaatwand te kijken is vaatschade geïnduceerd in de *Slc44a2*-deficiënte muis en de accumulatie van zowel bloedplaatjes als fibrine (het eindproduct van de stolling) gemeten. Een opmerkelijke bevinding is dat muizen zonder SLC44A2 een minder sterke reactie hebben op deze vaatschade in vergelijking met wildtype controle muizen. Hiermee bevestigen we de uit de GWAS volgende link tussen SLC44A2 en veneuze trombose. De bevindingen in dit hoofdstuk laten zien dat onder fysiologische omstandigheden, dus zonder pro-trombotische trigger, SLC44A2 geen groot effect heeft op verschillende aspecten van de bloedstolling (VWF-levels uitgezonderd). Ook dit is in overeenkomst met de GWAS waar variaties in het *SLC44A2*-gen geen effect hebben op de verschillende gemeten parameters voor hemostase in mensen.

In **hoofdstuk 3** gaan we van de fysiologische naar de pathofysiologische situatie, waarbij we *Slc44a2*-deficiënte muizen blootstellen aan twee verschillende modellen van veneuze trombose met als doel te kijken of SLC44A2 trombose beïnvloedt. In het eerst toegepaste model in dit hoofdstuk wordt de aanmaak van twee anti-stollingsfactoren (antitrombine en proteïne C) in de lever geremd door middel van siRNA. Als gevolg ontstaan er meerdere bloedstolsels in de grote venen van de kaak/hoofd van de muis. Wanneer wij dit model toepassen op muizen met *Slc44a2*-deficiëntie, zien wij geen verschil in het ontstaan van deze bloedstolsels. Wel is zichtbaar dat na de vorming van bloedstolsels, het aantal neutrofielen in het bloed hoger is bij muizen zonder SLC44A2 ten opzichte van controlemuizen. Het is bekend dat neutrofielen de incidentie van trombose niet beïnvloeden in dit model. Dit motiveerde ons om een tweede model voor veneuze trombose toe te passen, waar deze bloedcellen wel een belangrijke rol spelen; het stenose model. Voor dit model wordt door middel van een chirurgische ingreep een ligatuur geplaatst om de onderste holle ader waardoor er een 90% reductie van de bloedstroom ontstaat. 48 uur na het plaatsen van de

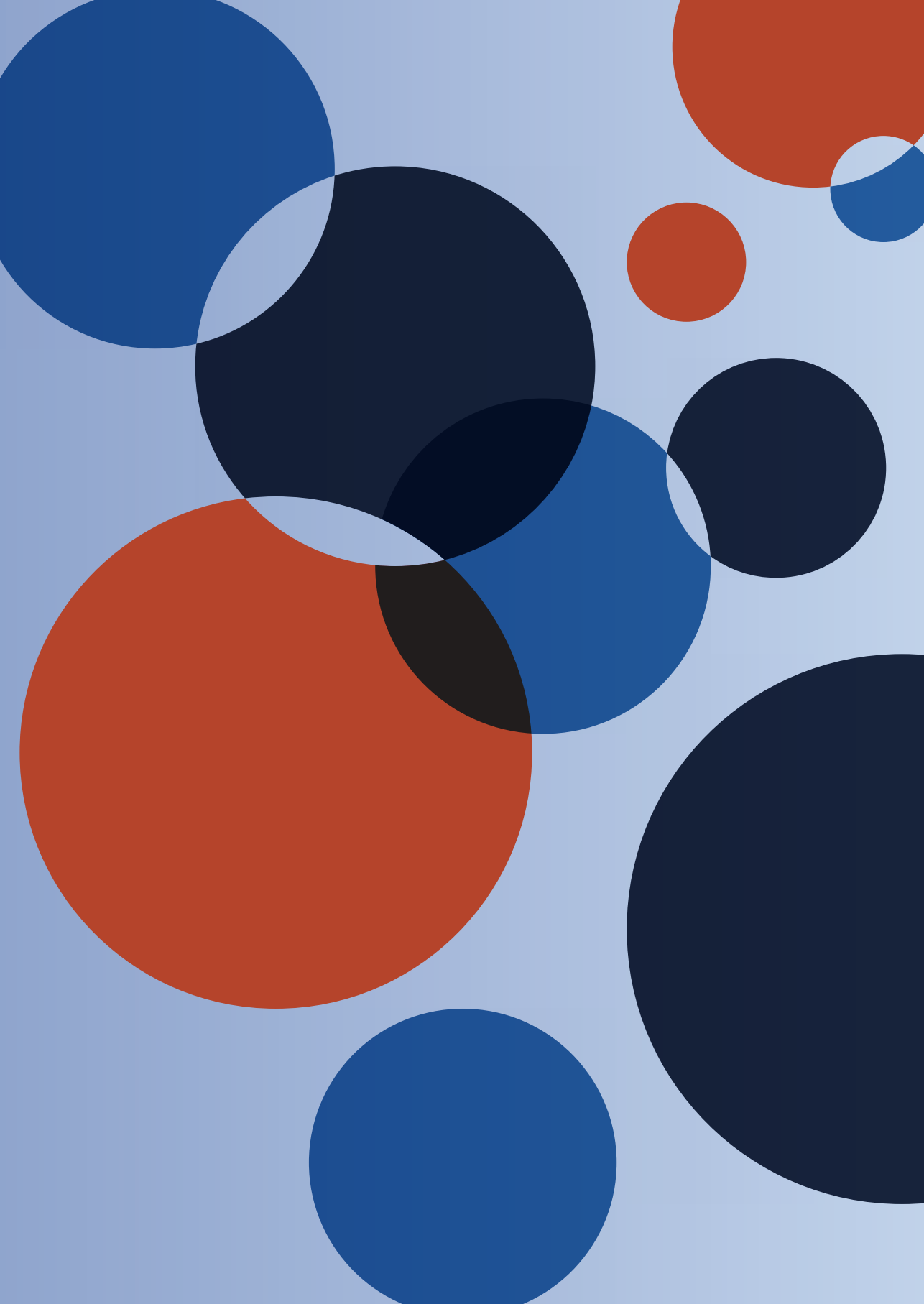
ligatuur is het aldus ontstane bloedstolsel significant kleiner in *Slc44a2*-deficiënte muizen ten opzichte van de controlemuizen. Tevens bevatten deze bloedstolsels minder bloedplaatjes. *Ex vivo* experimenten wijzen uit dat dit niet het gevolg is van een veranderende adhesie van bloedplaatjes aan VWF. Wanneer we ons meer richten op de initiatie van trombus vorming, na 6 uur stenose, is het effect van SLC44A2 nog uitgesprokener. Verder is zichtbaar dat veranderingen in uitscheiding van ontstekingsfactoren door het endotheel, activatie van bloedplaatjes, aggregatie van bloedplaatjes aggregatie en neutrofiel-activatie niet ten grondslag liggen van het waarneembare effect op trombose. Samenvattend laten de studies beschreven in **hoofdstuk 3** zien dat SLC44A2 duidelijk bijdraagt aan trombose in de muis. Door de verschillende waarnemingen bij de twee verschillende modellen kunnen wij concluderen dat het effect van SLC44A2 niet door stolling is gemedieerd, wat in lijn is met de bevindingen beschreven in **hoofdstuk 2**. De duidelijke invloed van SLC44A2 in het stenose model, leidt tot de hypothese dat deze invloed via een cellulair mechanisme plaatsvindt.

Bloedplasma bevat verschillende eiwitten waaronder de stollingsfactoren, complementfactoren, en talloze eiwitten betrokken bij de immuun response. Om een goed beeld te krijgen over fysiologie en pathofysiologie in cardiovasculair onderzoek is het meten van plasma-eiwitten cruciaal. Een groot obstakel hier is dat traditionele metingsmethoden lang niet voor alle eiwitten beschikbaar zijn, voornamelijk in het geval van eiwitten in muizen. Ook vereisen de traditionele methoden veelal een groot plasmavolume, wat nadelig is gezien muizen een klein bloedvolume hebben. In **hoofdstuk 4** is daarom een nieuw platform voor het meten van plasma-eiwitten gebruikt wat gebaseerd is op massaspectrometrie. In een plasma *sample* worden bij deze methode eiwitten enzymatisch gefragmenteerd en aan de hand van de massa van de peptide kunnen deze eiwitten vervolgens worden geïdentificeerd en gekwantificeerd. Traditionele massaspectrometrie heeft echter een beperkte exactheid en daarom gebruiken wij een zogenaamde *targeted approach* waarbij 375 eiwitten in het plasma kunnen worden gekwantificeerd met een hoge precisie doormiddel van stabiele isotopen-gelabelde peptide standaarden. Eerst wordt gekeken naar het effect van trombose op de plasma-eiwitten, waarbij we kijken naar het eerder benoemde model waarbij trombose ontstaat als gevolg van de remming van de aanmaak van antistollingsfactoren. Veneuze trombose heeft hier een sterk effect, met voornamelijk verschillen in de plasma hoeveelheid van eiwitten betrokken bij ontstekingen en eiwitten aanwezig in rode bloedcellen. Om inzicht te vergaren in een eventueel effect van SLC44A2 op plasma-eiwitten, is dezelfde techniek toegepast op muizen deficiënt voor *Slc44a2*, zonder de introductie van trombose. In deze groep muizen, waarin beide seksen (man en vrouw) zijn geïncludeerd, heeft sekse een grotere invloed dan SLC44A2. Voor *Slc44a2*-deficiëntie zijn er twee eiwitten welke verschillend zijn binnen beide sekse namelijk *glycosylation-dependent cell adhesion molecule-1* en *thrombospondin-1*. Voor beide eiwitten is geen directe rol in de bloedstolling bekend. Wel zijn deze betrokken bij cellulaire mechanisme in neutrofielen en bloedplaatjes respectievelijk. Het ontbreken van een effect van SLC44A2 op de plasmahoeveelheid van eiwitten betrokken bij de stolling is in overeenstemming met de bevindingen van **hoofdstuk 2** en met de bevindingen van de GWAS. Concluderend, in dit hoofdstuk een nieuwe technologie voor

het meten van plasma-eiwitten voor het eerst toegepast in cardiovasculair onderzoek gebruikmakend van muismodellen en zijn hiermee nieuwe inzichten verkregen in de effecten van trombose, sekse en SLC44A2 op deze eiwitten.

In bovenstaande hoofdstukken bestuderen wij het effect van SLC44A2 op hemostase, trombose en plasma-eiwitten waarbij wij gebruikmaken van een muismodel. In **hoofdstuk 5** worden deze bevindingen teruggebracht naar de mens waarbij de rol van SLC44A2, en specifiek het daarop aanwezige antigen HNA-3, in humane cellen is bestudeerd. Bevindingen vanuit het onderzoek naar TRALI, een ziekte waar SLC44A2 ook een rol speelt, duiden er op dat SLC44A2 via HNA-3 kan binden aan VWF en dat deze binding wordt beïnvloed door de variatie geassocieerd met trombose; rs2288904. Om dit verder te bestuderen is in HEK293T cellen, een veelgebruikt cel model in biomedisch onderzoek, SLC44A2 met HNA3-A of HNA3-B ingebracht. Vervolgens is in een model wat de stroming van het bloed door bloedvaten nabootst, gekeken naar de binding van deze cellen aan VWF. Cellen met HNA3-A vertonen een verhoogde binding ten opzichte van HNA3-B. Dit is tevens zichtbaar wanneer hetzelfde experiment wordt uitgevoerd met humane neutrofielen met HNA3-A of HNA3-B. Deze verhoogde binding kan resulteren in neutrofiel activatie na blootstelling aan een stimulus. Neutrofiel activatie kan leiden tot het uitscheiden van DNA wat een net (ook wel neutrofiele extracellulaire vallen (NETs)) vormt waar bloedcellen aan kunnen binnen. Deze NETs zijn recentelijk in verband gebracht met een verhoogd risico op trombose. Om de invloed van SLC44A2 op neutrofiel/vaatwand interactie te verifiëren, is gekeken naar de invloed van SLC44A2 op de interactie van neutrofielen en venen in de muis. Hier is zichtbaar dat neutrofielen van *Slc44a2*-deficiente muizen inderdaad minder aan de vaatwand kleven.

Samenvattend tonen de studies beschreven in dit proefschrift aan dat SLC44A2 in muizen geen effect heeft op de hemostase en de hoeveelheid van stollingseiwitten, met de uitzondering van een kleine verlaging in von Willebrand factor. Dit is in overeenstemming met bevindingen dat SLC44A2 geen invloed heeft op de ernst van de trombose in een model voor veneuze trombose, welke gevoelig is voor veranderingen in de bloedstolling. SLC44A2 heeft wel een invloed op een model waarvan bekend is dat bloedcellen en voornamelijk neutrofielen een belangrijke rol spelen. Hieruit kan de conclusie worden getrokken dat SLC44A2 via cellulaire mechanismen trombose beïnvloedt. In de studies met menselijke cellen is zichtbaar dat SLC44A2 een neutrofiel/VWF-interactie medieert, wat tot activatie van deze immuun cellen en het uitscheiden van NETs kan leiden. Deze studies hebben bijgedragen aan het ontrafelen hoe de nieuwe erfelijke factor SLC44A2 bijdraagt aan de ontwikkeling van veneuze trombose. Hierdoor begrijpen we beter hoe veneuze trombose ontstaat met hopelijk in de nabije toekomst concrete aanknopingspunten voor een alternatieve, betere en veiliger behandelingsstrategie voor veneuze trombose.



APPENDIX

A

Curriculum vitae

Julia Tilburg was born in Rotterdam on September 8th 1989. Following her secondary education at the Ring van Putten in Spijkenisse, she studied *Biologie en Medisch Laboratoriumonderzoek* at the Hogeschool Rotterdam, during which she worked as a teaching assistant. Her bachelor internship was performed at the department of Bone and Calcium Metabolism of the Erasmus Medical Center in Rotterdam under the supervision of Dr. J. van de Peppel. This research focused on genetic regulatory elements important for osteogenic and adipogenic lineage commitment in human mesenchymal stromal cells. After graduating in 2013, she continued her education with a master in Biology at the Leiden University. As part of this master, she performed two research projects, both with a focus on omics data. The first, at the RNA Biology and Applied Bioinformatics Research Group of the University of Amsterdam with Dr. R.J. Dekker, focused on the expression of small RNAs in embryonic vs. adult cells. The second project was conducted at the department of Molecular Epidemiology at the Leiden University Medical Center under the supervision of Prof. Dr. B.T. Heijmans in collaboration with Unilever R&D in Colworth, UK. Here, she studied the effect of ultraviolet exposure on DNA methylation in human dermal fibroblasts. In January 2016, Julia started her PhD research at the Department of Thrombosis and Hemostasis and Einthoven Laboratory for Vascular and Regenerative Medicine of the Leiden University Medical Center. This research, under the supervision of Dr. B.J.M. van Vlijmen and Prof. Dr. H.H. Versteeg, together with Dr. C.X. Maracle, was sponsored by the Trombosestichting Nederland. As part of this doctoral research, she performed studies in Ann Arbor (USA), Marseille (France) and Maastricht. Her most important research findings are outlined in this thesis. Julia is currently a research fellow in the laboratory of Dr. J.E. Italiano Jr. at Boston Children's Hospital and Harvard Medical School, Boston, USA. Here, she studies platelet production from megakaryocytes and platelet/megakaryocyte extracellular vesicles.

Publicaties

G. Zirka, J. Tilburg, P. Robert, C.X. Maracle, B.J.M. van Vlijmen, P. Legendre, M.C. Alessi, P.J. Lenting, P.E. Morange and G.M. Thomas SLC44A2/HNA-3a is involved in neutrophil adhesion and activation to Von Willebrand factor in humans and mice. *Manuscript under revision.*

J. Tilburg, D.M. Coenen, G. Zirka, S. Dólleman, A.M. van Oeveren-Rietdijk, M.F.A. Karel, H.C. de Boer, J.M.E.M. Cosemans, H.H. Versteeg, P.E. Morange, B.J.M. van Vlijmen, C.X. Maracle*, G.M. Thomas*. SLC44A2 deficient mice have a reduced response in stenosis but not in hypercoagulability driven venous thrombosis. *J Thromb Haemost.* 2020 Jul;18(7):1714–1727. (*:These authors contributed equally)

J. Tilburg, R.C. Slieker, H.E.C. Suchiman, A. Heath, D. van Heemst, P.E. Slagboom, F.R. de Gruijl, D.A. Gunn, B.T. Heijmans. Repeat UVA exposure of human skin fibroblasts induces both a transitionary and recovery methylation response. *Epigenomics.* 2020 Apr;12(7):563-573.

J. Tilburg, S.A. Michaud, C.X. Maracle′ H.H. Versteeg′ C.H. Borchers′ B.J.M. van Vlijmen*, Y. Mohammed*. Plasma Protein Signatures of a Murine Venous Thrombosis Model and *Slc44a2* Knockout Mice Using Quantitative-Targeted Proteomics. *Thromb Haemost.* 2020 Mar;120(3):423-436. (*:These authors contributed equally)

J. Tilburg*, R. Adili*, T.S. Nair, M.E. Hawley, D.C. Tuk, M. Jackson, H.M. Spronk, H.H. Versteeg, T.E. Carey, B.J.M. van Vlijmen, C.X. Maracle**, M.M. Holinstat**. Characterization of Hemostasis in Mice lacking the Novel Thrombosis Susceptibility Gene *Slc44a2*. *Thromb Res.* 2018 Nov;171:155-159. (*/**:These authors contributed equally)

J. van de Peppel, T. Strini, J. Tilburg, H. Westerhoff, A.J. van Wijnen, J.P. van Leeuwen. Identification of Three Early Phases of Cell-Fate Determination during Osteogenic and Adipogenic Differentiation by Transcription Factor Dynamics. *Stem Cell Reports.* 2017 Apr 11;8(4):947-960.

Dankwoord

Het werk beschreven in dit proefschrift is het resultaat van vele samenwerkingen. In het onderstaande stuk wil ik graag de personen die hieraan hebben bijgedragen bedanken. Maar, allereerst, wil ik een dank uitspreken aan jou, de lezer, voor de getoonde interesse in dit proefschrift.

Bart, je onbaatzuchtige en integere manier van wetenschap bedrijven siert je. Ik heb je coöperatieve instelling, wat ervoor gezorgd heeft dat ik in verschillende laboratoria een kijkje heb kunnen nemen, altijd erg gewaardeerd. Ik hoop je lessen mee te nemen in mijn verdere carrière "to expect the unexpected".

Henri, bedankt voor de rol die je als promotor hebt gehad tijdens mijn PhD.

Chrissta, thank you for everything! I enjoy your positivity and our trips to Marseille have been among the highlights of my PhD.

Marco, wat een fijne mede AIO, ik heb veel van je mogen leren. David en Lieke, jullie hebben als studenten een enorme bijdrage geleverd, bedankt!

Tom, I am grateful that you shared your *Slc44a2* knockout mice, they have made a pivotal contribution to my PhD. Tom, Thanku, Michael and Raymond, also many thanks for the wonderful time in Ann Arbor.

Pierre, Grace and Gaia. Thank you for the pleasant collaboration, I am very excited that you will continue the SLC44A2 work and assured you will discover amazing things.

Yassene, I really enjoyed diving into the world of plasma proteomics!

Judith en Daniëlle, bedankt voor jullie expertise en het warme welkom in Maastricht.

Hetty en Annemarie, bedankt voor de vele input!

Jeroen van de Peppel en Bas Heijmans, jullie hebben mijn enthousiasme voor de wetenschap altijd geprikkeld.

C7-collega's en D2 labmaten, ik heb enorm genoten van de geweldige dynamiek op onze afdeling, bedankt!

Joeri, Ik wil je bedanken voor de ongelofelijke steun die je bent geweest de afgelopen jaren.

Karlijn, ik waardeer onze duurzame vriendschap enorm.

Sophie, Kelley en Stam, ik voel me gezegend met jullie als werkvriendinnetjes.

Suzan, ik ben trots dat je mijn paranimf wil zijn, bedankt voor alles!

Rayna, ik kijk uit naar nieuwe avonturen.

Lief Idunn, en in het bijzonder Nina, Pien, Jantien, Lam, Felice, Daniek, Lisa, Marielle en Hannah, bedankt voor jullie interesse en vriendschap.

Fenneke en Elsemieke, wat ben ik blij met mijn Gravinnen.

Simone, onze vriendschap is fenomenaal!

Daan, Maartje, Eva, Joren en Lotte, bedankt dat ik altijd mijzelf kan zijn bij jullie.

Vader en moeder, het doet me goed dat jullie altijd in mij geloven.